Technical Report

TR-11-02

Assessment of the importance of mixing in the Yucca Mountain hydrogeological system

Javier B. Gómez, Luis F. Auqué, María Gimeno, Patricia Acero
Geochemical Modelling Group, Department of Earth Sciences
University of Zaragoza

Zell Peterman, Thomas A. Oliver
U.S. Geological Survey

Mel Gascoyne, Gascoyne Geoprojects Inc

Marcus Laaksoharju, Geopoint AB

February 2011

Svensk Kärnbränslehantering AB
Swedish Nuclear Fuel
and Waste Management Co

Box 250, SE-101 24 Stockholm
Phone +46 8 459 84 00

ISSN 1404-0344
SKB TR-11-02

Assessment of the importance of mixing in the Yucca Mountain hydrogeological system

Javier B. Gómez, Luis F. Auqué, María Gimeno, Patricia Acero
Geochemical Modelling Group, Department of Earth Sciences
University of Zaragoza

Zell Peterman, Thomas A. Oliver
U.S. Geological Survey

Mel Gascoyne, Gascoyne Geoprojects Inc

Marcus Laaksoharju, Geopoint AB

February 2011

Foreword

The M3 code (Multivariate Mixing and Massbalance calculations) is a statistical and mathematical groundwater modelling tool developed by SKB which models the obtained groundwater chemistry in terms of sources and sinks in relation to an ideal mixing model. The complexity of the measured groundwater data determines the configuration of the ideal mixing model. Deviations from the ideal mixing model are interpreted as being due to reactions or other processes such as evaporation.

M3 is used as one of the major groundwater modelling tool within the SKB site investigation programme. The code has previously been applied on groundwater data from Sweden, Finland, Canada, Japan, Jordan and Gabon. There is an increasing interest to use the code for various groundwater modelling tasks in shallow and deep groundwater environments in different countries. The purpose of this report is to test the code in a challenging groundwater environment such as the Yucca Mountain. The results are used as an important validation and verification exercise of the M3 code.

Summary

The Yucca Mountain area is the focus of a potential repository for high-level radioactive waste. The planned repository is located in the unsaturated zone at approximately 500 m below the eastern crest of Yucca Mountain. In the event of a confinement failure in the repository, contaminated waters will first percolate down to the underlying tuffaceous aquifer and then south and south-east to the Central Amargosa Valley. Here, a complex aquifer system will receive the plume and consequently it is of utmost importance to assess the degree of connection between the three main aquifers in the area: the Tertiary Tuffs Aquifer (directly connected to Yucca Mountain), the Quaternary Basin-fill Aquifer, and the regional (and deep) Palaeozoic Carbonate Aquifer. An upward leakage from the Palaeozoic Carbonate Aquifer would dilute the contaminant plume, while the reverse, downward leakage from the Tertiary Tuffs Aquifer or the Quaternary Basin-fill Aquifer into the Palaeozoic Carbonate Aquifer would contaminate a major aquifer system. The main objective of this study is to propose a mixing hypothesis for the Yucca Mountain groundwaters and to assess the degree of mixing between the different aquifers.

For this purpose, a large set of samples taken in deep and shallow boreholes, wells and springs are analysed from a hydro-geochemical point of view. These samples cover an area of ~280 km^2 (40 km in the east-west direction and 90 km in the north-south direction) with the northern boundary just north of the Yucca Mountain crests and the southern boundary near the locality of Death Valley Junction, CA. There is a general northeast-southwest topographic gradient, with maximum altitudes of 2,000 m above sea level in the Eleana Range and minimum altitudes of –80 m above sea level in Death Valley, which in a general way controls the regional flow of groundwaters in the area. For local groundwater flow, the maximum relief is of the order of 1,000 m, as occurs between the top of Yucca Mountain (1,507 m above sea level) and the bottom of the Amargosa River at Ash Meadows (around 650 m above sea level).

Hydrogeologically, the movement of groundwaters can be discussed in terms of local, intermediate, and regional flow systems. The first two are relatively shallow and water flow is restricted to individual basins. whereas regional flow is deeper and water flows from one basin to another. Regional groundwater flow is mainly through faults and fractures in the thick Palaeozoic carbonate rocks, whereas intermediate and local flow is in the Cainozoic volcanics and Quaternary basin-fill deposits. These three aquifer systems have a complex geometry and are separated by aquitards with sometimes lesser known confinement characteristics.

Five different water types contributing to the chemistry of any water parcel in the Yucca Mountain area have been identified: precipitation, surface waters, perched waters, unsaturated-zone pore waters, and saturated-zone groundwaters. In addition, the saturated-zone groundwaters have been grouped into 10 hydrofacies based on chemical, geographical and hydrogeological criteria. These 10 hydrofacies are (from north to south and west to east): Western Yucca Mountain, Eastern Yucca Mountain, Bare Mountains, South East Crater Flat, Jackass Flat, Western Rock Valley, Fortymile Wash, Amargosa River, Eastern Amargosa and Ash Meadows.

The initial dataset consists of 397 water samples, of which 39 are precipitation samples, 17 surface water samples, 6 perched water samples, 81 pore water samples and 254 are groundwater samples.

The analysis of the sample dataset has been carried out in two steps: a preliminary exploratory analysis where the processes affecting the chemistry of each sample are identified, followed by a multivariate statistical analysis for the assessment of mixing. The preliminary exploratory analysis is performed on the complete dataset (raw dataset, 397 samples). It serves to identify trends and outliers and, together with PHREEQC simulations, to eliminate from the raw dataset all the samples affected by non-mixing processes (water-rock interaction, evaporation, cation exchange, etc).

After the exploratory analysis, which was carried out in two phases, i.e. total system and by hydrofacies, a total of 157 samples were screened out. The distribution of eliminated samples is as follows:

(i) 38 precipitation samples (i.e. only one representative precipitation water, sample #6221, was retained),

(ii) 16 surface water samples because they were affected by strong water-rock interaction and evaporation (sample #275 was retained as a representative of the less evolved surface waters),

(iii) one perched water sample with a very anomalous chemistry (sample #336),

(iv) all 81 pore water samples, as the exploratory analysis showed that their chemistry was, in general, unrelated to the chemistry of the groundwaters and, in addition, cation exchange between pore waters and secondary minerals in the Tertiary tuffs was very apparent, and

(v) 18 groundwater samples (8 from the Ash Meadows hydrofacies, 4 each from the Fortymile Wash and Bare Mountains hydrofacies, and one each from the Eastern Amargosa and Western Rock Valley hydrofacies).

The main processes identified in the screened-out groundwater samples are evaporation (Ash Meadows hydrofacies), anthropic contamination (Fortymile Wash hydrofacies), calcite subsaturation in a carbonate aquifer (Bare Mountains hydrofacies), high chloride concentrations in an otherwise very diluted hydrofacies (Eastern Amargosa), and high bicarbonate, 400 mg/L, in a hydrofacies with a constant bicarbonate content of 160 mg/L (Western Rock Valley).

The final dataset (240 samples) is used as input to the multivariate geochemical code M3 in order to identify potential end-member waters and, most importantly, to bracket the *number* of end-members that can best explain the chemistry of the samples of the final dataset.

M3 (*M*ultivariate *M*ixing and *M*ass balance) is a Principal Component Analysis code that approaches the modelling of mixing and mass balance from a purely geometrical perspective (Laaksoharju et al. 1999, 2009, Gómez et al. 2006, 2009). As opposed to standard geochemical codes, M3 tries first to explain the chemical composition of a parcel of water by pure mixing, and only then are deviations from the pure mixing model interpreted as chemical reactions. The M3 computer program is a stand-alone program developed by SKB in the MATLAB 7.1 computational environment. M3 has been recently subjected to a verification and validation procedure (Gómez et al. 2009).

The main outcome of the M3 analysis is the identification of *mixing models* that are able to explain the overall chemistry of a large dataset in terms of mixing. Given a set of potential end-member waters, M3 explores all possible combinations of end-members and ranks these mixing models in terms of the number of samples inside the mixing polyhedron (coverage). Samples inside the mixing polyhedron are those whose chemistry can be explained by a mixture of the end-member waters that define the particular mixing model. The more samples in a mixing model inside the mixing polyhedron, the better the model is at explaining the chemistry of the complete dataset.

All the best mixing models identified by M3 (14 mixing models with coverage > 75%) are composed of three end-members (5 models) or four end-members (9 models). No five-end-member mixing model can compete with the three- and four-end-member mixing models in terms of coverage. Under closer inspection, the three-end-member mixing models are clearly inferior to the four-end-member ones as they exclude important subsets of samples from the mixing polyhedron. It is thus concluded that the Yucca Mountain hydro-system is best explained as a mixture of four end-member waters.

Another important result arising from the M3 analysis is that the samples defining the end-members in the good mixing models are only a small subset of the initial set of potential end-members. In other words, only a small number of samples can act as end-member waters so that, when they mix, they can reproduce the chemistry of the Yucca Mountain hydro-system. For obvious reasons, these end-member waters have been termed the Tertiary Tuffs Aquifer (TTA) end-member, the Regional Palaeozoic Carbonate Aquifer (RCA) end-member, the Quaternary Basin-fill Aquifer (QBfA) end-member, and the Altered Meteoric Water (AMW) end-member. The first three end-members are representative of each of the major aquifer systems in the area, while the fourth is representative of the meteoric waters (a precipitation sample, a surface water sample or a perched water sample). The TTA end-member is systematically defined by sample #211 (Eastern Yucca Mountain hydrofacies); the RCA end member is defined either by sample #264 (Bare Mountains hydrofacies) or by sample #40

(Ash Meadows hydrofacies); the QBfA end-member is defined either by sample #143 (Amargosa River hydrofacies) or by sample #291 (Jackass Flat hydrofacies); and the AMW end-member is defined either by precipitation sample #6221 or by perched water sample #345.

Six mixing models were finally selected from the initial 14 identified by M3. To rank the mixing models, two parameters have been considered: (i) coverage and (ii) a good match between the chloride contents of the actual samples and that of the reconstructed chemistry based on the computed mixing proportions. Once arranged in order, the best model has been taken as the reference mixing model. The mixing proportions computed with the reference model are the best approximation to the mixing processes that the waters at Yucca Mountain have undergone. The picture that emerges from this mixing model is the following:

1. The reference mixing model has sample #211 as the TTA end-member, sample #264 as the RCA end-member, sample #143 as the QBfA end-member, and sample #345 as the AMW end-member. The coverage is 81.4%, i.e. 195 samples out of 240 are inside the mixing polyhedron. Overall, the highest contribution to the chemistry of the samples in the final dataset comes from the AMW (49%), followed by the TTA (19%), the RCA (17%), and the QBfA (15%). Also, the AMW contribution is the most evenly spread among the samples.
2. The Eastern and Western Yucca Mountain hydrofacies samples are almost a binary mixture of the TTA and AMW end-members. The presence of an AMW component in these waters is somewhat surprising, and points to the rather widespread presence of an "old" meteoric water in many shallow sections of the local aquifers around Yucca Mountain.
3. Most Ash Meadows samples are almost a binary mixture of the RCA and AMW end-members (with a small contribution, ~8%, of the QBfA end-member). This concurs with a discharge of the regional Palaeozoic carbonate aquifer along the Gravity fault, followed by a mixture of the carbonate waters with (old) meteoric waters during ascent.
4. The samples from the Central Amargosa Valley (Amargosa River, Eastern Amargosa, Fortymile Wash, and Western Rock Valley hydrofacies) are particularly interesting because they occupy the area located down-gradient of Yucca Mountain. From the point of view of mixing, these waters are dominated by the QBfA and AMW end-members, although they always have contributions from at least one other end-member water. Based on hydrofacies, Amargosa River samples have the highest contribution of the QBfA end-member (between 75% and 100%), followed by the Eastern Amargosa samples (around 40%), and the Fortymile Wash samples (less than 20%). The Western Rock Valley samples have a varied contribution of the QBfA, between 0 and 50%. The "extra" contribution could be the TTA (as in one subset of the Western Rock Valley samples), the RCA (as in the Eastern Amargosa samples), or both (as in the Fortymile Wash samples). The high contribution of the RCA end-member in most samples of the Eastern Amargosa hydrofacies is compatible with their position intersecting the Gravity fault.

In summary, the ternary mixing that characterises most samples in the Central Amargosa Valley is a clear indication that the aquifers in the area are not completely sealed. On the contrary, it seems that mixing between chemically contrasting waters is widespread down-gradient of Yucca Mountain.

The study performed in this context was funded by the USGS and, apart from its intrinsic interest for the dynamics of the groundwater system at Yucca Mountain, it is highly recommended for application by any potential M3 users who may want to understand and apply the complete methodology to a different hydrogeological system. In this respect, the Yucca Mountain hydro-system has proved to be rather difficult, and the stringent methodological procedure devised to model the system could serve as a template for further studies.

Objectives

The main objective of this work is to assess the importance of mixing on the hydrochemistry of waters in and around Yucca Mountain, most importantly in those waters south of Yucca Mountain. Due to the general north-south gradient of groundwater flow in the Yucca Mountain area, leakage from the proposed high-level radioactive waste repository would have the greatest consequences in the saturated zone waters south of Yucca Mountain. In this area (Amargosa River, Amargosa Flat and Ash Meadows), three main aquifers interact: the Regional Palaeozoic Carbonate Aquifer (RCA), the Tertiary Tuffs Aquifer (TTA) and the Quaternary Basin-fill Aquifer (QBfA). One consequence of upward leakage from the Palaeozoic Carbonate Aquifer would be to dilute the contaminant plume should one develop from the radioactive waste repository at Yucca Mountain. The reverse, downward leakage from the Tertiary Tuffs Aquifer or the Quaternary Basin-fill Aquifer into the Palaeozoic Carbonate Aquifer would contaminate a major aquifer system. It is clearly of the utmost importance to explore the links between theses aquifer systems and to assess the degree of mixing between the groundwaters.

To attain this general objective, the following specific objectives have been either defined in advance or decided as being important during the development of the project:

1. Compile a dataset of water samples from the Yucca Mountain area. This dataset should contain samples from all the potential water types that contribute to the chemistry of the groundwaters in the aquifer systems in the area.
2. Perform a careful total-system exploratory analysis on the initial (raw) dataset in order to identify trends and outliers.
3. Perform a detailed exploratory analysis of each individual hydrofacies with the aim of identifying and eliminating from the raw dataset all the samples heavily affected by processes other than mixing (e.g. water-rock interaction, evaporation, cation exchange). PHREEQC simulations were performed in order to conduct such screening.
4. Analyse the final dataset with the multivariate geochemical code M3 in order to identify the end-member waters needed to explain the chemistry of the groundwaters in the Yucca Mountain area.
5. Define the best mixing model and compute the mixing proportions in terms of the selected end-member waters. Particularly important are the mixing proportions of the waters down-gradient of Yucca Mountain, in the Central Amargosa River area.

Contents

1 Introduction

1.1 Geography

The Yucca Mountain area (Figure 1-1) is located in the southern Great Basin, a sub-province of the Basin and Range physiographic province, which encompasses nearly the whole of Nevada as well as adjacent parts of Utah, Idaho, Oregon and California. It includes a large valley, the Amargosa Valley, and part of another valley, the Death Valley; two large mountain ranges, the Funeral Mountains to the southwest and the Spring Mountains to the east; and a broad volcanic plateau to the north. Most of the area has northwest-southeast trending physiographic features (the Amargosa River Valley, the Death Valley, the Funeral Mountains and the Spring Mountains), although Yucca Mountain itself is a north-south trending mountain (as is typical for the Basin and Range province). Much of the topographic relief is due to Late Cainozoic tectonic and volcanic activity. There is a general northeast-southwest topographic gradient, with maximum altitudes of 2,000 m above sea level (asl) in the Eleana Range and minimum altitudes of –80 m asl in Death Valley, which controls in a general way the regional flow of groundwaters in the area. An exception to this rule are the Spring Mountains, located to the southeast, where the maximum altitudes reach 3,600 m asl at Charleston Peak (outside the bounding box of Figure 1-1). Although this gives more than 3,500 m of topographic relief, the relief between valleys and adjoining mountains is of the order of 1,000 m, as occurs between the top of Yucca Mountain (1,507 m asl) and the bottom of the Amargosa River at Ash Meadows (approximately 650 m asl).

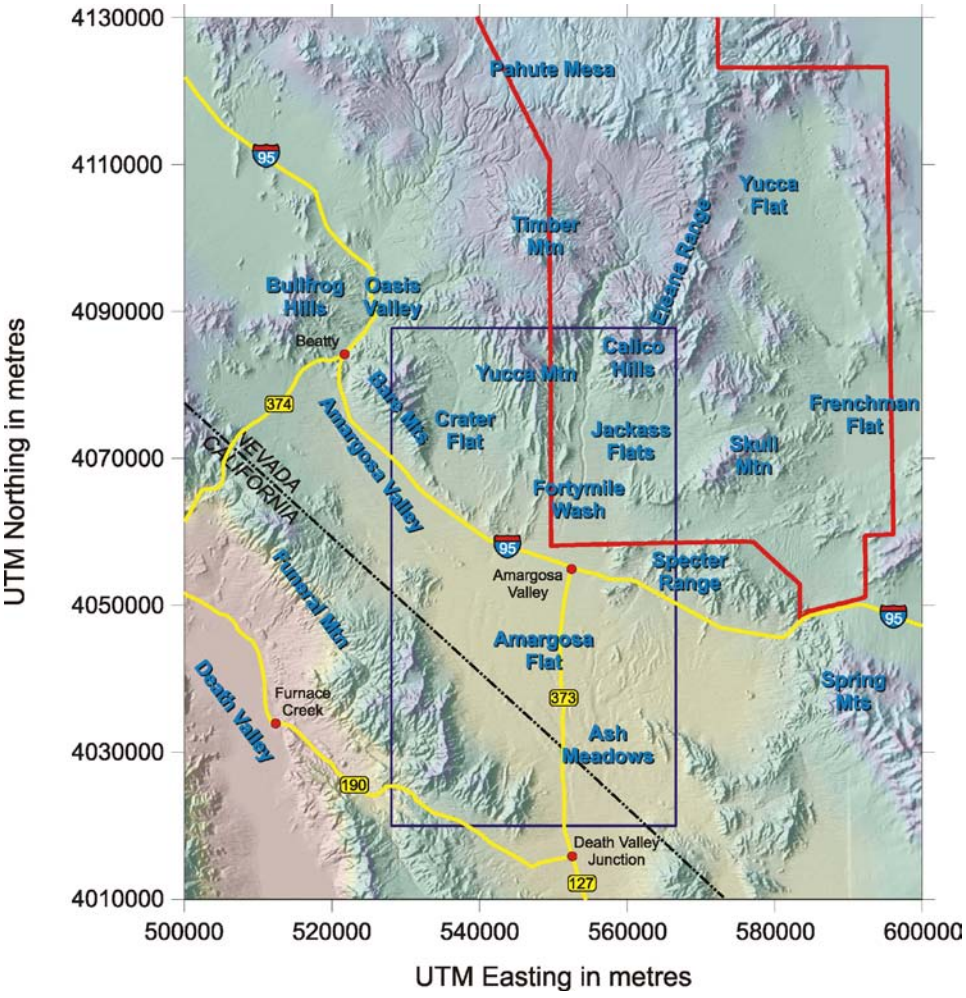

Figure 1-1. *Bounding box of the Yucca Mountain area as used in this report. Major geographical features are labelled. All groundwater samples used in this report are located inside the bounding box. The red polygon marks the boundary of the Nevada Test Site.*

Mountain ranges are separated by broad intermontane basins. The basins are filled with sediment and certain interbedded volcanic deposits that gently slope from the valley floors to the bordering mountain ranges (Peterson 1981). The valley floors are local depositional centres which usually contain playas that act as catchments for surface-water runoff (Grose and Smith 1989). Most of the basins seldom contain perennial surface water and many playas contain saline deposits that indicate the evaporation of surface water and/or shallow ground water from the playa surface. Playas affected by quaternary faulting contain springs in which ground water is forced to the surface by juxtaposed lacustrine and basin-fill deposits (Bedinger et al. 1989). The Amargosa Desert contains several spring pools (e.g. Ash Meadows) and human-engineered reservoirs that are supported by regional ground-water discharge.

From a climatic point of view, most of the Yucca Mountain Area forms part of the Mojave Desert, characterised by hot, dry summers and warm, dry winters. The northern sector, however, belongs to what has been called the Transition Desert, and here the climate is a mixture of the Mojave Desert climate and the Great Basin Desert climate, the latter being characterised by warm, dry summers and cold, dry winters.

Precipitation in the region is influenced by two distinct storm patterns, one occurring in the winter and the other in the summer. Winter precipitation (dominantly snow in the mountains and rain in the valleys) tends to be of low intensity and long duration, and covers great areas. In contrast, most summer rains (resulting from local convective thunderstorms), are of high intensity and short duration (Hales 1972, 1974).

The soils and vegetation are controlled to a substantial degree by climatic, geomorphic, and hydrologic factors, and are highly variable and complex. Soils in the Yucca Mountain area typically include soils weathered from bedrock on the mountains, medium- to coarse-textured soils on alluvial fans and terraces, and fine-grained, alluvial soils on the valley floors. In general, the soils of the mountains and hills are thin and coarse textured, with little moisture-holding capacity. The soils of the alluvial fans on the upper bajadas also are coarse textured but are thicker, so that infiltration rates are relatively high. Infiltration rates of the alluvial basin soils are low because the downward movement of water is frequently impeded by calcium carbonate-cemented layers (pedogenic carbonate), fine-grained playa deposits and, less commonly, silicified hardpans that form within the soils over time (Beatley 1976).

1.2 Geology and hydrogeology

The current tectonic setting of Yucca Mountain is a result of extensional tectonism and magmatism active during the middle and late Cainozoic Era. Three regional tectonic domains characterise the tectonic setting within 100 km of Yucca Mountain (Stuckless and Dudley 2002, Sweetkind et al. 2004) (Figure 1-2): the Walker Lane Domain, which includes the site; the Basin and Range Domain to the northeast and the Inyo-Mono Domain to the southwest. These domains represent structurally bounded blocks of crust, each characterised by a deformation history that differs substantially from adjacent domains. Most of the area shown in Figure 1-1 belongs to the Walker Lane Domain.

The northwest-trending *Walker Lane Domain* (Stewart 1988, Stewart and Crowell 1992) is a complex structural zone that is dominated by large right-lateral faults with northwest orientations, such as the Pahrump-Stewart Valley fault zone and the Las Vegas Valley shear zone. It has been subdivided into three structural blocks according to their style of deformation (Stewart 1988, Stewart and Crowell 1992): (i) the Goldfield block occupying the north-western part and notable for its lack of full-penetration strike-slip faults and relative lack of normal faults; (ii) the Spotted Range-Mine Mountain block characterised by east-northeast-trending, left-lateral strike-slip faults, such as the Rock Valley fault zone and the Cane Spring and Mine Mountain faults; (iii) the Spring Mountains block, which is a relatively intact block that is bounded by the Pahrump-Stewart Valley fault zone and the Las Vegas Valley shear zone.

Most of the deformation in the Walker Lane belt may have occurred during Middle Miocene time (Hardyman and Oldow 1991, Dilles and Gans 1995), although deformation in the vicinity of Death Valley continued into Late Miocene time (Wright et al. 1999, Snow and Wernicke 2000). Some structures in the belt, such as the Rock Valley fault zone, continue to be active (Rogers et al. 1987, von Seggern and Brune 2000).

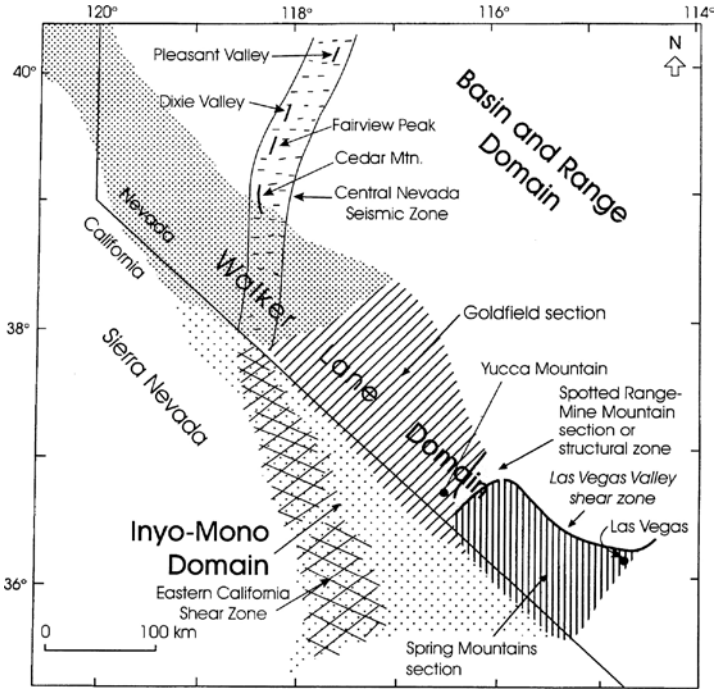

Figure 1-2. *Regional tectonic domains for Yucca Mountain including subsections of the Walker Lake Domain (after Stewart 1988; taken from Stuckless and Dudley 2002).*

More locally, the Yucca Mountain site (Goldfield block of the Walker Lane Domain, see Figure 1-2) consists of a series of fault-bounded blocks of ash-flow and ash-fall tuffs and a smaller volume of lava deposited between 14 and 11 Ma from a series of calderas located a few to several tens of kilometres to the north (Sawyer et al. 1994). Yucca Mountain itself extends southwards from the Pinnacles Ridge toward the Amargosa Desert, where the tuffs thin and pinch out beneath the basin-fill deposits. The tuffs dip 5 to 10 degrees to the east over most of Yucca Mountain. The Solitario Canyon Fault (Figure 1-3) separates Yucca Mountain from Crater Flat. Underlying Crater Flat are thick sequences of alluvial deposits, lavas and tuffs that have been locally cut by faults and volcanic dikes. East of Yucca Mountain, and separated from it by Fortymile Wash, is Jackass Flats, which is underlain by a thick sequence of alluvium and volcanic rocks. Timber Mountain, approximately 25 km to the north of the repository area, is a resurgent dome within the larger caldera complex that erupted the tuffs at Yucca Mountain.

Hydrogeologically, the Yucca Mountain area belongs to the Death Valley regional groundwater flow system (DVRFS), an extensive flow system of approximately 100,000 km^2. Ground water in this region is influenced by a combination of topography, climate and geology (Figure 1-3). Ground water moves through permeable zones under the influence of hydraulic gradients from areas of recharge in the mountains of central and southern Nevada to areas of discharge south and west of the Nevada Test Site and in Death Valley, California. This movement can be discussed in terms of local, intermediate and regional flow systems (D'Agnese et al. 1997). The first two systems are relatively shallow and water flow is restricted to individual basins. The regional flow system is deeper and water flows from one basin to another. Regional groundwater flow is mainly in the thick Palaeozoic carbonate rocks through faults and fractures, whereas intermediate and local flow is in the Cainozoic volcanics (through fractures) and Quaternary basin-fill deposits (porous flow).

The important hydrostratigraphic elements of the area around Yucca Mountain can be grouped into a series of aquifers separated by confining units (Figure 1-4). The groundwaters in the study area belong to three principal aquifers: the Palaeozoic Carbonate Aquifer, the Tertiary Tuffs Aquifer and the Quaternary Basin-fill Aquifer (Figure 1-5). The water table is very deep beneath the upland areas such as Yucca Mountain, where it is 500–750 m below the land surface (Stuckless and Dudley 2002). This means that there is a thick and potentially important non-saturated zone between the surface and the water table where pore waters and perched groundwaters are found. A more detailed description is given below of the three aquifers and their main subdivisions as presented in Figure 1-4.

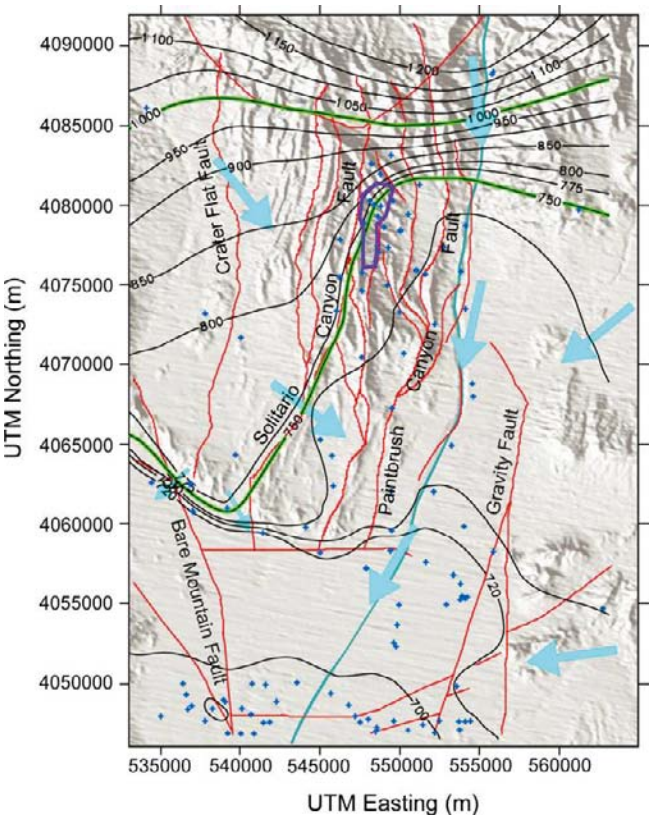

Figure 1-3. *Major faults, potentiometric surface and inferred flow directions in the Yucca Mountain area. The red lines are selected faults and the blue crosses indicate the location of hydraulic head measurements. The potentiometric surface is in black (with head in metres asl) and inferred flow directions are indicated with blue arrows. The outline (purple) of the proposed repository is included (from CRWMS M&O 2007).*

The oldest rocks that have some bearing on the saturated-zone groundwater flow belong to the *Proterozoic confining unit*, and are mainly Precambrian metasedimentary assemblages which grade upsection into Cambrian siliciclastic strata.

Resting on this confining unit is the *Lower Carbonate Aquifer*, the deepest and regionally most important aquifer. It has a thickness of several kilometres and is composed principally of Cambrian to Devonian dolomites and limestones, extending from central Utah to eastern California. The carbonate aquifer has negligible matrix permeability and derives its transmissivity from fractures. Just east of Yucca Mountain the aquifer was intersected by borehole UE-25 p#l at a depth of 1,244 m. At this location, the carbonate aquifer is hydrologically isolated from the overlying Tertiary units as indicated by an increase in hydraulic head of approximately 20 m at the contact (Stuckless and Dudley 2002).

Regionally, rocks from the Mississippian are fine clastic in origin, mainly argillites and shales (Eleana Formation) and behave as a confining unit (*Upper Clastic Confining Unit*). The regional extent of this unit is smaller than previous Palaeozoic units and it has not been intersected by boreholes near the Yucca Mountain site. However, it extends into the Nevada Test Site. In certain places, this confining unit is overlain by another Palaeozoic carbonate aquifer, the Upper Carbonate Aquifer, which is of much less importance for the regional groundwater flow than the Lower Carbonate Aquifer.

Mesozoic rocks do not play an important role in the hydrogeology of the Yucca Mountain area, and are absent from the bounding box in Figure 1-1. The nearest outcrops are at the Spring Mountains near Las Vegas (Belcher et al. 2002). When present, they can act as an aquifer or as a confining unit, depending on their fracture density.

The Cainozoic (Miocene) saturated volcanic units at and around Yucca Mountain have been grouped into two confining layers and two aquifers depending on the welded/non-welded character of the tuffs (Figure 1-4). In the Yucca Mountain region, north- to northeast-striking faults are more likely

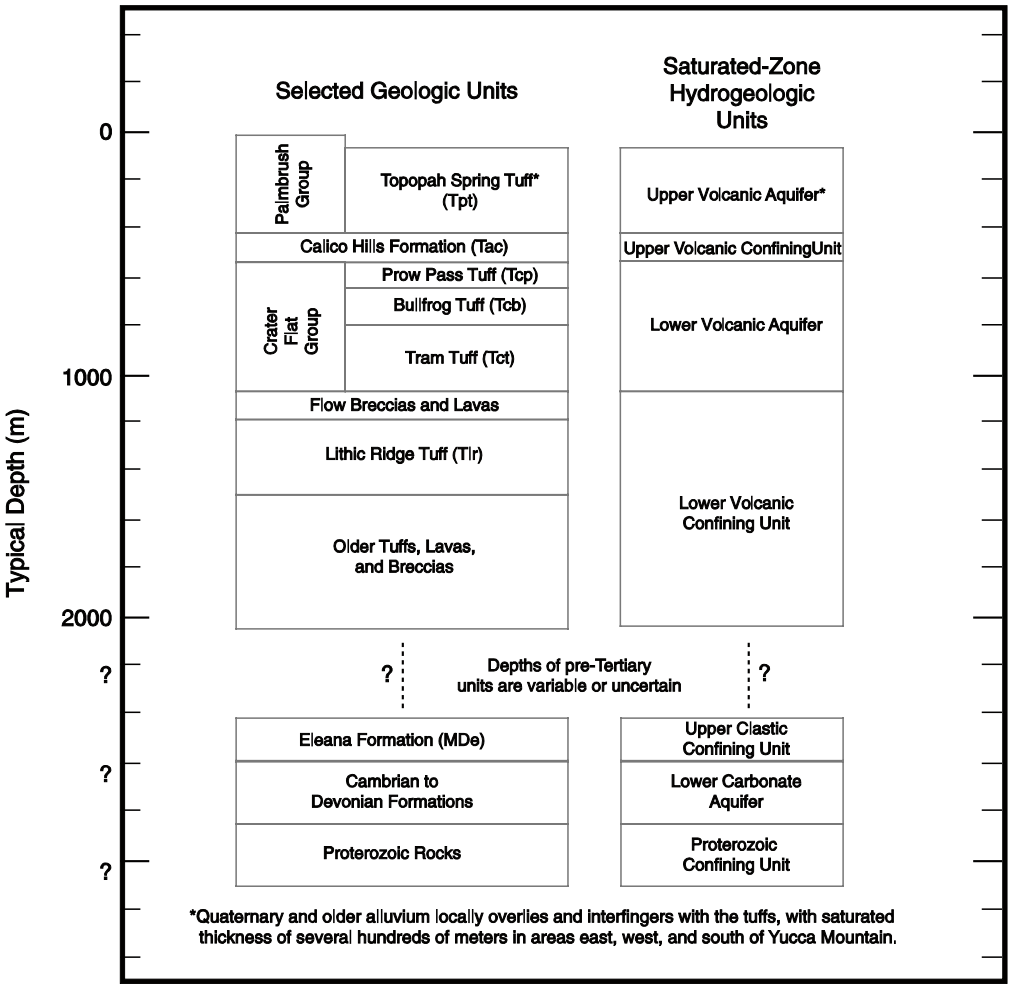

Figure 1-4. *Major saturated zone hydrogeologic and geologic units (Eddebbarh et al. 2003).*

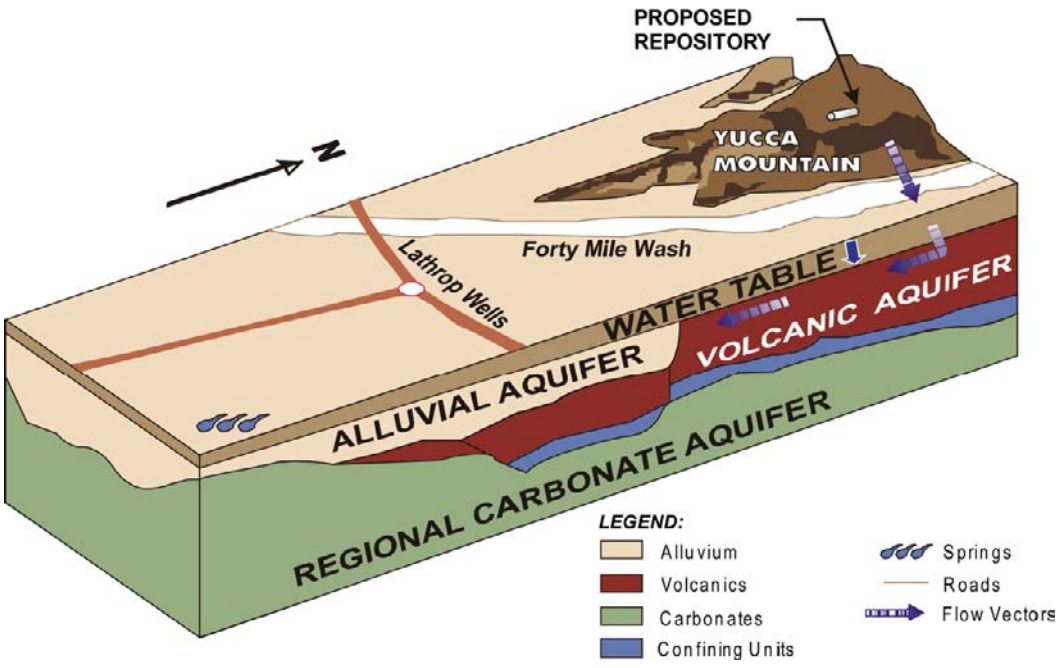

Figure 1-5. *Simplified 3D view of the main aquifers south of Yucca Mountain (courtesy of Drew Coleman and Zell Peterman).*

than those of other orientations to be permeable because they are approximately perpendicular to the least principal stress. These faults are favourably oriented for the transport of water from the highlands in the north (Timber Mountain, Pahute Mesa) to areas of discharge in the lower basins in the south (Amargosa Desert) and southwest (Death Valley), where it is consumed by evapotranspiration (Figure 1-6). Mineralogical alteration of the volcanic rocks (zeolitization) is more intense at depth, where it greatly diminishes rock permeability. Therefore, the deeper volcanic rocks generally impede groundwater flow and confine the underlying Palaeozoic carbonate aquifer where the Upper Clastic Confining Unit is not present (Stuckless and Dudley 2002).

As described by (Luckey et al. 1996), the Tertiary volcanic section at Yucca Mountain consists of a series of ash flow and bedded ash fall tuffs that contain minor amounts of lava and flow breccia. Ash flow tuffs range from non-welded to densely welded, and the degree of welding varies both horizontally and vertically in a single flow unit. Non-welded ash flow tuffs, when unaltered, have moderate to low matrix permeability but high porosity. Permeability is decreased by secondary alteration, and fractures are infrequent and often closed in the low-strength non-welded tuffs. Consequently, these rocks generally constitute laterally extensive confining units in the Yucca Mountain area. This is so in the case of the Calico Hills Formation, which constitutes the *Upper Volcanic Confining Unit*, and also of parts of the *Lower Volcanic Confining Unit*, a heterogeneous unit consisting of older tuffs, lavas and breccias.

The densely welded tuffs generally have minimal primary porosity and water-storage capacity, but they can be highly fractured. Where interconnected, fractures can easily transmit water, and highly fractured units function as aquifers, as is the case with the Topopah Spring Tuff (*Upper Volcanic Aquifer*) and the tuffs that form the Crater Flat Group (*Lower Volcanic Aquifer*). Together, the upper and lower volcanic aquifers form the Tertiary Tuffs Aquifer as used in this report.

Consolidated Cainozoic basin-fill units in the region range from late Eocene to Pliocene in age. They consist of a broad range of both volcanic and sedimentary rocks including lavas, welded and non-welded tuffs, and alluvial, fluvial, colluvial, aeolian, paludal, and lacustrine sediments. Together with the unconsolidated Cainozoic (mainly Pliocene to Holocene) basin-fill sediments (coarse-grained alluvial and colluvial deposits, fine-grained basin axis deposits, and local lacustrine limestones and spring discharge deposits), which constitute a regional unconfined aquifer, referred to in this report as the Quaternary Basin-fill Aquifer (although not all of its units are Quaternary).

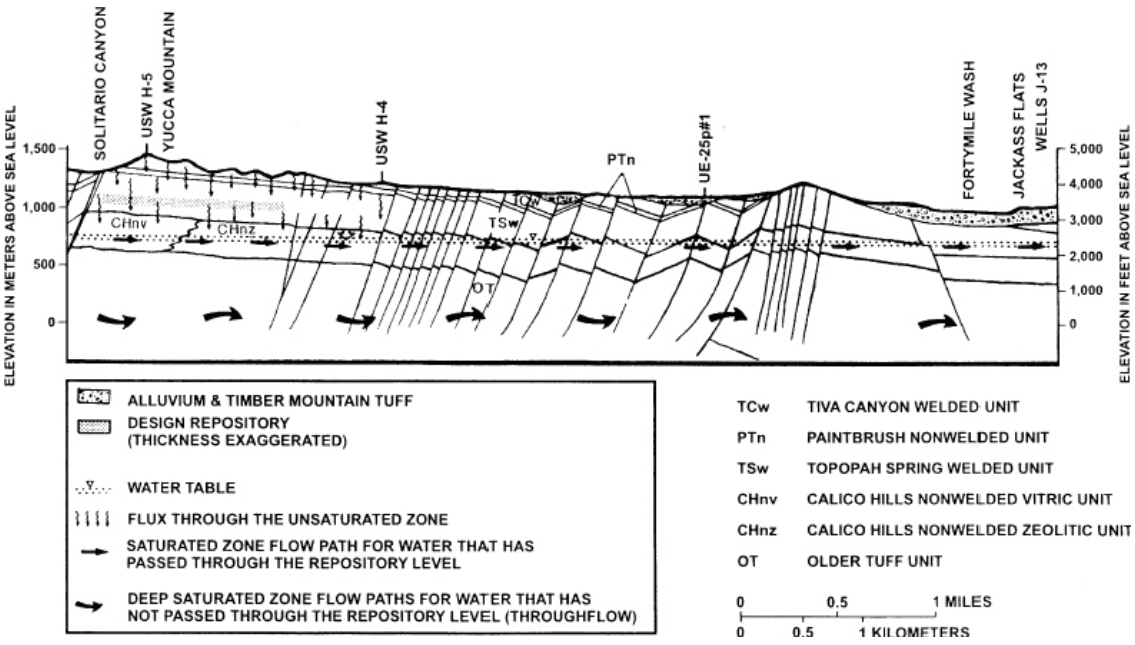

Figure 1-6. *Conceptual hydrogeologic cross-section through Yucca Mountain in a northwest to southeast direction showing the principal hydrostratigraphic units and the main boreholes (Stuckless and Dudley 2002).*

2 Analysis of hydrogeochemical data

2.1 Methodology

As the main objective of this work is assessing the importance of mixing in the chemistry of the groundwaters south of Yucca Mountain, the methodology has been tailored to this end. The procedure can be summarised as follows:

1. Start with the whole dataset (which will be referred to as the "raw dataset").
2. Perform a system-wide explorative analysis with the raw dataset in order to discriminate between conservative and non-conservative behaviour for specific elements.
3. Identify outliers in the raw dataset by means of ion-ion plots and Principal Component Analysis. These outliers are removed from the raw dataset (the focus of the work is on the general behaviour and trends in the chemistry of the different water types, and not on the peculiarities of specific samples).
4. Analyse the excluded samples one by one with PHREEQC (Parkhurst and Appelo 1999) to evaluate why they are special (i.e. which processes, natural or otherwise, have contributed to their "outlierness").
5. Perform an explorative analysis hydrofacies by hydrofacies (ion-ion plots and PCA) to locate samples where mixing is clearly not the principal process controlling their chemistry. These samples, affected by evaporation, water-rock interaction, or cation exchange (PHREEQC simulations are used to corroborate this) are also excluded from the raw dataset.
6. Identify end-member waters in the hydrofacies-by-hydrofacies exploratory analysis.
7. The above screening procedure results in a dataset in which all samples that may be suspected of having been affected drastically by non-mixing modifications of their chemistry have been excluded. This dataset is referred to as the "final dataset".
8. Use the end-member waters selected in (6) to calculate mixing proportions and deviations from the ideal (mixing-only) chemical composition. This step is carried out with the multivariate mixing and mass balance code M3 (Laaksoharju et al. 1999, Gómez et al. 2006, 2009).

The calculated mixing proportions for each sample are used to delineate the plausible mixing events and paths between the three main aquifer systems south of Yucca Mountain.

2.2 Hydrofacies, water types and water categories

The raw dataset consists of 397 water samples, of which 254 are groundwater samples, 6 are perched water samples, 81 are pore water samples, 17 are surface water samples, and 39 are precipitation samples. The data are summarised here for each sample location of the raw dataset in Tables 2-1 (location), 2-2 (major ions) and 2-3 (isotopes, minor ions and trace elements). Where multiple sets of data were available for a sampling point, the values have been averaged to derive the value shown in the table. The column headed "Sample-specific comments" in Table 2-1 shows this information for all the samples affected. Because the data collected in the table come from multiple sources, organisations and methods, and were collected over a time span of more than 20 years, the analytical precision and accuracy vary for different chemical analyses. As a rough estimate of the analytical accuracy, the following values can be used for recent measurements (CRWMS M&O 2007):

- ±10% for major anions, cations and strontium concentration, except for fluoride (±15%). In some cases strontium was determined by isotopic dilution mass spectrometry, for which data *eller* the data from which are more accurate (±0.5%),
- ±3 ‰ for $\delta^{2}H$, ±0.2 ‰ for $\delta^{18}O$, $\delta^{13}C$, and $\delta^{34}S$, and ±0.1 pmC for ^{14}C,
- Better than 1% for U and from 0.09% to 4.5% (mean of 0.73%) for $^{234}U/^{238}U$,
- $\pm 1 \cdot 10^{-5}$ for $^{87}Sr/^{86}Sr$ and ±0.01 ‰ for $\delta^{87}Sr$.

An additional guide to the reliability of individual water analyses is also provided by the calculated charge-balance errors listed in Table 2-2. Groundwaters from most sites used in this analysis have charge-balance errors of less than ±5% (85% of the samples), the remainder being mostly in the range ±5% to ±15%. When no charge balance is given for a sample (8 cases), it is because some of the ions used to compute the charge balance (usually nitrate and/or phosphate) are below the detection limit.

Table 2-1. Summary of water samples.

Sample ID	Local Name	USGS_SiteID	Facies	Sample Type[1]	UTM-x	UTM-y	Sample-specific comments
2	Grapevine Springs	YMP0350	Ash Meadows	sp	562,403.1	4,020,635.8	
3	Last Chance Spring	362120116162201	Ash Meadows	sp	565,249.4	4,023,430	Integrated major ion and isotope samples
4	Bole Spring	362145116161301	Ash Meadows	sp	565,467.9	4,024,201.9	Average of 3 samples
5	Big Spring	362230116162001	Ash Meadows	sp	565,158.7	4,025,555.4	Average of 10 samples
17	Jack Rabbit Spring	362405116161305	Ash Meadows	sp	564,823.9	4,027,001.1	Average of 2 major ion and 2 isotope samples; Rec #3829 and rec #3823 excluded from average
18	Indian Rock Spring	362343116160802	Ash Meadows	sp	565,565.0	4,027,838.6	
19	Well #3	362358116160101	Ash Meadows	gw	565,961.5	4,028,119	
20	East of Point of Rock Springs	YMP0367	Ash Meadows	gw	565,986.4	4,028,119.2	
21	King Pool	362407116162401	Ash Meadows	sp	565,362.5	4,028,268.5	Average of 2 samples
22	Well #2	362409116155601	Ash Meadows	gw	565,636.5	4,028,270.6	Average of 2 samples
23	18S/51E–7cbc	YMP0369	Ash Meadows	sp	564,938.8	4,028,296.1	
24	18S/51E–07dac	YMP0370	Ash Meadows	sp	565,635.8	4,028,363	
25	WELL 18S/51E–07db Ash Meadows	YMP0371	Ash Meadows	gw	565,560.3	4,028,454.9	
26	Well #4	362358116163301	Ash Meadows	gw	565,012.1	4,028,481.6	
27	Many Springs	YMP0372	Ash Meadows	sp	565,335.7	4,028,514.8	
28	Point of Rocks (King)	362410116161002	Ash Meadows	sp	565,410.4	4,028,515.4	Average of 4 samples; C-14 values were 1.7 and 11.1 PMC
29	Well #1	362410116160901	Ash Meadows	gw	565,958.4	4,028,519.5	
31	Point of Rocks (Small)	362410116161001	Ash Meadows	sp	565,508.9	4,028,670.2	Average of 2 samples
32	18S/50E–7aa	YMP0374	Ash Meadows	gw	556,040.0	4,029,158	
33	GMC (King) Spring	YMP0375	Ash Meadows	sp	555,840.4	4,029,219	Sr isotope data is average of 2 samples
34	18S/49E–11bbb	YMP0377	Ash Meadows	gw	551,306.8	4,029,283	
35	Well #5	362432116165701	Ash Meadows	gw	564,333.1	4,029,339.3	Average of 2 samples
36	Tenneco Well #3	362451116254100	Ash Meadows	gw	551,278.6	4,029,838	
37	Mom’s Place	362444116251001	Ash Meadows	gw	552,050.5	4,029,873	Average of 2 samples
38	18S/50E–6dac	YMP0380	Ash Meadows	gw	556,034.8	4,029,959	
39	Tenneco Well #2	362459116251000	Ash Meadows	gw	552,049.2	4,030,089	
40	Ash Meadows Ranger Station	YMP0942	Ash Meadows	gw	559,643.3	4,030,384	
41	Crystal Pool	362502116192301	Ash Meadows	sp	560,588.3	4,030,575.6	Average of 8 major ion and 9 isotope samples
43	Franklin Well	YMP0386	Ash Meadows	gw	548,234.0	4,030,929	
44	Tennaco	YMP0388	Ash Meadows	gw	553,164.0	4,031,051	

Sample ID	Local Name	USGS_SiteID	Facies	Sample Type[1]	UTM-x	UTM-y	Sample-specific comments
45	Spring (18S/49E–1aba)	YMP0387	Ash Meadows	sp	554,035.5	4,031,056	
46	230 S17 E51 31DDD 1 Unknown	362529116155801	Ash Meadows	gw	565,789.3	4,031,106.6	
47	Guerdon Industries Well #10	362529116171100	Ash Meadows	gw	563,871.6	4,031,123	Average of 2 samples
48	Devil's Hole	362532116172700	Ash Meadows	sp	563,572.4	4,031,182.4	Average of 13 major ion and 4 isotope samples
49	Ash Tree Spring	362535116244200	Ash Meadows	gw	552,739.7	4,031,202	Average of 3 samples
51	Garners Well	362555116205301	Ash Meadows	gw	558,437.9	4,031,855	Rec #3963 excluded; high TDS possibly contaminated
52	Scruggs Spring	362601116182800	Ash Meadows	sp	561,997.6	4,032,003	Integrated major ion and isotope samples; C-14 values were 1.1 and 2.6 and 14.7 PMC
56	Well 10	362627116213501	Ash Meadows	gw	557,631.5	4,033,298	
58	IMV#1	YMP0402	Amargosa River	gw	547,348.8	4,033,420	
59	IMV#2	362648116274601	Amargosa River	gw	548,145.4	4,033,425	Average of 3 samples
63	230 027N004E27D01S	362715116322301	Amargosa River	gw	541,245.7	4,034,221	
81	230 S17 E50 23B 1 Five Springs Area	362723116184101	Ash Meadows	sp	561,052.2	4,035,416.5	Average of 2 major ion and 2 isotope samples
82	Five Springs Well	362755116190401	Ash Meadows	gw	561,125.8	4,035,571.1	Average of 7 major ion and 2 isotope samples
84	17S/50E–19aab	362505116223001	Ash Meadows	gw	555,773.3	4,035,751	
85	Longstreet Spring	362751116192701	Ash Meadows	sp	560,427.1	4,035,812.7	Average of 2 samples and integrated major ion and isotope samples; C-14 values were 2.7 and 8.0 PMC
86	Purgatory Spring Well	362822116193801	Ash Meadows	gw	561,344.5	4,036,312.2	
88	Gilgans South Well	362835116264101	Eastern Amargosa	gw	549,744.6	4,036,731	Average of 5 samples
89	230 S17 E49 15BBD 1 Unknown	362839116263700	Eastern Amargosa	gw	549,843.4	4,036,854	
90	17S/50-15aca	362840116193701	Ash Meadows	gw	560,568.5	4,036,953.8	
92	Rogers Spring	362835116192101	Ash Meadows	sp	560,417.9	4,037,137.6	Integrated major ion and isotope samples; C-14 values were 1.5 and 12.1 PMC
93	Soda Ash Spring	362848116195901	Ash Meadows	sp	559,745.6	4,037,194.6	
94	Well 8	362858116195301	Ash Meadows	gw	559,968.0	4,037,411.8	
95	230 S17 E49 08DDB 1 Unknown	362904116280800	Fortymile Wash	gw	547,574.7	4,037,612	
96	Crane Domestic	YMP0424	Amargosa River	gw	543,591.8	4,037,930	
97	Lyle Records Well #2	362920116311000	Amargosa River	gw	543,043.6	4,038,081	
99	Fairbanks Spring	362924116203001	Ash Meadows	sp	559,015.9	4,038,361	Average of 13 samples; Rec #4079 (partial analysis) excluded
101	Mecca Club	362936116251500	Eastern Amargosa	gw	551,873.4	4,038,623	Average of 2 samples

Sample ID	Local Name	USGS_SiteID	Facies	Sample Type[1]	UTM-x	UTM-y	Sample-specific comments
102	Lyle Records Well	362938116300100	Fortymile Wash	gw	544,757.5	4,038,645	
103	AF Playa	362936116153001	Ash Meadows	gw	566,428.0	4,038,722.5	
104	Bill Copeland Well	362940116265800	Eastern Amargosa	gw	549,310.1	4,038,731	
105	Ponderosa Dairy #1	YMP0429	Eastern Amargosa	gw	549,384.7	4,038,731	
106	Ponderosa Dairy #1	YMP0429	Eastern Amargosa	gw	549,384.7	4,038,731	
107	Amargosa Motel (B)	YMP0432	Eastern Amargosa	gw	551,722.1	4,038,961	
116	230 S17 E48 01AB 2 Unknown	363028116302500	Fortymile Wash	gw	544,152.5	4,040,182	
117	Amargosa Estates #2	YMP0448	Fortymile Wash	gw	544,624.0	4,040,400	
120	16S/48E–36dcc	363044116303601	Amargosa River	gw	543,528.2	4,040,672	
121	16S/48E–36dcc	363044116303601	Amargosa River	gw	543,528.2	4,040,672	
122	Bray Domestic	YMP0451	Fortymile Wash	gw	546,662.2	4,040,688	
123	Oettinger Well	YMP0455	Eastern Amargosa	gw	551,685.2	4,040,963	
124	Good's Well	YMP0458	Eastern Amargosa	gw	551,980.3	4,041,520	
125	16S/48E–36a	YMP0459	Fortymile Wash	gw	543,721.8	4,041,720	
126	Mill's Well	YMP0460	Eastern Amargosa	gw	553,222.0	4,041,836	
127	Payton Domestic	YMP0463	Eastern Amargosa	gw	553,121.5	4,041,989	
128	Betty Smith Well	363128116302400	Fortymile Wash	gw	544,167.9	4,042,031	
129	Bradshaw's Well	363109116253101	Eastern Amargosa	gw	551,454.7	4,042,071	16S/49-35ba in Buqo
130	Mathew's Well	363132116240000	Eastern Amargosa	gw	553,717.1	4,042,208	Integrated major ion and isotope samples; major ion data from rec 4155 excluded (inconsistent K value)
131	Funeral Mountain Ranch Irrigation	YMP0486	Fortymile Wash	gw	541,376.3	4,043,311	
133	Anvil Ranch Irrigation	363205116271801	Fortymile Wash	gw	548,785.1	4,043,566	
136	Jacob's #1	363219116302400	Fortymile Wash	gw	544,159.9	4,043,602	
137	DeLee Large Irrigation	363203116295801	Fortymile Wash	gw	544,806.4	4,043,606	
138	16S/48E–23da	YMP0495	Fortymile Wash	gw	542,390.7	4,044,364	
139	Jacob's #2	363249116291900	Fortymile Wash	gw	545,771.2	4,044,535	
140	Rancho Amargosa Well	363252116323000	Fortymile Wash	gw	541,022.0	4,044,604	
141	Fox Well	YMP0903	Fortymile Wash	gw	542,414.0	4,044,672	
142	230 S16 E48 23AA 1	363244116320701	Fortymile Wash	gw	541,318.9	4,044,913	
143	Ohataz Well	YMP0497	Amargosa River	gw	536,122.0	4,045,105	
144	T&T Ranch	363313116302500	Fortymile Wash	gw	544,126.5	4,045,266	
145	Thiede's Well	YMP0498	Fortymile Wash	gw	547,432.9	4,045,284	
146	Albitre Well	363320116280900	Fortymile Wash	gw	547,506.3	4,045,500	

Sample ID	Local Name	USGS_SiteID	Facies	Sample Type[1]	UTM-x	UTM-y	Sample-specific comments
147	230 S16 E49 18DC 1 Unknown	363323116294400	Fortymile Wash	gw	545,144.1	4,045,579	
148	Ouimet's Well	YMP0500	Amargosa River	gw	536,045.4	4,045,598	
149	Tharpe's Well	YMP0502	Amargosa River	gw	534,826.7	4,045,747	
150	Spear's Well	363332116323501	Fortymile Wash	gw	540,519.0	4,045,834	
152	16S/48E–15ba	YMP0506	Amargosa River	gw	539,669.8	4,046,693	
153	230 S16 E48 17ABBB1	363342116345401	Amargosa River	gw	537,035.0	4,046,712	
154	Schoolhouse Well	YMP0505	Eastern Amargosa	gw	550,407.8	4,046,718	
155	230 S16 E48 15AA 1	363342116325101	Fortymile Wash	gw	540,787.8	4,046,821	
156	Selbach Domestic	363342116335701	Fortymile Wash	gw	539,147.2	4,046,844	
157	Nichol's Well	363405116324000	Fortymile Wash	gw	540,762.8	4,046,852	
158	Lowe Domestic	YMP0509	Eastern Amargosa	gw	552,121.2	4,047,005	
159	Amargosa Elementary School	363410116273500	Fortymile Wash	gw	548,342.9	4,047,045	
160	McCracken Domestic	YMP0511	Amargosa River	gw	537,381.5	4,047,052	
161	Sullivan Well	YMP0512	Amargosa River	gw	536,784.6	4,047,142	
162	K. Garey	363418116274200	Fortymile Wash	gw	548,167.5	4,047,291	
163	Perez Well	YMP0514	Eastern Amargosa	gw	553,833.9	4,047,386	
164	230 S16 E50 07C 1	363409116233701	Eastern Amargosa	gw	551,348.1	4,047,432	
165	Fox Well	363425116332000	Fortymile Wash	gw	539,765.7	4,047,463	
166	Cook's Well	363425116235000	Eastern Amargosa	gw	553,932.4	4,047,540	Average of 2 samples
167	Nelson Domestic	363428116240301	Eastern Amargosa	gw	553,608.7	4,047,631	
168	Cooks East Well	363428116234701	Eastern Amargosa	gw	554,006.4	4,047,633	
169	230 S16 E49 09CA 1	363415116275101	Fortymile Wash	gw	547,941.0	4,047,782	
170	Henderson's Well	YMP0519	Fortymile Wash	gw	546,723.1	4,047,806	
171	O'Neill Domestic	YMP0520	Fortymile Wash	gw	547,294.2	4,047,902	
172	Barrachman Dom/Irr	YMP0523	Amargosa River	gw	534,941.3	4,048,120	Average of 2 samples
173	Rose Well	YMP0524	Amargosa River	gw	534,841.7	4,048,181	
174	Finley's Well	YMP0526	Amargosa River	gw	534,791.2	4,048,366	
175	230 S16 E48 08BAAA1	363434116354001	Amargosa River	gw	536,654.9	4,048,405	
176	K. Finicial	363456116284100	Fortymile Wash	gw	546,694.7	4,048,453	
177	A. Sasse Well	363528116284200	Fortymile Wash	gw	546,664.5	4,049,439	
179	230 S15 E50 25BD 1 Nye County Land Company	363715116244500	Western Rock Valley	gw	549,538.0	4,052,639	

Sample ID	Local Name	USGS_SiteID	Facies	Sample Type[1]	UTM-x	UTM-y	Sample-specific comments
180	230 S15 E49 22DC 1 Unknown	363740116263900	Fortymile Wash	gw	549,697.3	4,053,524	
181	230 S15 E50 22 7 Unknown	363750116200000	Fortymile Wash	gw	549,672.3	4,053,554	
182	TW-5	363815116175901	Western Rock Valley	gw	562,604.5	4,054,686	
183	230 S15 E49 22AABA1	363742116263201	Fortymile Wash	gw	549,863.1	4,054,911	
184	Airport Well	363830116241401	Eastern Yucca Mountain	gw	552,818.2	4,054,929	Average of 4 samples
185	15S/50E–18cdc	YMP0537	Western Rock Valley	gw	553,934.3	4,055,151	
186	NDOT well	363835116234001	Western Rock Valley	gw	553,685.4	4,055,242	
187	NDOT-2 Well	363835116234002	Western Rock Valley	gw	553,685	4,055,242	
188	15S/50E–19b1	YMP0536	Western Rock Valley	gw	553,685.4	4,055,242	Average of 2 samples
189	15S/50E–18ccc	YMP0540	Western Rock Valley	gw	553,710.0	4,055,273	Average of 3 samples
190	Desert Farms Garlic Plot (DFGP)	YMP0541	Western Rock Valley	gw	553,287.7	4,055,301	
191	NC-EWDP-04PA	363925116241501	Western Rock Valley	gw	553,253.7	4,056,780	Average of 4 samples
192	NC-EWDP-04PB	363925116241401	Western Rock Valley	gw	553,278.5	4,056,780	Chemistry changing over time; keep separate
193	NC-EWDP-04PB	363925116241401	Western Rock Valley	gw	553,278.5	4,056,780	Chemistry changing over time; keep separate
194	NC-EWDP-04PB	363925116241401	Western Rock Valley	gw	553,278.5	4,056,780	Chemistry changing over time; keep separate
195	NC-EWDP-04PB	363925116241401	Western Rock Valley	gw	553,278.5	4,056,780	Chemistry changing over time; keep separate
196	NC-EWDP-04PB	363925116241401	Western Rock Valley	gw	553,278.5	4,056,780	Chemistry changing over time; keep separate
197	NC-EWDP-02D	363939116275401	Fortymile Wash	gw	547,814.1	4,057,180	bailed
198	NC-EWDP-Washburn-1X	363951116252402	Fortymile Wash	gw	551,544.5	4,057,569	
199	NC-EWDP-15P	364011116295001	Eastern Yucca Mountain	gw	544,929.2	4,058,150	Average of 2 samples
200	NC-EWDP-05SB	364011116223401	Western Rock Valley	gw	555,752.0	4,058,214	Chemistry changing over time; keep separate
201	NC-EWDP-05SB	364011116223401	Western Rock Valley	gw	555,752.0	4,058,214	Chemistry changing over time; keep separate
202	NC-EWDP-19D	364014116265301	Eastern Yucca Mountain	gw	549,322.3	4,058,267	Average of 3 samples; sample collected on 20031029 excluded from average
203	NC-EWDP-19D Zones 1–4	YMP0921	Eastern Yucca Mountain	gw	549,322.3	4,058,267	Average of 2 samples
204	NC-EWDP-19D Zone 1	YMP0922	Eastern Yucca Mountain	gw	549,322.3	4,058,267	
205	NC-EWDP-19D Zone 1	YMP0922	Eastern Yucca Mountain	gw	549,322.3	4,058,267	
206	NC-EWDP-19D Zone 1	YMP0922	Eastern Yucca Mountain	gw	549,322.3	4,058,267	

Sample ID	Local Name	USGS_SiteID	Facies	Sample Type[1]	UTM-x	UTM-y	Sample-specific comments
207	NC-EWDP-19D Zone 1	YMP0922	Eastern Yucca Mountain	gw	549,322.3	4,058,267	Collected at end of tracer test
208	NC-EWDP-19D Zone 2	YMP0923	Eastern Yucca Mountain	gw	549,322.3	4,058,267	Average of 2 samples
209	NC-EWDP-19D Zone 3	YMP0924	Eastern Yucca Mountain	gw	549,322.3	4,058,267	Average of 2 samples
210	NC-EWDP-19D Zone 4	YMP0925	Eastern Yucca Mountain	gw	549,322.3	4,058,267	Average of 2 samples
211	NC-EWDP-19D Zone 5–7	YMP0926	Eastern Yucca Mountain	gw	549,322.3	4,058,267	
212	NC-EWDP-19P	364015116265301	Eastern Yucca Mountain	gw	549,322.1	4,058,297	Average of 2 samples
213	NC-EWDP-19 IM-1	364015116265302	Eastern Yucca Mountain	gw	549,322.1	4,058,297	
214	NC-EWDP-19IM1 Zone 5	364015116265302	Eastern Yucca Mountain	gw	549,322.1	4,058,297	Average of 3 samples
215	NC-EWDP-19IM1 Zone 4	364015116265303	Eastern Yucca Mountain	gw	549,322.1	4,058,297	
216	NC-EWDP-19IM1 Zone 3	364015116265304	Eastern Yucca Mountain	gw	549,322.1	4,058,297	
217	NC-EWDP-19IM1 Zone 2	364015116265305	Eastern Yucca Mountain	gw	549,322.1	4,058,297	
218	NC-EWDP-19IM1 Zone 1	364015116265306	Eastern Yucca Mountain	gw	549,322.1	4,058,297	Average of 3 samples
219	NC-EWDP-19IM2	364015116265201	Eastern Yucca Mountain	gw	549,347.0	4,058,298	Average of 2 samples; sample collected on 20031028 excluded from average
220	NC-EWDP-19PB Zone 2	364014116264801	Eastern Yucca Mountain	gw	549,336.7	4,058,316	
221	NC-EWDP-19PB Zone 1	364014116264802	Eastern Yucca Mountain	gw	549,336.7	4,058,316	
224	NC-EWDP-03S Zone 3	364054116321302	Western Yucca Mountain	gw	541,348.3	4,059,457	Average of 3 samples; uranium concentration ranges from 4 ug/L to 18 ug/L
225	NC-EWDP-03S Zone 2	364054116321303	Western Yucca Mountain	gw	541,348.3	4,059,457	Average of 2 samples; sample colleced on 20031105 excluded from average because of contamination
226	NC-EWDP-03D	364054116321401	Western Yucca Mountain	gw	541,348.3	4,059,457	Average of 3 samples
227	NC-EWDP-29P	364057116265001	Eastern Yucca Mountain	gw	549,396.5	4,059,607	Average of 2 samples

Sample ID	Local Name	USGS_SiteID	Facies	Sample Type[1]	UTM-x	UTM-y	Sample-specific comments
228	Cind-R-Lite Well	364105116302601	Eastern Yucca Mountain	gw	544,026.9	4,059,840	
230	NC-EWDP-23P Zone 2	364105116234701	Western Rock Valley	gw	553,923.4	4,059,875	Chemistry changing over time; keep separate
231	NC-EWDP-23P Zone 2	364105116234701	Western Rock Valley	gw	553,923.4	4,059,875	Chemistry changing over time; keep separate
232	NC-EWDP-23P Zone 1	364105116234702	Western Rock Valley	gw	553,923.4	4,059,875	
233	NC-EWDP-12PA	364137116351001	Bare Mountains	gw	536,974.4	4,060,762	Average of 3 samples
234	NC-EWDP-12PB	364138116351101	Bare Mountains	gw	536,949.5	4,060,793	Average of 3 samples
235	NC-EWDP-12PC	364139116351101	Bare Mountains	gw	536,949.3	4,060,824	Average of 2 samples
236	NC-EWDP-09SX	364145116334401	South East Crater Flat	gw	539,107.4	4,061,018	Average of 4 samples
237	NC-EWDP-09SX Zone 4	364145116334402	South East Crater Flat	gw	539,107.4	4,061,018	Average of 4 samples
238	NC-EWDP-09SX Zone 3	364145116334403	South East Crater Flat	gw	539,107.4	4,061,018	Average of 4 samples
239	NC-EWDP-09SX Zone 2	364145116334404	South East Crater Flat	gw	539,107.4	4,061,018	Average of 4 samples
240	NC-EWDP-09SX Zone 1	364145116334405	South East Crater Flat	gw	539,107.4	4,061,018	Average of 4 samples
241	NC-EWDP-22S Zone 4	364215116250301	Fortymile Wash	gw	552,018.7	4,062,020	Average of 2 samples
242	NC-EWDP-22S Zone 3	364215116250302	Fortymile Wash	gw	552,018.7	4,062,020	Average of 2 samples
243	NC-EWDP-22S Zone 2	364215116250303	Fortymile Wash	gw	552,018.7	4,062,020	Average of 2 samples
244	NC-EWDP-22S Zone 1	364215116250304	Fortymile Wash	gw	552,018.7	4,062,020	Average of 2 samples
245	NC-EWDP-22PB Zone 2	364216116250303	Fortymile Wash	gw	552,037.7	4,062,037	
246	NC-EWDP-22PB Zone 1	364216116250304	Fortymile Wash	gw	552,037.7	4,062,037	
247	NC-EWDP-22PA Zone 2	364216116250301	Fortymile Wash	gw	552,020.1	4,062,038	Average of 2 samples
248	NC-EWDP-22PA Zone 1	364216116250302	Fortymile Wash	gw	552,020.1	4,062,038	Average of 2 samples
249	NC-EWDP-24P	364217116265001	Eastern Yucca Mountain	gw	549,385.6	4,062,056	Average of 2 samples
250	NC-EWDP-28P	364229116291601	Western Yucca Mountain	gw	545,745.6	4,062,393	
251	NC-EWDP-01DX Zone 2	364234116351502	Bare Mountains	gw	536,847.3	4,062,509	Sample from 19990524 excluded because of poor charge balance
252	NC-EWDP-01S	364233116351501	Bare Mountains	gw	536,842.8	4,062,518	
253	NC-EWDP-01S Zone 2	364233116351502	Bare Mountains	gw	536,842.8	4,062,518	
254	NC-EWDP-01S Zone 1	364233116351503	Bare Mountains	gw	536,842.8	4,062,518	

Sample ID	Local Name	USGS_SiteID	Facies	Sample Type[1]	UTM-x	UTM-y	Sample-specific comments
255	NC-EWDP-01DX	364234116351501	Bare Mountains	gw	536,842.8	4,062,518	Bailed
256	NC-EWDP-01DX Zone 2	364234116351502	Bare Mountains	gw	536,842.8	4,062,518	Sample from 19990524 excluded because of poor charge balance
258	NC-EWDP-16P	364329116291901	Western Yucca Mountain	gw	545,665.4	4,064,263	Sample from 20050920 excluded because of possible contamination from construction materials
259	NC-EWDP-7SC Zone 4	364332116332203	Bare Mountains	gw	539,631.9	4,064,317	
260	NC-EWDP-7SC Zone 3	364332116332204	Bare Mountains	gw	539,631.9	4,064,317	Average of 2 samples
261	NC-EWDP-7SC Zone 2	364332116332205	Bare Mountains	gw	539,631.9	4,064,317	Average of 2 samples
262	NC-EWDP-7SC Zone 1	364332116332206	Bare Mountains	gw	539,631.9	4,064,317	Average of 2 samples
263	NC-EWDP-7S	364332116332201	Bare Mountains	gw	539,638.1	4,064,317	
264	NC-EWDP-7SC	364332116332202	Bare Mountains	gw	539,638.1	4,064,317	
265	NC-EWDP-10S Zone 2	364349116241801	Fortymile Wash	gw	553,140.0	4,064,899	Average of 2 samples
266	NC-EWDP-10S Zone 1	364349116241802	Fortymile Wash	gw	553,140.0	4,064,899	Average of 2 samples
267	NC-EWDP-10P Zone 2	364349116241701	Fortymile Wash	gw	553,148.8	4,064,916	Average of 2 samples
268	NC-EWDP-10P Zone 1	364349116241702	Fortymile Wash	gw	553,148.8	4,064,916	Average of 2 samples
269	NC-EWDP-10S	YMP0941	Fortymile Wash	gw	553,128.5	4,064,945	
270	NC-EWDP-27P	364402116294801	Western Yucca Mountain	gw	544,935.2	4,065,275	Average of 2 samples
272	NC-EWDP-13P	YMP0943	South East Crater Flat	gw	543,471.2	4,066,433	
273	NC-EWDP-18P	364505116264701	Eastern Yucca Mountain	gw	549,415.5	4,067,233	Average of 2 samples
274	JF-3	364528116232201	Fortymile Wash	gw	554,498.3	4,067,974	
275	40-Mile Wash at J-12	364551116233700	Surface water	sw	554,121.9	4,068,680	
276	Well MR3	364556116413501	Amargosa River	gw	527,395.0	4,068,707	Average of 3 samples; C-14 value from 19890916 (1999 C-14 value excluded)
277	NECO Well #1	364600116413001	Amargosa River	gw	527,518.9	4,068,738	Average of 6 samples
278	MW315	364557116411801	Amargosa River	gw	527,816.4	4,068,739	
279	MW604	364557116411501	Amargosa River	gw	527,890.8	4,068,739	
280	MW311	364557116411401	Amargosa River	gw	527,915.6	4,068,739	
281	UE-25 J-12	364554116232401	Fortymile Wash	gw	554,443.6	4,068,775	Average of 8 major ion and 3 isotope samples; All samples collected before borehole deepened in 1968 excluded
282	MW 314	364600116412001	Amargosa River	gw	527,766.5	4,068,831	
283	U.S. Ecology-W001	364601116414101	Amargosa River	gw	527,245.8	4,068,860	
284	MW 316	364603116410801	Amargosa River	gw	528,063.7	4,068,924	

Sample ID	Local Name	USGS_SiteID	Facies	Sample Type[1]	UTM-x	UTM-y	Sample-specific comments
285	Precip Gauge, Waste Burial Site South of Beatty, Nv	364606116413101	Precipitation	me	527,493.2	4,069,015	
286	MW 313	364615116412401	Amargosa River	gw	527,665.8	4,069,293	Average of 2 samples
287	MW 600	364615116412402	Amargosa River	gw	527,665.8	4,069,293	Average of 2 samples
288	Precip Area 25	364652116172001	Precipitation	me	563,454.8	4,070,624	
289	UE-25 WT#12	364656116261601	Eastern Yucca Mountain	gw	550,168.1	4,070,659	Average of 7 major ion and 8 isotope samples
290	HRF Precipitation	364704116170302	Precipitation	me	563,873.4	4,070,997	
291	UE-25 J-11	364706116170601	Jackass Flat	gw	563,798.6	4,071,058	Average of 8 major ion and 4 isotope samples
293	USW VH-1	364732116330701	South East Crater Flat	gw	539,975.5	4,071,714	Average of 5 major ion and 4 isotope samples
294	Busted Butte Wash	364749116235100	Surface water	sw	553,751.9	4,072,314	
295	UE-25 WT#3	364757116245801	Eastern Yucca Mountain	gw	552,090.0	4,072,550	Average of 4 samples
296	USW VH-2	365821116343701	Bare Mountains	gw	537,738.3	4,073,214	Average of 5 major ion and 3 isotope samples
297	UE-25 WT #17	364822116262601	Eastern Yucca Mountain	gw	549,904.7	4,073,307	Average of 3 samples; three samples collected duiring early pumping excluded because of possible contamination
298	USW WT-10	364825116290501	Western Yucca Mountain	gw	545,964.3	4,073,378	Average of 2 samples
299	UE-25 J-13	364828116234001	Fortymile Wash	gw	554,016.7	4,073,548	Average of 9 major ion and 14 isotope samples
301	40-Mile Wash at Road H	364904116234700	Surface water	sw	553,836.4	4,074,625	
302	40-Mile Wash above Drill Hole Wash	364908116234600	Surface water	sw	553,860.4	4,074,749	
303	Drill Hole at Wash Mouth	364911116235200	Surface water	sw	553,711.2	4,074,840	
304	Drillhole Wash CSG	10251254	Surface water	sw	553,711	4,074,902	
305	UE-25 WT-7	364933116285701	Western Yucca Mountain	gw	546,151.2	4,075,474	
306	UE-25 p#1 (0–1200 m)	364938116252100	Western Yucca Mountain	gw	551,501.2	4,075,659	Thief sample
307	UE-25 p#1 (1,300–1,800 m)	364938116252102	Eastern Yucca Mountain	gw	551,501.2	4,075,659	For 6/15/98 sample, Sr concentration 0.0225ppm and 87Sr/86Sr was 0.70961
308	USW H-3 HTH	364942116280000	Western Yucca Mountain	gw	547,561.7	4,075,759	
309	UE-25 c#2 open	364947116254301	Eastern Yucca Mountain	gw	550,954.9	4,075,871	Values differ in (Claassen (1985) times may be incorrect
310	UE-25 c#2 Prow Pass	364947116254301	Eastern Yucca Mountain	gw	550,954.9	4,075,871	

Sample ID	Local Name	USGS_SiteID	Facies	Sample Type[1]	UTM-x	UTM-y	Sample-specific comments
311	UE-25 c#3 Bullfrog/Tram	364947116254501	Eastern Yucca Mountain	gw	550,930.0	4,075,902	Average of 9 major ion and 21 isotope samples; HCO_3 value of 175 and C-14 value of 73.02 PMC (rec#4977) excluded from average
312	UE-25 c#3 Prow Pass	364947116254501	Eastern Yucca Mountain	gw	550,930.0	4,075,902	
313	UE-25 c#1	364947116254300	Eastern Yucca Mountain	gw	550,954.6	4,075,933	Average of 3 samples
314	UE-25 c#3 open	364947116254302	Eastern Yucca Mountain	gw	550,954.6	4,075,933	
315	USW SD-7 Perched	YMP0556	Perched water	pw	548,375.0	4,076,503	Average of 4 major ion and 7 isotope samples; bailed sample (rec #7017) excluded from average
316	UE-25 ONC-1	YMP0557	Eastern Yucca Mountain	gw	550,479.9	4,076,608	bailed sample; For 3/16/95 sample, Sr concentration 3.3ppm and 87Sr/86Sr was 0.71015
317	USW H-4	365032116265401	Eastern Yucca Mountain	gw	549,187.8	4,077,309	
318	UE-25 WT#14	365032116243501	Eastern Yucca Mountain	gw	552,630.5	4,077,330	
319	USW SD-6 ST1	365040116275901	Western Yucca Mountain	gw	547,576.5	4,077,546	Average of 6 major ion and 10 isotope samples; bailed sample excluded from average
320	USW H-6 (525–1,220 m)	365049116285500	Western Yucca Mountain	gw	546,188.1	4,077,816	Average of 3 samples; C-14 values of 10.0 and 12.4 and 16.3 PMC
321	227A Split Wash below Quac Canyon Wash, NTS, NV	102512537	Surface water	sw	549,183.3	4,078,079	
324	UE-25 b#1	365108116262300	Eastern Yucca Mountain	gw	549,949.1	4,078,423	Average of rec #5075 and #5079; rec #5040 to #5074 excluded from average because of LiCl tracer
325	USW G-4	365114116270401	Eastern Yucca Mountain	gw	548,932.7	4,078,602	
326	UE-25 WT#15	365116116233801	Eastern Yucca Mountain	gw	554,033.6	4,078,694	
327	USW H-5	365122116275501	Western Yucca Mountain	gw	547,668.3	4,078,841	Average of 2 samples
329	227A Wren Wash at Yucca Mtn, NTS, NV	1025125356	Surface water	sw	548,656.7	4,079,217	
330	227A Wren Wash at Yucca Mtn, NTS, NV	1025125356	Surface water	sw	548,656.7	4,079,217	
331	227A Pagany Wash Number 1, NTS, NV	102512533	Surface water	sw	550,314.9	4,079,380	Rec #177 excluded (partial analysis)
332	USW H-1	365157116271201	Eastern Yucca Mountain	gw	548,727.0	4,079,926	Average of 2 samples

Sample ID	Local Name	USGS_SiteID	Facies	Sample Type[1]	UTM-x	UTM-y	Sample-specific comments
333	227A Yucca Wash nr Mouth, Nevada Test Site, NV	10251252	Surface water	sw	554,025.4	4,079,988	
334	227A Yucca Wash nr Mouth, Nevada Test Site, NV	10251252	Surface water	sw	554,025.4	4,079,988	
335	227A Yucca Wash nr Mouth, Nevada Test Site, NV	10251252	Surface water	sw	554,025.4	4,079,988	
336	Specie Spring	365207116393201	Perched water	sp	530,403.7	4,080,149	Average of 5 samples
337	USW UZ-14	365208116274001	Eastern Yucca Mountain	gw	548,031.8	4,080,261	Average of 2 samples; both samples bailed
338	USW UZ-14 Perched	365208116274001	Perched water	pw	548,031.8	4,080,261	Average of 2 major ion and 4 isotope samples; bailed samples and early pump samples excluded from average
340	USW WT-24 Saturated Zone	365301116271301	Eastern Yucca Mountain	gw	548,690.9	4,081,898	bailed sample
341	USW WT-24 Perched	365301116271301	Perched water	pw	548,690.9	4,081,898	Average of 2 samples Bailed samples (rec #5193 to rec #5199) excluded from average
343	Overland Flow in Fortymile Canyon	365320116231501	Surface water	sw	554,578.7	4,082,519	
344	USW G-2	365322116273501	Eastern Yucca Mountain	gw	548,142.7	4,082,542	Average of 5 major ion and 7 radioisotope samples
345	Cottonwood Spring	365353116233501	Perched water	sp	554,077.1	4,083,533	
350	ST3		Precipitation	me	565,435.804	4,085,318.96	
354	Topopah Spring	365620116160901	Perched water	sp	565,080.8	4,088,140	Two samples from 1950s excluded (rec #7074 and 7075)
355	ST2		Precipitation	me	566,766.554	4,088,188.01	
357	Overland Flow Near Pah Canyon	365627116223701	Surface water	sw	555,481.6	4,088,287	
359	UE-29 a #1	365629116222601	Fortymile Wash	gw	555,753.3	4,088,351	Integrated 1 major ion and 3 isotope samples; rec #5314 (poor charge balance) excluded from average
360	UE-29 a #2	365629116222602	Fortymile Wash	gw	555,753.3	4,088,351	Average of 3 samples
361	Pah Canyon Above Mouth	365634116221501	Surface water	sw	556,024.4	4,088,506	
363	ST1		Precipitation	me	565,880.739	4,088,794.35	
364	ST1		Precipitation	me	565,880.739	4,088,794.35	
426	RT3		Precipitation	me	563,189.256	4,109,018.47	
427	RT3		Precipitation	me	563,189.256	4,109,018.47	
428	227B Stockade Wash at Airport Road, NTS, NV	102512484	Surface water	sw	563,092.2	4,109,296	
443	RT2		Precipitation	me	569,484.623	4,112,544.89	
444	RT2		Precipitation	me	569,484.623	4,112,544.89	

[1] gw: groundwater; me: meteoric water (precipitation); pw: pore water; sp: groundwater from spring; sw: surface water.

Table 2-2. Chemical and physico-chemical composition of the samples used in this report: Major ions.

Sample ID	Facies[1]	Temp	Field pH[2]	FieldCond[2]	Charge Balance	Ca	Mg	Na	K	Cl	SO_4	HCO_3	NO_3	SiO_2
2	AM	15.50	8.75	4,910.00		7.60	15.000	1,200.00	69.00	330.00	1,100.00	1,246.80	< 0.20	18.00
3	AM		7.60		0.1	44.00	19.000	97.00	8.70	25.00	105.00	318.00		28.00
4	AM	21.63	7.55	838.00	–1.8	36.00	18.330	102.00	9.73	26.33	117.67	305.85	0.97	31.67
5	AM	28.70	7.43	778.57	–1.1	43.70	18.000	96.80	8.98	26.20	109.60	316.41	0.45	28.40
17	AM	28.00	7.30	742.00	–0.5	45.00	21.500	73.50	8.20	21.50	89.00	302.50	0.10	22.50
18	AM	33.50			–0.8	46.00	21.000	68.00	7.40	21.00	78.00	304.00	0.20	22.00
19	AM	29.50	8.30	1,000.00	5.6	59.00	30.000	130.00	9.10	76.00	230.00	183.00	5.60	24.00
20	AM	29.20	7.10	755.00	–0.5	43.00	21.000	72.00	7.70	21.00	83.00	296.46	0.53	23.00
21	AM	32.00			1.1	46.00	22.000	67.50	7.80	22.50	78.00	289.00	0.46	22.00
22	AM	26.60	7.50	3,400.00	–0.6	140.00	90.000	445.00	21.50	295.00	1,068.00	226.50	23.50	20.50
23	AM	28.30	7.40	680.00	1.3	52.00	20.000	69.00	8.40	23.00	79.00	298.00	1.20	23.00
24	AM		8.10	372.00	0.1	16.00	4.400	55.00	8.80	7.50	36.00	161.00	4.10	88.00
25	AM	31.00	7.10	720.00	–9.0	38.00	25.000	83.00	8.70	28.00	80.00	415.00	0.02	
26	AM	30.50	7.80	700.00	3.4	51.00	21.000	78.00	8.40	25.00	83.00	293.00	2.60	23.00
27	AM	31.00			9.5	45.00	20.000	69.00	8.20	21.00	74.00	223.00	0.20	22.00
28	AM	30.33	7.50	665.00	–0.6	49.00	20.250	67.25	7.53	21.75	78.25	303.70	0.30	21.75
29	AM	28.00			–1.1	60.00	36.000	170.00	11.00	95.00	330.00	263.00	7.10	23.00
31	AM	31.70	7.30	672.50	–0.6	49.00	20.000	67.00	7.70	21.00	78.00	305.00	0.20	22.50
32	AM	13.00	8.40		1.6	25.65	9.481	140.93	19.16	37.58	146.97	261.17		47.42
33	AM	20.00	7.50	1,370.00	–7.7	24.00	8.200	93.00	26.00	51.00	120.00	215.94	3.32	77.00
34	AM	25.00	7.56		3.6	34.00	8.600	99.00	11.60	31.00	90.00	221.00		78.30
35	AM	31.35	7.70	680.00	3.6	45.00	20.000	65.00	8.60	20.50	78.00	254.50	0.20	23.00
36	AM	24.00	7.40	730.00	–1.2	29.00	12.000	120.00	9.70	20.00	74.00	352.00	1.55	59.00
37	AM	23.00	7.81	534.00	–0.8	25.60	6.520	77.55	9.49	13.10	51.85	233.00	6.38	78.50
38	AM		8.22		3.2	24.00	12.000	103.00	14.00	21.00	107.00	230.00		80.00
39	AM	23.80	6.90	545.00	1.6	17.00	5.400	110.00	8.40	12.00	52.00	267.00	4.08	62.00
40	AM	23.30	7.40	712.00	–1.0	46.25	20.550	74.10	9.03	22.20	80.80	316.00	0.92	30.00
41	AM	30.87	7.32	708.44	–0.4	45.48	20.410	73.29	9.08	22.57	84.79	301.13	0.34	26.64
43	AM	12.80	8.00	4,740.00	10.6	64.00	54.000	1,020.00	68.00	150.00	530.00	1,690.00	1.10	125.00
44	AM	23.60	8.90	3,990.00	–2.0	1.30	1.000	940.00	10.00	250.00	700.00	1,236.00	19.00	11.00
45	AM	17.50	8.60	680.00	–1.8	24.00	12.000	95.00	19.00	18.00	100.00	263.00	–0.10	73.00
46	AM	25.50	8.20	718.00	1.5	30.00	12.000	120.00	6.20	19.00	90.00	313.00	0.70	22.00

Sample ID	Facies[1]	Temp	Field pH[2]	FieldCond[2]	Charge Balance	Ca	Mg	Na	K	Cl	SO_4	HCO_3	NO_3	SiO_2
47	AM	33.40	7.90	667.00	–1.1	46.00	20.000	69.50	8.35	20.00	84.00	300.50	0.20	23.50
48	AM	32.96	7.43	684.40	–0.3	49.74	21.420	67.75	7.86	22.43	80.67	306.72	0.72	22.74
49	AM	21.27	7.90	372.00	–2.5	15.00	4.470	52.00	8.23	6.77	37.33	157.00	5.75	79.33
51	AM	16.50	7.50	1,460.00		72.00	64.000	150.00	26.00	97.00	230.00	527.00	< 0.44	62.00
52	AM	35.00	8.00	668.00	0.4	46.00	22.000	68.00	8.40	21.00	76.00	302.00	0.00	25.00
56	AM	19.40	7.60	1,067.00	2.0	2.80	2.900	250.00	15.00	26.00	105.00	494.00	0.00	67.00
58	AR	21.00	7.60		3.9	54.00	15.000	160.00	15.90	70.00	187.00	271.00		71.90
59	AR	25.00	7.58	790.00	–0.8	45.17	10.180	102.33	11.67	28.90	92.17	299.00	10.95	70.97
63	AR	22.20	7.80	943.00	1.3	58.00	19.000	134.00	19.00	32.00	107.00	438.00	0.20	72.00
81	AM	34.15	7.31	600.00	0.9	46.50	20.500	70.00	7.95	20.50	81.00	289.50	0.25	22.00
82	AM	33.92	7.33	695.33	–1.5	45.71	20.000	67.71	8.09	22.29	81.86	296.86	0.22	21.86
84	AM	16.00	8.60		1.1	7.60	8.500	252.00	27.00	70.00	176.00	416.00		42.61
85	AM	27.20	7.43	600.00	–0.3	49.50	18.000	68.50	7.85	19.50	76.50	301.00	0.35	22.00
86	AM	34.50	7.30	670.00	–2.2	44.00	21.000	60.00	8.60	22.00	80.00	286.00	0.10	22.00
88	EA	24.20	8.03	308.58	–0.8	19.43	1.950	40.67	7.51	9.01	29.70	125.95	7.46	77.37
89	EA	22.50	8.10	321.00	–3.0	21.00	4.000	32.00	8.20	10.00	35.00	120.00	7.09	73.00
90	AM	19.40	7.60	665.00	–0.4	50.00	20.000	67.00	9.20	23.00	79.00	305.00	0.90	23.00
92	AM		7.60	677.00	0.2	47.00	21.000	69.00	7.80	21.00	78.00	302.00	0.00	23.00
93	AM		7.70	772.00	–0.9	36.00	17.000	106.00	10.00	27.00	93.00	330.00	0.00	35.00
94	AM	21.00			0.3	22.00	11.000	110.00	15.00	22.00	74.00	296.00	0.50	31.00
95	FmW	24.00	8.00	299.00	1.5	21.00	2.700	36.00	7.50	6.40	27.00	123.00	6.65	81.00
96	AR	26.30	7.19	1,120.00	–0.5	64.00	18.000	147.00	16.00	41.00	138.00	451.00	9.30	45.00
97	AR		7.70	1,290.00	–1.5	74.00	24.000	160.00	16.00	78.00	180.00	404.00	30.57	46.00
99	AM	27.72	7.33	690.00		47.13	20.100	69.31	7.97	21.40	81.45	302.33	< 0.20	22.04
101	EA	23.00	8.10	798.00	–0.6	34.50	14.000	103.50	15.00	27.00	150.00	232.50	0.37	48.00
102	FmW		8.00	363.00	–0.1	24.00	1.800	48.00	7.30	9.50	31.00	153.00	7.09	80.00
103	AM	16.50	8.25		–0.1	9.70	10.000	130.00	18.00	32.00	66.00	315.00	1.20	23.00
104	EA		7.90	422.00	–6.0	25.00	3.600	48.00	9.70	10.00	69.00	131.00	7.09	70.00
105	EA	28.30	7.98	507.00	–6.0	30.00	4.500	59.00	11.00	16.00	93.00	145.00	4.39	74.00
106	EA	27.0	8.00	457.00	–0.9	24.90	4.060	57.40	10.80	21.60	70.80	129.00	9.73	87.00
107	EA	24.00	7.60	852.00	–1.2	49.50	18.000	97.50	14.00	27.00	151.00	286.00	1.02	43.50
116	FmW	24.40	8.00	307.00	–1.9	19.00	1.500	40.00	7.10	6.30	25.00	135.00	6.65	79.00
117	FmW	24.00	8.09	296.00	1.3	20.00	2.100	38.00	6.80	6.50	22.00	134.00	7.93	79.00

Sample ID	Facies[1]	Temp	Field pH[2]	FieldCond[2]	Charge Balance	Ca	Mg	Na	K	Cl	SO_4	HCO_3	NO_3	SiO_2
120	AR		7.60	670.00	5.1	40.00	8.600	98.00	11.00	29.00	43.00	278.00	7.80	74.00
121	AR	26.00	7.20	830.00	–1.2	55.00	9.800	100.00	13.00	33.00	110.00	300.00	9.10	70.00
122	FmW	20.90	8.05	316.00	–1.1	22.00	1.800	35.00	8.80	7.90	25.00	131.00	7.48	74.00
123	EA	25.20	7.51	881.00	–2.1	50.00	16.000	103.00	15.00	29.00	157.00	291.00	1.59	39.00
124	EA		7.65		3.7	44.00	16.000	120.00	16.00	29.00	148.00	267.00		36.70
125	FmW	23.30	7.90	700.00	0.9	70.00	3.900	62.00	9.00	61.00	107.00	142.00	17.00	82.00
126	EA		7.65		1.4	45.00	20.000	110.00	16.60	24.00	156.00	288.00		42.80
127	EA	20.20	7.58	933.00	–1.4	51.00	19.000	107.00	16.00	41.00	155.00	290.00	6.15	36.00
128	FmW		7.90	301.00	–3.1	17.00	2.000	40.00	6.10	6.90	25.00	133.00	7.09	79.00
129	EA	24.40	7.41	796.00	0.9	53.00	18.000	113.00	13.00	31.00	170.00	278.50	0.50	37.50
130	EA		7.76		3.4	52.00	22.000	120.00	17.80	27.00	168.00	309.00		37.80
131	FmW	22.20	8.21	479.00	–3.1	12.00	2.400	80.00	7.00	12.00	43.00	200.00	6.59	87.00
133	FmW	20.50	7.92	681.00	–1.4	47.00	5.800	68.00	13.00	40.00	120.00	138.00	20.80	71.00
136	FmW		7.90	324.00	–2.3	19.00	0.800	43.00	7.30	9.30	28.00	133.00	7.53	72.00
137	FmW	14.60	8.02	312.00	–0.5	23.00	1.100	37.00	8.30	6.10	25.00	135.50	7.51	76.50
138	FmW	24.00	8.20		1.1	22.00	2.200	69.00	6.60	27.00	67.00	134.00		
139	FmW	26.40	7.90	324.00	–2.7	24.00	1.100	36.00	8.20	6.60	33.00	134.00	7.09	75.00
140	FmW		8.45	367.00	2.9	18.00	1.600	54.00	6.60	15.00	40.00	122.00		68.00
141	FmW		8.19		5.9	16.00	1.600	56.00	6.50	9.00	35.00	125.00		77.00
142	FmW	23.90	7.30	346.00	1.0	9.40	1.000	66.00	6.80	8.80	27.00	156.00	3.10	74.00
143	AR		7.69		3.2	66.00	11.000	170.00	12.00	83.00	235.00	235.00		78.00
144	FmW	27.00	7.00	321.00	0.5	18.00	0.700	54.00	6.90	7.80	30.00	147.00	7.09	79.00
145	FmW		7.87		0.9	30.00	2.000	40.00	4.30	8.00	51.00	130.00		77.00
146	FmW	25.00	7.56	368.00	–0.3	28.00	1.800	36.00	8.30	4.70	47.00	134.20		68.00
147	FmW		8.00	340.00	–2.2	20.00	2.700	42.00	8.80	7.40	28.00	150.00	6.65	59.00
148	AR		7.69		2.1	53.00	8.600	150.00	10.70	63.00	187.00	232.00		77.00
149	AR		7.98		1.6	55.00	11.000	150.00	11.70	61.00	190.00	267.00		79.80
150	FmW		7.97		4.5	18.00	5.900	71.00	7.30	12.00	47.00	173.00		71.42
152	AR	25.00	8.00		–0.2	60.00	7.800	147.00	9.80	66.00	199.00	264.00		37.00
153	AR	23.90	7.40	1,074.00	0.3	60.00	7.800	157.00	12.00	69.00	179.00	302.00	1.20	75.00
154	EA	23.80	7.70	650.00	–1.6	41.00	7.600	80.00	9.70	23.00	130.00	195.00	0.50	46.00
155	FmW		7.70	381.00	–0.3	12.00	3.200	65.00	3.20	8.00	30.00	166.00	4.10	76.00
156	FmW	23.90	7.99	631.00	–2.4	23.00	8.100	90.00	6.60	36.00	96.00	178.00	11.50	68.00

Sample ID	Facies[1]	Temp	Field pH[2]	FieldCond[2]	Charge Balance	Ca	Mg	Na	K	Cl	SO_4	HCO_3	NO_3	SiO_2
157	FmW	24.90	8.05	365.00	–2.3	9.90	3.450	59.50	5.65	5.85	32.00	161.90	6.00	65.50
158	EA	18.50	7.72	855.00	–1.8	44.00	11.000	111.00	11.00	30.00	147.00	274.00	2.30	43.00
159	FmW	23.30	7.60	430.00	–1.6	23.00	2.600	56.00	9.00	10.00	67.00	141.00	7.53	72.00
160	AR	21.70	7.50	1,431.00	–0.7	83.00	12.000	194.00	12.00	123.00	266.00	243.00	62.00	73.00
161	AR	23.30	7.60	950.00	0.3	48.00	6.800	160.00	10.00	67.00	180.00	264.00	2.90	68.00
162	FmW	24.00	7.40	432.00	1.0	33.00	3.300	56.00	9.40	14.00	76.00	144.00	7.53	75.00
163	EA		7.64		–7.5	46.00	17.000	120.00	4.30	24.00	160.00	284.00		20.20
164	EA		7.70	821.00	0.4	51.00	18.000	103.00	13.00	30.00	143.00	288.00	0.70	31.00
165	FmW	25.50	8.08	370.00	–2.5	8.85	3.400	60.50	5.60	5.90	33.00	162.30	4.50	62.50
166	EA	30.70	7.46	870.00	0.4	43.50	16.500	115.00	12.50	26.50	140.00	300.00	< 0.20	25.50
167	EA	29.40	7.54	897.00	–12.1	43.00	16.000	110.00	11.50	26.50	154.00	308.00	0.48	25.50
168	EA	32.00	7.60	888.00	2.5	44.00	16.000	120.00	11.00	27.00	150.00	273.00	0.44	28.00
169	FmW	23.90	7.20	383.00	0.9	28.00	3.400	46.00	7.60	10.00	53.00	142.00	3.30	56.00
170	FmW	25.80	7.90	316.00	–1.0	23.00	2.400	37.00	6.50	6.20	29.00	138.00	6.60	58.00
171	FmW	19.50	7.89	366.00	0.3	26.00	2.400	44.00	7.60	7.40	43.00	141.00	7.93	65.00
172	AR	22.75	7.55	999.50	–2.5	50.20	13.300	132.00	9.51	63.15	184.00	262.00	3.69	70.00
173	AR	24.20	7.70	960.00	0.0	47.00	16.000	130.00	9.20	62.00	180.00	239.00	2.50	64.00
174	AR	24.70	7.40	980.00	0.0	53.00	9.400	140.00	10.00	63.00	180.00	251.00	1.90	69.00
175	AR	25.00	7.90	1,160.00	1.3	59.00	6.300	180.00	13.00	80.00	203.00	296.00		38.00
176	FmW	23.00	7.00	314.00	–0.2	30.00	2.600	37.00	5.60	7.70	30.00	152.00	6.65	54.00
177	FmW		7.80	307.00	2.9	29.00	2.200	35.00	5.20	6.00	26.00	135.00	7.53	62.00
179	WRV	44.00	7.90	343.50	–1.3	22.00	1.300	49.00	2.55	7.45	38.00	149.00	0.34	20.50
180	FmW		7.80	337.00	–0.6	28.00	2.100	39.00	4.90	6.70	33.00	146.00	7.09	49.00
181	FmW		6.70	325.00	–0.2	27.00	2.000	43.00	4.60	8.50	33.00	149.00	6.20	49.00
182	WRV	30.00	7.80	875.00	–1.6	33.00	17.000	130.00	12.00	21.00	99.00	395.00		19.00
183	FmW	27.80	8.00	336.00	–0.9	25.00	2.400	41.00	5.20	8.00	33.00	145.00	3.50	52.00
184	EYM	27.55	8.69	353.00	–1.6	6.20	0.254	69.00	1.65	7.70	47.25	126.81	6.61	40.00
185	WRV	25.10	8.00	492.00	–0.5	12.00	0.700	93.00	3.90	17.00	78.00	153.00	6.40	38.00
186	WRV	26.31	8.00	548.09	–0.6	16.54	0.816	102.03	3.84	14.17	109.81	155.71	9.56	43.95
187	WRV	27.6	8.10	569.00	–0.1	17.40	0.940	104.00	3.76	12.70	113.00	160.00	9.47	47.00
188	WRV	23.90	8.05	743.00	–1.3	20.00	3.900	107.50	6.00	17.50	127.50	162.00	6.50	44.00
189	WRV		8.37	487.00	–0.1	15.67	1.500	106.00	4.23	19.33	109.00	161.00	4.55	39.33
190	WRV	26.20	7.78	523.00	–0.7	30.00	2.100	71.00	5.10	13.00	117.00	125.00	4.08	40.00

Sample ID	Facies[1]	Temp	Field pH[2]	FieldCond[2]	Charge Balance	Ca	Mg	Na	K	Cl	SO_4	HCO_3	NO_3	SiO_2
191	WRV	23.7	7.50	334.25	–1.7	13.45	0.330	57.73	2.89	7.43	53.33	116.50	6.59	31.75
192	WRV	23.5	7.90	396.00	–1.5	19.00	0.480	63.00	3.10	9.90	79.00	109.00	9.50	33.00
193	WRV	23.6	9.30	359.00	–0.2	7.50	0.040	72.00	2.10	5.60	37.00	152.31	3.85	33.00
194	WRV	25.9	9.20	353.00	–2.2	6.50	0.047	69.00	1.80	5.40	36.00	154.31		31.00
195	WRV	23.2	9.90	316.00	–1.0	6.20	0.030	60.00	1.80	5.50	31.00	130.48	2.36	32.00
196	WRV	25.4	9.30	308.00	–2.7	4.90	0.000	61.00	1.40	5.40	26.00	138.50	2.68	38.00
197	FmW		7.50	301.00	–4.3	19.00	1.200	42.00	4.10	6.10	22.00	149.00	5.73	49.00
198	FmW		7.70	295.00	0.1	21.00	2.700	38.00	5.60	6.90	27.00	128.00	8.29	52.00
199	EYM	29.9	7.80	434.00	–1.3	10.00	2.450	81.50	3.35	8.75	44.50	188.00	4.62	49.50
200	WRV	23.4	7.20	769.00	–2.6	23.00	2.800	136.00	9.30	31.00	125.00	268.00	1.23	27.00
201	WRV		7.60	573.00	–0.3	14.00	1.700	107.00	6.90	32.00	61.00	211.00	0.56	21.00
202	EYM	30.23	8.73	461.67	–1.2	1.73	0.056	107.50	3.60	6.22	28.00	246.85	3.41	61.00
203	EYM	31.0	8.60	438.50	–3.4	2.25	0.150	96.50	3.40	6.25	22.00	238.50	3.89	57.00
204	EYM	32.0	8.90	448.00	0.5	1.50	0.057	104.00	3.80	5.90	21.00	238.84	1.25	57.00
205	EYM		8.40	391.50	–0.7	5.90	0.560	79.00	3.60	6.30	23.00	190.00	3.79	59.00
206	EYM	28.6	8.40	384.00	3.7	7.80	0.800	76.00	4.30	6.50	21.00	175.00		58.00
207	EYM		8.00	314.00		16.00	1.700	49.50	3.85	6.30	21.00	144.00	< 0.20	56.00
208	EYM	28.9	8.25	327.00	0.4	10.65	0.975	60.50	3.75	6.30	21.50	153.00	5.73	60.50
209	EYM	30.8	8.45	440.50	–0.4	1.30	0.050	99.00	3.20	6.30	26.00	219.00	5.14	55.00
210	EYM	31.3	8.85	469.00	–1.0	0.93	0.033	107.50	3.40	5.65	18.50	256.00	2.08	60.00
211	EYM	30.9	8.90	475.00	–1.0	0.57	0.027	113.00	3.51	5.50	20.30	268.74	2.24	60.40
212	EYM	29.20	8.05	294.50	–2.1	16.00	1.215	47.00	3.65	7.80	22.00	141.52	4.81	54.00
213	EYM		8.60	422.00	–0.7	2.88	0.219	96.00	3.30	6.30	26.20	218.61	4.43	56.70
214	EYM	31.00	8.83	433.67	–1.3	0.55	0.050	101.33	3.14	5.55	17.00	244.91	2.08	58.37
215	EYM	30.90	9.00	450.00	–6.3	0.57	0.030	95.90	3.24	5.50	17.30	255.77	2.03	59.10
216	EYM	29.70	8.60	439.00	–3.7	1.08	0.033	98.10	3.40	6.25	25.70	235.49	4.42	56.75
217	EYM	29.10	8.50	366.00	–4.4	5.62	0.464	76.90	3.30	6.10	22.00	200.52	3.84	56.20
218	EYM	25.77	8.73	396.33	–1.1	2.55	0.285	93.07	3.21	5.71	19.87	223.33	2.06	54.47
219	EYM		8.70	408.00	0.7	4.14	0.343	90.90	3.37	6.50	27.08	205.22		56.58
220	EYM		8.20	382.00	–4.9	8.40	0.730	76.00	3.40	5.80	21.00	214.00	4.30	56.00
221	EYM		8.40	328.00	–2.8	13.00	1.400	55.00	4.30	6.50	28.00	153.00	4.80	43.00
224	WYM	32.60	8.87	608.67		0.81	0.097	136.67	2.93	9.53	47.33	304.06	< 0.22	48.17
225	WYM	32.20	8.65	565.50	–0.6	0.78	0.090	127.50	3.30	18.00	47.50	248.30	1.57	59.00

Sample ID	Facies[1]	Temp	Field pH[2]	FieldCond[2]	Charge Balance	Ca	Mg	Na	K	Cl	SO_4	HCO_3	NO_3	SiO_2
226	WYM	34.30	8.43	494.33	–2.0	0.51	0.073	113.00	2.97	8.97	45.00	235.21	2.10	54.00
227	EYM	25.10	8.20	313.00	0.3	13.90	1.100	53.95	3.86	6.49	23.00	143.50	5.86	58.50
228	EYM		8.00	441.67	–2.9	12.33	6.167	71.67	3.97	9.23	46.00	193.58	4.87	54.33
230	WRV	24.80	8.60	678.00	–1.5	5.96	0.776	137.00	4.00	11.10	159.00	166.05	12.70	34.40
231	WRV	24.50	8.40	634.00	–2.3	16.00	1.000	117.00	4.30	11.00	158.00	153.00	12.40	32.00
232	WRV	24.90	8.00	621.00	–4.6	26.00	5.300	86.00	8.30	14.00	130.00	175.00	11.70	39.00
233	BM	28.20	6.80	899.67	–2.2	30.37	8.080	143.83	27.03	14.28	105.00	407.67	2.69	68.83
234	BM	28.53	6.80	875.33	–2.0	30.30	8.000	139.67	27.20	14.33	108.33	390.67	2.56	68.00
235	BM	28.60	7.50	786.00	–0.4	53.00	27.500	72.00	9.95	14.00	123.50	323.00	3.32	55.50
236	SECF	28.40	7.90	482.00	–2.2	19.80	7.630	75.75	4.13	10.68	61.50	212.80	3.50	46.50
237	SECF	28.13	7.93	485.75	–2.3	19.23	7.420	73.70	3.70	9.82	59.18	209.00	3.39	49.25
238	SECF	27.85	8.15	475.50	–2.5	17.60	7.200	73.38	3.99	9.88	57.88	205.50	3.01	44.25
239	SECF	27.68	7.95	483.25	–8.9	18.20	7.210	73.93	4.20	10.50	58.88	206.00	3.34	47.13
240	SECF	26.83	8.30	475.50	–2.2	17.05	5.990	76.50	5.12	13.88	56.90	200.26	3.44	41.50
241	FmW	28.70	8.00	312.50	–0.7	21.75	2.620	41.40	5.00	6.35	20.30	155.00	5.13	50.60
242	FmW	28.40	7.85	304.50	–1.2	21.90	3.185	37.40	5.56	7.10	20.55	148.50	5.09	49.55
243	FmW	28.40	7.70	298.50	–0.7	18.65	2.960	38.08	5.14	6.63	20.98	135.50	4.19	47.28
244	FmW	27.60	7.50	283.00	–0.8	15.35	2.785	38.55	5.30	6.70	19.05	126.50	6.38	49.55
245	FmW	27.8	7.95	343.00	–1.1	22.60	3.020	44.90	4.97	6.35	27.50	159.00	8.08	43.30
246	FmW	28.9	7.95	331.50	–1.9	24.70	3.325	38.60	5.72	6.40	23.10	159.00	8.36	53.80
247	FmW	26.00	7.45	296.00	–2.6	18.85	2.910	36.00	5.49	6.95	21.70	133.00	8.12	56.50
248	FmW	28.2	7.40	293.50	–1.6	14.70	2.520	41.50	5.52	6.65	22.30	127.50	8.59	51.10
249	EYM	30.4	8.05	339.00	–0.8	15.45	1.205	56.65	3.42	6.74	24.35	159.00	3.72	44.50
250	WYM	28.6	8.75	460.00	–1.1	3.26	0.243	102.05	3.77	7.68	31.40	228.00	6.24	69.00
251	BM	30.5	6.70	2,230.00		77.10	9.710	376.00	83.00	199.00	122.00	933.00	< 0.20	49.00
252	BM	27.8	7.30	792.50	–2.1	59.00	31.000	67.50	8.55	15.00	127.00	358.00	3.54	55.00
253	BM	27.6	7.35	812.50	–2.4	56.80	31.040	67.34	8.82	15.08	125.50	356.80	2.80	50.00
254	BM	26.8	7.40	821.00	–1.9	58.60	31.475	69.30	8.85	15.28	128.50	360.25	3.41	53.00
255	BM		7.20	789.00	–3.6	55.50	31.000	73.50	10.00	16.00	136.00	369.00	3.71	46.50
256	BM	30.2	6.50	1,770.00		37.00	10.000	341.00	60.00	42.00	118.00	978.00	< 0.20	48.00
258	WYM		8.60	484.00	1.3	0.66	0.000	109.00	1.70	8.60	57.00	190.00	5.49	45.00
259	BM		8.20	734.00	–5.3	24.50	27.000	81.00	8.50	16.00	132.50	289.00	< 0.20	26.00
260	BM	21.4	7.65	975.00		70.90	36.700	86.90	7.08	16.90	151.00	450.00	< 0.20	25.90

Sample ID	Facies[1]	Temp	Field pH[2]	FieldCond[2]	Charge Balance	Ca	Mg	Na	K	Cl	SO_4	HCO_3	NO_3	SiO_2
261	BM	18.95	7.30	949.50	–1.8	78.60	36.950	83.50	5.74	15.50	160.50	444.00	2.03	21.80
262	BM	26.1	7.40	962.50	–3.4	73.00	34.750	81.70	5.80	15.60	160.00	432.00	2.16	20.90
263	BM	21.5	7.30	994.00	–0.6	77.00	37.000	86.00	8.15	19.50	167.00	420.00	2.39	23.00
264	BM		7.15	1,020.00	–0.7	82.50	38.250	90.00	6.10	22.50	179.00	429.00	3.48	24.00
265	FmW	26.7	8.15	308.50	–4.1	10.30	1.760	50.50	5.44	7.35	20.90	147.50	5.20	50.30
266	FmW	25.6	7.85	290.50	–2.6	13.90	2.480	41.80	6.06	7.00	19.80	134.00	6.92	57.20
267	FmW	25.7	7.70	293.50	–1.1	14.75	2.405	42.05	5.95	6.55	19.95	130.50	8.17	58.30
268	FmW	26.1	7.65	295.00	–1.6	13.75	2.230	43.75	6.10	7.00	20.10	132.00	8.38	57.95
269	FmW	28.2	7.50	284.00	–0.6	14.60	2.380	41.10	5.76	6.30	20.40	126.00	7.69	59.40
270	WYM	31.5	8.35	489.50	–1.3	4.63	0.865	105.45	3.22	9.27	40.65	229.00	3.25	43.50
272	SECF	28.5	7.70	616.00	0.2	21.00	18.000	87.50	11.20	14.70	71.10	271.00	12.90	73.00
273	EYM	30.8	8.10	353.00	–3.7	9.56	0.152	67.20	1.76	7.15	21.10	175.50	4.44	46.30
274	FmW	26.75	7.65	314.84	–1.9	17.84	3.150	39.34	8.55	10.90	31.34	123.00	8.75	56.00
275	SW		8.20	59.00	–3.85	6.70	0.70	2.40	6.30	2.00	6.30	31.72		4.50
276	AR	28.50	7.61	1,137.67	–2.0	47.67	18.000	164.33	10.67	79.33	193.33	322.33	1.42	68.33
277	AR	25.22	7.60	1,106.67	–0.7	54.25	13.250	172.50	10.25	79.50	186.75	328.50	0.39	63.75
278	AR	24.50	7.57	1,130.00	–1.5	54.00	13.000	170.00	10.00	81.00	190.00	325.00	0.80	69.00
279	AR	25.00	8.18	1,030.00	–0.6	26.00	14.000	180.00	10.00	72.00	170.00	300.00	0.94	69.00
280	AR	24.50	7.76	1,120.00	–5.9	48.00	15.000	160.00	10.00	83.00	190.00	348.00	0.98	62.00
281	FmW	26.72	7.40	287.00	–1.7	14.64	2.142	39.93	4.79	7.62	22.02	119.38	8.34	50.57
282	AR	26.00	7.65	1,190.00	–1.3	57.00	13.000	170.00	10.00	84.00	190.00	325.00	0.89	70.00
283	AR	23.00	7.70	1,150.00	–4.4	53.00	16.000	150.00	11.00	74.00	200.00	324.00	1.39	67.00
284	AR	24.00	7.18	1,260.00		69.00	18.000	170.00	13.00	65.00	230.00	382.00	< 0.20	68.00
285	P			8.00	–14.66	0.40	0.20	0.10	0.10	0.20	0.30	2.00	0.84	0.05
286	AR	24.50	7.60	1,134.00	–3.5	52.00	16.000	158.00	12.00	69.50	207.50	328.00	0.94	70.50
287	AR	24.50	7.95	1,005.00	–3.5	19.50	11.130	169.00	9.10	70.00	151.50	292.00	1.03	59.50
288	P		7.30		–43.43	0.14	0.01	0.32	0.05	0.05	0.41	2.83		0.10
289	EYM		7.58	365.00	–2.4	13.57	0.234	62.43	2.27	6.94	23.79	165.03	5.25	45.64
290	P		5.00	12.00	–65.30	0.11	0.03	0.05	0.05	0.30	1.00	1.25		0.05
291	JaF	35.02	7.90	1,164.63	0.6	80.81	14.410	154.48	16.00	22.42	467.19	100.61	7.90	56.33
293	SECF	34.50	8.10	358.00	1.3	11.42	1.680	74.10	2.11	8.83	39.60	160.25	2.83	49.27
294	SW		8.30	120.00	3.73	12.00	1.80	7.00	8.10	1.70	7.90	57.34		23.00
295	EYM	31.80	7.63	289.50	–1.7	11.24	1.036	49.09	3.89	5.97	18.12	140.21	5.64	56.66

Sample ID	Facies[1]	Temp	Field pH[2]	FieldCond[2]	Charge Balance	Ca	Mg	Na	K	Cl	SO_4	HCO_3	NO_3	SiO_2
296	BM	32.37	7.03	891.33	–1.6	78.40	30.000	70.40	8.10	15.40	141.40	397.00	1.48	26.20
297	EYM	28.70	7.25	291.33	–0.2	9.66	0.666	49.63	2.45	6.39	18.16	129.73	4.69	40.10
298	WYM	38.70	8.39	404.50	–0.7	2.60	0.038	96.00	0.95	7.80	33.50	195.97	4.40	46.50
299	FmW	30.53	7.29	287.57	–1.2	12.89	2.010	43.95	4.96	7.24	19.29	125.93	7.72	59.73
301	SW	21.30	8.00	170.00	3.25	21.00	2.90	8.20	9.10	1.40	10.00	91.50		24.00
302	SW		8.40	70.00	–5.24	8.10	0.90	4.10	5.60	1.30	6.20	43.92		8.70
303	SW		8.30	100.00	–1.00	9.50	1.30	8.60	7.40	2.20	12.00	51.24		20.00
304	SW		8.40	125.00	0.56	11.00	1.10	8.10	6.30	2.40	4.20	53.00	6.23	22.00
305	WYM		8.70	422.00	–0.4	2.40	1.900	98.50	1.95	13.00	7.20	252.00	0.02	20.00
306	WYM	57.00	6.70	1,220.00	–3.0	94.00	31.000	150.00	12.00	26.00	78.00	753.00		44.00
307	EYM	56.00	6.60	1,330.00	–2.3	100.00	39.000	150.00	12.00	28.00	160.00	694.00		41.00
308	WYM	26.50	9.20	523.00	–11.7	0.80	0.020	120.00	1.10	9.50	31.00	334.30	0.22	46.00
309	EYM	36.60	7.82	297.00	–2.5	12.00	0.350	53.50	2.05	7.05	22.00	140.00	6.31	53.50
310	EYM	32.70	7.94	299.00	–2.9	6.08	0.032	60.63	1.22	5.74	16.73	150.00	4.40	42.20
311	EYM	39.50	7.65	301.93	–0.1	11.54	0.304	54.53	1.95	6.49	19.66	136.71	5.15	54.52
312	EYM	34.90	7.89	299.00	0.7	8.62	0.078	56.44	1.42	5.48	16.81	139.07	0.11	49.92
313	EYM	41.47	7.57	303.67	–0.8	11.67	0.367	56.33	2.12	7.53	21.83	140.70	5.00	56.33
314	EYM	40.80	7.70	298.00	–8.7	11.00	0.400	55.00	1.90	7.20	22.00	167.10	5.76	53.00
315	PW	22.75	8.12	257.00	2.5	13.03	0.091	45.38	5.38	4.11	9.05	128.13	14.37	55.75
316	EYM		8.70	302.00	2.7	13.30	1.100	50.60	3.60	7.10	23.60	132.90	1.20	26.50
317	EYM	34.80	7.40	340.00	3.8	17.00	0.290	73.00	2.60	6.90	26.00	173.00		46.00
318	EYM		7.30	256.00	–2.4	9.62	0.795	43.70	5.27	7.85	20.30	119.00	1.86	57.50
319	WYM	35.0	8.35	391.50	–1.5	0.40	0.007	91.20	1.55	6.78	26.70	187.00	6.19	46.30
320	WYM	38.87	8.05	379.00	–6.1	3.40	0.060	87.33	1.37	7.40	28.67	212.97		48.00
321	SW		8.16	199.00	9.59	24.00	3.40	9.30	8.80	3.70	8.70	88.00		19.00
324	EYM	36.60	7.29	295.50	–0.5	17.50	0.655	46.00	3.15	8.00	21.50	135.40	4.03	51.50
325	EYM	35.60	7.70	312.00	3.7	13.00	0.200	57.00	2.10	5.90	19.00	139.00		45.00
326	EYM		7.50	347.00	1.6	11.60	1.700	61.80	4.60	11.50	16.10	168.00	0.02	53.00
327	WYM	35.90	7.85	276.50	1.9	1.95	0.010	60.00	2.10	6.35	16.00	126.50		48.00
329	SW		8.20	258.00	8.05	28.00	3.90	16.00	11.00	5.80	16.00	109.00		21.00
330	SW	5.50	8.00	184.00	11.39	22.79	3.06	9.00	8.22	4.61	13.00	72.00		15.00
331	SW	3.40	8.00	250.00	1.04	27.84	3.28	17.00	6.99	5.24	29.00	108.00		20.00
332	EYM	33.85	7.60	256.50	–7.9	5.35	0.050	51.00	2.00	5.75	18.50	144.55		43.50

Sample ID	Facies[1]	Temp	Field pH[2]	FieldCond[2]	Charge Balance	Ca	Mg	Na	K	Cl	SO_4	HCO_3	NO_3	SiO_2
333	SW	7.00	7.60	133.00	13.43	15.00	2.30	11.00	4.10	4.40	6.00	55.00		24.00
334	SW		8.10	117.00	11.63	15.00	2.10	6.00	4.10	2.00	4.00	53.00		22.00
335	SW	5.70	8.00	136.00	3.79	16.33	2.71	7.00	4.15	2.40	6.00	70.00		25.00
336	PW	22.50	7.10	1,100.00	–5.3	147.71	41.606	24.88	7.46	0.96	4.30	810.00		61.48
337	EYM	25.70	8.38	354.50	1.0	0.34	0.027	72.04	1.93	7.19	13.80	140.70		45.54
338	PW		7.87		2.5	26.0	2.15	35.00	1.75	6.50	14.55	144.50		34.50
340	EYM		7.88	262.00	2.6	0.28	0.034	59.10	1.59	6.71	14.90	118.76	0.11	53.20
341	PW	22.95	8.36	286.00	–2.2	20.54	1.351	37.33	2.68	8.95	15.93	134.41	0.91	41.40
343	SW	5.80	8.09	164.00	8.75	20.00	2.90	8.40	4.50	2.60	8.50	72.00		23.00
344	EYM	33.75	7.53	245.13	2.7	7.91	0.475	47.20	5.62	6.44	14.42	123.53	2.73	51.13
345	PW	23.00	8.73	231.00	–2.0	7.05	0.916	16.30	6.38	3.03	4.88	70.42		65.17
350	P				69.51	48.4	5.88	6.09	10.20	2.60	8.20	22.70		
354	PW	20.70	7.70	149.00	–7.4	12.09	2.868	12.35	6.55	2.55	6.44	80.00		40.86
355	P				8.54	30.8	4.7	3.92	15.60	3.20	9.20	111.00		
357	SW		7.75	134.00	22.26	15.00	2.80	4.90	3.70	3.40	7.80	34.00		18.00
359	FmW	22.20	7.55	265.00	1.4	16.00	2.390	35.60	4.31	8.34	16.50	112.00	10.32	57.20
360	FmW	23.13	7.40	248.33	–3.0	10.83	0.700	41.83	1.87	9.59	19.50	108.67	6.98	42.13
361	SW		7.90	145.00	11.72	16.00	2.90	8.20	4.30	4.00	7.60	55.00		30.00
363	P				12.04	4.13	0.32	0.72	0.76	0.80	1.80	9.90		
364	P				26.87	25.4	3.79	1.94	20.40	1.80	5.40	66.90		
426	P				6.36	3.45	0.36	0.60	0.64	0.70	0.80	10.90		
427	P				27.84	15.2	2.05	1.90	7.28	0.80	3.00	36.00		
428	SW	4.00	7.50	122.00	10.60	15.00	3.10	6.40	4.30	3.10	6.50	54.90		24.00
443	P				15.67	1.33	0.1	0.20	0.16	0.20	0.90	2.40		
444	P				24.58	17.5	3.04	5.70	7.28	0.90	4.00	50.90		

[1] See Table 2-4 for hydrofacies' abbreviations.
[2] Figures in italics refer to lab pH or lab conductivity (when the *in situ* value was not measured).

Table 2-3. Chemical and physicochemical composition of the samples used in this report: Minor ions and isotopes.

Sample ID	Facies[1]	F	I	Br	As	B	Sr	Li	U	$\delta^{2}H$	$\delta^{18}O$	$\delta^{13}C$	^{14}C	$\delta^{34}S$	$\delta^{87}Sr$
2	AM	3.60		1.10		8,900.00	380.00	350.00							5.87
3	AM	1.40								–91.30	–12.40				12.41
4	AM	1.13		0.16		635.00	900.00	136.67	0.20	–100.40	–14.60				13.89
5	AM	1.43		0.16		547.00	962.50	112.86	2.90	–101.60	–13.42	–4.60	3.08		11.08
17	AM	1.60		0.16		400.00	840.00	90.00		–107.50	–14.60	–5.50	3.70		4.62
18	AM	1.50				350.00		90.00							
19	AM	1.70					1,500.00	120.00							
20	AM	1.60				360.00	940.00	93.00							4.73
21	AM	1.45				80.00		80.00							
22	AM	1.50					4,300.00	200.00							
23	AM	1.20				310.00	1,100.00	100.00							
24	AM	2.00					< 100.00		1.60						
25	AM	1.30					710.00	30.00							
26	AM	1.70					930.00	90.00							
27	AM	1.50						80.00							
28	AM	1.63				280.00	833.33	88.33	3.10	–103.00	–13.65	–5.55	6.40		
29	AM	1.50						120.00							
31	AM	1.35				475.00	820.00	88.67	2.90			–7.40	7.20		
32	AM														
33	AM	2.90		0.13		1,600.00	660.00	91.00							4.93
34	AM	2.75					486.00								
35	AM	1.60					910.00	80.00							
36	AM	3.70					590.00	130.00							
37	AM	2.74	0.02	0.07	20.00	366.00	326.50	91.00	1.80	–103.50	–13.25	–4.58	12.30		10.32
38	AM														
39	AM	4.50					530.00	70.00							
40	AM	1.87	0.05	0.10	14.50	340.50	1,003.00	97.00	2.67	–104.25	–13.45	–4.80	8.80	15.65	
41	AM	1.70		0.15		368.62	942.23	88.60	3.21	–102.50	–13.73	–4.30	11.00		4.61
43	AM	8.00			< 10.00	1,200.00	1,400.00		4.80						2.55
44	AM	15.00				12,000.0	240.00	90.00							
45	AM	2.90					650.00	150.00							
46	AM	1.60					770.00	120.00							

Sample ID	Facies[1]	F	I	Br	As	B	Sr	Li	U	$\delta^{2}H$	$\delta^{18}O$	$\delta^{13}C$	^{14}C	$\delta^{34}S$	$\delta^{87}Sr$
47	AM	1.75				295.00	930.00	85.00							
48	AM	1.54		0.15		296.86	804.63	83.13	3.33		–13.60	–5.90	3.15		4.46
49	AM	2.57				285.00	230.00	65.00		–102.00	–12.40		13.80		
51	AM	3.20													
52	AM	1.70				320.00	820.00	90.00				–6.03	6.17		
56	AM	3.20				1,400.00	7,700.00	140.00	4.00						
58	AR	2.60					750.00								
59	AR	2.92	0.03	0.14	13.00	426.25	446.67	123.50	3.66	–103.00	–13.48	–4.96	7.60	19.40	10.55
63	AR	3.60				400.00	600.00	140.00	4.20						
81	AM	2.10				310.00	940.00	82.50		–102.00	–13.60	–11.00	11.40		
82	AM	1.66		0.15		353.00	863.33	84.00	3.05	–103.75	–14.19				4.64
84	AM														
85	AM	1.70				355.00	875.00	92.50	3.00	–103.15	–13.80	–5.80	5.35		4.78
86	AM	1.60					920.00	90.00							
88	EA	1.61	0.01	0.05	8.90	179.54	142.97	50.00	0.75	–99.80	–13.10	–8.30	30.45	9.40	5.17
89	EA	1.40					100.00	40.00							
90	AM	1.20				280.00	800.00	100.00							
92	AM	1.50				270.00	820.00	90.00		–103.15	–13.60	–5.77	6.80		4.77
93	AM	2.00				950.00	770.00	100.00				–5.00	2.90		
94	AM	2.10					8.20	140.00							
95	FmW	1.40					90.00	50.00		–102.00	–13.00		27.80		
96	AR	3.30		0.17		577.00	674.00	177.00	3.90	–109.00	–13.40	–4.30	7.90		12.91
97	AR	6.80					670.00	160.00							
99	AM	1.79				364.33	825.68	89.67	2.65	–103.66	–13.88	–5.16	6.28		4.98
101	EA	2.80				500.00	760.00	140.00							
102	FmW	1.70					100.00	60.00		–104.00	–12.70		10.00		
103	AM														4.34
104	EA	1.20					130.00	50.00		–105.00	–12.80		18.90		
105	EA	1.20		0.09		274.00	248.00	58.00	2.10	–105.50	–13.30	–7.20	14.19	16.00	4.17
106	EA	1.41	0.02	0.08	10.00	211.00	328.00	73.00	1.39	–100.50	–13.20	–8.00	19.20	10.00	
107	EA	2.95		0.13		481.50	954.00	148.00	1.60	–109.00	–13.65	–3.00	1.94		5.58
116	FmW	1.70					80.00	50.00		–104.00	–13.00		18.40		

Sample ID	Facies[1]	F	I	Br	As	B	Sr	Li	U	$\delta^{2}H$	$\delta^{18}O$	$\delta^{13}C$	^{14}C	$\delta^{34}S$	$\delta^{87}Sr$
117	FmW	1.60		0.05		150.00	129.00	50.00	1.20	–104.25	–13.10	–10.60	21.60		5.16
120	AR	2.80				280.00	700.00	100.00	2.90						
121	AR	2.80					460.00	140.00							
122	FmW	0.97		0.06		130.00	101.00	43.00	1.50	–103.00	–13.20	–10.00	23.50		3.43
123	EA	3.30		0.14		490.00	915.00	152.00	1.40	–108.50	–13.80	–2.55	1.40		5.71
124	EA	3.90					920.00								
125	FmW	1.40							4.70						
126	EA	4.00					1,100.00								
127	EA	3.90		0.22		481.00	1,069.00	163.00	1.00	–109.70	–13.80	–2.65	3.30		5.73
128	FmW	1.60					60.00	40.00		–98.50	–12.60				
129	EA	4.05				420.00	1,035.00	180.00	1.60						
130	EA	1.80					1,080.00			–104.00	–13.70	–4.40			
131	FmW	2.30		0.09		227.00	114.00	60.00	1.30	–107.00	–13.70	–5.40	6.50		10.49
133	FmW	1.10		0.21		279.00	319.00	53.00	2.00	–104.20	–13.10	–10.40	11.80		3.82
136	FmW	1.30					80.00	50.00		–102.00	–13.00		19.30		
137	FmW	1.10		0.05		141.00	109.50	43.50	1.50	–104.13	–13.25	–8.43	20.50		3.51
138	FmW														
139	FmW	1.00					60.00	40.00		–101.00	–13.10		20.80		
140	FmW	1.70					100.00	70.00		–99.00	–11.90	–8.40	28.42		
141	FmW	2.10					120.00			–99.00	–13.20	–8.40	27.40		
142	FmW	2.00				150.00	1,800.00	60.00	2.20						
143	AR	1.60					530.00								
144	FmW	1.50					80.00	80.00							
145	FmW	0.62					185.00			–97.50	–13.20	–5.20	24.80		
146	FmW	0.60					120.00	40.00		–97.50	–11.60	–5.20	25.81		
147	FmW	1.20					70.00	40.00		–102.00	–12.60		28.40		
148	AR	4.80					430.00			–104.00	–13.60	–5.70			
149	AR	1.66					520.00								
150	FmW	2.02					180.00								
152	AR														
153	AR	1.20				570.00	600.00	200.00	6.20						
154	EA	0.80					350.00	60.00		–105.00	–13.80	–3.40			
155	FmW	3.00				90.00		0.00							

Sample ID	Facies[1]	F	I	Br	As	B	Sr	Li	U	$\delta^{2}H$	$\delta^{18}O$	$\delta^{13}C$	^{14}C	$\delta^{34}S$	$\delta^{87}Sr$
156	FmW	1.40		0.20		289.00	217.00	86.00	2.60	–103.15	–12.90	–8.05	30.70		7.79
157	FmW	1.80					80.00	65.00		–103.00	–13.20	–7.10	17.53		
158	EA	1.40		0.16		402.00	724.00	147.00	2.80	–101.60	–13.80	–2.98	1.20		5.43
159	FmW	0.90					110.00	40.00		–103.00	–13.40	–7.30	21.90		
160	AR	1.70		0.58		642.00	600.00	247.00	5.20	–102.70	–12.90	–12.10	32.90		7.53
161	AR	1.80					310.00	210.00							
162	FmW	0.80					200.00	40.00		–100.00	–13.20				
163	EA	3.70					884.00								
164	EA	4.00				360.00	1,200.00	140.00	1.40						
165	FmW	1.75					75.00	70.00		–101.50	–12.80	–5.30	16.05		
166	EA	3.95					860.00	185.00		–104.50	–13.60	–3.80	7.26		
167	EA	3.79		0.13		497.50	829.50	173.50	1.70	–110.20	–13.80	–1.98	0.94		5.48
168	EA	3.80													
169	FmW	0.70				160.00	900.00	60.00	1.50						
170	FmW	0.70					80.00	40.00							
171	FmW	0.79		0.06		169.00	109.00	43.00	1.60	–101.80	–13.20	–6.65	17.70		3.05
172	AR	1.93	0.05	0.21	19.00	785.00	456.50	162.00	4.54	–105.43	–13.50	–5.65	19.50	21.10	11.99
173	AR	2.00					460.00	160.00		–102.00	–13.10	–6.20	31.40		
174	AR	1.90					440.00	180.00							
175	AR														
176	FmW	0.70					80.00	40.00		–99.50	–13.20	–6.80	21.40		
177	FmW	1.00					50.00	50.00		–103.00	–13.20	–7.10	19.30		
179	WRV	0.85					65.00	45.00							
180	FmW	1.00					50.00	40.00		–102.00	–12.80		15.60		
181	FmW	0.90					80.00	40.00		–102.00	–12.80	–10.20			
182	WRV	3.40		0.08		580.00	980.00	190.00		–113.20	–15.40				8.25
183	FmW	1.40							1.50						
184	EYM	1.80	< 0.002	0.06		147.67	27.33	78.00	< 1	–103.83	–13.77	–11.80	13.55	8.55	0.91
185	WRV	2.50				180.00	100.00	80.00				–7.40	11.80		
186	WRV	1.90		0.12		288.34	102.16		2.53						2.26
187	WRV	1.70	0.03	0.07	22.00	262.00	108.00	87.00	2.77	–104.00	–13.45	–6.95	7.40	8.50	
188	WRV	1.40					< 100		3.25						
189	WRV	2.00				290.00	80.00	90.00	1.80						

Sample ID	Facies[1]	F	I	Br	As	B	Sr	Li	U	$\delta^{2}H$	$\delta^{18}O$	$\delta^{13}C$	^{14}C	$\delta^{34}S$	$\delta^{87}Sr$
190	WRV	0.83		0.12		185.00	144.00	59.00	1.20	–106.35	–13.10	–9.05	8.84		0.75
191	WRV	1.21	0.01	0.15	8.30	127.88	66.38	49.38	0.80	–100.25	–13.21	–10.49	23.10	8.79	0.48
192	WRV	1.20	0.01	0.08		145.00	88.00	55.00	< 1	–107.00	–13.50	–12.65		8.30	1.04
193	WRV	1.70	0.01	0.04		159.00	40.00	47.00	< 1	–111.00	–13.80	–10.15		9.20	1.34
194	WRV	1.70	< 0.002	0.04		166.00	36.00	50.00	< 1	–107.00	–13.90	–10.50	13.50	9.20	1.47
195	WRV	1.60	0.01	0.03		155.00	32.00	39.00	M	–107.50	–13.90	–9.45	18.20	9.90	1.59
196	WRV	1.70	< 0.002	0.04	38.00	105.00	34.00	35.00	0.57	–106.00	–13.80	–9.90	8.70	9.50	1.27
197	FmW	1.60	< 0.002	0.05		154.00	53.00	42.00	1.00	–104.00	–14.10	–8.30	23.50	11.90	3.40
198	FmW	1.40	< 0.002	0.05	5.80	175.00	66.00	44.00	0.49	–98.00	–13.10	–9.45	22.40	9.30	
199	EYM	2.25	< 0.002	0.06		193.50	50.50	81.00	3.00	–106.38	–13.80	–6.25	12.40	13.15	4.54
200	WRV	0.90	0.11	0.16		698.00	322.00	178.00	< 1	–108.00	–13.25	–2.55	3.60	16.30	4.40
201	WRV	1.20	0.08	0.18		650.00	204.00	147.00	M	–106.00	–13.50	–0.50	4.30	20.70	
202	EYM	2.20	< 0.002	0.05		177.17	3.33	129.33	2.00	–105.50	–13.80	–7.57	12.40	9.05	2.05
203	EYM	2.20	< 0.002	0.05		182.50	7.50	117.50	2.00	–108.75	–13.75	–7.10	12.35	10.65	2.59
204	EYM	2.20	0.01	0.05		162.00	5.00	130.00	2.00	–108.00	–13.90	–6.80	19.90	9.80	2.38
205	EYM	1.80	< 0.002	0.05		166.00	25.00	93.00	1.00	–110.00	–13.80	–7.10	15.20	10.40	2.82
206	EYM	2.00	0.16	15.00		163.00	34.00	84.00	1.00	–107.50	–13.85	–7.65		10.30	2.92
207	EYM	1.90	0.01	0.11		147.50	62.00	53.00	M	105.25	–13.80	–7.80	19.40	10.90	
208	EYM	1.65	< 0.002	0.04		157.00	36.00	68.00	1.00	–104.00	–13.60	–7.60	21.00	10.60	2.77
209	EYM	2.00	< 0.002	0.04		190.00	3.00	126.00	2.00	–106.25	–13.55	–6.60	12.50	10.90	1.44
210	EYM	2.60	< 0.002	0.04		185.00	2.00	132.00	2.00	–110.40	–13.95	–6.40	12.60	11.65	2.14
211	EYM	2.20	< 0.002	0.05		186.00	1.10	145.00	2.56	–106.00	–13.20	–7.10	9.20	9.60	1.48
212	EYM	1.75	< 0.002	0.05	1.40	138.00	58.50	42.00	0.77	–101.75	–13.53	–8.68	22.95	11.50	3.06
213	EYM	2.00	< 0.002	0.06		185.00	8.00	114.00	1.71	–104.50	–13.40	–8.50		9.30	2.28
214	EYM	2.12	< 0.002	0.05	31.00	134.67	1.87	137.67	1.95	–105.00	–13.75	–7.33	8.40	11.05	1.61
215	EYM	2.40	< 0.002	0.05		160.00	1.09	132.00	1.44	–101.50	–12.10	–7.45	9.00	11.20	0.98
216	EYM	2.10	< 0.002	0.07		186.50	1.88	133.00	1.79	–103.00	–13.00	–7.00	11.40	9.80	1.74
217	EYM	2.10	< 0.002	0.08		151.00	16.90	98.20	1.95	–100.00	–11.75	–9.50	14.90	9.20	2.10
218	EYM	2.05	< 0.002	0.05	30.00	137.00	16.87	116.33	2.06	–103.00	–13.25	–7.48	12.50	9.80	0.62
219	EYM	1.95	< 0.002	0.06		172.00	9.60	109.00	1.69	–102.63	–13.20	–8.49		8.70	2.79
220	EYM	1.80	< 0.002	0.05	14.00	173.00	35.00	86.00	2.33	–102.00	–13.40	–6.80	12.00	9.80	
221	EYM	2.00	0.01	0.06	8.40	154.00	75.00	47.00	1.52	–100.00	–13.20	–8.35	22.10	8.00	
224	WYM	4.18	0.02	0.05		289.67	4.00	266.83	10.00	–106.00	–14.13	–5.10	8.40	9.82	2.14

Sample ID	Facies[1]	F	I	Br	As	B	Sr	Li	U	$\delta^{2}H$	$\delta^{18}O$	$\delta^{13}C$	^{14}C	$\delta^{34}S$	$\delta^{87}Sr$
225	WYM	2.95	0.01	0.06		234.00	2.50	180.00	3.00	–104.75	–14.25	–8.38	21.50	10.85	1.53
226	WYM	2.87	0.01	0.05		237.33	1.33	161.67	2.00	–105.83	–14.40	–6.83	10.00	11.17	1.47
227	EYM	1.94	0.01	0.04	9.25	137.00	66.00	46.50	0.95	–101.00	–13.40	–8.26	21.20	10.80	1.84
228	EYM	2.47		0.07			110.00	68.00	2.50	–102.00	–13.65				4.22
230	WRV	1.30	0.01	0.09		238.00	62.90	51.50	4.32	–104.00	–13.10	–9.85	22.60		–0.07
231	WRV	1.10	< 0.002	0.08	18.00	171.00	137.00	57.00	2.99	–104.50	–13.50	–11.30	20.70	2.10	0.44
232	WRV	1.40	0.06	0.10	13.00	275.00	131.00	58.00	5.85	–101.00	–13.10	–10.55	24.40	5.05	1.80
233	BM	4.11	0.01	0.08	8.25	341.50	306.17	320.67	1.06	–102.08	–13.58	–3.40	4.70	16.23	8.98
234	BM	3.99	0.01	0.11	5.40	321.67	298.67	288.00	1.01	–100.67	–13.60	–3.60	4.75	16.23	7.59
235	BM	0.95	< 0.002	0.09		213.50	461.50	77.50	9.00	–101.75	–13.40	–5.25	9.00	14.70	5.09
236	SECF	2.15	< 0.002	0.07		183.25	146.75	78.00	4.25	–104.90	–13.85	–6.53	11.70	13.43	4.66
237	SECF	2.04	< 0.002	0.07	11.00	178.00	146.63	79.75	4.99	–104.73	–14.05	–6.39	11.00	16.40	4.74
238	SECF	2.03	0.01	0.07	11.00	180.00	143.50	76.00	4.41	–104.17	–14.00	–6.23	10.90	14.40	4.64
239	SECF	2.01	0.01	0.05	11.00	178.63	146.50	74.88	4.74	–104.67	–14.07	–6.70	11.40	13.90	4.52
240	SECF	2.01	0.01	0.05	9.20	184.50	132.25	77.50	4.52	–104.00	–14.07	–6.80	12.20	14.17	4.63
241	FmW	1.00	0.01	0.04	6.20	150.50	76.30	41.95	0.84	–98.50	–12.95	–8.28	20.80	8.90	1.73
242	FmW	1.10	0.01	0.05	3.90	154.00	91.25	36.70	0.72	–98.75	–13.10	–8.15	20.60	9.90	1.75
243	FmW	1.70	0.01	0.05	4.90	144.25	72.38	36.80	0.53	–98.75	–13.10	–7.88	21.05	9.88	1.79
244	FmW	1.70	< 0.002	0.05	5.80	146.50	60.15	37.75	0.44	–99.00	–13.10	–9.15	24.10	9.25	2.44
245	FmW	0.88	< 0.002	0.05	7.20	123.50	77.00	37.50	1.52	–97.50	–13.10	–10.70	22.30	8.15	2.21
246	FmW	1.05	< 0.002	0.05	4.55	124.75	95.20	35.60	1.09	–97.75	–13.14	–9.57	20.80	8.77	1.79
247	FmW	1.60	< 0.002	0.05	5.40	131.00	67.30	35.35	0.53	–97.50	–13.30	–10.00	22.50	9.50	2.01
248	FmW	1.95	< 0.002	0.05	6.20	123.50	64.00	36.90	0.79	–99.25	–13.10	–10.60	25.00	8.40	2.13
249	EYM	2.11	0.01	0.04	4.90	149.00	55.50	54.00	0.95	–104.00	–13.65	–7.65	17.60	12.10	1.85
250	WYM	2.17	0.01	0.04	14.50	193.00	27.50	62.50	4.02	–102.25	–13.55	–11.30	16.45	9.38	0.49
251	BM	6.67	0.03	0.03	10.00	844.00	1,550.00	649.00	< 0.06	–105.00	–14.10	–1.80		27.50	
252	BM	0.60	< 0.002	0.08		216.00	557.00	72.50	8.00	–100.00	–13.88	–5.65	6.40	14.60	5.19
253	BM	0.56	0.01	0.09	5.25	204.80	550.75	67.63	7.24	–101.00	–13.67	–5.44	7.05	15.13	5.19
254	BM	0.59	< 0.002	0.09	5.70	208.00	583.00	69.00	8.71	–101.67	–13.53	–5.60	7.65	14.70	5.04
255	BM	0.70	0.04	0.12		212.50	509.50	73.50	5.00	–101.30	–13.53	–4.50		14.60	5.08
256	BM	6.50	0.03	0.12		942.00	967.00	647.00	< 1	–107.50	–13.80	–2.00	2.50	27.60	5.31
258	WYM	2.80	0.01	0.06	10.00	154.00	7.40	69.00	3.85	–99.50	–13.60	–8.50	17.60	4.70	–0.36
259	BM	0.82	0.02	0.09	1.25	234.50	352.00	122.00	0.20	–97.75	–13.40	–5.70	7.25	21.65	4.33

Sample ID	Facies[1]	F	I	Br	As	B	Sr	Li	U	$\delta^{2}H$	$\delta^{18}O$	$\delta^{13}C$	^{14}C	$\delta^{34}S$	$\delta^{87}Sr$
260	BM	0.81	0.02	0.17	2.00	247.00	497.50	106.00	2.89	–98.00	–13.25	–4.80	6.40	16.10	5.15
261	BM	0.86	0.01	0.10	< 1.2	246.50	488.00	108.00	5.29	–98.50	–13.30	–4.70	5.75	14.25	5.93
262	BM	0.89	0.01	0.10	< 1.2	241.50	482.00	136.50	5.25	–98.75	–13.30	–4.80	5.80	14.30	5.89
263	BM	0.95	0.01	0.11		273.00	630.00	116.00	6.00	–98.00	–13.00	–4.85	8.40	14.30	5.66
264	BM	0.90	0.01	0.15		283.00	560.50	115.00	5.50	–99.88	–13.50	–4.90	6.50	13.30	
265	FmW	2.05	0.01	0.06	10.00	108.00	54.95	39.05	0.87	–97.25	–13.15	–8.40	25.30	9.20	1.99
266	FmW	2.05	0.01	0.06	9.30	118.50	61.65	35.75	0.69	–99.50	–13.10	–9.10	24.95	9.85	2.35
267	FmW	2.05	< 0.002	0.05	10.00	133.50	62.30	37.50	0.90	–96.75	–13.15	–10.05	24.80	9.70	2.23
268	FmW	2.10	< 0.002	0.05	11.00	121.50	61.25	39.10	0.88	–98.50	–13.10	–10.20	25.70	9.55	2.06
269	FmW	1.90	< 0.002	0.07		142.00	53.10	41.30	0.65	–100.00	–12.70	–8.75	26.20	9.70	2.93
270	WYM	3.51	0.02	0.05	12.50	216.00	41.00	92.50	4.29	–102.00	–13.65	–7.00	12.90	11.30	0.70
272	SECF	0.94		0.00	12.00	209.00	373.00	52.00	4.78						
273	EYM	2.60	0.01	0.05	6.70	150.00	25.20	63.15	2.54	–102.25	–13.65	–8.13	21.75	12.20	2.22
274	FmW	1.60		0.05				37.17	1.30	–97.25	–13.17	–8.60	30.70		3.00
275	SW	0.05	< 0.002	0.01	0.50		31.00	5.00							
276	AR	3.30	0.01	0.33		550.00	369.50	250.00	6.70	–108.25	–14.23	–6.60	26.20	20.10	3.86
277	AR	3.70	0.02	0.31		496.67	363.33	256.67	8.00	–107.00	–14.03	–5.90	28.80		
278	AR	3.60	0.02	0.31		500.00	350.00	240.00		–105.00	–14.00				3.89
279	AR	3.10	0.01	0.29		640.00	440.00	180.00		–104.00	–13.91	–7.80	13.80		
280	AR	3.70	0.01	0.35		610.00	350.00	230.00		–104.00	–13.89	–6.50	17.10		
281	FmW	1.83		0.06	9.80	115.57	47.19	37.71	0.74	–96.50	–12.95	–7.88	30.80		3.52
282	AR	4.00	0.02	0.32		410.00	410.00	240.00		–106.50	–13.95				3.33
283	AR	3.10	< 0.002	0.31		610.00	380.00	240.00		–104.00	–13.99	–6.70	25.00		
284	AR	2.50	0.02	0.24		610.00	690.00	280.00		–105.00	–13.80				1.30
285	P														
286	AR	4.05	0.06	0.30		592.00	405.50	263.00	8.00	–108.25	–14.00	–6.20	14.70	21.80	3.90
287	AR	4.18	0.01	0.30		649.75	342.13	127.63	5.00	–106.50	–14.18	–8.25	17.93	19.60	3.99
288	P	0.05		0.01				2.00							
289	EYM	2.98	< 0.002	0.08			25.00	59.93	1.98	–102.50	–13.69	–7.07	11.40		1.01
290	P	0.05		0.01		8.00	0.50	2.00	0.50	–56.75	–7.50				1.22
291	JaF	1.11	0.02	0.02		1,410.00	264.00	43.00	2.40	–105.00	–13.45	–11.00	12.30	8.80	0.21
293	SECF	2.64	< 0.002	0.06		174.50	62.30	86.20	3.26	–106.67	–14.03	–7.22	12.77	12.95	2.57
294	SW	0.30	< 0.002	0.01	3.00		86.00	17.00							

Sample ID	Facies[1]	F	I	Br	As	B	Sr	Li	U	$\delta^{2}H$	$\delta^{18}O$	$\delta^{13}C$	^{14}C	$\delta^{34}S$	$\delta^{87}Sr$
295	EYM	2.32		0.05		120.44	32.43	48.07	0.50	–101.76	–13.36	–8.47	22.25	10.81	2.12
296	BM	1.12	< 0.002	0.10		204.00	567.00	88.67	6.13	–102.00	–13.80	–4.80	7.00	14.70	5.36
297	EYM	2.00		0.21		115.34	46.73	70.09	0.50	–100.84	–13.53	–8.24	17.50	10.67	4.26
298	WYM	3.70	< 0.002	0.16			4.00	86.00		–103.00	–13.82	–6.08	7.32		1.18
299	FmW	2.35		0.06		116.00	59.66	47.79	0.63	–95.61	–12.73	–8.03	30.67	10.45	3.03
301	SW	0.20	0.01	0.01	2.00		100.00	7.00							
302	SW	0.05	< 0.002	0.01	0.50		34.00	6.00							
303	SW	0.30	< 0.002	0.01	2.00		66.00	14.00							
304	SW	0.30	0.01	0.20		87.00	74.00	10.00	0.50	–82.50	–11.30	–13.15			
305	WYM			0.21				150.00			–13.95	–9.01			1.51
306	WYM	4.90					490.00	310.00		–107.00	–13.80	–2.80			
307	EYM	4.70					450.00	590.00		–106.00	–13.80	–2.20	2.30		3.59
308	WYM	5.50	0.01	0.18			1.00	220.00		–101.00	–13.90	–4.90	10.50		
309	EYM	2.05	< 0.002	0.04			45.00	93.00		–100.50	–13.40	–7.00	15.95		
310	EYM	2.12	0.08	0.04		122.02	22.35	126.47	1.99	–102.15	–13.90	–9.25	11.65	10.90	0.72
311	EYM	2.11	0.01	0.18		110.70	53.39	82.98	1.11	–99.64	–13.39	–6.94	16.18		0.85
312	EYM	1.97		0.05			22.37	73.77		–101.30	–13.45	–8.01	14.45	10.80	0.58
313	EYM	2.15	< 0.002	0.03			34.50	143.33		–102.00	–13.50	–7.10	15.00		
314	EYM	2.00	< 0.002	0.05			44.00	110.00		–103.00	–13.50	–7.50	15.70		
315	PW						30.00	20.00		–99.78	–13.33	–9.48	28.33		3.29
316	EYM					120.00	280.00	84.00							2.04
317	EYM	4.60					27.00	130.00		–104.00	–14.00	–7.40	11.80		
318	EYM	1.80		0.45				50.00		–97.50	–12.75	–12.70	24.10		
319	WYM	4.59	< 0.002	0.06		203.80	0.50	64.33	4.50	–105.30	–14.37	–9.42	15.01	12.60	2.87
320	WYM	4.43					6.33	72.00		–106.00	–13.93	–7.30	12.90		
321	SW	0.20		0.01			160.00	9.00							3.27
324	EYM	1.60					42.50	170.00		–100.25	–13.45	–9.50	17.80		
325	EYM	2.50					17.00	67.00		–103.00	–13.80	–9.10	22.00		
326	EYM			0.06				550.00		–97.50	–13.20	–11.80	21.60		
327	WYM	1.40					6.50	66.50		–102.00	–13.60	–10.30	19.80		
329	SW	0.20		0.01			200.00	19.00							
330	SW	0.05					160.90	9.60							3.33
331	SW	0.05					184.60	12.10							3.33

Sample ID	Facies[1]	F	I	Br	As	B	Sr	Li	U	$\delta^{2}H$	$\delta^{18}O$	$\delta^{13}C$	^{14}C	$\delta^{34}S$	$\delta^{87}Sr$
332	EYM	1.10					12.50	40.00		–102.00	–13.45	–11.40	21.90		
333	SW	0.20					45.00	10.00							
334	SW	0.20		0.01			44.00	2.00							3.75
335	SW	0.05					54.40	5.20							
336	PW	0.45		0.26						–89.57	–11.63				2.45
337	EYM	6.51		0.08			2.10	129.06		–100.48	–14.00	–12.83	22.88	11.40	0.73
338	PW	0.70					250.00	20.00		–97.35	–13.40	–9.85	27.20		4.38
340	EYM	0.92		0.05			1.47	39.90		–101.05	–13.20	–10.70	27.34		1.77
341	PW	0.75	0.04	0.53			148.65	36.00		–99.98	–13.47	–11.28	30.49	10.85	4.07
343	SW	0.20		0.01			97.00	10.00							3.68
344	EYM	1.03	0.01	0.05		116.67	10.40	45.87	1.30	–98.93	–13.30	–11.25	20.45		2.12
345	PW	0.22		0.02		110.95	10.11	2.00	0.50	–73.10	–9.90				3.70
350	P														
354	PW						22.97	4.31		–89.50	–12.40				3.71
355	P														
357	SW	0.05		0.01			89.00	8.00							3.46
359	FmW									–90.60	–12.57	–11.00	75.70		2.65
360	FmW	0.95		0.10			36.00	105.00		–92.50	–12.73	–12.00	65.07		1.94
361	SW	0.30		0.01			23.00	2.00							3.50
363	P														
364	P														
426	P														
427	P														
428	SW	0.05					80.00	9.00							
443	P														
444	P														

[1] See Table 2-4 for hydrofacies' abbreviations.

The 254 groundwater samples contained in the raw dataset have been grouped into 10 “hydrofacies” by geographical and/or chemical similitude (Oliver and Patterson 2002), although the groupings are not intended to be either rigorous or comprehensive. The 10 hydrofacies of the groundwater samples, together with the four other water types (perched waters, pore waters, surface waters, and precipitation) gives a total of 14 different “categories” of water samples. Each water category has been given a different colour, a different symbol type and a different abbreviation, which is maintained throughout the report. 0 collects the colour code, symbol type and abbreviation for each category and Figure 2-1 shows the general distribution of the samples of each water category on a shaded relief map. We will call hydrofacies to each category, even recognising that we are using the term “hydrofacies” in a broad sense.

Table 2-4. Hydrofacies used in this report. The colour code, symbol type, and abbreviations used throughout the report are included.

Hydrofacies	Water type	Colour code	Symbol	Abbreviation
Amargosa River	Groundwater		+	AR
Eastern Yucca Mountain	Groundwater		□	EYM
Fortymile Wash	Groundwater		×	FmW
Bare Mountain	Groundwater		△	BM
Eastern Amargosa	Groundwater		○	EA
Ash Meadows	Groundwater		⊕	AM
Western Yucca Mountain	Groundwater		■	WYM
Western Rock Valley	Groundwater		✳	WRV
South East Crater Flats	Groundwater		◁	SECF
Jackass Flat	Groundwater		■	JAF
Perched Water	Perched water		●	PW
Surface Water	Surface water		▲	SW
Precipitation	Precipitation		▽	P
Pore Water	Pore water		●	PW

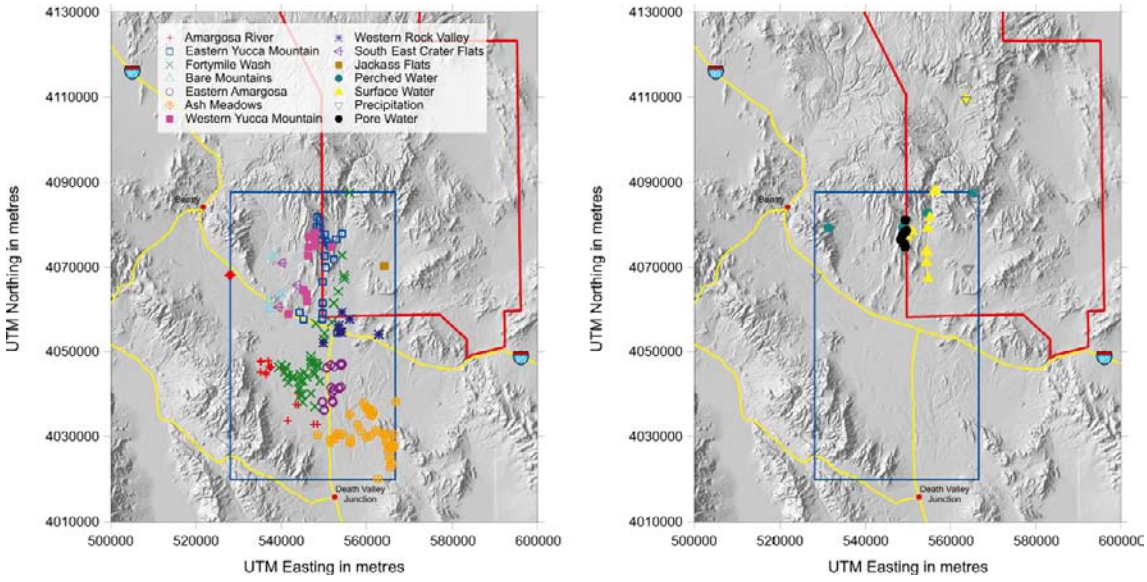

Figure 2-1. *Map with the location of the samples of the raw dataset. The left-hand map plots the groundwater samples (all 10 hydrofacies), and the map on the right plots the non-groundwater samples (perched waters, surface waters, pore waters and precipitation). The red polygon marks the boundary of the Nevada Test Site.*

2.3 Water types

The following five water types can be identified in the Yucca Mountain area:

Precipitation. This is the starting point for all water types. Evapotranspiration of precipitation waters in the soil zone appears to be a very important process in the control of vadose zone pore waters, perched waters and saturated zone ground water compositions in this area (Meijer 2002).

Surface waters. Surface waters in these desert areas are short-lived and ephemeral. Cl concentrations are higher relative to precipitation, indicating that they have either dissolved Cl-bearing solids and/or that they have experienced evapo-transpiration, although the former interpretation seems more plausible. The fact that SO_4 to Cl ratios in these samples are similar to the precipitation samples suggests also dissolution of SO_4-bearing solids and/or evapo-transpiration. The elevated HCO_3 to Cl ratios in these samples strongly suggest that CO_3-bearing solids have also been dissolved by these surface waters (Meijer 2002). Silica has very low concentrations in precipitation samples (< 1.0 mg/l). However, surface waters show concentrations of up to 37 mgL^{-1} with an average value of approximately 25 mg L^{-1}. Given that the age of surface waters is in the range of hours to days, these data indicate there is a very soluble form of silica in surface soils that is rapidly dissolved by surface waters.

Pore waters. These are waters extracted from the unsaturated zone (volcanic tuffs) in the Yucca Mountain area. Extraction was performed by either uniaxial/triaxial compression or ultra-centrifugation. Pore waters have ratios of Ca, Na, HCO_3 and SO_4 to Cl that are all lower than those found in precipitation. The lower ratios probably reflect the precipitation of alkaline earth carbonates and possibly sulphates in the soil zone (Meijer 2002). Downward matrix flow in the unsaturated zone is indicated by ion exchange within zeolitised layers. The upper portions of these layers have gained Sr, Mg, and Ca from percolating water and lost Na, K and Rb. The fact that this exchange is most pronounced at the tops of zeolitised layers and absent in stratigraphically lower zeolitised layers when multiple layers exist provides strong evidence of downward percolation of water (Stuckless and Dudley 2002).

Perched waters. Perched waters are groundwaters in perched aquifers or aquitards above the main water table. They are chemically more diluted than the pore waters, but appear to have gained their solutes by similar mechanisms. Sulphates were dissolved in the soil zone in addition to carbonates and chlorides. The dissolution of the less soluble phases (i.e. alkaline earth carbonates and sulphates) in the soil zone implies that perched waters were infiltrated under wetter climatic conditions (Meijer 2002).

Groundwaters. Saturated zone groundwaters originated by processes similar to those that formed the perched groundwaters, except that the former were subject to more extensive ion exchange reactions. Groundwaters in the shallow saturated zone beneath Yucca Mountain appear to include a significant component that was locally infiltrated. Deeper saturated zone waters probably infiltrated further upgradient in the direction of Pahute Mesa (Meijer 2002). Two main facies have been recognised: (1) pH-neutral, $Na+Ca+Mg+SO_4+HCO_3$ water with moderate to high total-dissolved solids; and (2) alkaline, $Na+HCO_3+CO_3$ water with high total dissolved solids.

2.4 Exploratory analysis

The aim of the exploratory analysis is twofold: (1) to assess the global relationships between all the water categories and (2) to screen the dataset for outliers, both on a total system basis and on a hydrofacies basis. The first part of the exploratory analysis defines the basic compositional characteristics of the whole dataset, the main hydrochemical trends and the compositional range of the most important chemical variables. The outcome of this analysis gives a distinction between conservative and non-conservative variables and a first identification of samples with extreme chemical signatures (outliers). The total-system exploratory analysis is carried out by means of ion-ion plots and Principal Components Analysis (PCA).

The second part of the exploratory analysis is performed on a hydrofacies basis. Each hydrofacies is treated separately and its behaviour compared with that of other hydrofacies. This permits the identification of samples strongly affected by non-mixing processes (evaporation, water-rock interaction, ion exchange, etc) and the preliminary selection of potential end-member waters.

2.4.1 Total-system exploratory analysis

Piper diagrams and box-and-whiskers plots

The Piper diagram in Figure 2-2 provides an immediate grasp of the general chemistry and trends in the raw dataset. In Figure 2-2, samples are colour-coded by hydrofacies and symbol size is proportional to Total Dissolved Solids (TDS, in mgL^{-1}). Most waters are low-TDS of a sodium-bicarbonate type, although exceptions to this rule do exist. The most obvious ones are: (1) the calcium-sodium bicarbonate-sulphate waters from the Bare Mountain (cyan; medium-TDS) and Ash Meadows (orange; high-TDS) hydrofacies; (2) the calcium-magnesium bicarbonate waters that include both precipitation (grey) and surface waters (yellow), both very low-TDS; and (3) the calcium-magnesium sulphate-chloride signature of some, generally low-TDS pore waters (black). Minimum TDS is 0.061 $meqL^{-1}$ (2.78 mgL^{-1}) and maximum TDS is 108.2 $meqL^{-1}$ (3968.4 mgL^{-1}), with a mean value for the whole dataset of 12.4 $meqL^{-1}$ (470.1 mgL^{-1}) and a median value of 9.1 $meqL^{-1}$. (368.0 mgL^{-1})

Several trends are also apparent: (1) pore waters have a very broad compositional range, from a pure sodium bicarbonate type to a calcium-magnesium sulphate-chloride type; (2) the Bare Mountain hydrofacies waters are also quite variable, defining a trend from a sodium bicarbonate type to a calcium-magnesium bicarbonate-sulphate type; and (3) the Ash Meadows hydrofacies waters follow a similar trend but even more pronounced, extending to the calcium-magnesium sulphate (-chloride) type.

In order to gain a general idea of the concentration range for the major ions, minor ions and isotopes, box-and-whiskers plots are very suitable. In the box-and-whiskers plots that follow Figures 2-3, 2-4 and 2-5, the box has the 75th and 25th percentiles as its upper and lower limits, and the middle line represents the median of the distribution (50th percentile), while the whiskers mark the 95th and 5th percentiles. In addition, the square is the mean, crosses are the 99th and 1st percentiles, and the horizontal bars are the maximum and minimum values.

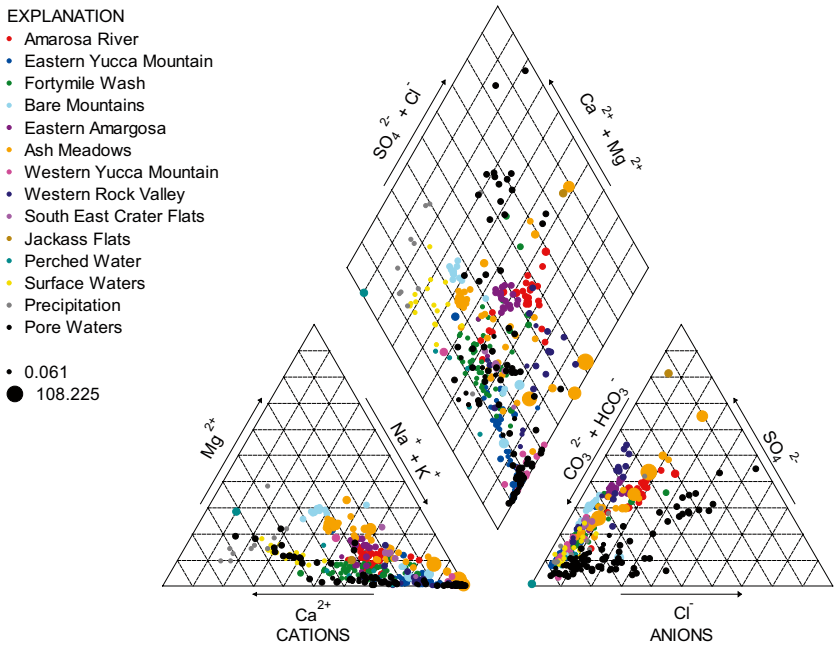

Figure 2-2. *Piper diagrams for the raw dataset, including all water categories. Symbol size is proportional to the Total Dissolved Content of the sample, expressed in $mmolL^{-1}$. As stated in the legend, the lowest TDS is 0.061 $meqL^{-1}$ (2.78 mgL^{-1}) and the highest 108.225 $meqL^{-1}$ (3968.4 mgL^{-1}).*

Figure 2-3 plots the relevant statistics for the major ions and Table 2-5 gives their numerical values. As already mentioned, concentrations of the major ions are generally low. Bicarbonate is the principal anion, with a median value of 162 mgL^{-1} (mean value = 200.3 mgL^{-1}), followed by sulphate and then chloride. Sodium is the principal cation (median = 67.3 mgL^{-1}; mean = 80.8 mgL^{-1}), followed by calcium, potassium and magnesium. All the distributions are skewed to the right (i.e. the median value is smaller than the mean value, and the coefficient of variation (standard deviation divided by the mean value) is considerably larger for sulphate, chloride and magnesium than for the other major ions (Table 2-5). Bicarbonate has the lowest coefficient of variation, indicating that the dispersion of values around the mean is smaller than for the other ions.

As regards the minor and trace elements (Figure 2-4), the most abundant of them is fluoride (median value = 1,700 μgL^{-1}, mean value = 1,996 μgL^{-1}; 365 samples), followed by boron (165 samples), strontium (268 samples), lithium (249 samples) and bromide (188 samples), all of them with median concentration values of the order of 100 μgL^{-1}. Finally, arsenic (54 samples), iodine (106 samples) and uranium (136 samples) have median concentrations between 2 and 9 μgL^{-1}.

Table 2-5. Basic statistics for the main ions in the raw dataset.

Species	Mean	Standard dev	Coeff of var	P25	P75	Median
Ca	26.3	25.2	0.96	7.05	44	19
Mg	6.92	10.5	1.52	0.304	9.9	2.121
Na	80.76	100.6	1.25	42	102	67.295
K	7.47	7.95	1.06	3.51	9.1	6.15
Cl	24.5	37.5	1.53	6.4	26.2	11.4
HCO_3	200.3	164.4	0.82	127.5	263	162
SO_4	67.4	104.5	1.55	15.3	92.17	28.835
NO_3	7.31	9.62	1.31	1.42	8.12	4.61

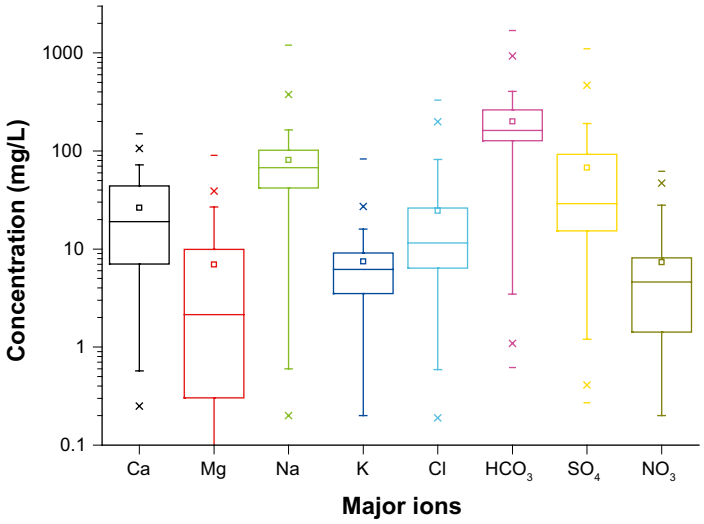

Figure 2-3. *Box-and-whiskers plot for the major ions in the raw dataset. Concentrations are expressed in mgL^{-1}. Box: 75th and 25th percentiles; middle line: median (50th percentile); whiskers: 95th and 5th percentiles; square: mean; crosses: 99th and 1st percentiles; horizontal bars: maximum and minimum values.*

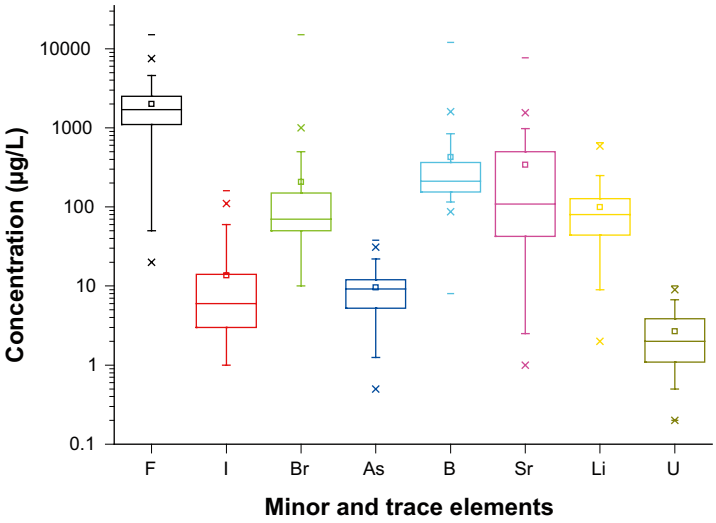

Figure 2-4. *Box-and-whiskers plot for minor ions in the raw dataset. Concentrations are expressed in μgL^{-1}. Box: 75th and 25th percentiles; middle line: median (50th percentile); whiskers: 95th and 5th percentiles; square: mean; crosses: 99th and 1st percentiles; horizontal bars: maximum and minimum values.*

The isotopes (Figure 2-5) have less skewed distributions than the major and minor ions, and have very similar mean and median values. The median value for δ^2H is –102.7 ‰ (218 samples), for $\delta^{18}O$ it is –13.5 ‰ (220 samples), for $\delta^{13}C$ it is –7.4 (173 samples) and for ^{14}C it is 15.2 pmc (168 samples). Because not all samples in the raw dataset have been analysed for all the elements, the number of samples contributing to the statistics is different in each case. The numbers specified refer to samples analysed and with a concentration above the detection limit for each specific element (i.e. samples analysed for a specific element but with a concentration below the detection limit have not been included in the box-and-whiskers plots or in the tables with statistical data). Table 2-6 gives the number of samples above the detection limits for each element in each of the 14 water categories.

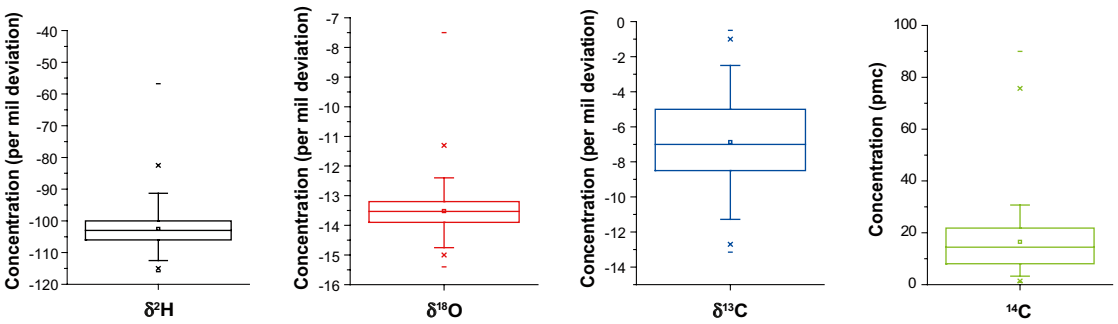

Figure 2-5. *Box-and-whiskers plot for the main isotopes: δ^2H, $\delta^{18}O$, $\delta^{13}C$ and ^{14}C. Box: 75th and 25th percentiles; middle line: median (50th percentile); whiskers: 95th and 5th percentiles; square: mean; crosses: 99th and 1st percentiles; horizontal bars: maximum and minimum values.*

Table 2-6. Number of samples above detection limit for each element, grouped by hydrofacies.

Element	Water category														Totals
	AR[1]	EYM	FmW	BM	EA	AM	WYM	WRV	SECF	JaF	PW	SW	P	PrW	
Ca	28	46	55	16	20	49	13	19	7	1	6	17	39	81	397
Mg	28	46	55	16	20	49	13	19	7	1	6	17	39	81	397
Na	28	46	55	16	20	49	13	19	7	1	6	17	39	81	397
K	28	46	55	16	20	49	13	19	7	1	6	17	39	81	397
Cl	28	46	55	16	20	49	13	19	7	1	6	17	39	81	397
HCO_3	28	46	55	16	20	49	13	19	7	1	6	17	39	81	397
SO_4	28	46	55	16	20	49	13	19	7	1	6	17	39	81	397
NO_3	21	38	49	12	16	41	9	17	7	1	2	1	18	77	309
SiO_2	28	46	54	16	20	48	13	19	7	1	6	17	24	76	375
NH_4	5	13	12	9	7	7	5	4	5	1	1	1	2	0	72
PO_4	17	27	37	3	13	17	8	11	7	1	2	1	5	0	149
F	26	44	53	16	20	45	12	19	7	1	4	17	23	78	365
I	12	28	11	16	2	2	9	12	6	1	1	6	0	0	106
Br	14	40	26	16	8	10	10	15	7	1	3	12	4	22	188
As	2	8	14	7	2	3	3	5	5	0	0	5	0	0	54
B	17	31	27	16	11	28	7	17	7	1	1	1	1	0	165
Sr	26	44	49	16	19	39	12	18	7	1	5	17	15	0	268
Li	22	46	48	16	15	40	13	17	7	1	5	17	2	0	249
U	11	30	29	14	10	14	7	10	7	1	1	1	1	0	136
δ^2H	16	45	46	16	12	14	12	14	6	1	6	1	29	0	218
$\delta^{18}O$	16	45	46	16	12	15	13	14	6	1	6	1	29	0	220
$\delta^{13}C$	13	44	37	16	11	14	13	14	6	1	3	1	0	0	173
^{14}C	12	41	43	14	10	15	11	12	6	1	3	0	0	0	168

[1]See Table 2-4 for abbreviations.

Ion-ion plots

Although most combinations of chemical variables have been explored, only those depicting clearly the main trends, limiting values and outliers are included here. The chemical variables that have given the most valuable information in the Yucca Mountain system are: major ions (Ca, Na, K, Mg, SO_4, Cl, HCO_3), the Na/Cl ratio, stable isotopes (deuterium, ^{18}O, and ^{13}C) and ^{14}C. Figure 2-6 to 2-9 plot the behaviour of the major ions and isotopes with respect to several compositional variables (chloride and bicarbonate in most cases, but also with respect to calcium, oxygen-18 and carbon-13) both in linear and logarithmic scales (in the latter case to better appreciate the low-concentration end). Chloride has been selected in most graphs as a tracer of "evolution" due to its conservative behaviour in most systems. Bicarbonate is also a good indicator of evolution in carbonate systems, although it is not necessarily a conservative element.

The word "trend" is used throughout the discussion that follows. It should be understood in a qualitative way, and not in its statistical sense (this is why the word "correlation" has not been used). In most cases the presence of a trend (meaning literally "following a general course" or "showing a tendency") will be clear from the scattergram. In other cases, where more than one trend can be appreciated in a single scattergram, two copies of it are presented: a "clean" copy and an annotated one, where the trends (already visible in the "clean" copy) are visually enhanced by means of coloured lines or arrows to guide the reader in the discussion.

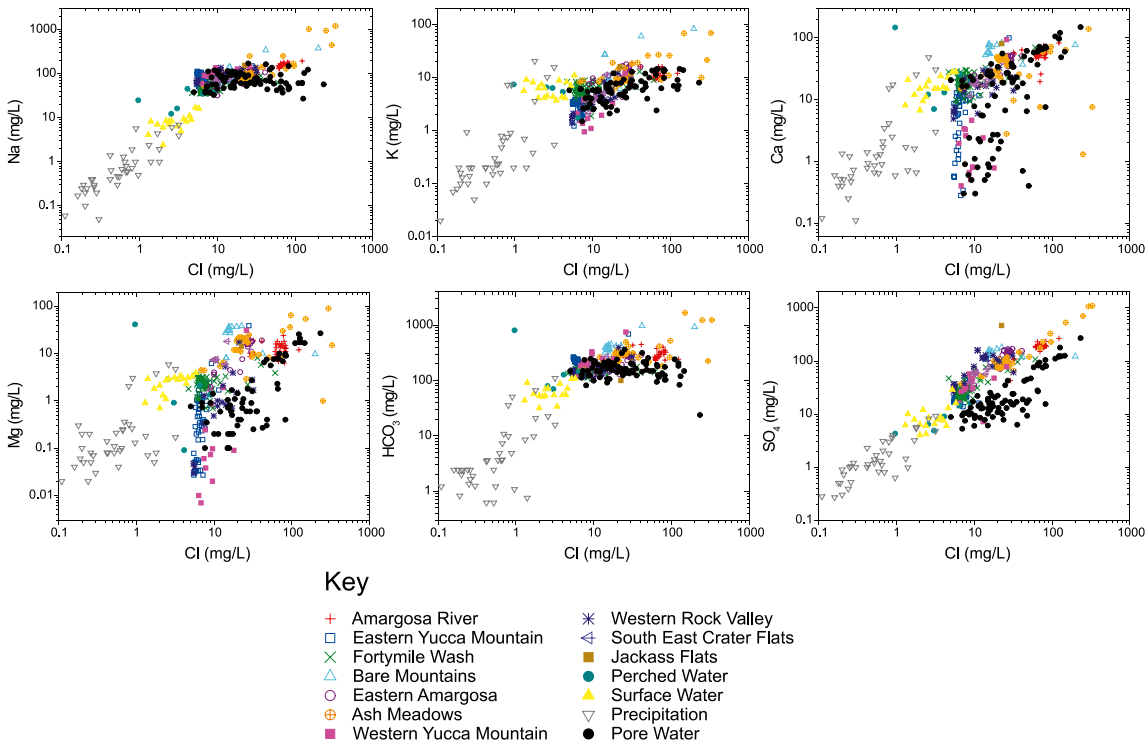

Figure 2-6. *Chloride versus the other major ions and isotopes in log-log scales*

Trends

Three observations are worth noting from the figures: (1) the presence of clear trends in some graphs, (2) the existence of limiting or threshold values in the concentration of specific elements and (3) the presence of outliers. We will deal with each observation separately.

Figure 2-6 shows that the best linear trend (in log-log scales) in the chloride plots is with sulphate. In general, the only water category that does not fit the correlation line is the pore water category (black circles), which is depleted in sulphate. The existence of this Cl-SO_4 trend means that sulphate is generally a conservative element in the system. The 1:1 *molar* ratio of chloride to sulphate for the entire range of compositions from 0.1 mg/L to 500 mg/L of Cl reflects the original ratio in Southern Nevada precipitation (Meijer 2002, CRWMS M&O 2007). This is an important point to remember.

As indicated in Figure 2-7, apart from the Cl-SO_4 trend, there are several other trends between Ca and Mg, Ca and Na, as well as between bicarbonate and the Na/Cl ratio. In Figure 2-7 two copies of the same graph are drawn side by side: the copy on the left is a non-annotated scattergram, while the copy on the right is an annotated version, in which specific samples are labelled and trends are visually marked using coloured lines.

The first trend worth mentioning is seen in Figure 2-7a: calcium and magnesium increase together in a linear way in log-log scales, with samples belonging to water categories interacting with the Tertiary Tuffs Aquifer in the lower left-hand corner, and those interacting with the Palaeozoic Carbonate Aquifer in the upper right-hand corner. Samples #306 and 307 (arrowed ellipse in the graphs in Figure 2-7) correspond to the two samples from borehole UE 25 p#1 that penetrate the deep carbonate aquifer underlying the thick volcanic pile at Yucca Mountain. They are clearly grouped together with the other water categories of the “carbonate trend” (Ash Meadows, Bare Mountains and South East Crater Flat). Although the scatter in the data is large, this can be appreciated in Figure 2-7b, where bicarbonate is plotted against the sodium-chloride ratio. There, waters from Bare Mountains, Ash Meadows and South East Crater Flat follow a separate trend, with samples #306 and 307 taken from the Palaeozoic Carbonate Aquifer belonging to this trend. In Figure 2-7b, not only are the two trends evident, but also the existence of a “mixing region” near the intersection of both trends in the lower left-hand corner of the graph. This is a first hint, which is substantiated below, to the effect that mixing actually takes place between the Palaeozoic Carbonate Aquifer, the Tertiary Tuffs Aquifer

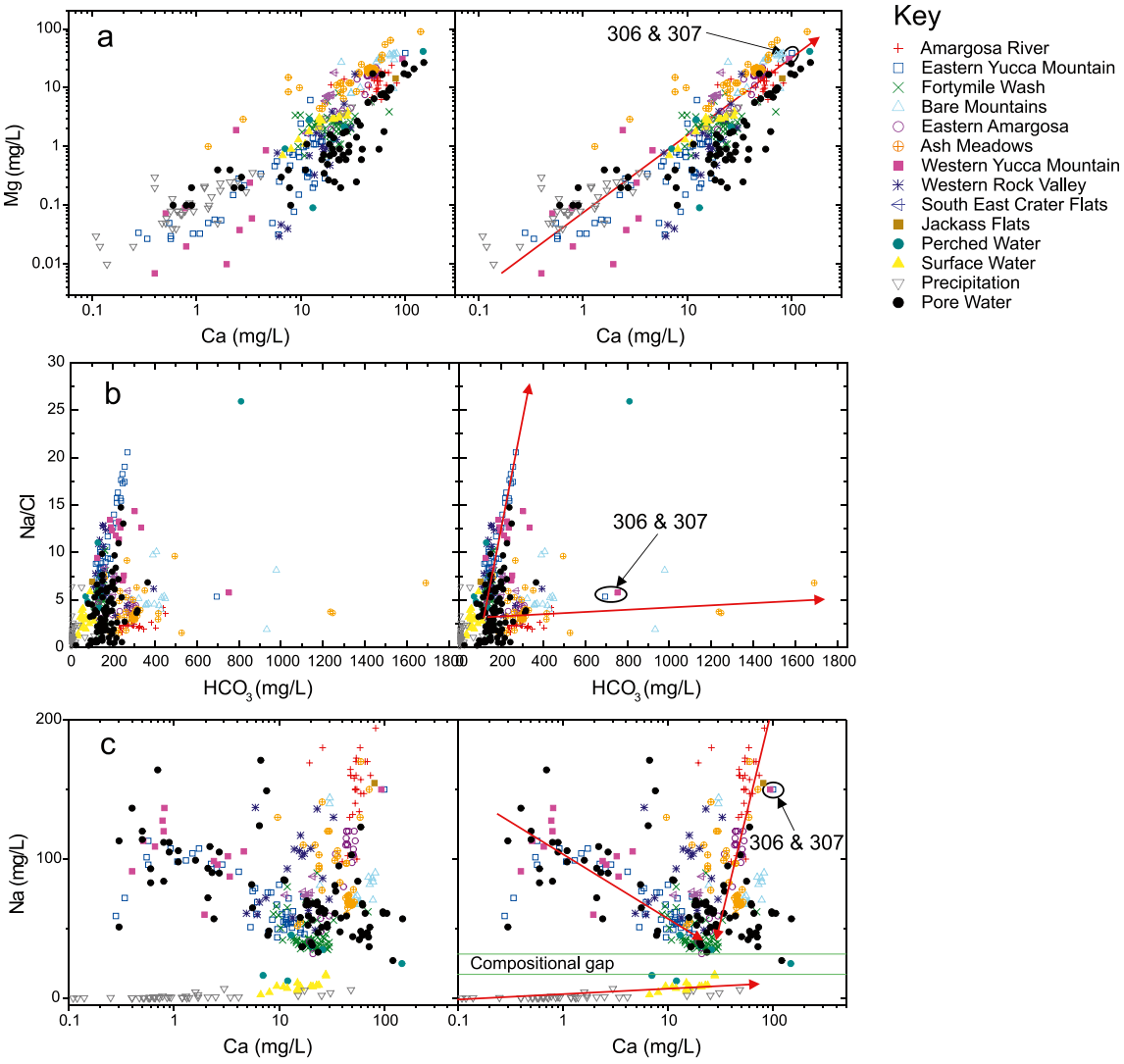

Figure 2-7. *Important trends in the raw dataset with respect to Mg, Ca, Na and bicarbonate. The graphs in the left-hand column are non-annotated, while their copies in the right-hand column are annotated. In this right-hand column, red trend arrows are drawn by eye and are not statistical fits. Ca and bicarbonate are always in the horizontal axis, while the vertical axis is occupied by Mg, Na or the Na/Cl relation. Note that the different axis scales for plots (a) are in log-log scales, for plots (b) they are in normal-normal scales and for plots (c) they are in log-normal scales.*

and the Quaternary Basin-fill Aquifer. The Tertiary Tuffs Aquifer appears to evolve through a rapid increase in the Na/Cl ratio with HCO_3, while the Palaeozoic Carbonate Aquifer evolves through a very slow increase in the Na/Cl ratio. Here also, samples #306 and 307 concur well with the "Palaeozoic Carbonate Aquifer trend", while all the other samples from the same water categories (belonging to the Eastern and Western Yucca Mountain hydrofacies) follow the "Tertiary Tuffs Aquifer trend".

The last row of graphs in Figure 2-7 shows the behaviour of Ca and Na in log-normal scales. Clearly, surface waters and precipitation samples follow a separate trend from the rest of the water categories. It is interesting to note the existence of a "compositional gap" between the Na concentration of the most concentrated surface waters (17 mg/L) and the Na concentration of the most diluted groundwaters of 35 mg/L (those from the Fortymile Wash hydrofacies). Only one perched water sample and one pore water occupy this compositional gap. This observation suggests that surface waters and precipitation do not play an important role (at the present time) in the main water budget of the Yucca Mountain area. On the other hand, the perched water samples seem to have continuity with the remainder of the groundwaters, occupying the position where the two trends followed by

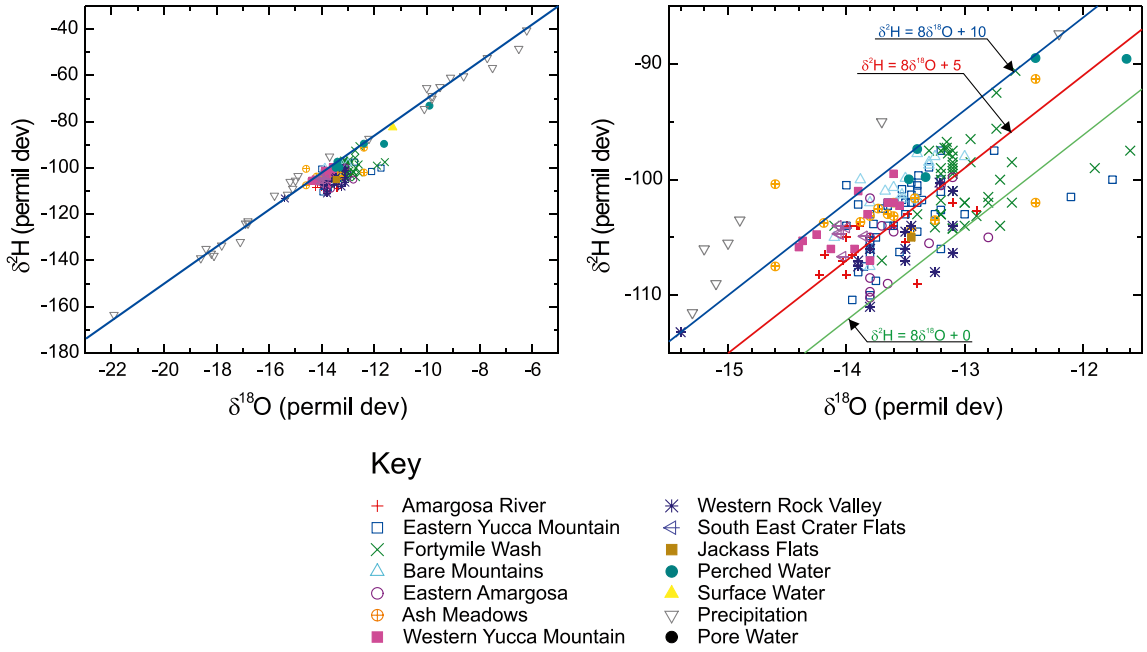

Figure 2-8. *Oxygen-18 versus deuterium plot. The graph on the left plots the complete range of values and the graph on the right only the central part, excluding most precipitation samples. The blue line is the global meteoric water line, the red line is a local palaeometeoric water line for southern Nevada and the green line marks the approximate location of waters affected by evaporation (to the right of the green line).*

the groundwater samples converge (Figure 2-7c, right-hand graph). The behaviour of the two trends differs. In one, Na and Ca increase together, while in the other Na and Ca change inversely (there is a decrease in Na when Ca increases). This latter trend is followed by the Eastern and Western Yucca Mountain hydrofacies, both of which interact with the Tertiary Tuffs aquifer. It has been suggested (Vaniman et al. 2001, Meijer 2002) that cation exchange between these two ions is an important process in the volcanic rocks in the Yucca Mountain area, and this inverse trend could be evidence of the actuation of such a process. However, there are other potential explanations, and a mixing hypothesis is favoured when the Eastern and Western Yucca Mountain hydrofacies are treated in detail below.

The final trend analysed here is that of oxygen-18 versus deuterium. Figure 2-8a shows the entire range of delta values including precipitation samples, whereas part (b) zooms in on the central part, excluding most precipitation samples. In both graphs, the blue line marks the global meteoric water line (Craig 1961). In the graph on the right, two other parallel lines are plotted: the red line is a local palaeometeoric water line for southern Nevada (White and Chuma 1987), and the green line is the "evaporation line" in the sense that waters plotting to the right of this line are probably affected by evaporation (Thomas et al. 1996). In this graph we again have a hint as to the role that is possibly played by evaporation in the waters of the Yucca Mountain area.

Limiting and threshold values

Several threshold values and limits are apparent in the raw dataset from a total-system perspective, as illustrated by Figure 2-9. Graph (a) shows how chloride in groundwaters has a minimum value of approximately 6 mgL^{-1}, whereas graphs (b) and (c) point to a minimum value for bicarbonate in groundwaters of some 110 mgL^{-1}. There are, of course, precipitation samples and surface water samples with lower Cl and HCO_3 concentrations, but no *groundwater* samples seem to fall below this threshold. Figure 2-6 also shows clearly the chloride threshold for groundwaters when plotted against calcium and magnesium. The most reasonable way of interpreting these threshold values is by invoking the existence of end-member waters with extreme compositions, which upon mixing with other waters give a range of compositions *limited* by these threshold values. This hypothesis is further developed below.

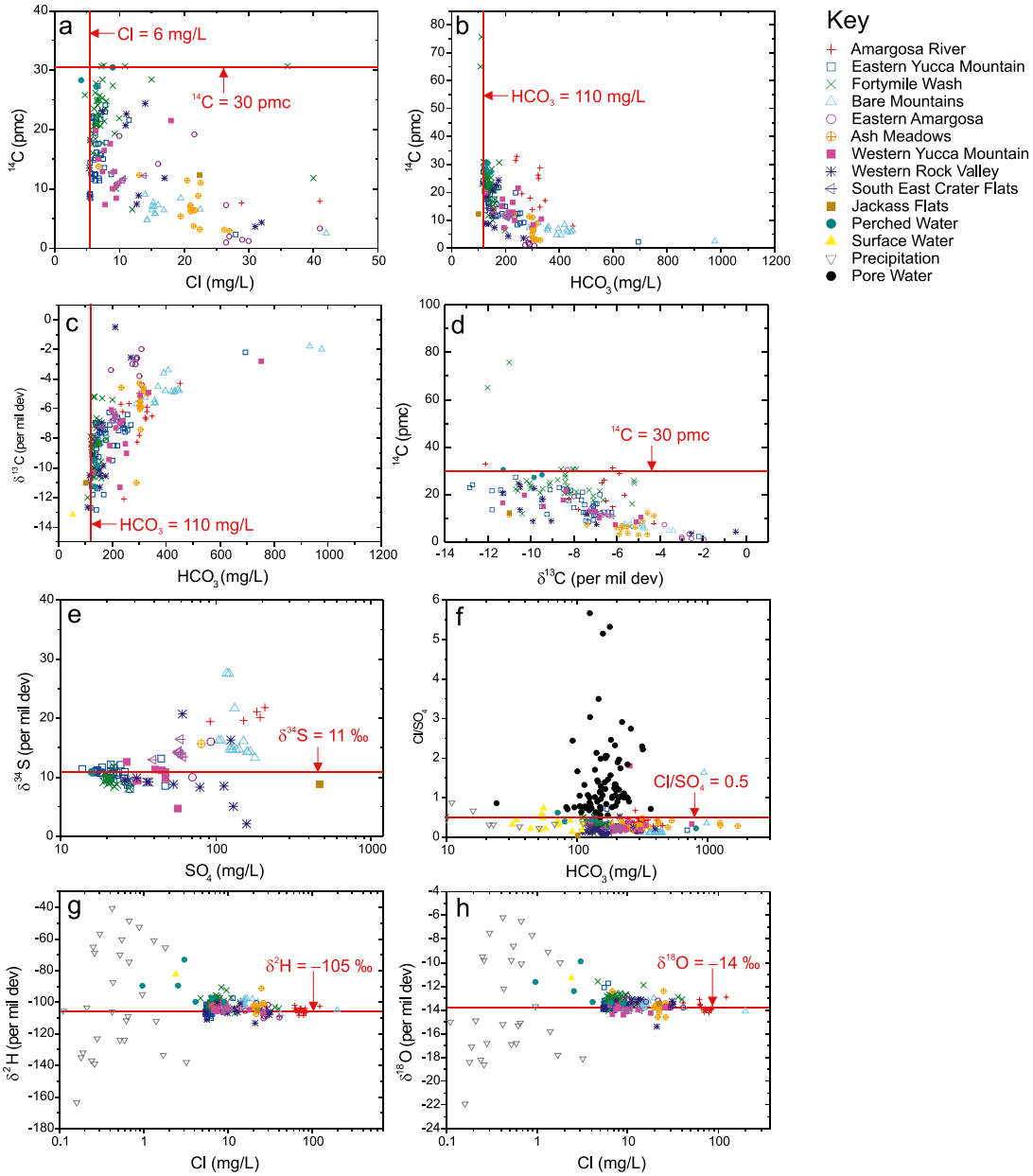

Figure 2-9. *Main limiting values discernible from the total-system exploratory analysis.*

Figure 2-9a, b and c show the existence of a threshold for ^{14}C. With the exception of two samples from the Fortymile Wash hydrofacies, no groundwater in the Yucca Mountain areas has a content of ^{14}C above 30 pmC. These same graphs also indicate the existence of a decreasing trend in ^{14}C against chloride, bicarbonate and $\delta^{13}C$.

As regards the Cl/SO_4 ratio, all groundwater, surface water, perched water and precipitation samples fall below the 1:2 ratio ($Cl/SO_4 < 0.5$). On the other hand, most pore waters have a Cl/SO_4 ratio above 0.5, although there is convergence in Cl/SO_4 ratio between pore waters and the remaining water types for a bicarbonate content close to the lower threshold of 110 mgL^{-1}. The connection zone is occupied by most of the perched water samples. This again points to the important role played by perched waters in the Yucca Mountain system.

Finally, the δ^2H, $\delta^{18}O$ and $\delta^{34}S$ values seem to converge to specific limiting values as chloride or sulphate content increase. Deuterium converges to –105 ‰, oxygen-18 to –14 ‰ and sulphate-34 to 11 ‰.

Outliers

The last observation that is worth noting from the total-system ion-ion plots is the existence of samples that are clearly way off the centre of gravity of the entire dataset. Figure 2-10 identifies the most obvious outliers (i.e. samples #2, #43, #44) together with some other potential ones (i.e. sample #256 or #160). The number of these samples is small but indicates the occurrence of extreme (and isolated) compositions that either do not follow specific trends or are separated by compositional gaps from the other samples. The total-system PCA that is presented below (see Figures 2-11 and 2-12) is also very useful for the identification of outliers and serves to improve this preliminary assessment. The samples identified as outliers will have a particular treatment when the hydrofacies exploratory analysis is carried out below.

Table 2-7 gives the maximum and minimum concentration values for all major and minor ions, stable isotopes and ^{14}C. It gives the concentration and the sample number, together with the hydrofacies to which the sample belongs. Only groundwater samples (including perched waters) have been used to compile the table in order to clearly appreciate their heterogeneity. From the table it is clear that the upper concentration values for many chemical species (10 species) are found in water samples from the Ash Meadows hydrofacies (samples #2, 22, 43, 44, and 56). The ranking is followed by the perched water samples, which have maximum values in three chemical species (samples #336 and 345), then the Eastern Yucca Mountain (sample #206), Western Rock Valley (samples #196 and 201) and the Bare Mountain hydrofacies (#251, 254) with maximum values in two species, and finally the Amargosa River (#160), Western Yucca Mountain (#224) and Fortymile Wash (#359) hydrofacies with maximum values in one chemical species.

It is also interesting to note that two hydrofacies (Ash Meadows and Eastern Yucca Mountain) have samples with the minimum and maximum concentration values. This is the case for SiO_2, where the minimum concentration is found in sample #44 (Ash Meadows) and the maximum concentration in sample #43 (Ash Meadows), and for iodine, with samples #314 (Eastern Yucca Mountain) having the minimum concentration value and sample #206 (Eastern Yucca Mountain) the maximum. This is an indication of extreme variability inside a hydrofacies, although it does not mean that all these samples are outliers. The hydrofacies exploratory analysis performed below will distinguish between outliers and extreme compositions.

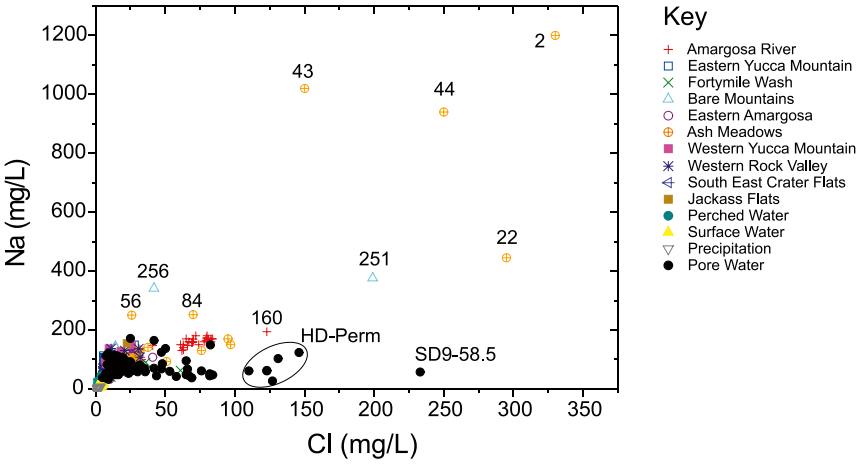

Figure 2-10. *Potential outlier samples identified in a Cl-Na ion-ion plot. Other potential outliers are also identified in Figure 2-12 below.*

Table 2-7. Maximum and minimum values for major and minor ions, stable isotopes and 14C. Only groundwater and perched water samples are included.

Species	Minimum Value	Sample #	Maximum Value	Sample #
Ca (mg/L)	0.28	340	147.7	336
Mg (mg/L)	0.007	319	90	22
Na (mg/L)	12.35	354	1,200	2
K (mg/L)	0.95	336	83	2
Cl (mg/L)	0.96	336	330	2
HCO_3 (mg/L)	70.4	345	1,690	43
SO_4 (mg/L)	4.3	336	1,100	2
NO_3 (mg/L)	0.02	25, 305, 326	62	160
SiO_2 (mg/L)	11	44	125	43
F (mg/L)	0.22	345	15	44
I (mg/L)	0.0005	314	0.16	206
Br (mg/L)	0.02	291, 345	15	206
As (µg/L)	1.25	259	38	196
B (µg/L)	80	21	12,000	44
Sr (µg/L)	0.5	319	7,700	56
Li (µg/L)	2	345	649	251
U (µg/L)	0.2	4, 259	10	224
δ^2H (‰)	–113.2	182	–73.1	345
$\delta^{18}O$ (‰)	–15.4	182	–9.9	345
$\delta^{13}C$ (‰)	–12.83	337	–0.5	201
$\delta^{34}S$ (‰)	2.1	231	27.6	254
^{14}C (pmc)	0.94	167	75.7	359

Principal Component Analysis

Principal Component Analysis (PCA) is a powerful multivariate statistical technique for the analysis of large datasets using at the same time information from multiple compositional variables (Gómez et al. 2006). In this sense, it resembles a multidimensional version of the ion-ion plots presented in the previous section. The ability to simultaneously plot many compositional variables allows a better visual understanding of the system, pointing to the presence of trends, correlation and outliers that cannot be seen in any of the previous ion-ion plots in isolation.

Figure 2-11 plots the PCA performed on the raw dataset. The three first principal components have been plotted in three different graphs: pc1-pc2 (upper left-hand graph), pc1-pc3 (upper right-hand graph), and pc2-pc3 (lower graph). Each principal component is clearly related to a particular chemical property of the water samples:

- The first principal component, pc1, is related to the total content of dissolved species, as indicated by the original variables (shown as an axis *eller* axes in the figure). All the ionic variables point to the left-hand side of the plot, indicating that the content of all the chemical species increases to the left. Only the Na/Cl ratio, which is not a concentration, does not follow this rule.
- The second principal component, pc2, is related to the Na/Cl ratio, which increases downwards in the pc1-pc2 graph and to the left in the pc2-pc3 graph. Consequently, samples with a high Na/Cl ratio have a large and negative pc2 co-ordinate.
- The third principal component, pc3, is related to the general water chemistry of the samples: Na-Cl waters (positive pc3 co-ordinate) versus Ca-Mg-HCO_3 waters (negative pc3 co-ordinate).

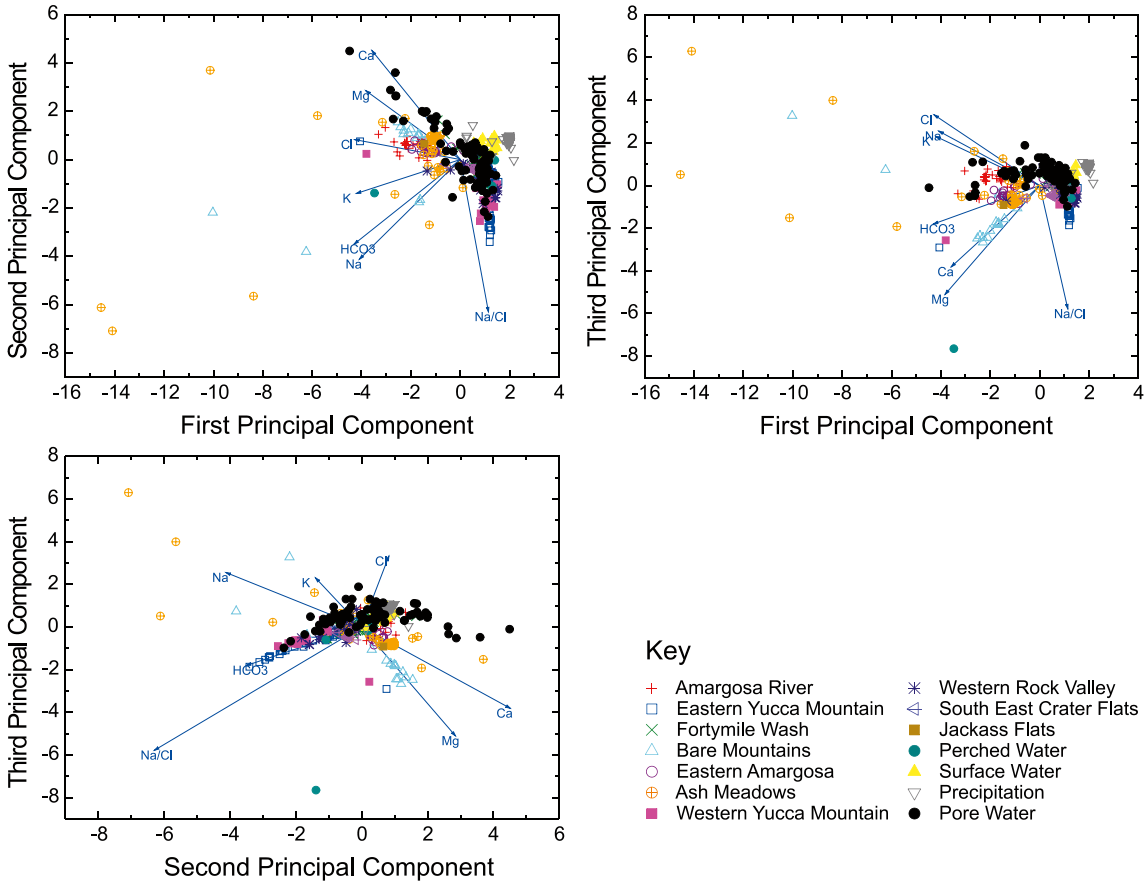

Figure 2-11. *Three views of the Principal Component Analysis of the raw dataset. The upper left-hand graph plots the first and second principal components, the upper right-hand graph plots the first and the third principal components and the lower graph plots the second and the third principal components. Blue vectors are the original variable axes.*

A PCA plot similar to the one in Figure 2-11 combines the information in a Piper diagram with that contained in several ion-ion plots viewed at the same time (amounting to all the possible combinations of two compositional variables). The usefulness and versatility of a PCA plot resides precisely in its ability to view the dataset from the most advantageous viewpoints, i.e. those that maximise the variance of the dataset in several mutually perpendicular axes. These axes are linear combinations of the original compositional variables and each one explains a decreasing amount of dataset variability. So, the first principal axis, pc1, "stores" the maximum amount of variance, followed by the second principal axis, pc2, which is perpendicular to the first one, and by the third principal axis, pc3, which is perpendicular to the other two. Each subsequent principal axis explains less and less variance, and is usually not taken into account.

Several trends are evident in the PCA plot of Figure 2-11. The most obvious ones are "the Na/Cl trend"– with a vertical orientation in the pc1-pc2 graph – which includes most samples from the Western and Eastern Yucca Mountain hydrofacies, and the "carbonate trend"– best observed in the pc1-pc3 and pc2-pc3 graphs following the Ca and Mg vectors – which includes many of the samples from the South East Crater Flat, Bare Mountains and Ash Meadows hydrofacies, together with samples #306 (Eastern Yucca Mountain) and #307 (Western Yucca Mountain), taken at depth in the Palaeozoic Carbonate Aquifer under Yucca Mountain.

In addition to identifying trends, PCA plots are excellent tools for outlier screening, as the location of a sample in the plot is more extreme (in the sense of being far from the centre of gravity of the dataset, located at the origin of coordinates) the more extreme its *global* composition is (as opposed to extreme compositions in only one or two compositional variables). Figure 2-12 labels the most obvious outliers (numbered) identified in the PCA of the raw dataset. Again, as in the case of outlier

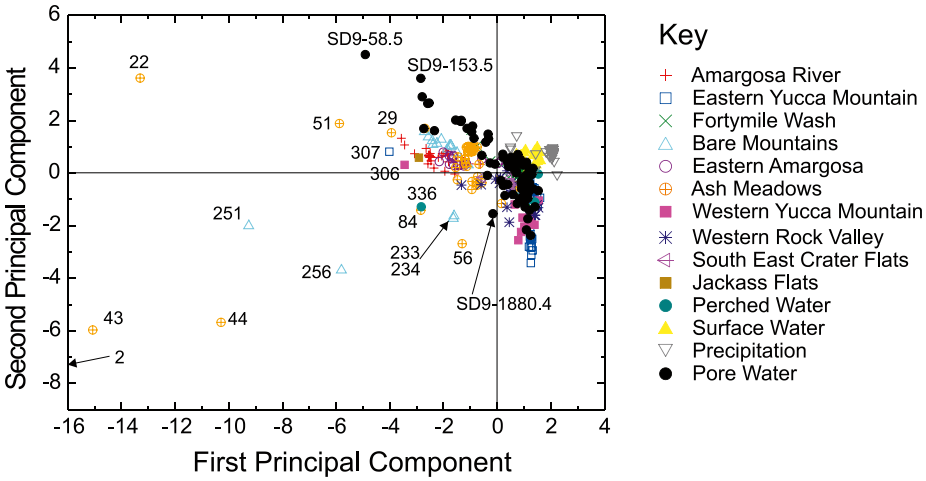

Figure 2-12. *Most obvious outlier samples identified in the PCA (labelled with sample ID).*

screening by means of ion-ion plots, few samples belong to the category of outliers (remember that an outlier is defined here as a sample plotting far from the centre of gravity of the whole dataset); and if we compare the samples labelled in this figure with those labelled in Figure 2-10 and those presented in Table 2-7, we see many coincidences. All these samples will be analysed in the hydrofacies exploratory analysis.

2.4.2 Hydrofacies exploratory analysis

This section is dedicated to the exploratory analysis of each water category. The analysis starts with the ten groundwater categories and then continues with the other four water categories (perched waters, pore waters, surface waters and precipitation). The analysis of the groundwater hydrofacies starts with those at Yucca Mountain itself, followed by hydrofacies to the west and east of Yucca Mountain, and finally the hydrofacies south of Yucca Mountain (in the Amargosa River Valley).

Eastern Yucca Mountain (□)

The samples of the Eastern Yucca Mountain hydrofacies have been collected from several boreholes in the eastern reaches of Yucca Mountain itself (Figure 2-13), in a north-south transect of approximately 30 km.

The southern samples are from Nye County EWDP boreholes, and several of them actually perforate the Quaternary basin-fill deposits before reaching the Tertiary Tuffs Aquifer. The northern samples belong to several UE-25 and USW boreholes, and all of them perforate the Tertiary volcanic unsaturated formations before reaching the saturated zone, also in Tertiary volcanic rocks. Only borehole UE-25 p#1 reaches the Palaeozoic carbonate rocks located under the pile of Tertiary volcanic tuffs. Sample #307 was taken at the bottom of the borehole and is one of only two samples (sample #306 is the other) that can be used as being "representative" of the groundwaters in the Palaeozoic Carbonate Aquifer flowing under Yucca Mountain.

From the samples taken in NC-EWDP boreholes at several depths, cutting different aquifers, those from NC-EWDP 9D borehole are especially interesting because they show a mixing line between the Tertiary Tuff and Quaternary Alluvial waters. Figure 2-14 shows a summary lithology log of borehole 19D with the location of the packed-off sections where the samples were taken. Samples #204 to 207 are special as they were collected during a tracer test in which there was in-borehole mixing of waters from the two aquifers, i.e. the Quaternary Basin-fill Aquifer, where the samples were taken, and the Tertiary Tuffs Aquifer below. Consequently, sample #204 is the most "contaminated" with waters from the lower tuffs aquifer, while sample #207 is the least contaminated. The linear mixing trends resulting from this artificial mixing are evident from the graphs in Figure 2-14, especially in the one for HCO_3-Na. The other packer-isolated samples collected in the same borehole also follow this mixing line, although no in-borehole contamination was reported in this case. An especially

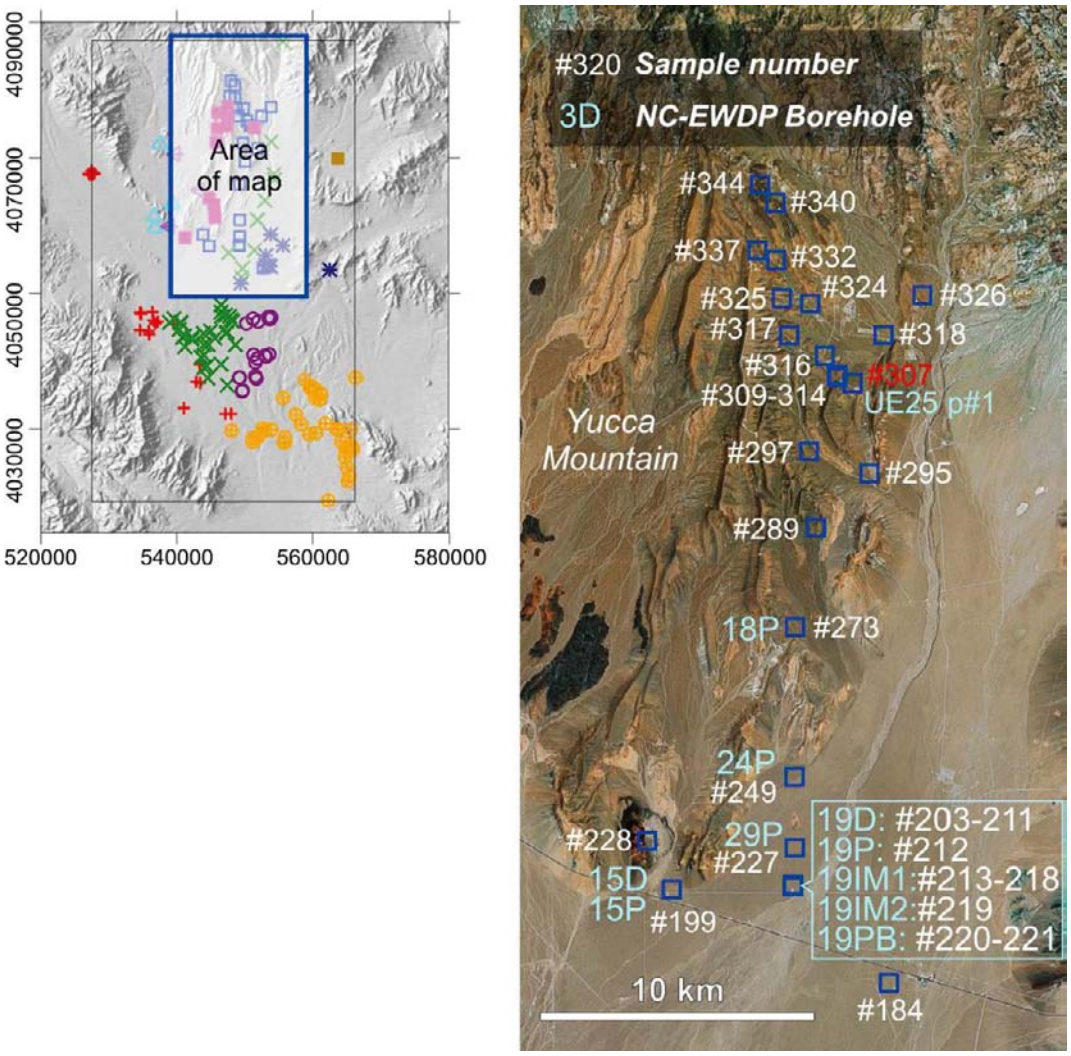

Figure 2-13. *Location map of the samples from the Eastern Yucca Mountain hydrofacies. Sample #307 from borehole UE25 p#1 was taken in the Palaeozoic Carbonate Aquifer that underlies the thick pile of Tertiary tuffs at Yucca Mountain. This sample has been omitted from the analysis carried out in this section (as the analysis is aimed at the behaviour of the Tertiary Tuffs Aquifer), but is not excluded from the final dataset and will be used in a subsequent section.*

interesting aspect is that most of the other samples from the Eastern Yucca Mountain hydrofacies, coming from other boreholes, also follow the same mixing line (Figure 2-14), which suggests that both aquifers have a hydraulic connection.

The two mixed waters have a very similar chloride concentration, as the Cl-Na graph shows, with values of approximately 6 mg/L for both end-member waters. On the other hand, the concentrations of bicarbonate, calcium and sodium are very different. Also, from the HCO_3-^{14}C plot, it appears that the Tertiary Tuff waters below Yucca Mountain have a ^{14}C content of approximately 10 pmC, while that of the Quaternary basin-fill waters is higher (30 pmC).

In summary, sample #211 seems to be most representative of the composition of the Tertiary Tuff aquifer waters and is thus proposed for selection as a candidate end-member. Several samples can be proposed as candidates for the Quaternary basin-fill end-member (e.g. sample #207) although it is quite possible that some mixing with the Tertiary Tuff end-member is present even in the most extreme waters (those located in the lower left-hand corner of the HCO_3-Na graph in Figure 2-14). Table 2-8 summarises the main chemical characteristics of both potential end-members.

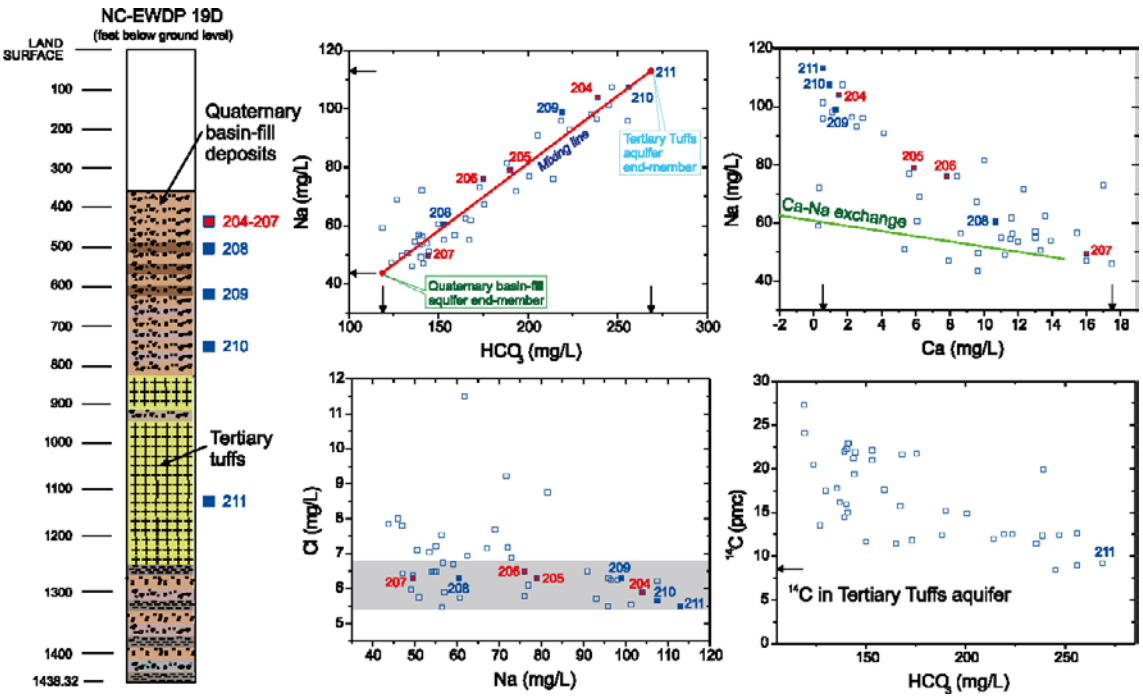

Figure 2-14. *Mixing line between the Tertiary Tuffs and Quaternary Basin-fill Aquifers.*

Table 2-8. Chemical characteristics of two potential end-member waters.

Ion	Tertiary tuffs end-member (#211)	Quaternary basin-fill end-member
pH	8.9	8.0
Cl (mg/L)	5.5	6–8
HCO_3 (mg/L)	268.7	120–140
SO_4 (mg/L)	20.3	15–25
Ca (mg/L)	0.57	16–18
Na (mg/L)	113	40–50
^{14}C (pmC)	9.2	20–35

The general trend of the Ca-Na graph in Figure 2-14 is reminiscent of a cation-exchange process. This process has been identified in pore waters in the unsaturated zone at Yucca Mountain (Meijer 2002, Vaniman et al. 2001). However, cation-exchange is a thermodynamically fast process that occurs in zeolitised sections of the tuffs, already in the unsaturated zone. By the time these waters reach the saturated zone, they have acquired the cation-exchange signature of low divalent cation (Ca+Mg), high monovalent cation (Na+K) concentrations. For this reason, the main trends shown in Figure 2-14 are interpreted as mixing. The imprint of a Ca-Na exchange is the subset of samples that plot near the 1:2 molar ratio line and that clearly depart from the main mixing line in the Ca-Na graph in Figure 2-14. This additional trend suggests that some of the waters in the Tertiary Tuff Aquifer have passed through zeolitised tuffs before reaching the saturated zone whereas others have not. Few unsaturated-zone waters have been analysed for strontium isotopes, but the few that do have Sr isotopes data would appear to support this hypothesis (Sonnenthal and Bodvarsson 1999).

Western Yucca Mountain (■)

As the name suggests, the samples belonging to this hydrofacies are generally located on the west side of the crests that conform to the topmost part of Yucca Mountain. In addition to these samples, several others – located south of the main elevation – have been collected in NC-EWDP boreholes (Figure 2-15). Most samples were taken in Tertiary tuffs, although the boreholes in the southern part have Quaternary and Tertiary basin-fill deposits near the surface. Sample #306, collected at the bottom of borehole UE 25 p#1 in the Palaeozoic Carbonate Aquifer, has been omitted from the analysis.

Figure 2-16 plots the samples from the Eastern and Western Yucca Mountain hydrofacies together, using the same ion-ion and ion-isotopes plots as in Figure 2-14. As the geographic location and rock types are very similar in both hydrofacies, it is likely that their chemistry is also similar. In general terms, the plots confirm this hypothesis, although there are also obvious differences. In the bicarbonate-sodium plot, samples from this hydrofacies follow the mixing trend defined by the Eastern Yucca Mountain samples. As the occurrence of Quaternary basin-fill deposits in the Western Yucca Mountain hydrofacies is low compared with the Eastern part, most samples plot near the Tertiary tuffs end-member (two samples even further apart). Sample #327 seems to be an exception and a difficult one to interpret because this sample comes from the northernmost site, where no Quaternary basin-fill deposits exist. However, the Ca-Na graph shows that this sample plots on the Ca-Na exchange line, not on the mixing line.

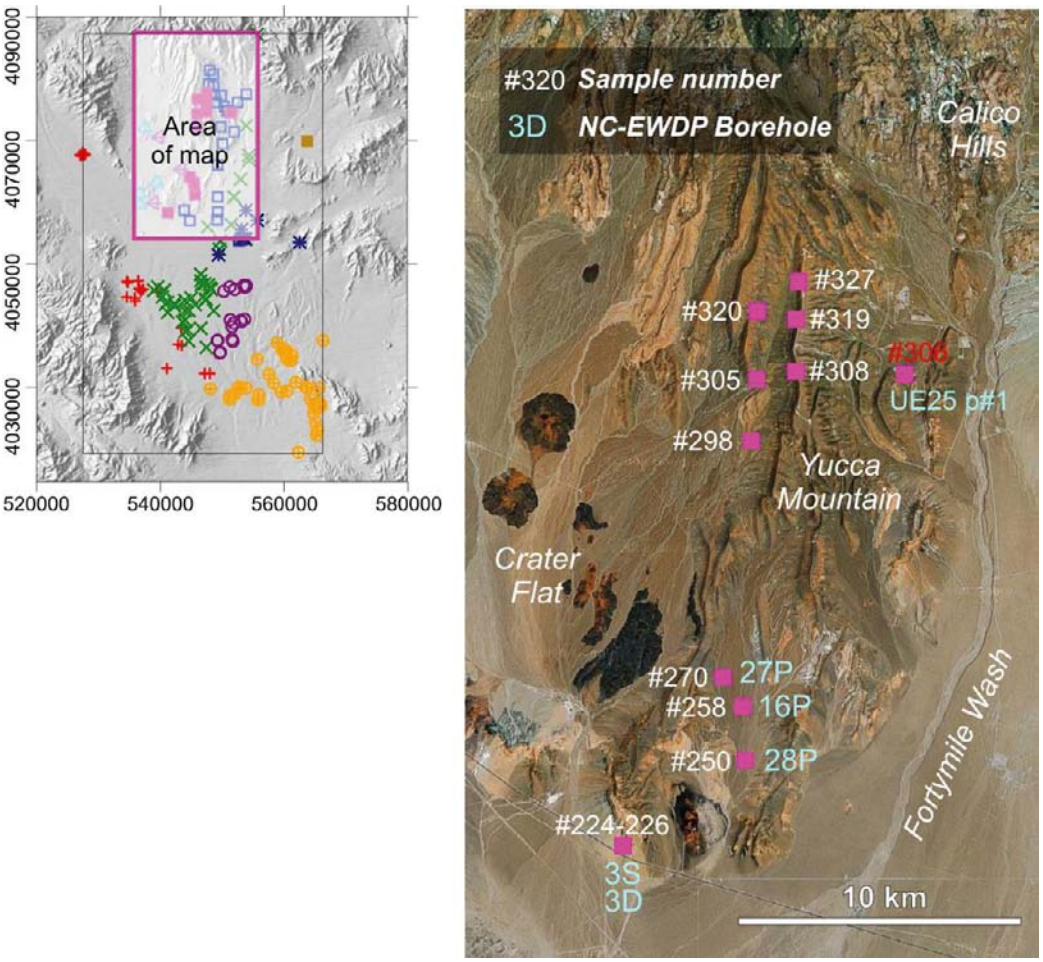

Figure 2-15. *Location map of the samples from the Western Yucca Mountain hydrofacies. Sample #306 from borehole UE25 p#1 was taken in the Palaeozoic Carbonate Aquifer that underlies the thick pile of Tertiary tuffs at Yucca Mountain. This sample has been omitted from the analysis carried out in this section.*

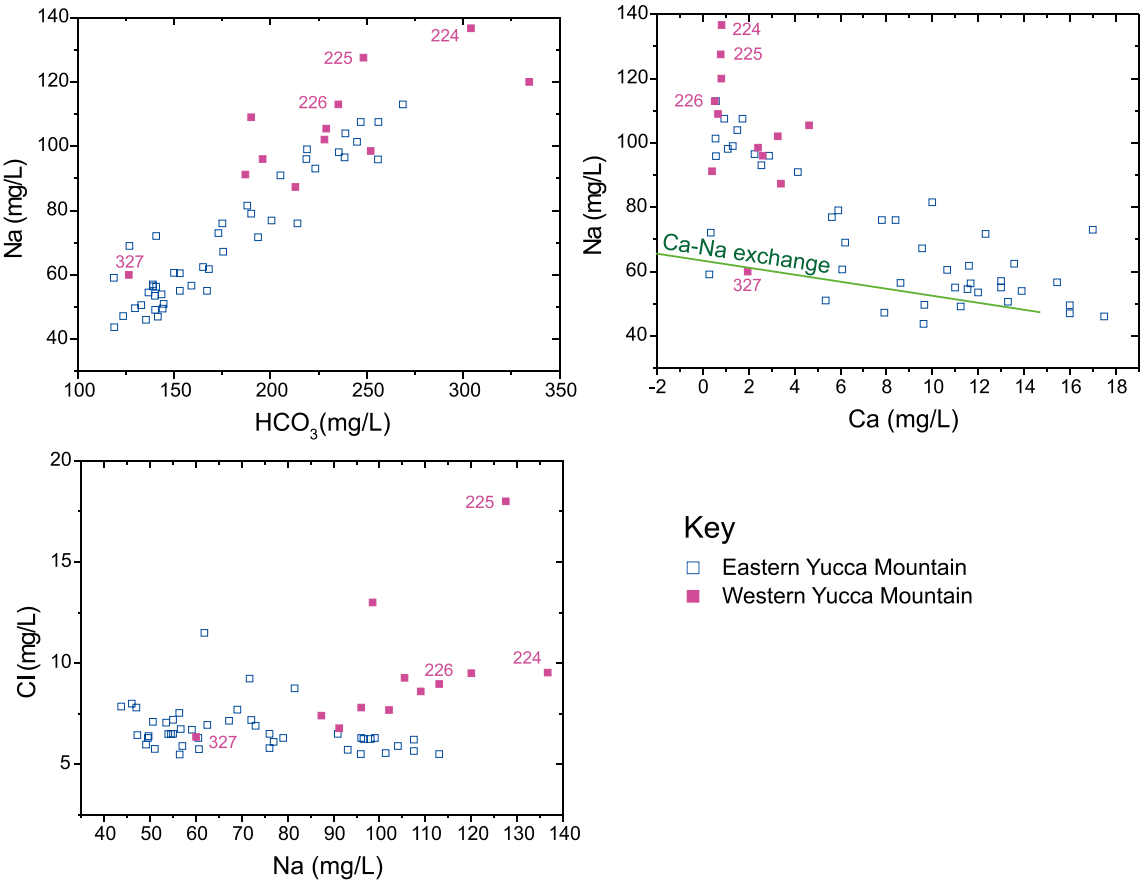

Figure 2-16. *Comparison of compositional trends in the Western and Eastern Yucca Mountain hydrofacies.*

The Ca-Na plot shows that several Western Yucca Mountain samples are more depleted in Ca than their Eastern Yucca Mountain counterparts, suggesting a more widespread occurrence of cation-exchanged waters. This highly exchanged water comes from boreholes NC-EPDP 3S and 3D in the southernmost part of the area.

Chloride concentration is also somewhat higher than in the Eastern Yucca Mountain samples. However, with the exception of these differences, it can be safely concluded that both hydrofacies are affected by the same basic processes, i.e. mixing and cation-exchange, although the intensity of both is reversed.

Bare Mountain (△) and South East Crater Flat (◁)

The samples of these two hydrofacies are similar both geographically and chemically. They are located in Crater Flat, a smooth surface limited in the west by the Bare Mountains and in the east by Yucca Mountain (Figure 2-17). Several samples have been collected close to the southern border of the area, near the Amargosa River Valley. Most samples come from packed sections in NC-EWDP boreholes, except for samples #293 (Bare Mountains hydrofacies) and #296 (South East Crater Flat hydrofacies), which were taken in open boreholes USW VH-1 and USW VH-2, respectively.

Chemically, the waters of both hydrofacies have a clear carbonate signature (see Figures 2-7 and 2-11 above). However, they have different TDS, with the South East Crater Flat samples being a diluted version of the Bare Mountains samples, as shown by Figure 2-18.

Four samples are clearly anomalous, as shown in the graphs in Figure 2-18. Sample #251 has very high Cl contents and sample #256 very high bicarbonate contents. Both also have a very poor charge balance, suggesting some kind of analytical error. On the other hand, samples #233 and 234 are anomalous in their Ca/HCO_3 and Mg/HCO_3 ratios, which is translated into a rather large degree of undersaturation with respect to calcite (and also dolomite). For these reasons, samples #233, 234, 251, and 256 have been omitted from further analysis.

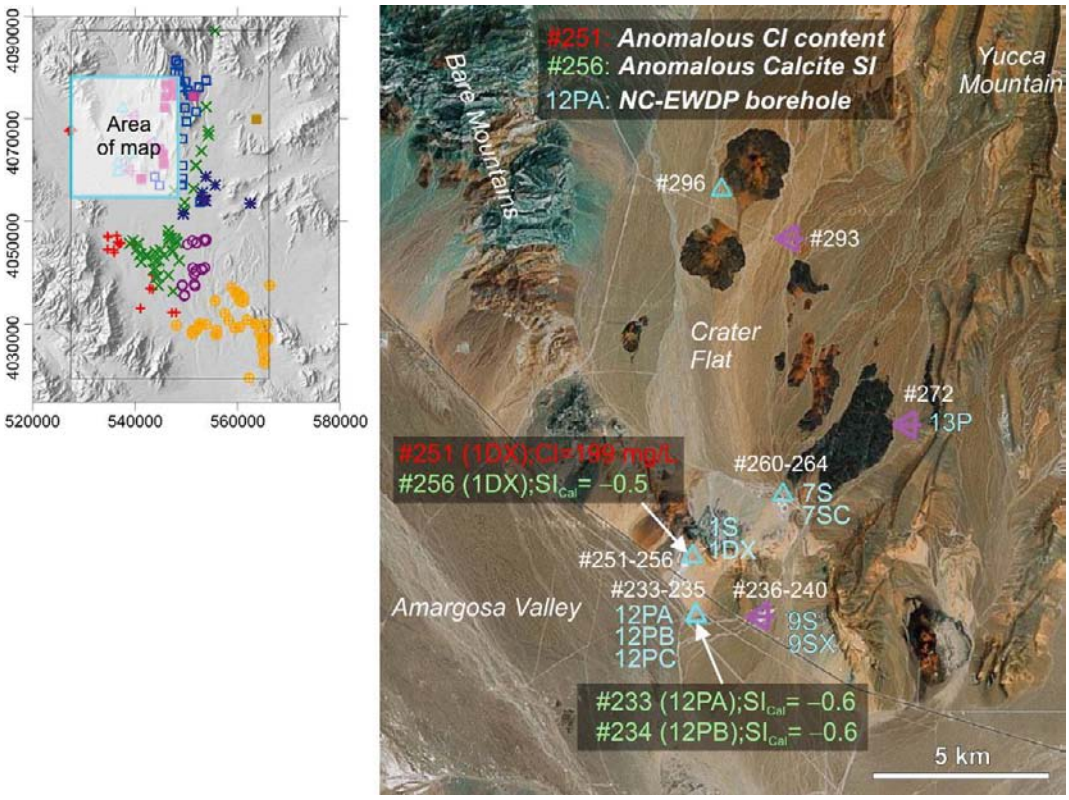

Figure 2-17. *Location map of the samples from the Bare Mountain (up triangle) and South East Crater Flat (barred left triangle) hydrofacies. Samples with anomalous Cl concentrations and calcite saturation indices have been highlighted.*

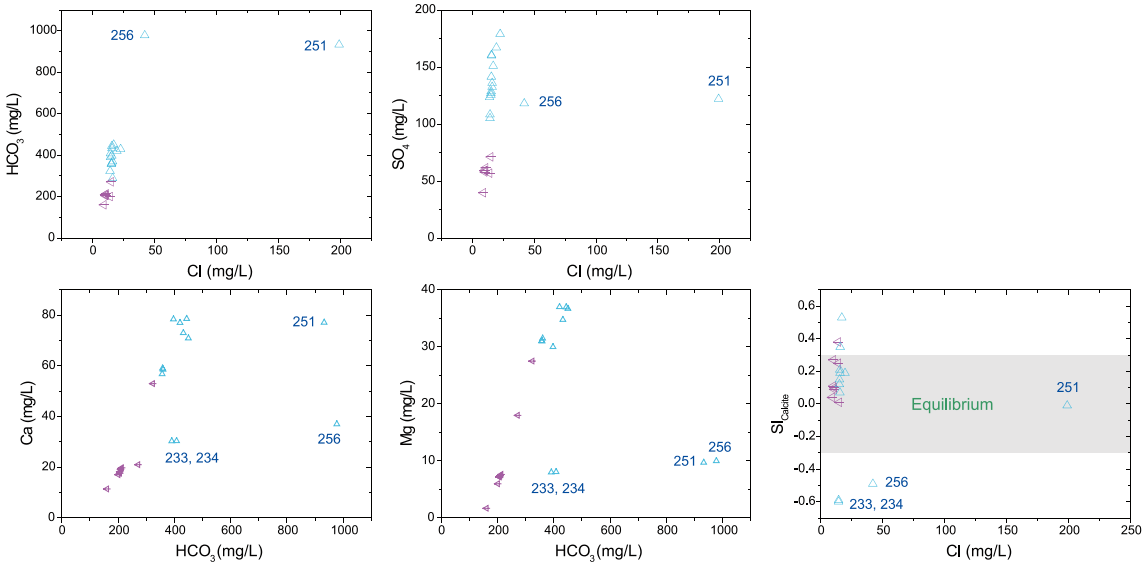

Figure 2-18. *Anomalous samples in the Bare Mountains (up triangles) and South East Crater Flat (barred left triangles) hydrofacies. All four anomalous samples have been eliminated from further analysis.*

Once these four samples have been eliminated, the remaining samples follow clear trends when SO_4 is used as a proxy for evolution. Here, "evolution" could mean water-rock interaction, evaporation, mixing, or any other process that gradually changes the chemistry of the waters. Among all possible processes, dedolomitisation has been invoked elsewhere as the main process controlling the hydrochemistry of carbonate aquifers in contact with gypsum (Plummer et al. 1990).

The trends followed by samples from the Bare Mountains and South East Crater Flat hydrofacies are reminiscent of a dedolomitisation process (Figure 2-19), except for the increase in bicarbonate with sulphate.

Dedolomitisation in a carbonate aquifer is a process driven by the presence of gypsum in the matrix or the fractures of the aquifer. At the start of the process, the waters are undersaturated with respect to gypsum. The dissolution of gypsum increases the concentration of Ca in the groundwaters which is then followed, promoted by the common ion effect, by the precipitation of calcite. As calcite precipitation takes place, pH and alkalinity decrease and the partial pressure of CO_2 increases. This generates an undersaturation state for dolomite, which is thus dissolved, thereby increasing the concentration of Mg in the waters. In summary, as the concentration of sulphate increases, Ca, Mg and P_{CO2} also increase, and pH and alkalinity decrease. As Figure 2-19 shows, all the trends – except for alkalinity – are compatible with a dedolomitisation process.

To assess quantitatively the dedolomitisation hypothesis, several PHREEQC reaction-path simulations have been performed. Two different samples have been used as the initial water: #240 and #293 (both from the South East Crater Flat hydrofacies). The addition of gypsum is the irreversible process that drives dedolomitisation; a total of 1.5 mmol of gypsum in 100 steps have been added to span the

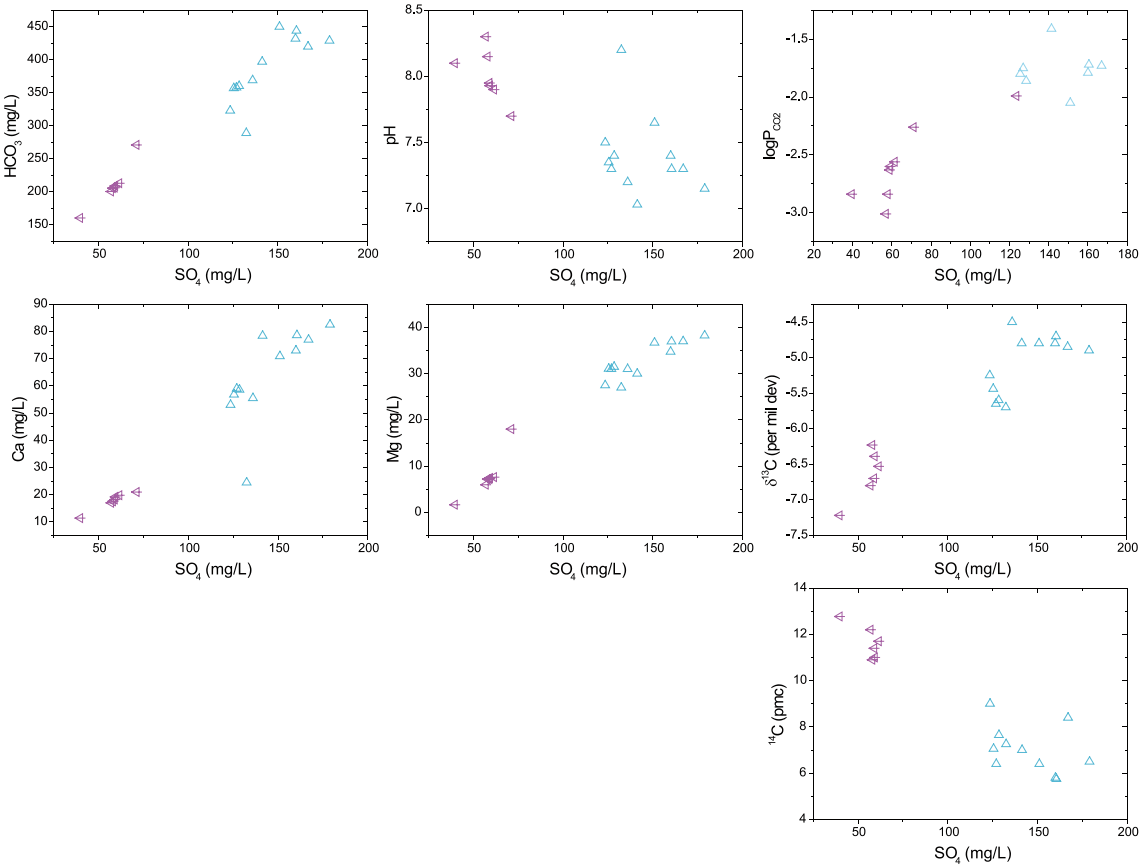

Figure 2-19. *Evolution trends in the chemistry of the waters from the Bare Mountains (up triangles) and South East Crater Flat (barred left triangles) hydrofacies. Sulphate has been selected as a tracer of evolution because dedolomitisation is a plausible process.*

measured sulphate concentration in groundwaters. In each reaction step, equilibrium with calcite and ordered dolomite has been imposed in a set of simulations, or with calcite and disordered dolomite in another set of simulations. The thermodynamic data have been taken from the WATEQ4F database distributed with the PHREEQC code.

Figure 2-20 shows, as a red line, the results from one of the dedolomitization simulations (sample #240 as initial water; equilibrium with calcite and ordered dolomite). The other simulations are not presented as the results are quantitatively very similar. It can be appreciated that no trend is quantitatively reproduced, although qualitative tendencies are compatible with a dedolomitisation process in all cases apart from the alkalinity (bicarbonate) trend. Here the discrepancy is large because dedolomitisation implies a decrease in alkalinity with reaction progress. However, the observations made in the South East Crater Flat and Bare Mountain samples indicate the opposite trend: a large increase in alkalinity with sulphate. We conclude that dedolomitisation is not the process that is responsible for the chemistry of these waters.

However, dedolomitisation is not the only process that is capable of explaining the trend shown in Figure 2-19. Mixing between two suitable end-member waters is also a possibility. Another set of PHREEQC simulations has been performed with samples #264 and 293 as end-members. These are the most and least "evolved" waters in the combined Bare-Mountains + South East Crater Flat dataset. As Figure 2-19 shows, mixing between these two end-member waters could explain the trends observed, although with a certain scatter in several of the graphs. This points to the intervention of other processes on top of first order mixing. The chemical composition of the two end-member waters is presented in Table 2-9. Sample #264 can be considered as a potential end-member for the Palaeozoic Carbonate Aquifer waters. The more diluted SECF samples have a large contribution from a shallower component, either a shallow basin-fill groundwater or a "meteoric" water.

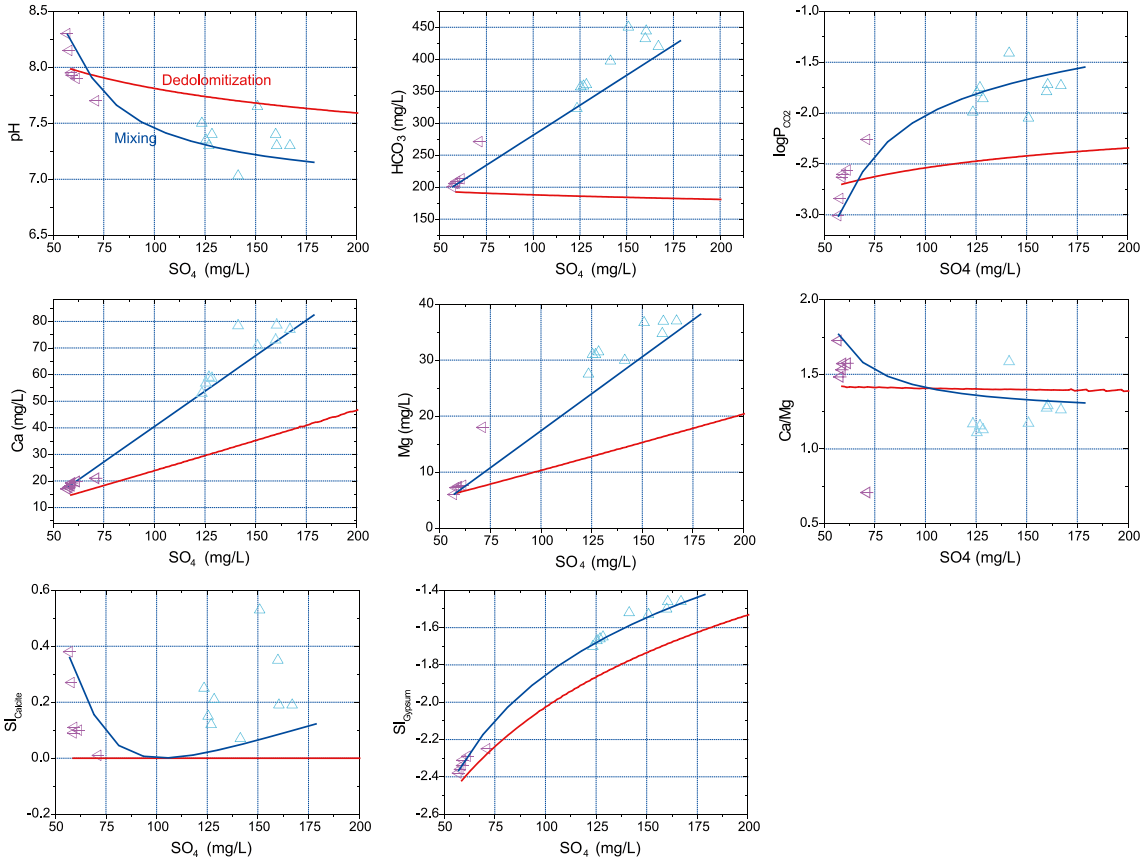

Figure 2-20. *PHREEQC simulations of dedolomitisation (red line) and binary mixing (blue line) superimposed onto the Bare Mountains (up triangles) and South East Crater Flat (barred left triangles) samples.*

Table 2-9. Chemical characteristics of the two end-member waters used in the mixing simulations carried out with PHREEQC.

	Initial water (#293) (South East Crater Flat)	Final water (#264) (Bare Mountains)
pH	8.1	7.15
Cl (mg/L)	8.8	22.5
HCO_3 (mg/L)	160.3	429.0
SO_4 (mg/L)	39.6	179.0
Ca (mg/L)	11.4	82.5
Mg (mg/L)	1.7	38.5
Na (mg/L)	74.1	90.0
$\delta^{18}O$ (‰)	–14.3	–13.5
^{14}C (pmC)	12.8	6.5

Jackass Flat (■)

Jackass Flat is a smooth area east of Yucca Mountain, separated from it by Fortymile Wash. Its northern limit is the Calico Hills and its southern limit the Skull Mountains. Fortymile Wash connects Jackass Flat with the Amargosa River Valley to the South (Figure 2-21).

Only one sample (#291) is available from this region, collected in borehole UE25-J11. The water table was intersected at a depth of 317 m (REF) and the sampling interval includes the whole length of the borehole down to 405 m (open borehole sampling). The rocks of the saturated zone at the borehole site are tertiary basalts and tuffs. (CRWMS M&O 2007) made the assumption of considering this sample as being representative of the waters that flow under Jackass Flat. In this assessment, a different point of view is taken. Sample #291 is not considered *a priori* representative of the chemistry of the groundwaters in this part of the studied domain. An *a posteriori* decision will be taken based on the mixing analysis carried out with the M3 code below. Thus, sample #291 is selected as a potential end-member water and its main chemical characteristics are shown in Table 2-10.

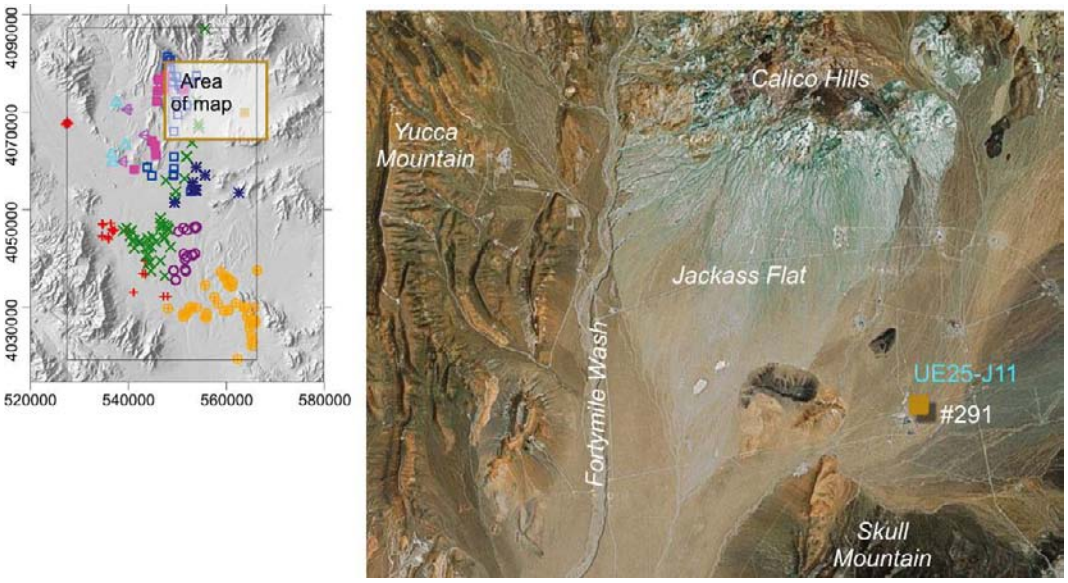

Figure 2-21. *Location map of the sample from the Jackass Flat. Only one sample is available from this geographical area and hydrofacies (sample #291, borehole UE25-J11).*

Table 2-10. Chemical characteristics of sample #291 (Jackass Flat hydrofacies).

Ion	Jackass Flat (sample #291)
pH	7.9
Cl (mg/L)	22.4
HCO_3 (mg/L)	100.6
SO_4 (mg/L)	467.2
Ca (mg/L)	80.8
Mg (mg/L)	14.4
Na (mg/L)	154.5
^{14}C (pmC)	12.3

Western Rock Valley (✳)

Samples from the Western Rock Valley hydrofacies are located near the south-eastern end of Yucca Mountain, between Fortymile Wash and the Specter Range (Figure 2-22). All samples except one have been taken in the flat area delimitated by Fortymile Wash and the foothills of the Specter Range. The only exception is sample #182, which was collected in a hilly area of the Specter Range.

This dataset consists of 18 samples with Cl contents of between 5 and 32 mgL^{-1} following quite simple increasing trends with Na, HCO_3, Mg, etc. The only clear departure from this trend is sample #182, which has high HCO_3 and Mg values (actually this sample is oversaturated in dolomite and in equilibrium with magnesite, whereas all the other samples in the dataset are undersaturated in dolomite and magnesite). For all these reasons, sample #182 has been excluded from the dataset.

The Cl-^{14}C plot again suggests a mixture with a low-Cl, high-^{14}C end-member. When this mixing proportion is low (low ^{14}C values), the Cl content of the waters is in the range of 30 mgL^{-1}. This is a further indication that the Quaternary Alluvial waters, when not "contaminated" by the precipitation end-member, have a Cl concentration of the order of 30 mgL^{-1}. Although low in comparison with groundwaters elsewhere, this amount of chloride (30 mgL^{-1}) seems to be the highest in the whole Yucca Mountain dataset when evaporation is excluded.

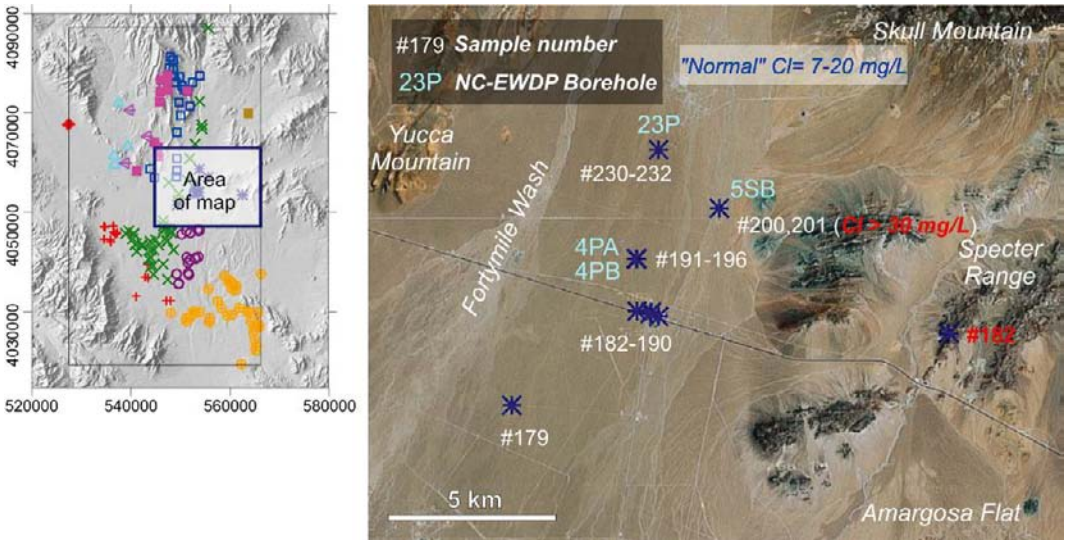

Figure 2-22. *Location map of the samples from the Western Rock Valley. Two samples with an anomalous chloride concentration are highlighted (samples #200 and 201). Sample #182 has been excluded from the final dataset, as discussed in the text.*

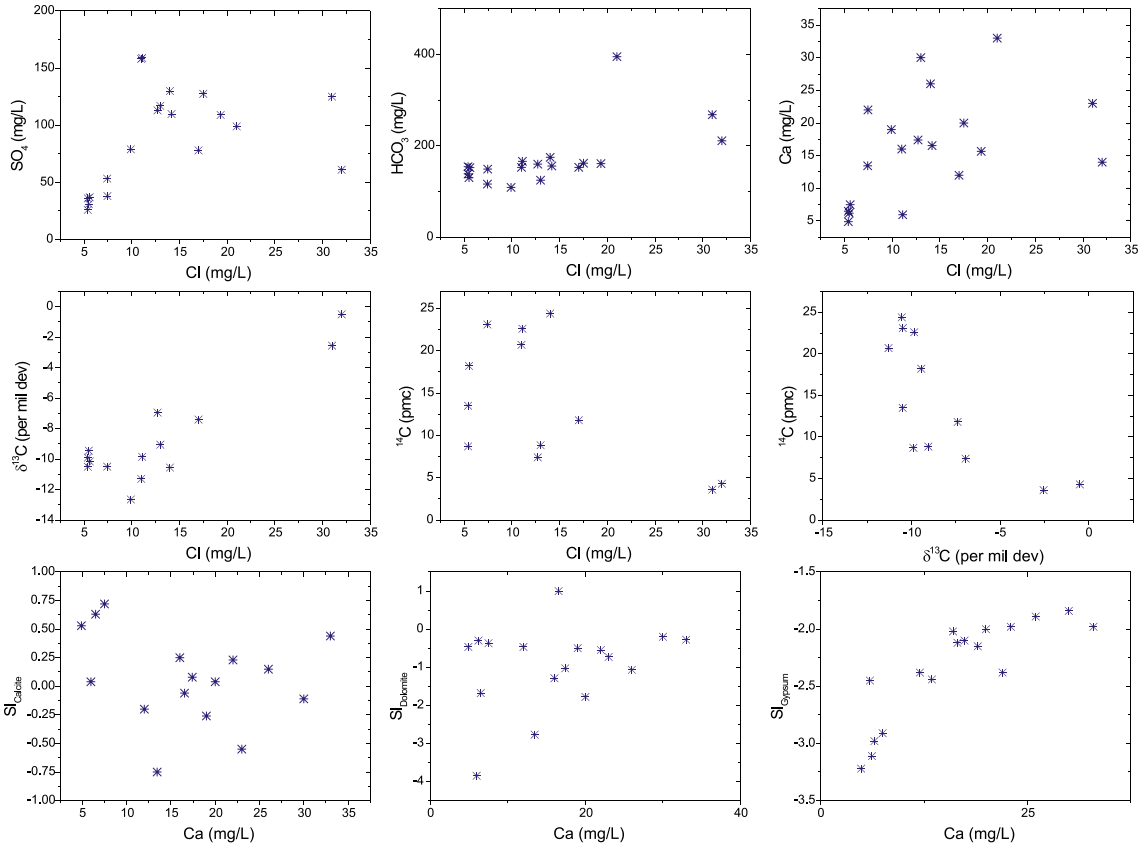

Figure 2-23. *Main trends in the Western Rock Valley hydrofacies.*

Fortymile Wash (⨯)

The 55 samples assigned to the Fortymile Wash hydrofacies come from a broad region that encompasses a sizable part of the Fortymile Wash river, from its northern reaches in the Calico Hills down to the Amargosa River Valley (Figure 2-24). The southern samples are flanked to the west by the Amargosa River hydrofacies and to the east by the Eastern Amargosa hydrofacies. The samples have been collected in packed-off NC-EWDP boreholes and in other open-hole boreholes, including water wells and irrigation wells, all of them in Quaternary basin-fill deposits.

In general, the chemistry of this hydrofacies is rather diluted, with average Cl contents of 6 to 12 mgL^{-1}, although four samples (#125, 133, 138, and 156) have higher chloride concentrations of up to 61 mgL^{-1} (sample #125). Actually, the samples from the Fortymile Wash hydrofacies have the lowest TDS of all the groundwaters in the dataset.

The four samples with higher Cl contents (highlighted in Figure 2-24) seem to have an evaporation signature (all of them are located in the centre of the Amargosa Valley). Also, two of these high-Cl samples (#125 and #133) have raised concentrations of NO_3, possibly due to contamination with fertilizers (these two samples come from the Amargosa Farms region, an area where artificial irrigation is widespread). Consequently, the four samples with Cl > 15 mgL^{-1} have been excluded from the final dataset.

As regards ^{14}C contents, all samples except two (#359 and 360) have $^{14}C < 32$ pmC. This ^{14}C value was identified in the total-system exploratory analysis as a threshold for the complete dataset, not only for the Fortymile Wash hydrofacies. The two samples enriched in ^{14}C, clearly contaminated by recent meteoric water, come from the northern part of the region (Figure 2-24), where precipitation is higher.

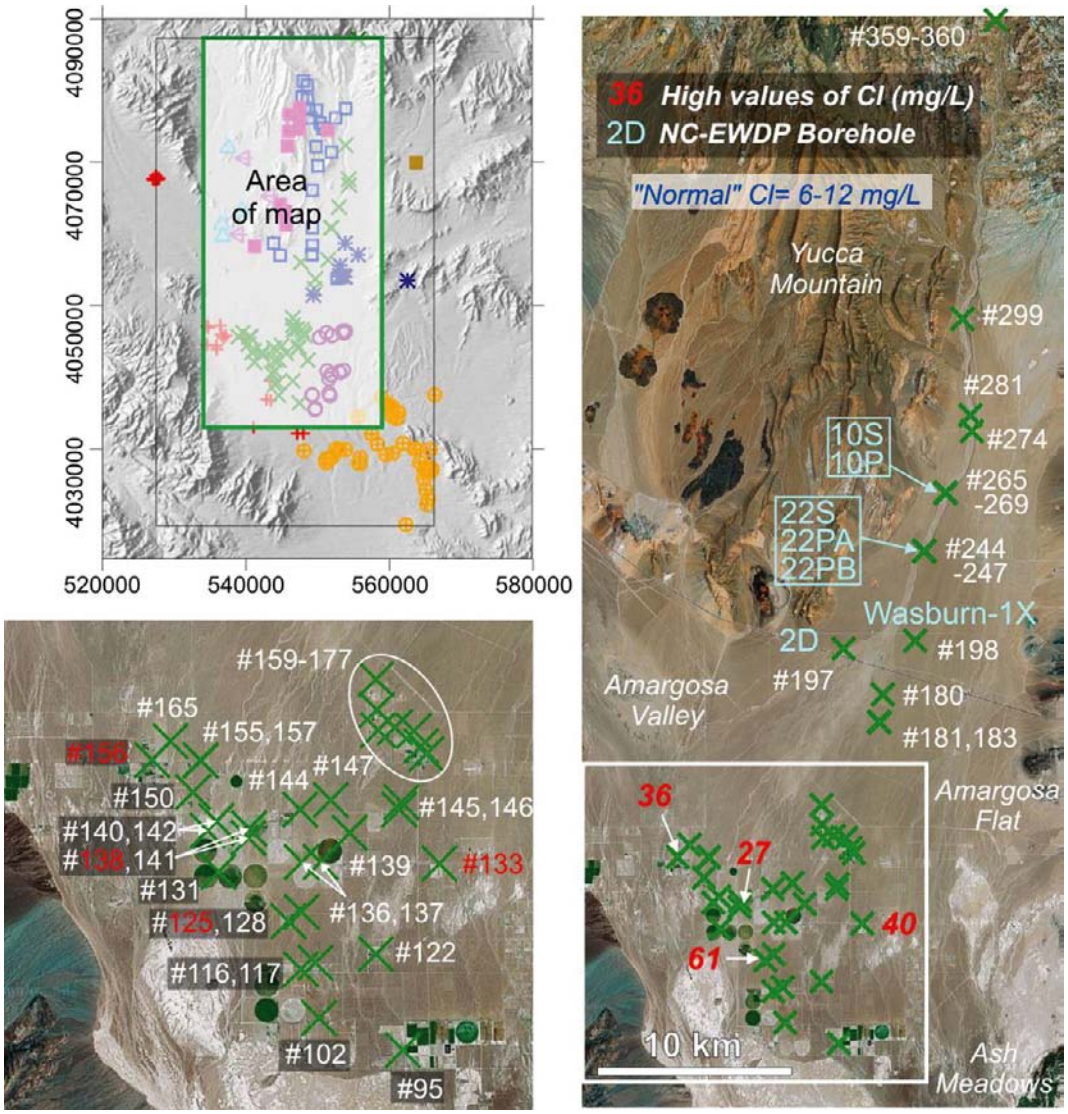

Figure 2-24. *Location map of the samples from the Fortymile Wash hydrofacies. Samples with anomalously high chloride contents are highlighted. The southern end of the area has been enlarged (image lower left).*

The last graph in Figure 2-25 is a Principal Component Analysis including only samples from the Fortymile Wash hydrofacies. The graph shows the pc1-pc2 plane and here it is obvious that most samples occupy a compact region near the origin of coordinates. Several samples lie further apart, including the four samples with high contents of Cl.

Apart from outliers, the identification of trends in a dataset is important in order to interpret its origin and evolution. As Figure 2-26 shows, trends are not very clear. It is worth noting that the variability in Cl contents is much smaller than in other ions or isotopes. This gives vertical "trends" for many ions and isotopes when plotted against chloride. It should be noted that the two samples with a high ^{14}C value systematically lie in the lower concentration range of these vertical "trends". In other words, these samples are more diluted that most samples, although their Cl content is similar to the others. One possible interpretation is mixing between two waters with the same concentration of chloride (approximately 10 mgL^{-1}) but different concentration of the other ions and isotopes. From the graphs in Figures 2-25 and 2-26, the range of concentration values summarised in Table 2-11 can be deduced for the Quaternary (Fortymile Wash) basin-fill end-member water.

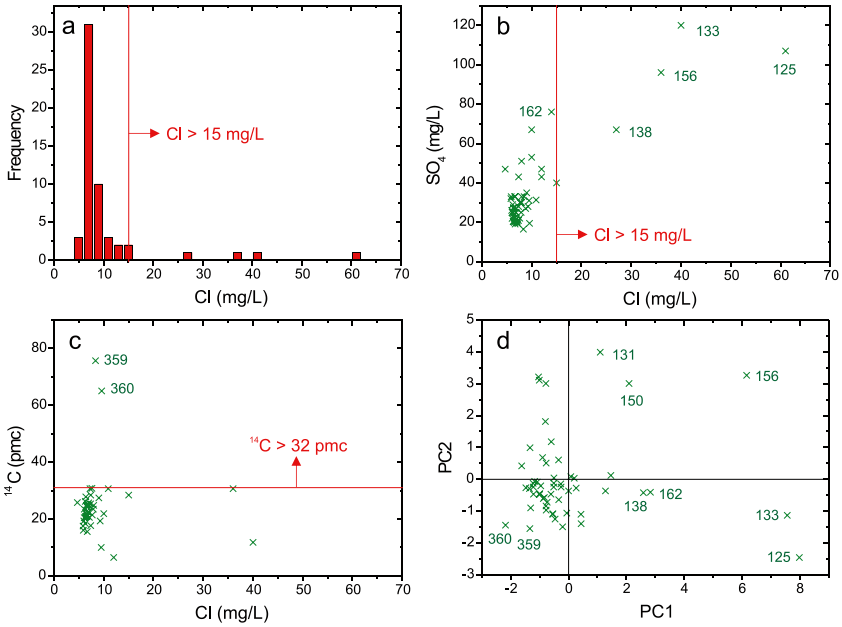

Figure 2-25. *Outliers in Fortymile Wash hydrofacies. Samples with Cl > 15 mg/L and ^{14}C > 32 pmc are considered anomalous. (a) Frequency histogram of chloride concentrations; (b) Cl-SO_4 ion-ion plot; (c) Cl-^{14}C plot; (d) pc1-pc2 view of a PCA using only the Fortymile Wash samples.*

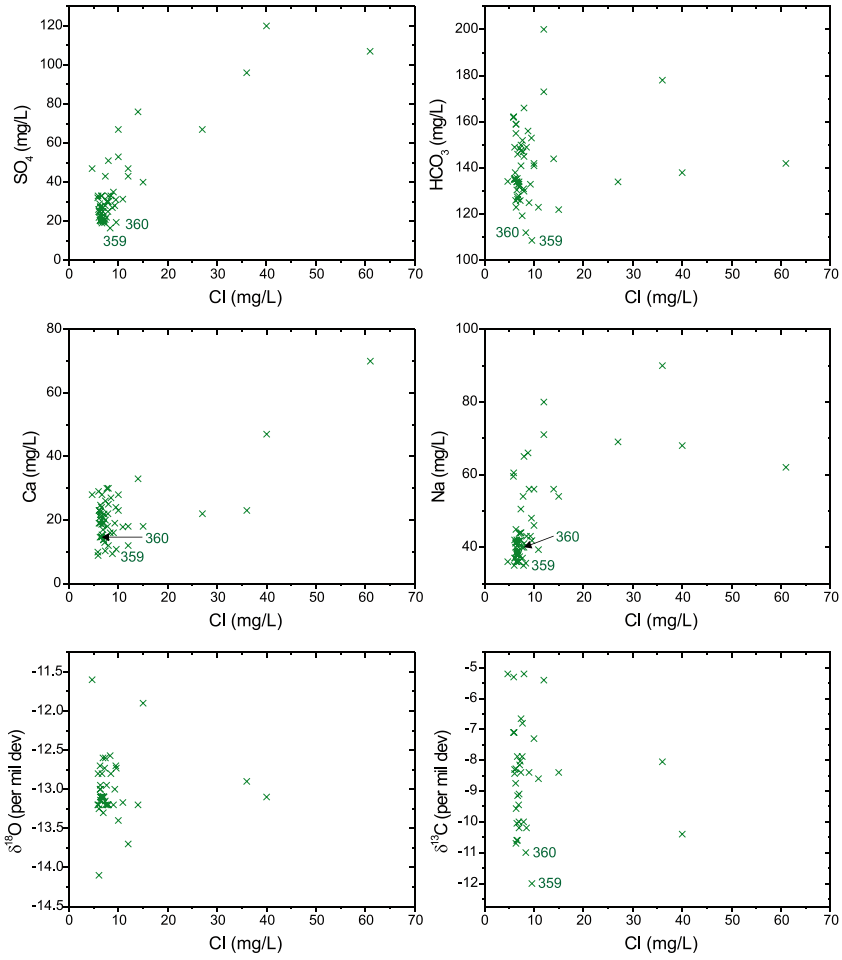

Figure 2-26. *Ion-ion and ion-isotopes plots for the Fortymile Wash hydrofacies. Samples #359 and 360, with an anomalously high value of ^{14}C, are labelled.*

Table 2-11. Chemical characteristics of a potential end-member water for the Quaternary Basin-fill Aquifer (second column), compared with the composition suggested for the same end-member after analysis of the Eastern Yucca Mountain samples (appended here as Column 3).

Ion	Quaternary basin-fill end-member (Fortymile Wash)	Quaternary basin-fill end-member (from Table 2-8)
pH	7.5–7.9	8.0
Cl (mg/L)	6–8	6–8
HCO_3 (mg/L)	120–160	120–140
SO_4 (mg/L)	20–30	15–25
Ca (mg/L)	20	16–18
Na (mg/L)	40	40–50
^{14}C (pmC)	18–30	20–35

If the values shown in the second columns of Table 2-11 are compared with those shown in the last column of Table 2-8 for the potential Quaternary basin-fill end-member as deduced from Eastern Yucca Mountain samples (appended here as Column 3), their similarity is obvious. Although the pH value is slightly lower in the potential end-member deduced from the Fortymile Wash samples (7.5–7.9 versus 8), and the Ca content slightly higher (20 mgL^{-1} versus 16–18 mgL^{-1}), it had already been noted that the potential end-member deduced from the Eastern Yucca Mountain hydrofacies was quite possibly contaminated to some extent by waters from the Tertiary Tuffs Aquifer. As a consequence, the pH and concentration values shown in Table 2-11 could be a better approximation to the "pure" Quaternary basin-fill end-member water.

Amargosa River (+)

Samples from the Amargosa River hydrofacies occupy the central and north-western parts of the Amargosa Valley (Figure 2-27). Most of them come from an area where irrigation is widespread and have been collected from shallow water wells. A group of samples have been collected near the southern end of the Bare Mountains (samples #276–287), some 30 km northwest of the remaining samples.

Three groups of water samples can be distinguish with respect to chloride: a low-Cl group, with chloride contents of between 30 and 40 mgL^{-1}; a medium-Cl group, with chloride contents ranging from 60–85 mgL^{-1}; and a high-Cl group (sample #160), with Cl = 123 mgL^{-1}. In general, chloride concentrations are high compared with the other elements in this hydrofacies (the mean Cl content is 24.5 mgL^{-1} and the median value is 11.4 mgL^{-1} for the whole raw dataset, see Figure 2-3 and Table 2-5).

This hydrofacies is difficult to interpret. Cl trends are not easily attributed to evaporation, as most ions do not increase their concentration with chloride, with the exception of SO_4. In particular, Ca and Mg are more or less independent of the concentration of Cl, although Mg (not Ca) does tend to increase with bicarbonate (Figure 2-28). Calcite and dolomite are in equilibrium or slightly oversaturated in these samples, suggesting precipitation of calcite and/or dolomite. Samples #97 (Cl = 78 mg/L) and #160, from the Amargosa Farms region, have high concentrations of NO_3, which suggests the possibility of contamination by fertilizers.

^{14}C trends are also intriguing (Figure 2-28), as the percentage of modern carbon seems to increase with Cl and decrease with HCO_3. This is unexpected from both the evaporation and mixing points of view.

The lowest Cl contents are approximately 30 mgL^{-1}, much higher than in the Quaternary Alluvial end-member deduced from the Eastern Yucca Mountain and Fortymile Wash datasets.

A more reliable interpretation of this hydrofacies has been deferred to the Results section, when several hydrofacies from the Quaternary Basin-fill Aquifer in the Amargosa River Valley (Amargosa River, Eastern Amargosa, Western Rock Valley and Fortymile Wash hydrofacies) will be plotted together.

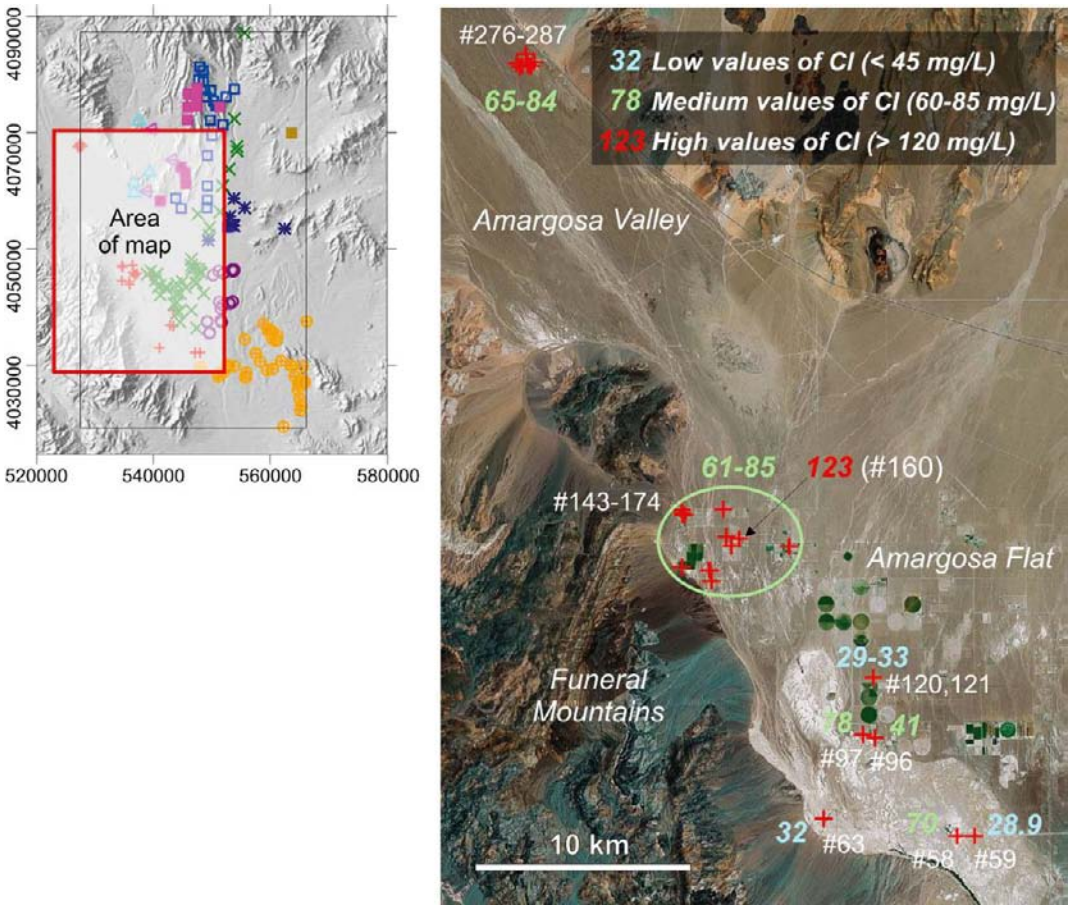

Figure 2-27. *Location map of the sample from the Amargosa River hydrofacies. Samples have been divided into three groups with respect to their Cl contents.*

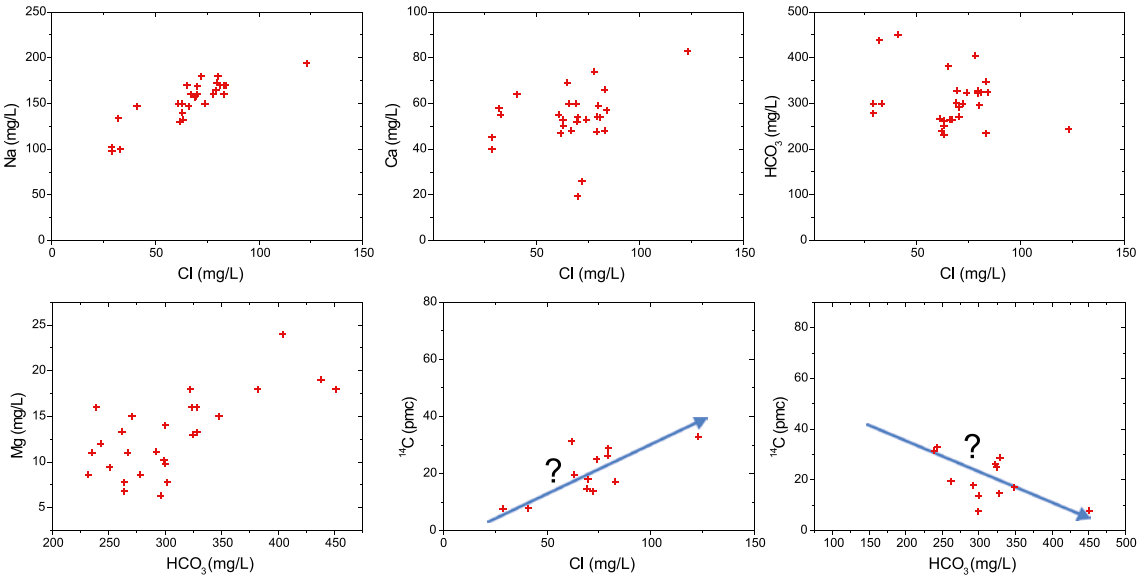

Figure 2-28. *Main ion-ion and ion-isotopes trends in the Amargosa River hydrofacies.*

Eastern Amargosa (○)

The samples belonging to the Eastern Amargosa hydrofacies occupy a compact area in the central part of the Amargosa River Valley, between the Fortymile Wash samples to the east and the Ash Meadows samples to the southwest (Figure 2-29). All samples were taken from shallow water wells, either for domestic use or for irrigation. The water table in the area is at a depth of 5 to 50 metres below ground level, saturating Quaternary basin-fill deposits.

Hydrochemically, the composition of the samples is fairly homogeneous. The normal chloride content in the waters of this hydrofacies ranges from 16 to 31 mgL^{-1}, although three samples have anomalously low Cl (9–10 mgL^{-1}) and one sample has an anomalously high Cl of 41 mgL^{-1} (these samples are highlighted in Figure 2-29).

Figure 2-30 shows several ion-ion, ion-isotope and isotope-isotope plots which together suggest that the waters from the Eastern Amargosa hydrofacies can be described as a rather simple mixture of two end-member waters: a low-Cl, high-^{14}C, heavy-$\delta^{18}O$ end-member and a high-Cl, low-^{14}C, light-$\delta^{18}O$ end-member. A representative composition of both end-members is displayed in Table 2-12

The low-Cl end-member water has a chemical composition compatible with the potential Quaternary Basin-fill Aquifer end-member suggested by the analysis carried out with Eastern Yucca Mountain and Fortymile Wash hydrofacies, although the concentration of Na is higher here (100–120 mgL^{-1} versus 40–50 mgL^{-1}). The high-Cl end-member, however, has not been identified in the analysis of the previous hydrofacies. Only some samples from the Amargosa River hydrofacies (those lowest in chloride) have a chemical signature similar to the high-Cl end-member identified here. The significance and origin of this end-member will be discussed below in a combined analysis of all the hydrofacies connected with the Quaternary Basin-fill Aquifer (i.e. the Amargosa River, Eastern Amargosa, Fortymile Wash and Western Rock Valley hydrofacies).

Sample #127 has the highest Cl concentration and departs from most trends as shown in Figure 2-30. For this reason, it has been excluded from the final dataset. Sample #104 is anomalous in the $\delta^{18}O$-^{14}C plot, but since it behaves "normally" in the other plots it has been retained in the final dataset.

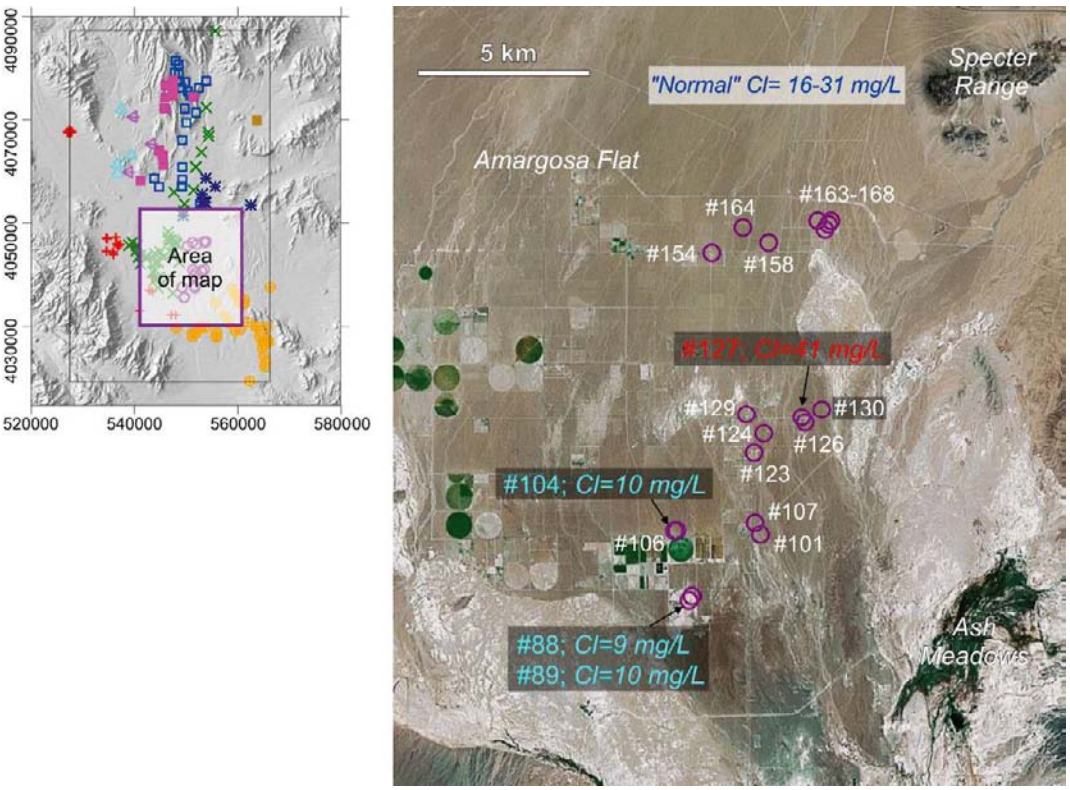

Figure 2-29. *Location map of the sample from the Eastern Amargosa hydrofacies. Samples low and high in chloride have been highlighted. The normal chloride contents in this hydrofacies are between 16 and 31 mgL^{-1}.*

Table 2-12. Chemical characteristics of two potential end-member waters from the Eastern Amargosa hydrofacies.

	High-Cl end-member (Eastern Amargosa)	Low-Cl end-member (Eastern Amargosa)
pH	7.5–7.7	8.0–8.1
Cl (mg/L)	25–32	7–10
HCO_3 (mg/L)	270–320	100–125
SO_4 (mg/L)	140–170	20–30
Ca (mg/L)	45–55	15–20
Mg (mg/L)	12–21	2–4
Na (mg/L)	100–120	18–25
K (mg/L)	10–18	7–10
$\delta^{18}O$ (‰)	13.8	13 to 12.8
^{14}C (pmC)	0–5	25–35

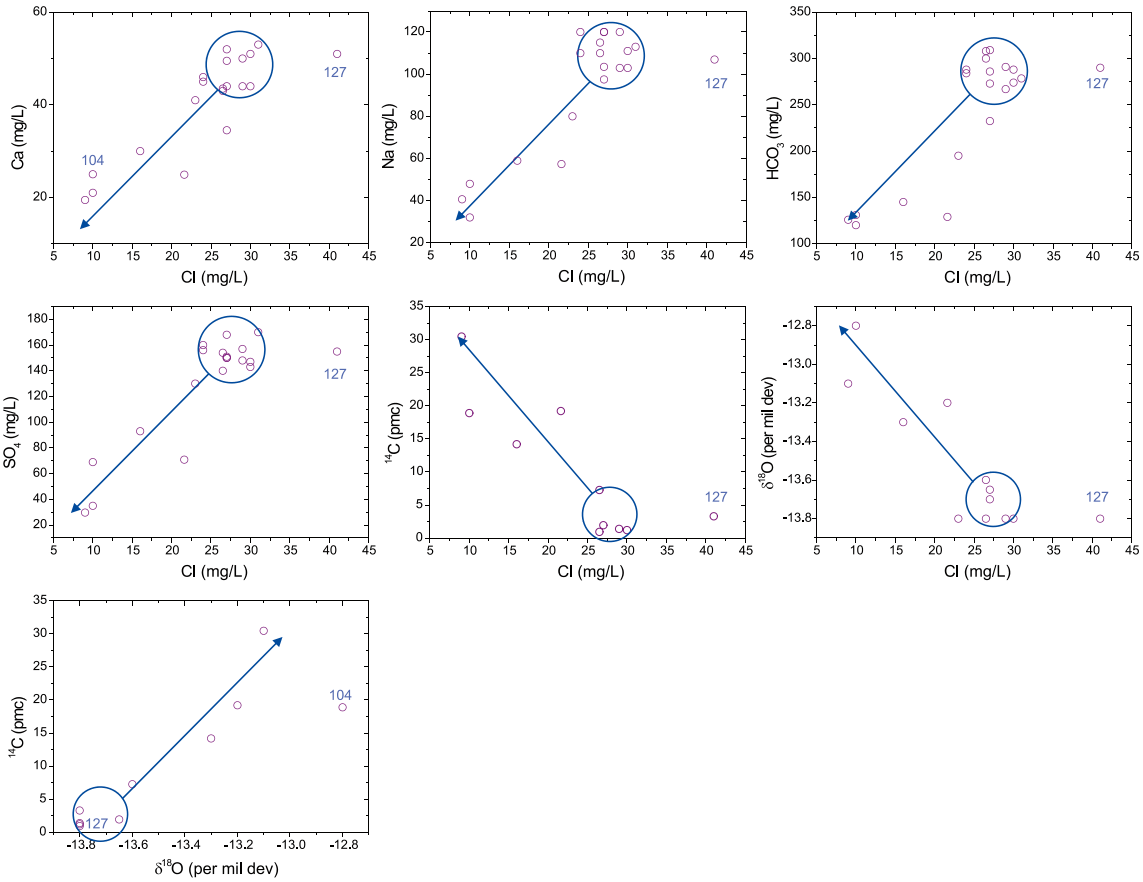

Figure 2-30. *Chloride trends (visual aid only) for the Eastern Amargosa hydrofacies. These trends are compatible with a binary mixture of two end-member waters. The high-Cl, low-^{14}C end-member is marked with a blue circle. Sample #127 is anomalous as it departs from most trends. Also, its chloride content is the highest.*

Central Amargosa Valley combined analysis

After dealing in the last four sections with the four hydrofacies geographically located around the central section of the Amargosa River Valley (Amargosa River, Eastern Amargosa, Fortymile Wash, and Western Rock Valley), a combined analysis is performed here with the aim of characterising, from a broader viewpoint, the common trends and the heterogeneity. For this purpose, several ion-ion plots and a PCA will be used. All the samples from these hydrofacies were sampled in the Quaternary Basin-fill Aquifer.

Figure 2-31 shows several ion-ion and ion-isotopes plots for the combined dataset. It is immediately obvious that the four hydrofacies share a common evolution, with the Fortymile Wash hydrofacies being those that are less "evolved" (i.e. more diluted), and the Amargosa River hydrofacies those that are most "evolved" (i.e. less diluted). Samples from the Eastern Amargosa hydrofacies systematically plot in a middle position, while samples from the Western Rock Valley hydrofacies tend to plot close to the Fortymile Wash ones, although the scatter is greater.

The end-member water already identified in the previous sections is here even more patent. It has been marked with a red ellipse in several of the plots in Figure 2-31. Inside the ellipse, samples from the Fortymile Wash, Eastern Amargosa and Western Rock Valley are found, which means that this "pure" end-member water has a widespread occurrence in the alluvial deposits.

The "evolved" end of the trends behaves differently. This part of the trend is only occupied by the Amargosa River hydrofacies when chloride or sulphate are used as markers of evolution or shared with some of the Eastern Amargosa hydrofacies when bicarbonate is used for that purpose (but bicarbonate is not a conservative element in this system). Sample #160 seems to be an outlier, although it follows the common trends in most graphs. Sample #143 has also been highlighted in Figure 2-31 as the most evolved sample in the cluster that can be observed in the Cl plots. The composition of this sample is summarised in Table 2-13 and it will be added to the potential end-member list.

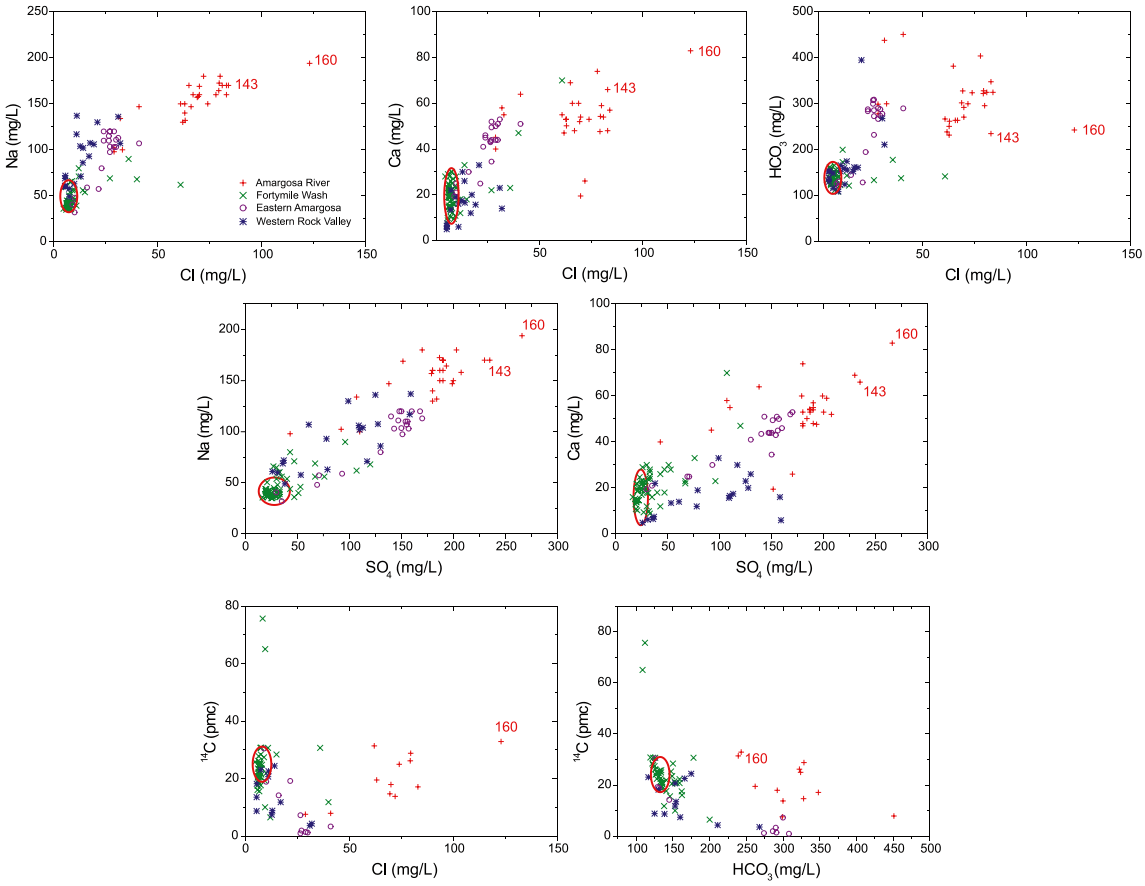

Figure 2-31. *Main trends for all the hydrofacies of the central part of the Amargosa Valley.*

Table 2-13. Chemical characteristics of sample #143 (Amargosa River hydrofacies) as potential end-member water for the high-Cl Quaternary Basin-fill Aquifer waters.

	High-Cl end-member (Amargosa River)
pH	7.69
Cl (mg/L)	83
HCO_3 (mg/L)	235
SO_4 (mg/L)	235
Ca (mg/L)	66
Mg (mg/L)	11
Na (mg/L)	170
K (mg/L)	12
$\delta^{18}O$ (‰)	Not analyzed
^{14}C (pmC)	Not analyzed

Ash Meadows (⊕)

The Ash Meadows region is located in the south-eastern corner of the domain studied (Figure 2-32). The region belongs to the Amargosa River Valley and is the exit point for the superficial waters in the domain, which flow south and then west towards Death Valley. Groundwaters in this area flow through Quaternary basin-fill deposits of varied lithology, ranging from coarse siliciclastic to tuffaceous to evaporitic. The dataset consists of 49 samples taken from shallow wells (27 samples) and springs (22 samples). Most of the springs are located in a spring line which is the surface expression of the Gravity Fault.

As was already evident in the total-system exploratory analysis, this hydrofacies contains several of the most extreme samples, which points to the operation of an array of processes that modify in a rather strong way the original chemistry of the groundwaters. Because many samples have been collected in springs and shallow irrigation boreholes, evaporation is an issue here and must be taken into account. Also, the presence of scattered playa deposits with highly soluble evaporitic minerals should be borne in mind when trying to interpret the hydrochemistry of several samples.

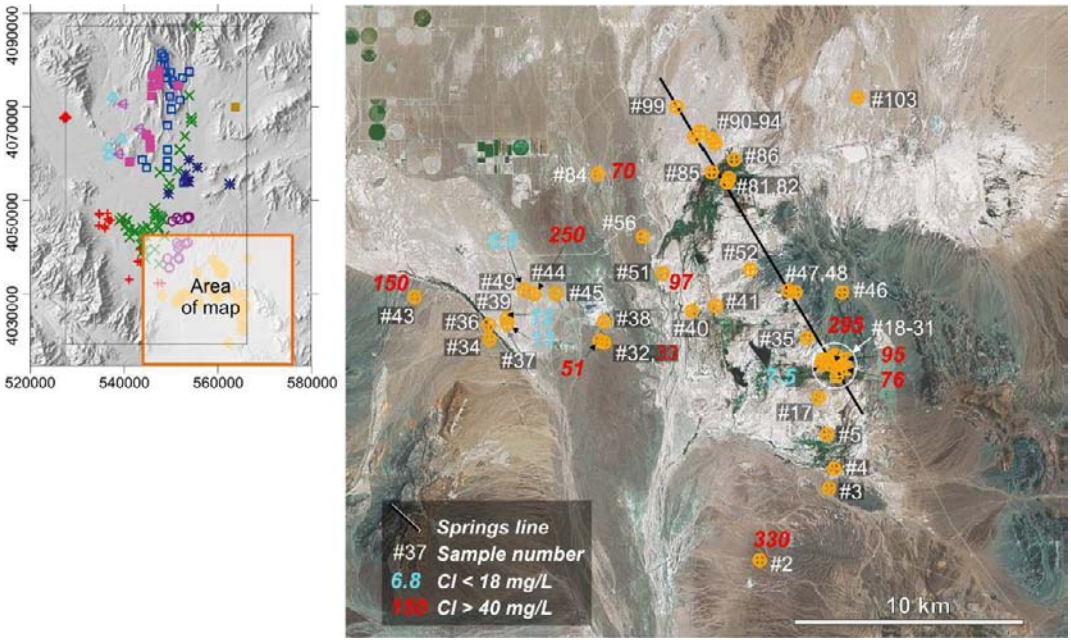

Figure 2-32. *Location map of the sample from the Ash Meadows hydrofacies. Samples low and high in chloride have been highlighted.*

Chloride ranges from 6.8 to 330 mgL^{-1}, sulphate from 37 to 1,100 mgL^{-1}, bicarbonate from 157 to 1,690 mgL^{-1}, Na from 52 to 1,200 mgL^{-1}, Ca from 1.3 to 140 mgL^{-1}, Mg from 1 to 90 mgL^{-1} and K from 6.2 to 69 mgL^{-1}. All of these upper values are the highest in all the groundwater hydrofacies (see Table 2-7).

Figure 2-33 plots the main trends in the Ash Meadows hydrofacies. Outliers already discovered in the total-system analysis are also detected here. As none of the high-TDS samples were analysed for isotopes (^{2}H, $\delta^{18}O$, $\delta^{34}S$, $\delta^{13}C$ and ^{14}C), trends of chloride against the isotopes are incomplete, spanning only the 0–30 mgL^{-1} Cl range (Figure 2-34). This is problematic as several of these trends could distinguish between evaporation and other processes responsible for raised concentrations of chloride (e.g. dissolution of evaporitic minerals).

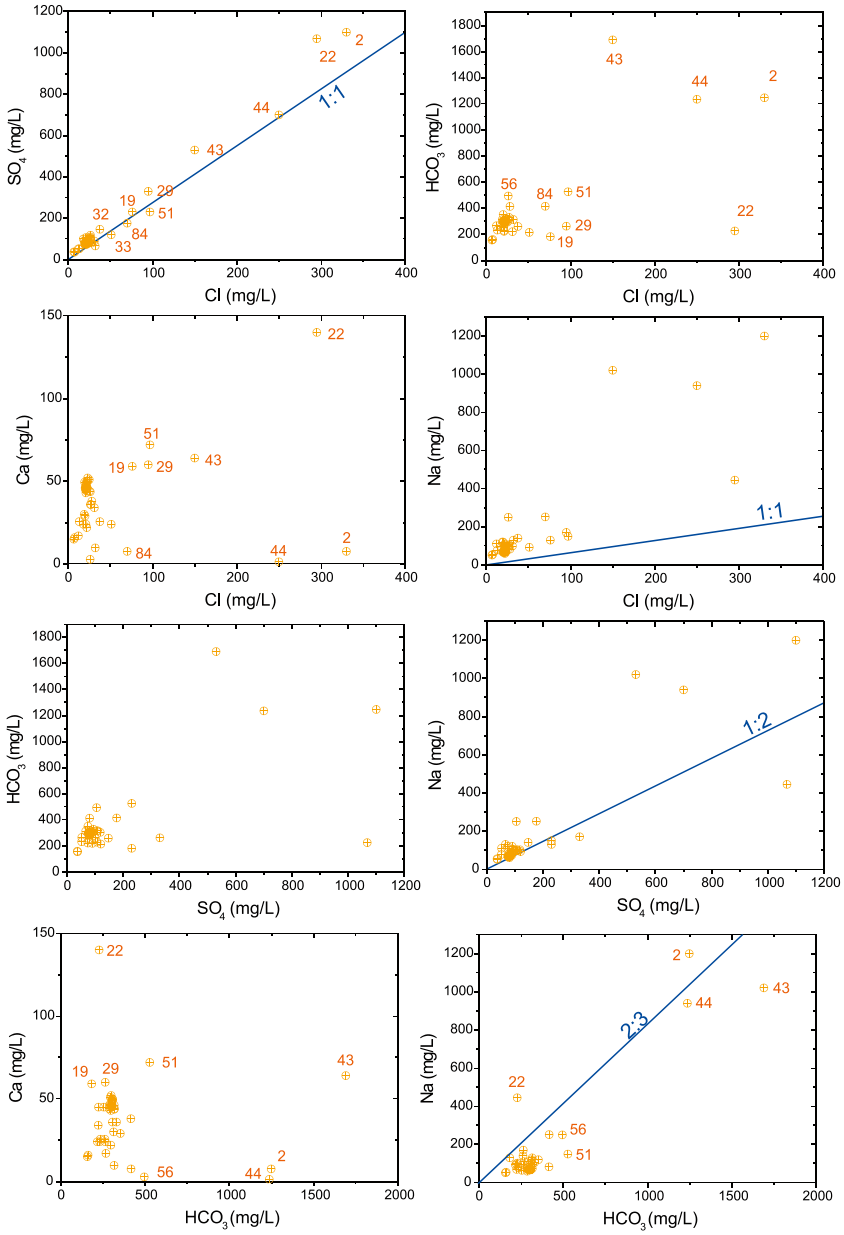

Figure 2-33. *Main trends in the Ash Meadows samples. High-TDS samples are labelled. The blue line in several plots marks the molar ratio of the two ions. The 1:1 line in the Cl-Na plot represents halite dissolution, the 1:2 line in the SO_4-Na plot represents thenardite dissolution and the 2:3 line in the HCO_3-Na plot represents trona dissolution.*

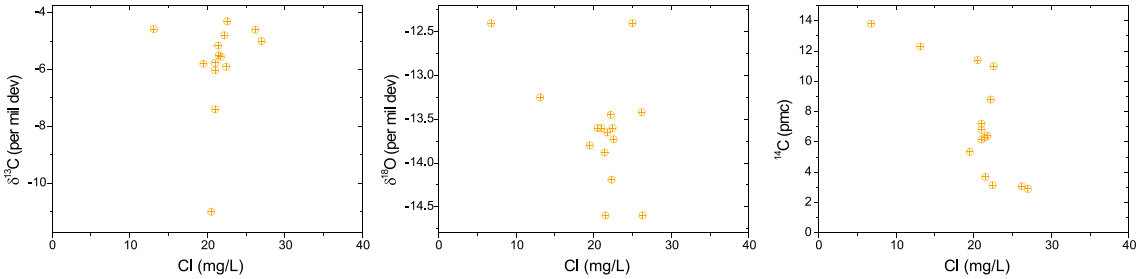

Figure 2-34. *Isotopic trends in the Ash Meadows system. As only low-TDS samples have isotopic data, the trends are limited to the 0–30 mg/L Cl range.*

The only good chloride trend is with sulphate. Sodium also increases with chloride, although the scatter is greater. Chloride-bicarbonate and chloride-Ca plots are quite erratic. Clearly, sulphate behaves as a conservative element, while bicarbonate and calcium are reactive. The bicarbonate and sulphate trends again point to a general increase in Na with both, while HCO_3-Ca and SO_4-Ca plots follow no simple pattern. The simplest explanation for these trends taken together is that the dissolution of several sodium minerals (trona, thenardite, halite) has occurred as a result of groundwater flows through evaporitic playa deposits. Evaporitic playa deposits are common in the Amargosa basin, both north and south of Ash Meadows (D'Agnese et al. 1997, Belcher et al. 2002).

Several PHREEQC simulations have been performed to test the two basic hypotheses of evaporation and dissolution of evaporitic minerals in playa deposits. The aim is to assess whether the chemistry of these samples could be the result of mixing or, as it seems, is the result of the actuation of non-mixing processes (either evaporation or dissolution). In the first case, the samples would be retained in the final dataset, while on the other hand they would be eliminated.

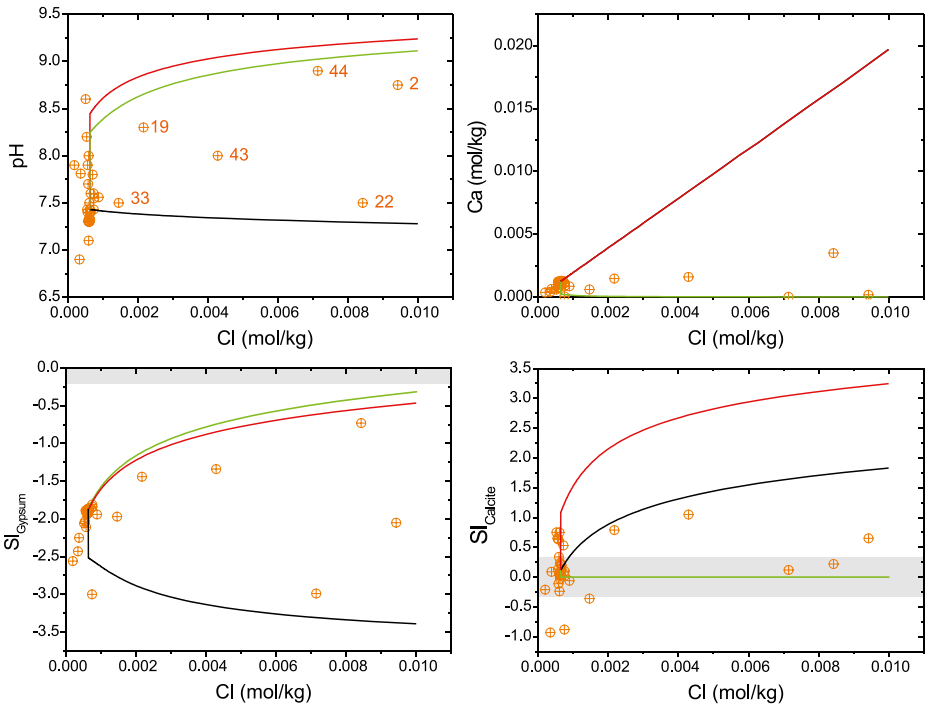

Figure 2-35. *PHREEQC simulations of three evaporation scenarios in the Ash Meadows system: (1) closed system with respect to CO_2 (red line), (2) re-equilibration at log P_{CO2} = –3 (black line) and (3) re-equilibration at log P_{CO2} = –3 and calcite equilibrium (green line). The shaded areas in the gypsum and calcite saturation indices plots represent equilibrium.*

Three different constraints have been imposed in the evaporation simulations: (1) closed system with respect to CO_2, (2) re-equilibriation at $P_{CO2} = 10^{-3}$ (normal CO_2 partial pressure in the unsaturated zone at Yucca Mountain) and (3) re-equilibration at $P_{CO2} = 10^{-3}$ and equilibrium with calcite. These three types of simulations span the main potential scenarios during evaporation in the Ash Meadows area.

Figure 2-35 presents the results using chloride as the variable that defines the degree of evaporation. The red line represents the evolution in the closed-system scenario, the black line the evolution in the re-equilibrium at $P_{CO2} = 10^{-3}$ scenario and the green line the evolution in the scenario where both re-equilibrium at $P_{CO2} = 10^{-3}$ and equilibrium with calcite are imposed. None of the scenarios match the evolution of the whole dataset, although the third scenario, in which precipitation of calcite is allowed, correlates better with the low concentration of Ca in most high-TDS samples. In light of these results, it is concluded that evaporation does not seem to be the key process responsible for the anomalous chemistry of some of the Ash Meadows waters, although it may have affected them.

In addition to evaporation simulations, several mass-balance calculations using the inverse-problem methodology implemented in the PHREEQC code were also performed. Sample #40 was used as the initial water (diluted initial state), while samples #2 and #44 were the final waters (concentrated final state). Several evaporitic minerals were included in the calculations: calcite, gypsum, halite, trona ($Na_3H(CO_3)_2:2H_2O$), natron ($Na2CO_3:10H_2O$) and several borates. This set of minerals has been selected as they are cited as feasible phases in playa deposits from the Amargosa River and Death Valley regions (Claassen 1985). Borates have also been included as samples #2 and #44 are highly enriched in boron (8.9 ppm in sample # and 12 ppm in sample #44), and large borate deposits are known in the region.

PHREEQC gives 36 different models, which vary in the number of phases included and the amount of dissolution (mass transfer) for each mineral. However, most of them give precipitation of calcite and the dissolution of gypsum, halite, trona and several borates. These mass transfers are capable of explaining the compositional change between the initial and the final waters, including, most importantly, the change in alkalinity, sodium, and boron, and the reduced pH of the final waters (approximately 8.9). Consequently, it can be concluded that the dissolution of evaporitic minerals would appear to be the cause of the anomalous compositions of most high-TDS samples in the Ash Meadows area, although evaporation could also have played a minor role. For all these reasons, the following samples have been eliminated from the dataset (in decreasing chloride concentration): 2, 22, 44, 43, 51, 29, 19, 84, 33 and 32. Sample #56 is also eliminated because it is anomalous with respect to bicarbonate.

Apart from the obvious heterogeneity of compositions in the Ash Meadow hydrofacies as a whole, there is a group of samples (24 in all, i.e. 50% of all the hydrofacies samples) with a narrow range of values for many of the major ions. The average composition of these waters is summarised in Table 2-14. In addition to the chemical parameters in Table 2-9, the representative waters of the Ash Meadows hydrofacies have a rather high CO_2 partial pressure ($\log P_{CO2} = -2.0$).

Table 2-14. Chemical characteristics of the representative samples from the Ash Meadows hydrofacies.

	Representative samples (Ash Meadows)
pH	7.3–7.5
Cl (mg/L)	20–24
HCO_3 (mg/L)	280–320
SO_4 (mg/L)	80–100
Ca (mg/L)	42–52
Mg (mg/L)	20–23
Na (mg/L)	70–100
$\delta^{18}O$ (‰)	13.9 to 13.2
^{14}C (pmC)	4–12

Geographically, most of these samples are located on or near the surface expression of the Gravity Fault, which is a discharge area for groundwaters that seem to have flowed through the Palaeozoic Carbonate Aquifer (their temperature is systematically higher than that of other samples in the Ash Meadows area). Samples with higher or lower concentrations are located west and south of the Gravity Fault, although three high-Cl samples are also on the fault line (Figure 2-32), indicating either evaporation or dissolution of evaporitic minerals.

The set of 20 samples with a narrow range of concentrations will be considered as being representative of the unaltered hydrochemistry of the Ash Meadows waters. "Unaltered" means not modified by evaporation and/or dissolution of evaporitic minerals, although mixing with other types of water could be the reason for their (rather small) range of compositions. This set of samples, together with the samples eliminated from the dataset, are displayed in Table 2-15

Perched waters (●), pore waters (●), surface waters (▲), and precipitation (▽)

Apart from the groundwater samples, the raw dataset contains four other water categories: pore waters, perched waters, surface waters and precipitation. The location and sample number of all these non-groundwater samples is shown in Figure 2-36. This dataset contains 6 perched water samples, 81 pore water samples, 17 surface water samples and 39 precipitation samples. Some or all of these water categories should represent the "initial state" from which the chemistry of the already described groundwaters evolves (by evaporation, water-rock interaction, mixing, etc).

Table 2-15. Ash Meadows samples separated into three groups: representative samples, excluded samples and non-representative but non-excluded samples.

Representative samples (24)	Excluded samples (8)	Non-representative, non-excluded samples (18)
3, 17, 18, 20, 21, 23, 26, 27, 28, 31, 35, 36, 40, 41, 47, 48, 52, 81, 82, 85, 86, 90, 92, 99	2, 19, 22, 29, 32, 33, 43, 44, 51, 56, 84	4, 5, 24, 25, 34, 36, 37, 38, 39, 46, 49, 54, 93, 94, 103

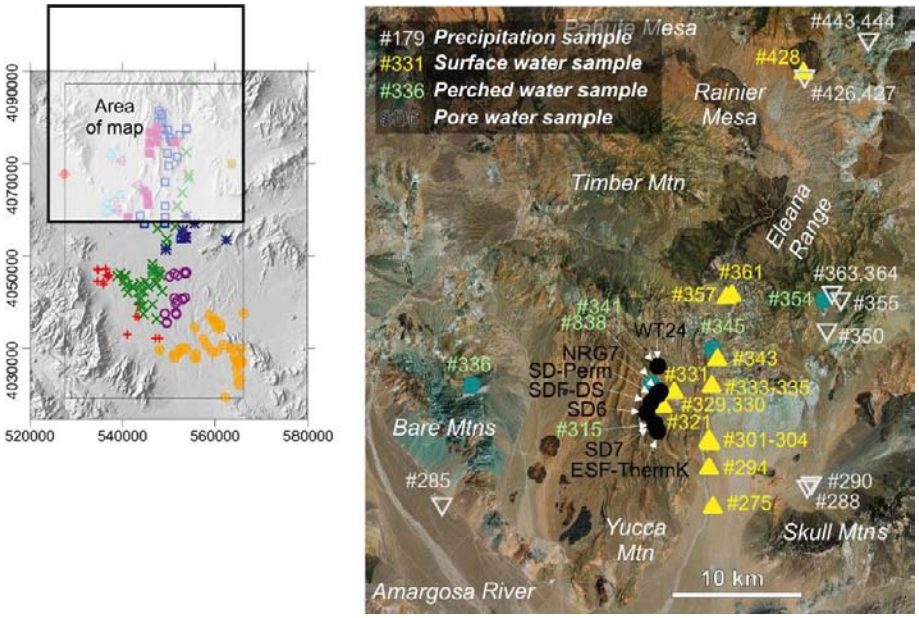

Figure 2-36. *Location and sample number of the four non-groundwater water categories in the raw dataset.*

In this sense it is important to assess the similarities and differences between these water categories in order to identify the most probable initial state. This "initial state water" would be one of the basic end-members from which the chemistry of the groundwater samples should be built. The basic pre-requisite for a water to be the initial state for groundwater evolution is that a smooth and continuous chemical transition exists between the initial water and the most dilute groundwaters.

With this objective in mind, Figure 2-37 plots the most interesting ionic trends in the non-groundwater dataset. Chloride is used as the marker of evolution in the first three plots, bicarbonate in the fourth and calcium in the other two. The Cl-SO_4 plot, as already commented on in the total-system exploratory analysis, shows a very good correlation between the concentrations of both ions. The red line gives the 1:1 Cl to SO_4 *molar* ratio. All samples follow this line apart from certain pore waters, which are depleted in sulphate (for a given value of chloride).

In the Cl-HCO_3, Cl-Na, HCO_3-SO_4 and Ca-Na graphs in Figure 2-37 two trends are clearly distinguishable: one followed by the precipitation and surface water samples, and another followed by the pore water samples. In all cases, the perched water samples plot in the intersection of both trends (blue circle). As will be seen later, *this is also the convergence point for the most diluted groundwaters* in the dataset (Fortymile Wash hydrofacies).

Another crucial observation to be made from Figure 2-37 is the existence of a compositional gap between precipitation and surface waters on the one hand and the pore waters on the other, which is better appreciated in the Cl-Na and Ca-Na plots. Perched water samples fill this gap, giving continuity to the geochemical evolution of the waters. In other words, the perched waters seem to be playing the role of a "hinge" between the evolution trends of surface waters (including precipitation) and pore waters. It should be noted, however, that certain surface waters (and even some of the most concentrated precipitation samples) plot also in this compositional gap (see, for example, the Cl-SO_4 plot in Figure 2-37).

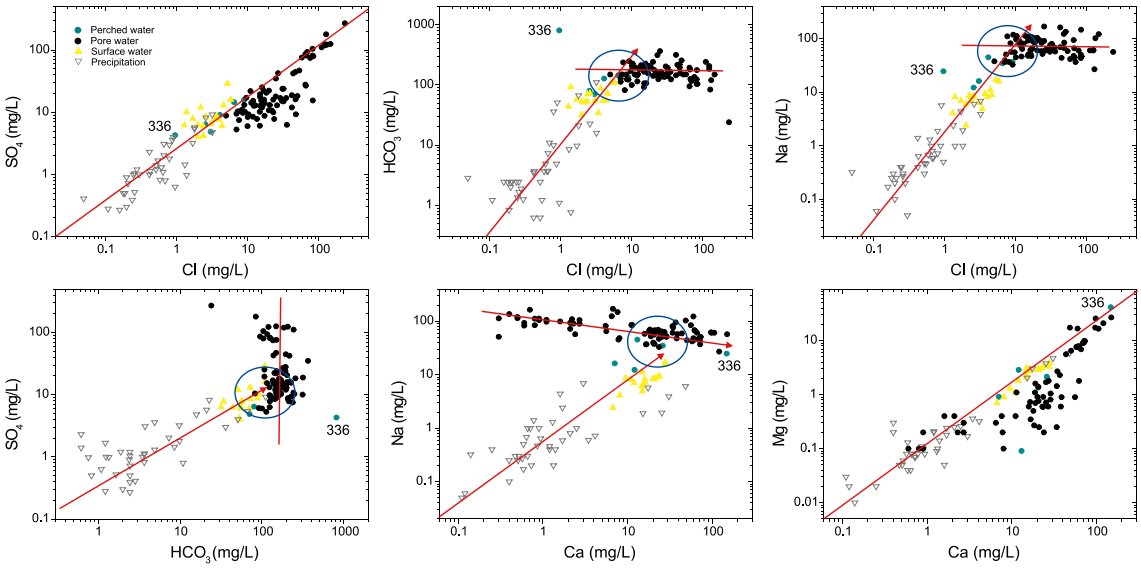

Figure 2-37. *Main ionic trends in the non-groundwater samples. The perched water sample #336, with an anomalous chemistry, is labelled.*

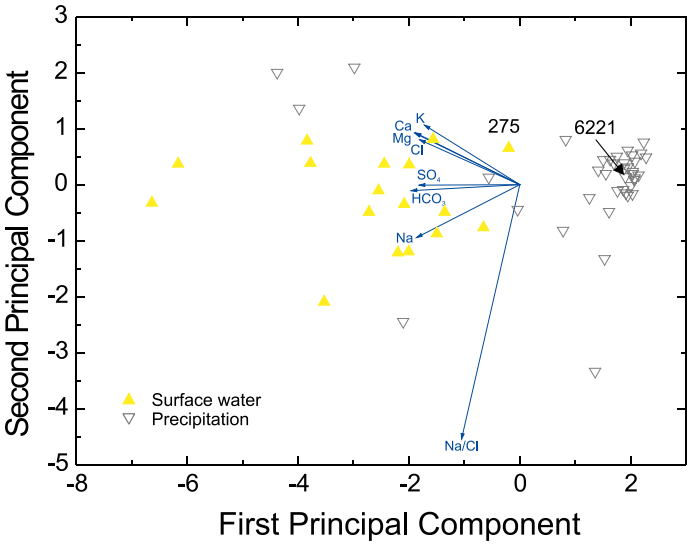

Figure 2-38. *Principal component analysis of the precipitation and surface waters. The two samples selected as potential end-members are labelled.*

All the above observations point to the important role that perched waters play in the Yucca Mountain system. Precipitation and surface waters are, of course, more "pristine" than perched waters, but they are not justifiable as the initial water from which the evolution of the groundwaters starts. This function seems to be neatly fulfilled by the perched waters.

Nevertheless, precipitation and surface waters will also be used as potential end-members in the next section. For this purpose, two candidate samples will be selected here by means of a Principal Components Analysis to serve as end-members. Figure 2-38 shows the result of the PCA in the pc1-pc2 plane. The original compositional variables are also included to establish that all the variables point to the left of the graph. This means that samples to the left of the pc1 = 0 coordinate have a higher TDS than the others. In other words, more diluted samples (less evolved ones) are on the right and less diluted samples (more evolved) are on the left. A compact cluster of precipitation samples is evident in the right-hand part of the graph. These are precipitation samples with a low TDS that share a similar chemical signature. Thus, a sample near the centre of this cluster could be a good candidate for the precipitation end-member. Sample #6221, labelled in Figure 2-38 has been selected.

With regard to the surface water samples, it is also clear from the PCA plot that there is a trend towards increasing TDS. This could be related to evaporation and/or dissolution of minerals during surface flow. Consequently, a good candidate for a potential surface water end-member would be the less evolved sample (minimum TDS). For this reason, sample #275 has been selected.

For the M3 analysis that is carried out in the next section, only the two samples from the surface water and precipitation dataset will be used.

The pore water samples have a wide compositional range. Some samples are diluted and similar in chemistry to the perched waters and the most diluted groundwaters (e.g. those of the Fortymile Wash hydrofacies). However, other samples, which are located far from the convergence zone between the surface waters and precipitation trend on the one hand and the pore waters trend on the other, are clearly affected by additional processes (evaporation, ion-exchange, dissolution and/or precipitation of minerals, Meijer 2002). Furthermore, the PCA carried out in the total-system exploratory analysis (see Figure 2-11 above) demonstrates that these samples follow specific trends, different from those followed by the groundwaters. Owing to the clear chemical discrepancies, it has been decided that the pore water samples should be excluded from the final dataset.

2.4.3 Conclusions of the exploratory analysis

- Following the hydrofacies exploratory analysis, three main groups of groundwater hydrofacies are apparent: (1) hydrofacies related to the Regional Palaeozoic Carbonate Aquifer (Bare Mountains, South East Crater Flat, Ash Meadows and samples #306 and 307), (2) hydrofacies clearly related to the Tertiary Tuffs Aquifer (Eastern and Western Yucca Mountain) and (3) hydrofacies related to the Quaternary Basin-fill Aquifer (Amargosa River, Eastern Amargosa, Fortymile Wash and Western Rock Valley). This last group of waters seems to be the most heterogeneous and difficult to interpret.
- To these three groups of groundwater, the perched waters should be added as the "initial" water from which all the others evolve. Modern precipitation and surface waters are not taken into account as they do not seem to be directly related to the general dynamics of the Yucca Mountain hydro-system. However, one sample of the precipitation samples and another from the surface water samples will be included in the following M3 analysis as potential end-member waters.
- A preliminary identification of end-member waters for each group of hydrofacies has been carried out and their chemical characteristics summarised in tables.
- From the total-system and hydrofacies exploratory analysis, several samples have been identified as being the results of the actuation of a varied array of processes which have drastically modified their chemical composition. These samples, collected in Table 2-16, have been excluded from the final dataset. None of the analyses carried out in the next section include these samples. In summary, the final dataset has 240 samples.

Table 2-16. Excluded samples after the total-system and hydrofacies exploratory analyses.

Hydrofacies	Water type	Symbol	Excluded samples
Amargosa River	Ground water	+	
Eastern Yucca Mountain	Ground water	□	
Fortymile Wash	Ground water	×	#125, #133, #138, #156
Bare Mountain	Ground water	△	#233, #234, #251, #256
Eastern Amargosa	Ground water	○	#127
Ash Meadows	Ground water	⊕	#2, #19, #22, #29, #33, #43, #44, #51
Western Yucca Mountain	Ground water	■	
Western Rock Valley	Ground water	✳	#182
South East Crater Flats	Ground water	◁	
Jackass Flat	Ground water	■	
Perched Water	Perched water	●	#336
Surface Water	Surface water	▲	All except sample #275
Precipitation	Precipitation	▽	All except sample #6221
Pore Water	Pore water	●	All

3 M3 analysis: selection of end-member waters and calculation of mixing proportions

M3 is a Principal Component Analysis code that approaches the modelling of mixing and mass balance from a purely geometrical perspective (Laaksoharju et al. 1999, Gómez et al. 2006, 2009). Unlike standard geochemical codes, M3 tries first to explain the chemical composition of a parcel of water by pure mixing, and only then are deviations from the pure mixing model interpreted as chemical reactions.

The M3 multivariate approach uses several chemical and physicochemical variables (conservative and non-conservative) to construct an ideal linear mixing model of the groundwater system. This is done by performing a Principal Component rotation of an $n \cdot n$ covariance matrix, where n is the number of chemical and physicochemical variables (e.g. Gershenfeld 1999). Each element of the covariance matrix expresses the degree of correlation of a pair of variables. Graphically, this is equivalent to the rotation of a reference frame composed of n orthogonal axes (one axis for every variable) until one axis, the first principal component, points in the direction of the maximum variability of the data set; another axis, the second principal component, points in the perpendicular direction with the second-largest variability and so on for the other axes. Once the samples and the end-members have been expressed in the Principal Component co-ordinates, mixing proportions are calculated in a straightforward way as the local co-ordinates of each sample in a hyper-tetrahedron whose vertices are the end-members (Gómez et al. 2006). This hyper-tetrahedron is a simplex, and therefore always has as many dimensions as end-members minus one.

Because there is one co-ordinate (i.e. one axis) for each input variable, at least as many input variables as end-members minus one are needed to obtain the mixing proportions (e.g. if three input variables are being used, say the concentration of Cl, Br and ^{18}O, it would be possible to give mixing proportions between two, three or a maximum of four end-member waters).

M3 calculates the mixing proportions with an algorithm referred to as "*n*-principal component mixing" (Gómez et al. 2006). This algorithm uses all principal components to compute the mixing proportions (geometrically, it works in an *n*-dimensional space, where n is the number of input compositional variables).

Once the mixing proportions have been calculated, the constituents that cannot be described by mixing are described using reactions by simple elemental mass balance supported by independent knowledge of the system. Reactions are inferred heuristically (by inspection) from the difference, for each sample, between the actual value of an input variable and the value computed by M3 assuming pure mixing. For example, if there is a deficit of both Ca and HCO_3 in the computed composition compared with the actual Ca and HCO_3 contents, it could be inferred that calcite has precipitated. There is no rigorous statistical test to decide whether a deviation between the computed and the analysed concentration of an element in a sample is sufficient to invoke a reaction.

3.1 Selection of end-member waters

Throughout the previous section, a number of water compositions have been collected in tables. Some have already been identified as potential end-members, others were used as initial or final waters in PHREEQC simulations and others were simply catalogued as being "representative" of a particular hydrofacies (e.g. the Ash Meadows hydrofacies). Table 3-1 compiles all these samples with their main chemical characteristics. In those cases where a range of concentrations has been specified for a potential end-member, a specific sample from the dataset is chosen, complete with the concentration of all the key chemical elements within the proposed range (i.e. representative of the given compositional range).

Table 3-1. Potential end-member waters used in the M3 analysis.

Sample	Hydrofacies	Ca	Mg	Na	K	Cl	HCO_3	SO_4	Cl/Na
143	AR (+)	66.00	11.000	170.00	12.00	83.00	235.00	235.00	2.05
207	EYM (□)	16.00	1.700	49.50	3.85	6.30	144.00	21.00	7.86
211	EYM (□)	0.57	0.027	113.00	3.51	5.50	268.74	20.30	20.5
359	FmW (×)	16.00	2.390	35.60	4.31	8.34	112.00	16.50	4.27
264	BM (△)	82.50	38.250	90.00	6.10	22.50	429.00	179.00	4.00
88	EA (○)	19.43	1.950	40.67	7.51	9.01	125.95	29.70	4.51
164	EA (○)	51.00	18.000	103.00	13.00	30.00	288.00	143.00	3.43
40	AM (⊕)	46.25	20.550	74.10	9.03	22.20	316.00	80.80	3.34
293	SECF (◁)	11.42	1.680	74.10	2.11	8.83	160.25	39.60	8.39
291	JaF (■)	80.81	14.410	154.48	16.00	22.42	100.61	467.19	6.89
345	PW (●)	7.05	0.916	16.30	6.38	3.03	70.42	4.88	5.37
275	SW (▲)	6.70	0.70	2.40	6.30	2.00	31.72	6.30	1.20
6221	P (▽)	0.64	0.04	0.68	0.23	0.59	0.82	3.66	1.15

If the end-members have been correctly chosen for the given dataset, all samples should plot inside an n –1-dimensional hyper-volume defined by the n end-members (Gómez et al. 2006). This is a generalisation of the property of triangular coordinates, i.e. any point inside the triangle has all three triangular coordinates positive, and any point outside the triangle has at least one negative coordinate. By applying this rule, it is easy to know which samples fall inside the hyper-volume defined by the n end-members: those with all their mixing proportions positive. Only these samples can be "explained" by pure conservative mixing of the selected end-members. The closer the number of explained samples is to the total number of samples, the better the combination is (in the sense that more samples can be explained as a mixing of the selected end-members). In other words, a set of end-members is properly selected for a specific dataset when most of the waters in the dataset fall inside the mixing hyper-volume. For three end-members, the mixing hyper-volume is simply a triangle; for four end-members, a tetrahedron and for five or more end-members, a hyper-tetrahedron (Gómez et al. 2006).

M3 performs a systematic search of combinations, starting from two end-members and ending with the maximum number of end-members included as input potential end-members (Gómez et al. 2006). The total number of combinations grows rapidly with this maximum number. For 13 potential end-members, those compiled in Table 3-1, the total number of combinations is 8,178. In other words, M3 solves the mixing problem for all the samples in the dataset a total of 8,178 times, each time selecting a different combination of potential end-members and computing the percentage of samples (coverage) that can be explained by mixing the chosen end-members. The "best" combinations of end-member waters are those with a higher coverage; in other words, with a higher percentage of samples inside the mixing polyhedron. Table 3-2 shows all the combinations of end-member waters with a coverage of at least 75%. This means that at least three quarters of the samples in the final dataset are inside the hyper-tetrahedron defined by the end-members that are listed in the first column of the table. The calculations were made using the same 8 compositional variables already used in the total-system exploratory analysis, i.e. Ca, Mg, Na, K, Cl, HCO_3, SO_4 and the Cl/Na ratio.

The "best" combination has a coverage of 92.4% and is defined by end-members #143, 211, 264 and 6221. Sample #143 is the high-Cl sample from the Amargosa River hydrofacies, sample #211 is the "Tertiary Tuffs aquifer" end-member selected from the Eastern Yucca Mountain hydrofacies, sample #264 is the final water (more evolved) in the PHREEQC mixing and dedolomitisation calculations from the Bare Mountain and South East Crater Flat hydrofacies (the water with the clearest signature of the Palaeozoic Carbonate aquifer) and sample #6221 is the precipitation sample that was chosen as representative of all the precipitation samples in the raw dataset.

Table 3-2. Combinations of end-member waters with a coverage > 75%. Selected mixing models are highlighted in blue.

Rank	End-member combination	Coverage	Mixing model
1	[143 211 264 6221]	92.4	MM1
2	[143 211 264 275]	88.6	
3	[211 264 291 6221]	88.1	MM2
4	[211 264 275]	85.1	
5	[211 264 275 291]	84.3	
6	[211 264 6221]	85.1	
7	[211 264 345]	82.6	
8	[143 211 264 345]	81.4	MM3
9	[40 143 211 6221]	80.9	MM4
10	[211 264 291 345]	79.7	MM5
11	[40 211 291 6221]	79.2	MM6
12	[211 275 291]	77.9	
13	[40 143 211 275]	75.8	
14	[143 211 275]	75.3	

The second "best" combination, with a coverage of 88.6%, shares with the best combination three of the four end-members. However, the precipitation sample #6221 has been substituted here by surface water sample #275. The third "best" combination again has the same end-members as the first, except for sample #143, which in this combination has been substituted by sample #291 (the lone sample from the Jackass hydrofacies).

The analysis of Table 3-2 shows that only a subset of all the potential end-member waters participates in "good" combinations. For example, all of the 14 combinations shown in the table include sample #211 (the Tertiary Tuffs Aquifer end-member), and 9 combinations (out of 14) include sample #264 (the Palaeozoic Carbonate Aquifer end-member).

But even more interesting than the specific end-members which are included in good combinations is the observation that *only combinations with three and four end-member waters* appear in Table 3-2. Considering that M3 has systematically computed all the possible combinations, starting with two end-members and ending with 13 end-members, this is a clear indication that the Yucca Mountain hydro-system must be the result of mixing between a maximum of four different water types. The best combination of 5 end-members, [143 211 264 345 6221], only explains 42.2% of the samples, and the best 6 end-member combination, [40 143 211 291 345 6221], just 36.6% of the samples. Both combinations are far from the 92.4% coverage that the best 4 end-member combination provides.

Figure 3-1 shows on pc1-pc2 plots the coverage of the end-member combinations listed in Table 3-2. It is clear from the figure that 3 end-member combinations are worse that 4 end-member combinations (even 3 end-member combinations with a higher coverage than 4 end-member combinations) as they leave an important part of the volume occupied by the samples outside the mixing hyper-tetrahedron. This is evident, for example, when comparing the best 3 end-member combination (rank 4 in Table 3-2, located in the second row, first column in Figure 3-1; coverage: 85.1%), with 4 end-member combination rank 6 (second row, third column in Figure 3-1; coverage: 84.3%). Although the coverage is slightly higher in the 3 end-member combination, a large group of samples located in the upper right-hand corner of the pc1-pc2 plot are not explained by mixing. On the other hand, in the 4 end-member combination most of these samples are inside the mixing hyper-tetrahedron[1]. Thus, coverage is only a fast way of ranking the mixing models, but the actual principal component analysis results must

[1] Notice that the area inside the triangle defined by the three end-members in 3 end-member combinations is the actual mixing "hyper-volume", but that the area inside the four-sided polygon defined by the four end-members in 4 end-member combinations is only the projection on to the pc1-pc2 plane of a three-dimensional tetrahedron. This is why some of the samples that appear to be inside this projected tetrahedron are actually outside it in the real three-dimensional mixing space.

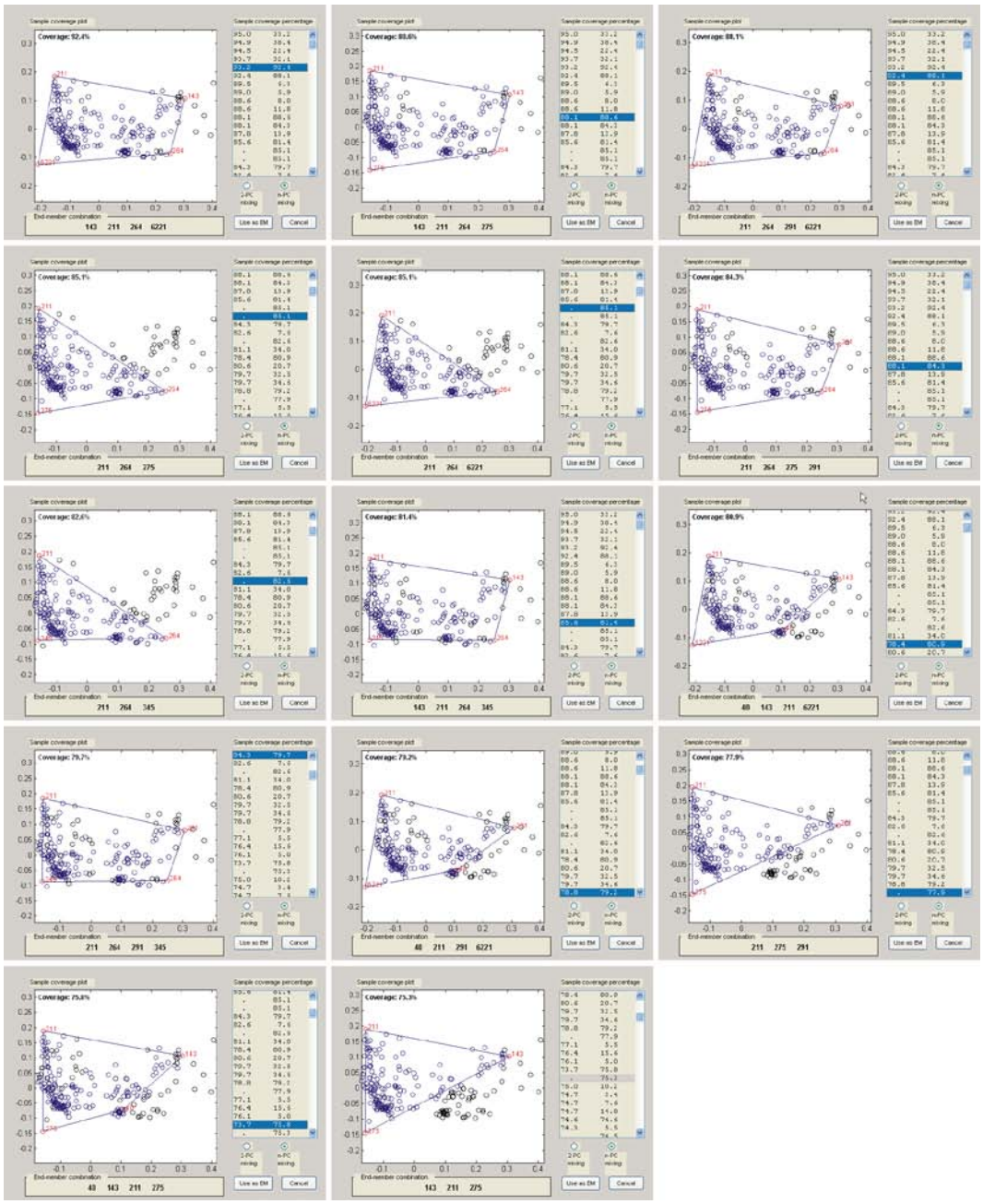

Figure 3-1. *M3 screenshots showing the 14 combinations of end-members with a coverage > 75%, ordered by decreasing coverage from the upper left to the lower right. Results of the principal components analysis are projected on to the pc1-pc2 plane (pc1 runs horizontally and pc2 vertically). The end-members that define each combination are labelled. Samples inside the mixing polyhedron are coloured in blue while those outside it are coloured in black.*

also be taken into account. Based on both the coverage and the actual distribution of the excluded samples, it is concluded that 3 end-member combinations are not able to correctly model the mixing behaviour of waters at Yucca Mountain. Therefore, only 4 end-member combinations are further analysed. *In other words, 4 end-member mixing models explain the hydrochemistry of the Yucca Mountain area better than 3 end-member mixing models*.

The first three entries in Table 3-2 are 4 end-member combinations. The end-members that are included in these three combinations are only 7 (of the potential 13 end-member listed in Table 3-1): one is always the sample that was considered as being representative of the Tertiary Tuffs Aquifer (TTA) (sample #211), another is always the sample considered as being representative of the Regional Palaeozoic Carbonate Aquifer (RCA) (sample #264), another is always a “meteoric water” sample

(either surface water #275 or precipitation water #6221) while the fourth is always a sample representative of the Quaternary Basin-fill Aquifer (QBfA) (the high-Cl samples #143 from the Amargosa River hydrofacies, or sample #291 from the Jackass Flat hydrofacies).

It is interesting to note that the next best 4 end-member combination (rank eight in Table 3-2) has as "meteoric" end-member, the perched water sample #345. This confirms the comment in the hydrofacies exploratory analysis section on the important role that perched waters play in the Yucca Mountain system.

So, it is observed that either a precipitation sample, a surface water sample or a perched water sample always appears as an end-member water in all the good 4 end-member combinations. To combine all three possibilities under one name for this end-member, the term "altered meteoric water" (AMW) end-member will be used from now on. The name can be a little misleading when the "pure" precipitation sample #6221 is used as the actual AMW end-member, but it is preferable to the plain "meteoric end-member", as it emphasizes that water-rock interaction processes have already modified the chemistry of this end-member water. Precipitation sample #6221 is the less modified "altered meteoric" end-member, and perched water sample #345 is the most evolved "altered meteoric" end-member, while surface water sample #275 lies somewhere in between. Thus, mixing proportions obtained with mixing models that include sample #275 would lie within the range defined by mixing models that use sample #6221 or #345. As the *range* of mixing proportions is most interesting, all 4 end-member combinations in which sample #6221 or #345 defines the altered meteoric end-member will be tested, and all combinations in which sample #275 is the altered meteoric end-member will be omitted.

Figure 3-2 shows three perpendicular views of the PCA performed on the final dataset. The end-members giving good coverage are labelled in the figure. It can be observed that they actually occupy extreme positions in the Principal Components graphs.

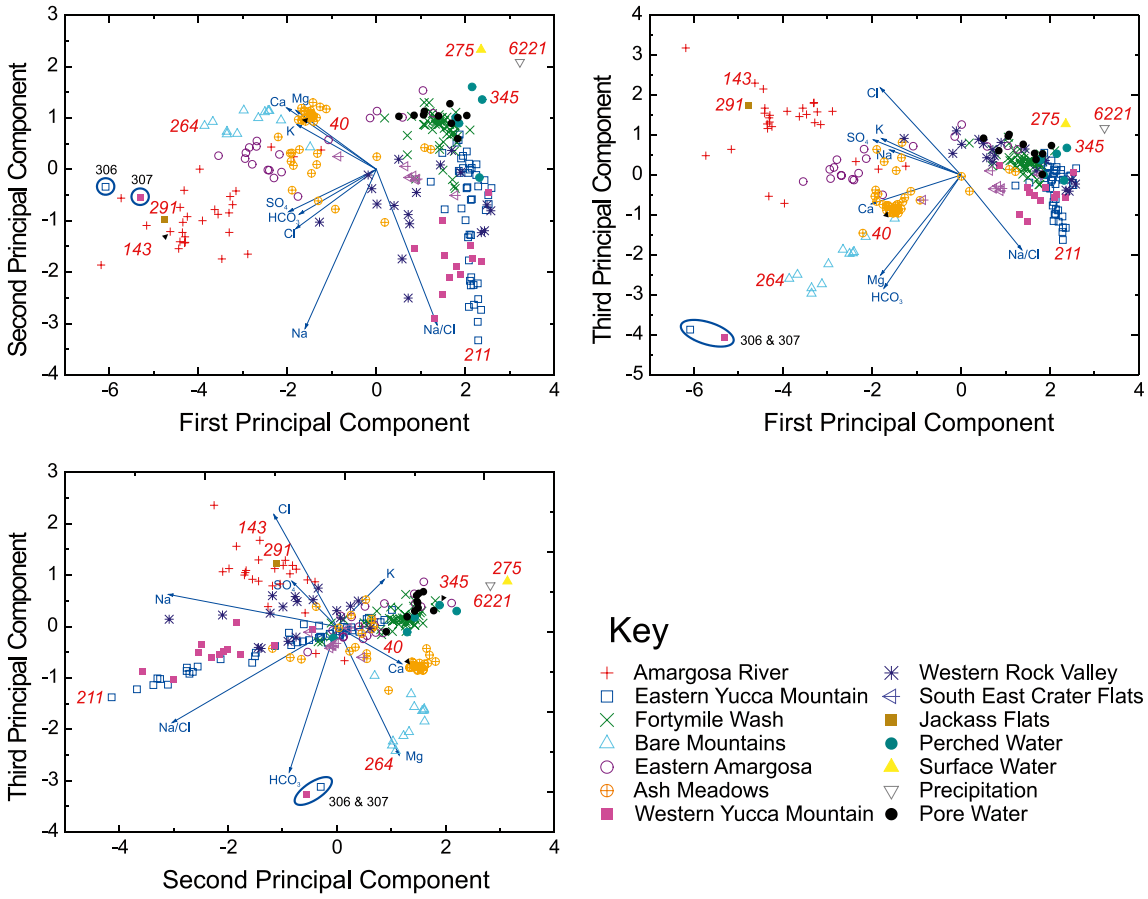

Figure 3-2. *Three perpendicular views of the PCA carried out with the final dataset. The end-member waters identified with M3's End-member Selection Module and belonging to mixing models with a coverage > 75% are labelled. Also, special samples 306 and 307 are labelled and encircled.*

It should also be noted that the two samples collected in the Palaeozoic Carbonate Aquifer in borehole UE-25 p#1 (samples #306 and 307) are outside the mixing polyhedron. This means that the chemical composition of samples #306 and 307 cannot be explained by a pure mixture of the four end-member waters (samples #143, 211, 264, and 6221). Other M3 runs were performed using the other combinations of end-members listed in Table 3-2, and in each case samples #306 and 307 were outside the mixing polyhedron. Two possible explanations for this difference in chemistry are: (1) the groundwaters of the carbonate aquifer under Yucca Mountain do not mix with other groundwaters included in the final dataset nor discharge inside the studied domain and (2) other processes besides mixing have change their chemistry, "pushing" both samples outside the mixing polyhedron.

3.2 Test of mixing models

The analysis carried out in the preceding section has shown that 4 end-member mixing models are superior to 3 end-member models. All the 4 end-member mixing models with > 75% coverage (Table 3-2) have several properties in common, which are important to stress in this context:

- From the 13 potential end-member waters listed in Table 3-1 only 8 appear in "good" combinations (those with > 75% coverage, as listed in Table 3-2). These are samples #40 (AM), #143 (AR), #211 (EYM), #264 (BM), #275 (SW), #291 (JaF), #345 (PW) and #6621 (P).
- Every 4 end-member combination in Table 3-2 has an Altered Meteoric end-member (sample #6621, sample #345 or sample #275), a Palaeozoic Carbonate Aquifer end-member (either sample #264 or sample #40), a Tertiary Tuffs Aquifer end-member (sample #211) and a Quaternary Basin-fill Aquifer end-member (either sample #143 or sample #291).
- Altered Meteoric end-member waters are of three types: precipitation (#6621), surface water (#275) and perched water (#345). Surface waters have a chemical signature intermediate between precipitation and perched waters (see, for example, Figures 2-37 and 3-2), which is the reason why mixing models that have sample #275as Altered Meteoric end-member surface water are not taken into account. Also, surface water samples could have been subjected to water-rock interaction processes that are not representative of those that characterise the recharge waters which eventually enter the groundwater system. Thus, only mixing models in which the Altered Meteoric end-member is occupied by precipitation sample #6621 or perched water sample #354 have been selected. These mixing models, highlighted in Table 3-2, are compiled in Table 3-3 indicating which sample occupies the Altered Meteoric Water (AMW), the Regional Palaeozoic Carbonate Aquifer (RCA), the Tertiary Tuffs Aquifer (TTA) and the Quaternary Basin-fill Aquifer (QBfA) end-member. Also, a specific label (MM1 for mixing model #1, MM2 for mixing model #2, and so on) is given to each of them for further reference (in order of decreasing coverage).

However, coverage is not the only attribute of a "good" mixing model (as already observed when comparing three- and four-end-member mixing models). Obviously, a key aspect for classifying a mixing model as being good or bad is how well the chemical composition of conservative elements (such as chloride) can be reproduced. This is easily performed once the mixing proportions have been computed. An example using Cl as the conservative element will clarify the procedure.

Table 3-3. Selected mixing models indicating the sample acting as end-member (sample number and hydrofacies) and the coverage.

Mixing model	End-member combination				Coverage
	AMW	RCA	TTA	QBfA	
MM1	6221▽	264△	211□	143+	92.4
MM2	6221▽	264△	211□	291■	88.1
MM3	345●	264△	211□	143+	81.4
MM4	6221▽	40⊕	211□	143+	80.9
MM5	345●	264△	211□	291■	79.7
MM6	6221▽	40⊕	211□	291■	79.2

▽: Precipitation; ●: Perched water; △: Bare Mountain; ⊕: Ash Meadows; □: Eastern Yucca Mountain; +: Amargosa River; ■: Jackass Flat.

Assuming that the mixing proportions of sample #3 (from the Ash Meadows hydrofacies) calculated with mixing model #1 (MM1) are: AMW = 22.1%, RCA = 48.3%, TTA = 9.0% and QBfA = 20.6%, the chloride contents of the four end-member waters are (Table 3-1): AMW (#6621) = 0.59 mgL^{-1}; RCA (#264) = 22.5 mgL^{-1}; TTA (#211) = 5.5 mgL^{-1}) and QBfA (#143) = 83.0 mgL^{-1}. Thus, the predicted chloride concentration of sample #3 under mixing model #1 is:

$$Cl_{\text{Sample \#3}} = \frac{Cl_{AM} \cdot 22.1\% + Cl_{PCA} \cdot 48.3\% + Cl_{TTA} \cdot 9.0\% + Cl_{QBfA} \cdot 20.6\%}{100} = 28.6 \text{ mg/L}.$$

As the actual chloride concentration of sample #3 is Cl = 25.0 mgL^{-1}, mixing model #1 overestimates the Cl content by 3.6 mgL^{-1} in absolute terms (12%). Therefore, when plotting the calculated Cl concentration of each sample against its actual concentration on an XY graph, a good model should have most samples along the 1:1 diagonal line.

Figure 3-3 plots the measured and calculated chloride concentrations in the six mixing models, with the measured concentration in the horizontal axis and the calculated one in the vertical axis. Each mixing model is represented by two plots: the left-hand plot is drawn with linear scales and the right-hand one with log-log scales to better appreciate the low-concentration end. Visually, it seems clear that models MM2 and MM5 are the worst of the group, whereas models MM1, MM3 and MM4 perform much better. Model MM6 appears to lie somewhere in between.

Obviously, a more quantitative assessment of the quality of each mixing model is needed. The whole procedure can be boiled down into a goodness-of-fit exercise, where the "model" is the diagonal line in Figure 3-3 and the "observations" are the samples. The closer to the diagonal line the samples are, the better the fit and the smaller the mismatch between measured and computed concentrations (residuals). Two goodness-of-fit statistics have been used to compare the six mixing models: the coefficient of determination (R^2), which is appropriate for absolute deviations, and the chi-square statistics, χ^2, which is useful for assessing relative deviations.

The coefficient of determination is defined as:

$$R^2 = 1 - \frac{SS_{err}}{SS_{tot}},$$

where SS_{tot} is the total sum of squares and SS_{err} is the sum of squared errors (or residual sum of squares),

$$SS_{tot} = \sum_{i=1}^{N} (x_i^{ob} - \mu_i^{ob})^2,$$

$$SS_{err} = \sum_{i=1}^{N} (x_i^{ob} - x_i^{cal})^2.$$

In the expression for SS_{tot}, μ refers to the mean value of variable x. For linear regression, as here, the coefficient of determination is the square of the well-known correlation coefficient and is a statistical measure of how well the regression line approximates the real data points. An R^2 of 1.0 indicates that the regression line fits the data perfectly, while an R^2 of 0.0 indicates that none of the variance in the data is explained by the proposed model. An intermediate value (such as $R^2 = 0.7$) means that part of the variance in the data is captured by the model (in the example, 70%), but another part (here 30%) is not explained and can be assigned to unknown variables or inherent variability. When comparing different models, the best model is the one with an R^2 value closest to 1. Table 3-4 gives the coefficient of determination for the six mixing models. We can see that the "intuitive" ranking of the models based on Figure 3-3 is qualitatively correct. Models MM1, MM3 and MM4 all have R^2 values of between 0.82 and 0.87, whereas models MM2 and MM5 have R^2 values of approximately 0.32, and model MM6 is intermediate, with $R^2 = 0.47$.

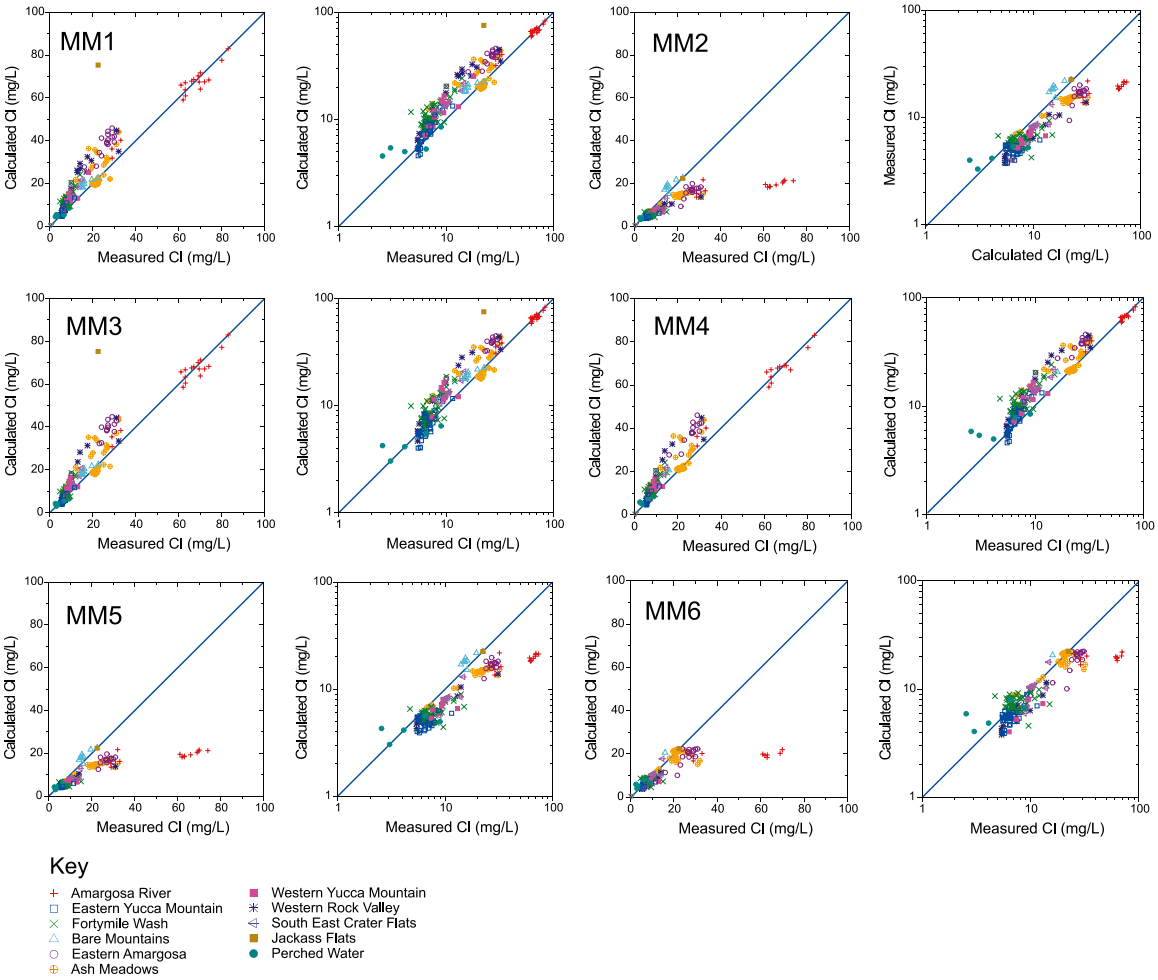

Figure 3-3. *Measured versus calculated chloride concentrations in the six mixing models. Each mixing model is represented by two plots, the left-hand plot in linear scales and the right-hand one in log-log scales.*

The χ^2 goodness-of-fit statistics are defined as

$$\chi^2 = \sum_{i=1}^{N} \frac{\left(x_i^{ob} - x_i^{cal}\right)^2}{x_i^{ob}} ,$$

where x is the variable to be fitted, and superscripts "ob" and "cal" refer to observed and calculated values for each of the N entries in the dataset. Because models with different number of samples are being compared, a better format in this case is the reduced χ^2, χ^2_{red},

$$\chi^2_{red} = \frac{1}{\nu} \sum_{i=1}^{N} \frac{\left(x_i^{ob} - x_i^{cal}\right)^2}{x_i^{ob}} ,$$

where ν is the number of degrees of freedom, $\nu = N–n–1$, being n the number of fitted parameters in the model. Here n is zero because both the intercept and the slope of the diagonal line (the model) cannot be chosen, which means that $\nu = N–1$. The advantage of the reduced chi-squared is that it already normalises for the number of data points and model complexity. As a rule of thumb, a large χ^2_{red} indicates a poor model fit. However, $\chi^2_{red} < 1$ indicates that the model 'over-fits' the data (either the model is improperly fitting noise, or the error bars have been over-estimated). A $\chi^2_{red} > 1$ indicates that the fit has not fully captured the data (or that the error bars have been under-estimated). In principle,

a $\chi^2_{red} = 1$ is the best fit for the given data and error bars. When comparing different models, the best model is the one with a χ^2_{red} closest to 1 (from above). Table 3-4 gives the reduced χ^2 for the six mixing models. Contrary to the coefficient of determination results, in this case model MM6 is the "best" one, followed by models MM3 and MM4, while model MM5, as was the case with R^2, is the "worst" one.

Table 3-4. Chloride goodness-of-fit for the six mixing models highlighted in Table 3-2.

Mixing model	N	SS_{tot}	SS_{err}	R^2	Rank	χ^2	Rank
MM1	222	57,738.9	10,635.1	0.816	3	2.80	5
MM2	210	37,934.0	25,545.8	0.327	5	2.71	4
MM3	196	56,312.9	7,939.1	0.859	2	2.10	2
MM4	194	47,546.7	5,995.0	0.874	1	2.12	3
MM5	189	36,705.3	25,061.8	0.317	6	2.86	6
MM6	187	27,364.4	14,524.4	0.469	4	1.66	1

As the coefficient of determination is, in this case, a measure of the goodness-of-fit of a linear regression model by least squares (minimisation of the sum of squared errors), outliers can drastically affect the quality of the fit. This is clearly the case with model MM6: it has a low R^2 of 0.47 (rank 4) but is the model with the lowest reduced χ^2 (rank 1). Going back to Figure 3-3 it can be appreciated that a group of outlier samples in the high-Cl end (samples from the Amargosa River hydrofacies) is obviously increasing the sum of squared errors (and thus reducing the overall coefficient of determination). On the other hand, models MM3 and MM4 do not have these outliers (see again Figure 3-3) and the overall R^2 is much higher (0.86 and 0.87, respectively).

However, it is important to note that the six mixing models have a different number of samples ("observations"). Although this is somehow taken into account by both the R^2 approach (via the total sum of squares) and the χ^2_{red} approach (via the number of degrees of freedom, ν), the exclusion of different samples in each case can, if these samples are far from the average deviation, influence the outcome of the statistical test. To take this asymmetry into account, both R^2 and χ^2_{red} for the subset of samples *common to the six mixing models* (this subset is composed of 164 samples) have been recomputed. Table 3-5 gives the new results. Now, on a common basis of the same 164 samples, MM3 emerges as the "best" model in both the R^2 and χ^2_{red} senses while MM6 ranks second from the χ^2_{red} point of view and fourth from the R^2 point of view.

Combining the rankings from coverage, R^2 and χ^2 (Table 3-6), mixing model MM3 emerges as the "best" model overall, followed (closely) by MM1 and by MM4 in the third position. So, MM3 will be taken as the reference mixing model in the next section and the mixing proportions obtained from it will be compared with the other mixing models in order to assess the variability of the results. Summating ranks of different statistics (coverage, R^2, χ^2) does not seem very appropriate, more so when the statistics have been obtained in rather different ways. And it would really be inappropriate if each set of statistics gave a completely different ranking. However, this is not the case, as model MM3 is the best model in both the R^2 *and* χ^2 senses. This is the only factor necessary in order to give model MM3 the status of "reference model". Below, reference model MM3 will be compared to the other models, and in making these comparisons the actual ranking of the other models (as summarised in Table 3-6) becomes quite irrelevant.

Table 3-5. Chloride goodness-of-fit (reduced to a common set of samples) for the six mixing models highlighted in Table 3-2.

Mixing model	N	SS_{tot}	SS_{err}	R^2	Rank	χ^2	Rank
MM1	164	26,013.3	4,891.1	0.812	3	2.09	3
MM2	164	26,013.3	16,524.9	0.365	5	2.36	5
MM3	164	26,013.3	3,646.0	0.860	1	1.36	1
MM4	164	26,013.3	4,782.7	0.816	2	2.10	4
MM5	164	26,013.3	16,700.2	0.358	6	2.41	6
MM6	164	26,013.3	14,203.5	0.454	4	1.80	2

Table 3-6. Final ranking of the six mixing models taking into account coverage, R^2 and c^2 rankings (▽: Precipitation; ●: perched water; △: Bare Mountain; ⊕: Ash Meadows; □: Eastern Yucca Mountain; +: Amargosa River; ■: Jackass Flat).

Mixing model	End-member combination				Rank Cov	Rank R^2	Rank χ^2	Σranks	Final rank
	AMW	RCA	TTA	QBfA					
MM3	345●	264△	211□	143+	3	1	1	5	1
MM1	6221▽	264△	211□	143+	1	3	3	7	2
MM4	6221▽	40⊕	211□	143+	4	2	4	10	3
MM2	6221▽	264△	211□	291■	2	5	5	12	4
MM6	6221▽	40⊕	211□	291■	6	4	2	12	5[1)]
MM5	345●	264△	211□	291■	5	6	6	17	6

[1)] Although mixing models MM2 and MM6 have the same sum of ranks, MM6 is given a lower final rank due to its smaller coverage.

3.3 Mixing proportions

Mixing model MM3 gives the best overall performance for the description of the Yucca Mountain hydro-system in terms of mixing. Here "best" is used qualitatively, meaning better global performance. However, as we have seen above, mixing model MM3 is also the best model in both the quantitative R^2 sense as well as in the quantitative χ^2 sense. For this reason, model MM3 is regarded as the reference mixing model and the mixing proportions obtained with it are considered as being the "good ones". Table 3-7 gives the mixing proportions of all samples in the final dataset for reference mixing model MM3. Samples outside the mixing polyhedron are included in the table but have no mixing proportions. Samples are ordered in increasing sample number (abbreviated to ID# in the table heading) and the symbol identifying the hydrofacies (see above) has been added to facilitate the visual analysis of the table.

Table 3-7. Mixing proportions of samples in the final dataset for mixing model MM3.

ID#	TTA	RCA	QBfA	AMW	ID#	TTA	RCA	QBfA	AMW
3⊕	0.065	0.466	0.195	0.274	197×	0.167	0.077	0.011	0.745
4⊕	0.073	0.400	0.256	0.271	198×	0.057	0.090	0.040	0.813
5⊕	0.055	0.444	0.220	0.281	199□	0.404	0.028	0.092	0.477
17⊕	0	0.530	0.087	0.384	200✳	0.233	0.017	0.505	0.245
18⊕	0	0.536	0.053	0.411	201✳	0.156	0	0.376	0.468
20⊕	0	0.518	0.076	0.406	202□	0.831	0	0.041	0.128
21⊕	0	0.516	0.066	0.419	203□	0.738	0.005	0.026	0.231
23⊕	–	–	–	–	204□	0.829	0	0.026	0.145
24⊕	0.141	0.108	0.087	0.664	205□	0.542	0	0.035	0.423
25⊕	0.049	0.660	0.067	0.225	206□	0.477	0	0.047	0.476
26⊕	0	0.506	0.118	0.376	207□	0.230	0.054	0.018	0.698
27⊕	–	–	–	–	208□	0.347	0.014	0.031	0.608
28⊕	0	0.527	0.062	0.411	209□	0.729	0	0.043	0.228
31⊕	0	0.529	0.059	0.412	210□	0.919	0	0.005	0.077
34⊕	0	0.157	0.387	0.456	211□	1.000	0	0	0
35⊕	–	–	–	–	212□	0.154	0.045	0.041	0.759
36⊕	0.267	0.341	0.220	0.172	213□	0.707	0	0.040	0.253
37⊕	0.133	0.204	0.154	0.509	214□	0.868	0	0	0.132
38⊕	0.056	0.206	0.346	0.392	215□	0.824	0.017	0	0.160
39⊕	0.398	0.144	0.179	0.279	216□	0.747	0	0.035	0.218
40⊕	0	0.533	0.091	0.375	217□	0.552	0.012	0.019	0.417
41⊕	0	0.505	0.105	0.390	218□	0.755	0	0.009	0.236
45⊕	0	0.277	0.334	0.390	219□	0.634	0	0.047	0.318
46⊕	0.311	0.290	0.210	0.189	220□	0.568	0.044	0	0.389
47⊕	0	0.519	0.075	0.407	221□	0.272	0.038	0.039	0.651
48⊕	0	0.541	0.063	0.397	224■	0.831	0	0.143	0.026
49⊕	0.158	0.105	0.069	0.668	225■	–	–	–	–
52⊕	0	0.540	0.055	0.405	226■	0.643	0	0.128	0.229
58+	0	0.134	0.820	0.046	227□	0.265	0.028	0.034	0.673
59+	0.028	0.312	0.327	0.334	228□	0.295	0.112	0.062	0.530
63+	0.025	0.600	0.370	0.005	230✳	–	–	–	–
81⊕	0	0.511	0.073	0.416	231✳	–	–	–	–
82⊕	0	0.500	0.083	0.418	232✳	0.143	0.080	0.293	0.484
85⊕	0	0.510	0.068	0.421	235△	0	0.691	0.025	0.283
86⊕	–	–	–	–	236◁	0.262	0.169	0.082	0.488
88○	0	0.065	0.099	0.836	237◁	0.281	0.164	0.064	0.490
89○	–	–	–	–	238◁	0.275	0.153	0.071	0.502

ID#	TTA	RCA	QBfA	AMW	ID#	TTA	RCA	QBfA	AMW
90	–	–	–	–	239	0.256	0.154	0.082	0.508
92	0	0.534	0.060	0.406	240	0.188	0.116	0.142	0.553
93	0.100	0.408	0.241	0.251	241	0.129	0.118	0.007	0.746
94	0.107	0.259	0.315	0.319	242	0.055	0.126	0.019	0.800
95	0.024	0.093	0.055	0.829	243	0.084	0.094	0.020	0.802
96	–	–	–	–	244	0.086	0.069	0.028	0.816
97	–	–	–	–	245	0.158	0.123	0.013	0.706
99	0	0.519	0.075	0.406	246	0.084	0.149	0.008	0.759
101	0	0.237	0.415	0.348	247	0.049	0.095	0.028	0.828
102	0.042	0.097	0.099	0.762	248	0.112	0.059	0.039	0.791
103	0.108	0.169	0.458	0.265	249	0.286	0.047	0.028	0.639
104	0	0.091	0.167	0.742	250	0.642	0	0.086	0.272
105	–	–	–	–	252	0	0.764	0	0.236
106	–	–	–	–	253	0	0.758	0	0.242
107	–	–	–	–	254	0	0.774	0	0.226
116	0.083	0.075	0.054	0.788	255	0	0.782	0.009	0.209
117	0.059	0.089	0.044	0.808	258	–	–	–	–
120	0.033	0.265	0.280	0.422	259	0.087	0.519	0.089	0.305
121	0	0.317	0.366	0.318	260	–	–	–	–
122	0	0.091	0.083	0.826	261	–	–	–	–
123	–	–	–	–	262	–	–	–	–
124	0	0.316	0.445	0.239	263	0	0.959	0	0.041
126	0	0.422	0.358	0.220	264	0	1.000	0	0
128	0.080	0.069	0.050	0.801	265	0.183	0.038	0.054	0.725
129	0	0.376	0.406	0.218	266	0.099	0.064	0.044	0.793
130	0	0.467	0.391	0.142	267	0.115	0.062	0.039	0.784
131	0.237	0.053	0.163	0.546	268	0.114	0.054	0.050	0.782
136	0.018	0.051	0.107	0.825	269	0.118	0.057	0.036	0.789
137	0.038	0.092	0.062	0.808	270	0.580	0	0.120	0.300
139	0.008	0.093	0.077	0.822	272	0.125	0.374	0.126	0.374
140	0.005	0.007	0.182	0.806	273	0.404	0.008	0.026	0.562
141	0.125	0.017	0.120	0.738	274	–	–	–	–
142	0.230	0.007	0.117	0.646	275	–	–	–	–
143	0	0	1.000	0	276	–	–	–	–
144	0.152	0.045	0.095	0.708	277	–	–	–	–
145	0.041	0.099	0.068	0.792	278	–	–	–	–
146	0.082	0.115	0.056	0.747	279	0.200	0.010	0.790	0
147	0.036	0.110	0.077	0.777	280	–	–	–	–
148	0.036	0.024	0.790	0.150	281	0.077	0.043	0.048	0.832
149	0.031	0.115	0.755	0.100	282	–	–	–	–
150	0.141	0.108	0.142	0.609	283	0.042	0.193	0.765	0
152	0.039	0.064	0.790	0.108	284	–	–	–	–
153	0.050	0.093	0.813	0.044	286	0.057	0.192	0.751	0
154	0	0.171	0.324	0.505	287	0.209	0	0.755	0.036
155	0.304	0.053	0.045	0.598	289	0.353	0.020	0.029	0.599
157	0.335	0.060	0.032	0.573	291	0	0.111	0.887	0.002
158	0.046	0.256	0.415	0.282	293	0.354	0	0.083	0.563
159	0.045	0.070	0.177	0.709	295	0.255	0.024	0.018	0.703
160	–	–	–	–	296	0	0.841	0	0.159
161	0.105	0	0.811	0.084	297	0.260	0	0.019	0.721
162	–	–	–	–	298	–	–	–	–
163	0.211	0.347	0.280	0.162	299	0.125	0.038	0.045	0.792

ID#	TTA	RCA	QBfA	AMW	ID#	TTA	RCA	QBfA	AMW
164○	0	0.398	0.339	0.263	305■	0.455	0.038	0.089	0.418
165×	0.344	0.054	0.035	0.567	306■	–	–	–	–
166○	0.058	0.374	0.354	0.214	307□	–	–	–	–
167○	0.061	0.375	0.348	0.216	308■	0.773	0.061	0.064	0.102
168○	0.082	0.322	0.380	0.216	309□	0.269	0.003	0.029	0.699
169×	0	0.117	0.121	0.762	310□	0.427	0	0	0.573
170×	0.060	0.108	0.038	0.794	311□	0.304	0	0.020	0.676
171×	0.050	0.107	0.087	0.756	312□	0.394	0	0	0.606
172+	0.013	0.140	0.684	0.164	313□	0.271	0	0.040	0.689
173+	0.001	0.148	0.658	0.193	314□	0.294	0.028	0.018	0.660
174+	0.027	0.073	0.735	0.165	315●	0.325	0.015	0	0.660
175+	–	–	–	–	316□	0.210	0.018	0.044	0.729
176×	0.018	0.148	0.036	0.799	317□	0.430	0.024	0.040	0.506
177×	0.055	0.126	0.015	0.804	318□	0.107	0	0.072	0.821
179✳	0.186	0.067	0.037	0.709	319■	–	–	–	–
180×	0.077	0.122	0.029	0.772	320■	0.581	0	0.042	0.377
181×	0.065	0.110	0.052	0.773	324□	0.144	0.036	0.043	0.778
183×	0.055	0.109	0.051	0.785	325□	0.357	0	0.010	0.633
184□	–	–	–	–	326□	0.170	0.038	0.093	0.699
185✳	–	–	–	–	327■	–	–	–	–
186✳	–	–	–	–	332□	0.331	0	0.002	0.667
187✳	–	–	–	–	337□	–	–	–	–
188✳	0.234	0	0.348	0.417	338●	0.104	0.116	0	0.781
189✳	–	–	–	–	340□	–	–	–	–
190✳	0.106	0.014	0.254	0.625	341●	0.058	0.069	0.024	0.848
191✳	0.244	0	0.094	0.662	344□	0.187	0	0.053	0.760
192✳	0.177	0	0.162	0.661	345●	0	0	0	1.000
193✳	0.517	0	0.032	0.451	354●	0	0.061	0	0.939
194✳	0.518	0	0.019	0.463	359×	0.028	0.050	0.041	0.882
195✳	0.410	0	0.022	0.568	360×	0.099	0	0.054	0.847
196✳	0.442	0	0.008	0.550	6221▽	–	–	–	–

In the following sections, a description is given of each mixing model. Mixing model MM3 is described in detail, while the remainder are described in comparison to MM3, stressing the most important differences.

3.3.1 Mixing model MM3 (reference mixing model)

Figure 3-4 summarises in a graphical manner the mixing proportions for the reference mixing model. Six plots are included in the portrait in order to represent all the binary combinations of end-members. In the first row, the RCA end-member is plotted against the other three end-members, in the second row the QBfA end-member is plotted against the two remaining end-members (TTA and AMW) and in the third row the AMW end-member is plotted against TTA. Mixing proportions are expressed on a unit basis (mixing fractions) instead of on a percentage basis

The diagonal line on each plot represents a binary mixture of the two end-members occupying the axes. In other words, samples that can be explained as a mixture of only two end-member waters will plot on this diagonal line when the two end-members contributing to its composition define the axes of the graph (see, for example, the Bare Mountains samples in the AMW-RCA graph in Figure 3-4 or many of the Eastern Yucca Mountain samples in the TTA-AMW graph in the same figure). Also, a sample plotted on one axis has a zero contribution from the end-member occupying the other axis, a sample near the origin of coordinates has a zero contribution from the two end-members that define the two axes in the corresponding graph and a sample located in the interior of the triangular area defined by the two axes and the diagonal line has contributions from at least three (possibly more) different end-member waters (the two end-members defining the axis plus, at least, one more end-member).

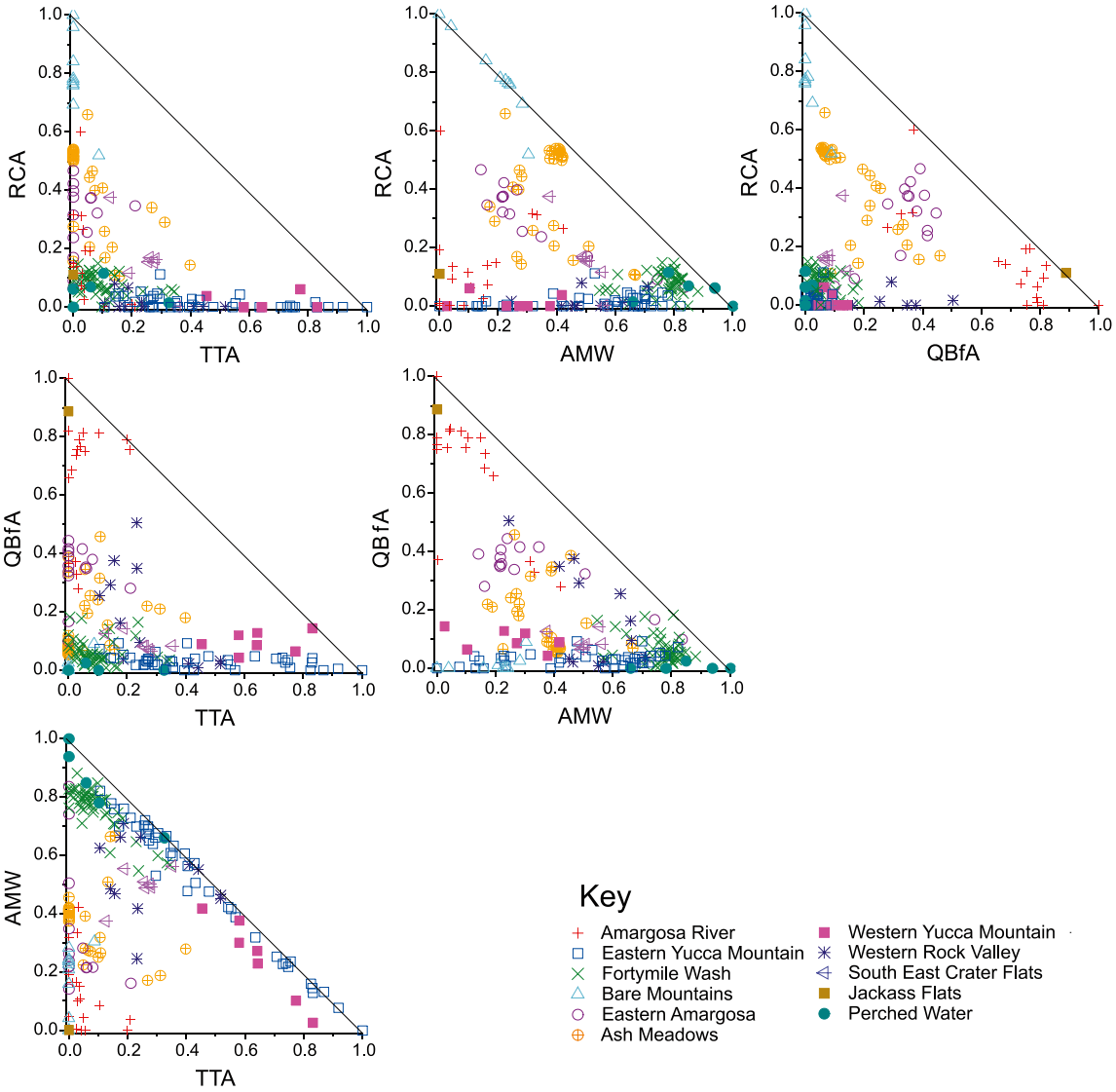

Figure 3-4. *Mixing proportions for mixing model MM3 (TTA=211; RCA=264; QBfA=143; AMW=345).*

MM3 has sample #211 as the TTA end-member (this sample is common to all selected mixing models, see Table 3-2 above), sample #264 as the RCA end-member, sample #143 as the QBfA end-member and sample #345 as the AMW end-member. The coverage is 81.4%, i.e. 195 samples out of 240 are inside the mixing polyhedron and can thus be explained by a mixture of the corresponding end-member waters (the remaining 45 samples plot outside the mixing polyhedron and their chemistry cannot be reproduced by mixing).

As Figure 3-5 shows, the highest contribution to the chemistry of the samples in the final dataset comes from the AMW (49%), followed by the TTA (19%), the RCA (17%) and the QBfA (15%). Also, the AMW contribution is more evenly spread among the samples (similar height of the histogram bars in the AMW graph).

In the following sections, the most important mixing trends affecting each hydrofacies, as evidenced on the graphs in Figure 3-4 are discussed. For this purpose, on the graphs in Figure 3-6 colour-coded trends are superimposed in order to assist in the visual understanding of the following explanations.

Ash Meadows hydrofacies

Figure 3-6 (left-hand graph) shows that the cluster of Ash Meadows (AM) samples (representative samples, see Table 2-14 above) is almost a binary mixture of the RCA and AMW end-members (with a small contribution, ~8%, of the QBfA end-member). This is in agreement with a discharge of the regional Palaeozoic Carbonate Aquifer along the Gravity Fault, as already mentioned. Apart from the cluster of representative samples, which have the highest contribution of the RCA end-member among all the AM samples, several other AM samples are "contaminated" to a lesser or greater extent by QBfA waters (up to 50% of the QBfA end-member). Two branches can be recognised as shown in Figure 3-6: one with a continuous increase in the proportion of the QBfA end-member (best seen in the right-hand graph in Figure 3-6), and another with an initial increase in the proportion of the QBfA end-member followed by an increase in the proportion of the AMW end-member (best seen in the left-hand graph in Figure 3-6 as the thick orange arrow). The samples contaminated by QBfA and/or AMW waters are those located at a considerable distance from the spring line that delineates the Gravity Fault. This contamination is a logical outcome, as in these samples the interaction with shallow groundwaters residing in the basin-fill aquifers is much more likely.

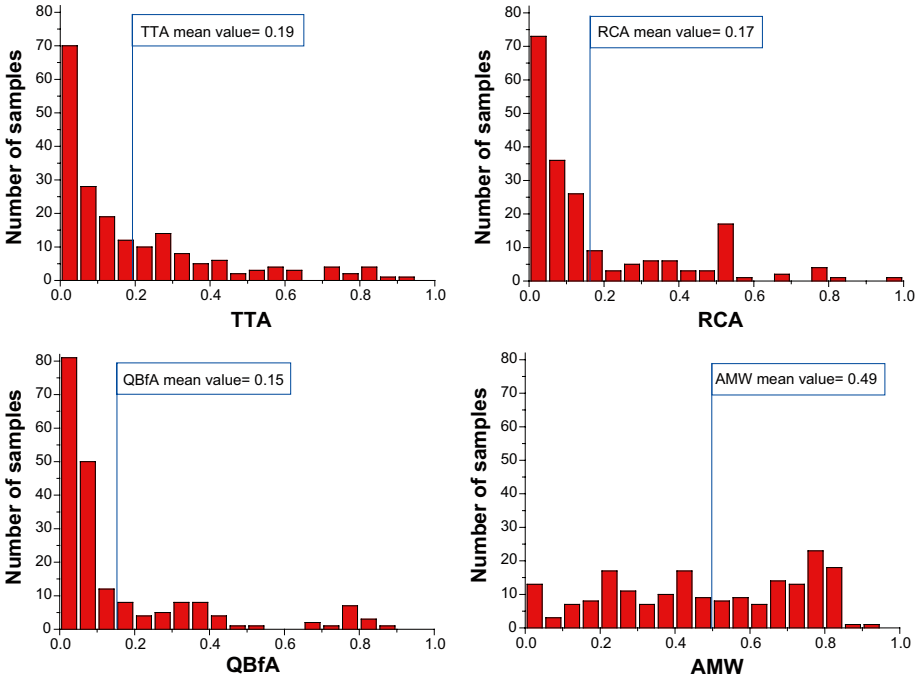

Figure 3-5. *Distribution of mixing proportions for each end-member water in the final dataset. The mean value is indicated. Note that the contribution of the AMW end-member (lower right plot) is more evenly distributed than the other end-members.*

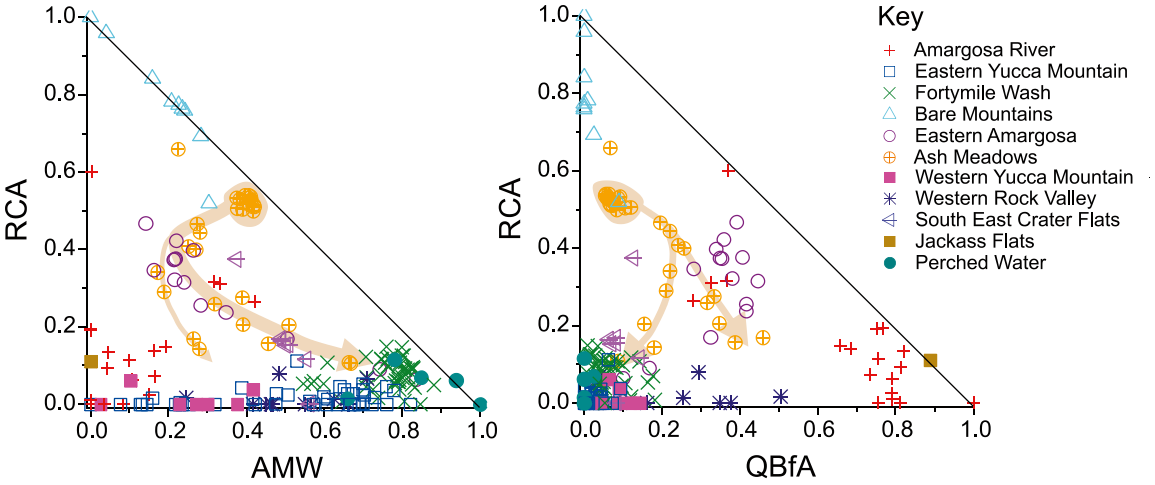

Figure 3-6. *Main trends affecting Ash Meadows samples.*

Eastern and Western Yucca Mountain hydrofacies

The Eastern and Western Yucca Mountain hydrofacies samples are almost a binary mixture of the TTA and AMW end-members (Figure 3-7). The proportion of the AMW end-members ranges from 0 to 80% in the EYM hydrofacies and from 0 to 40% in the WYM hydrofacies. This is a rather unexpected result. In Section 2.4.2 (Hydrofacies exploratory analysis) it was stated that the EYM waters seem to be a binary mixture of TTA *and QBfA waters*. This conclusion was reached after a detailed analysis of samples in borehole NC-EWDP 19D. The lithology summary log of the borehole shows sections with Quaternary basin-fill sediments, and samples taken from there were assumed to be representative of the QBfA end-member water.

But the mixing analysis carried out here shows that the chemistry of the waters in the basin-fill sediments in the area is characteristic of the AMW end-member and *not* of the QBfA end-member. This result is very interesting in itself, and points to the rather widespread presence of an “old” meteoric water in many shallow sections of the local aquifers around Yucca Mountain.

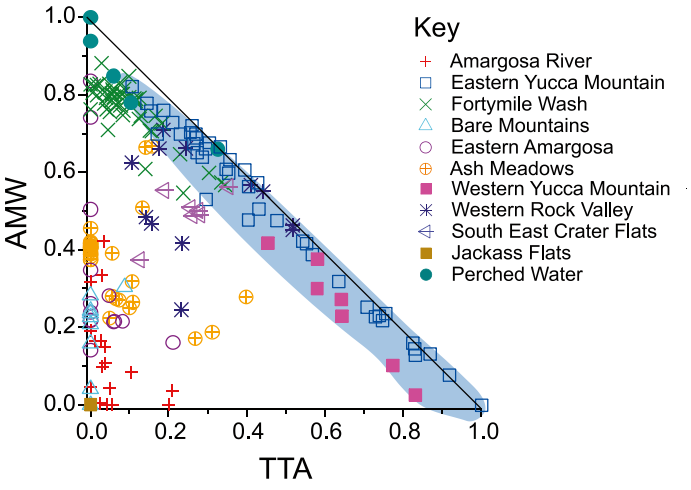

Figure 3-7. *Binary mixing trend in the Eastern and Western Yucca Mountain samples.*

Bare Mountains and Southeast Crater Flat hydrofacies

The Bare Mountains and Southeast Crater Flat samples follow a trend starting at the RCA end-member[2] (upper left-hand corner in the three plots of Figure 3-8), along the diagonal line in the AMW-RCA plot (upper graph in Figure 3-8) and ending inside the mixing triangle. Most BM samples are a binary mixture of the RCA and AMW end-members, while the SECF samples also have an important contribution from the TTA end-member (around a 30%), best seen in the lower left-hand graph if Figure 3-8, near the arrow head. As was the case with the EYM samples, the main additional component in the mixture is the AMW end-member despite the fact that most samples were collected in basin-fill sediments. The TTA component is apparent in those SECF samples that come from the deepest sections in the boreholes, where the Tertiary Tuffs are intersected (boreholes NC-EWDP 9SX and NC-EWDP 13P). In summary, the mixing trend starts at the RCA end-member and progresses by mixing with the AMW end-member, first alone (up to the point where the trend leaves the diagonal line in the RCA-AMW plot), and then with extra contributions from the TTA (up to 30%) and QBfA (up to 20%) end-members. In the last stages, the QBfA contribution diminishes and the samples are a mixture dominated by the AMW end-member (50%), with contributions from the TTA end-member (30%), the RCA end-member (15%) and the BQfA (5%).

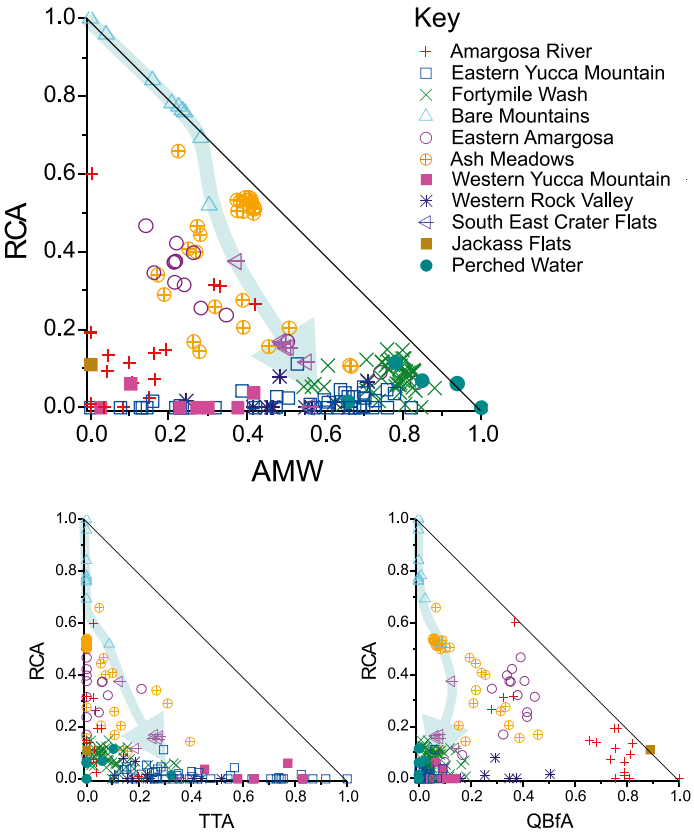

Figure 3-8. *Main mixing trend in Bare Mountain and South East Crater Flat samples.*

[2] The RCA end-member water, sample #264, belongs to the BM hydrofacies.

Central Amargosa Valley hydrofacies

The samples from the Central Amargosa Valley (Amargosa River, Eastern Amargosa, Fortymile Wash and Western Rock Valley hydrofacies) are particularly interesting because they occupy the area down-gradient of Yucca Mountain. In the case of a confinement failure in the repository, the contaminated waters are likely to end here. Therefore, an assessment of the composition of these waters in terms of mixing could shed light on the issue of the degree of isolation between aquifers.

From the point of view of mixing (Figure 3-9), these waters are dominated by the QBfA and AMW end-members, although they always have contributions from at least one other end-member water. By hydrofacies, Amargosa River samples have the highest contribution of the QBfA end-member (between 75% and 100%), followed by the Eastern Amargosa samples (around 40%) and the Fortymile Wash samples (less than 20%). This is best seen in the left-hand graph in Figure 3-9, starting near the upper left corner (100% of QBfA) and going down diagonally by increasing the amount of the AMW end-member. Thus, as a first approximation, the Central Amargosa Valley samples are a "binary" mixture of the QBfA and AMW end-members.

Two important exceptions to this general trend are worth commenting on here. First, samples from the Eastern Amargosa hydrofacies (purple circles) have an important contribution of the carbonate end-member, as is clearly shown on the right-hand graph in Figure 3-9 (cluster of AR samples coloured in purple). This contribution ranges from less than 20% up to 50%. The high contribution of the RCA end-member in most samples of the EA hydrofacies is compatible with their position intersecting the Gravity Fault, where more to the south a line of springs in the Ash Meadows region has a clear signature of the RCA end-member

The second important exception to the QBfA-AMW binary mixture trend affects a subset of samples from the Western Rock Valley hydrofacies (dark blue stars). This is the part of the blue trend following the diagonal line in the middle graph in Figure 3-9, which has end-members AMW and TTA as axes. This means that this subset of WRV samples is a binary mixture of these two end-members (instead of a binary mixing of the AMW and QBfA end-members, as most Central Amargosa Valley samples are). The contribution of the Tertiary Tuffs Aquifer end-member ranges from a minimum of 20% to a maximum of 55%. The 20% contribution of TTA is common to the other subset of WRV samples (vertical branch in the middle graph in Figure 3-9). All the samples with an increased contribution of the TTA end-member come from borehole NC-EWDP-04PB, the borehole that experienced problems during sampling (see comments on samples #192 to #196 in Table 2-1). Therefore, this branch of the mixing trend affecting the WRV is probably an artefact (this hypothesis is strengthened by the fact that borehole NC-EWDP-04PB does not intersect volcanic tuffs).

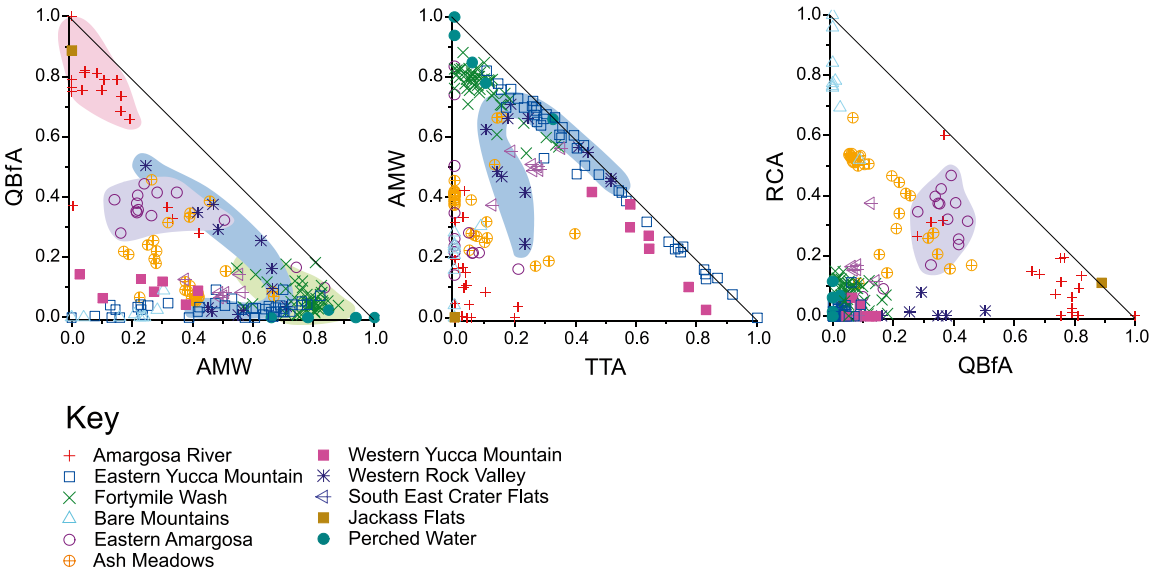

Figure 3-9. *Mixing trends in the Central Amargosa Valley samples. Included here are the following hudrofacies: Amargosa River (red trend, Western Rock Valley (blue trends), Fortymile Wash (green trend) and Eastern Amargosa (purple trend).*

3.3.2 Mixing model MM5

The comparison of reference mixing model MM3 with the other mixing models is carried out using XY plots in which the mixing proportions given by MM3 always appear in the X axis and the corresponding ones from the other mixing model in the Y axis. Because there are four end-member waters, four different XY graphs for each mixing model are used. The diagonal line of these XY graphs has a special meaning: a perfect match of mixing proportions between two mixing models would result in all the samples plotted on this line. The more discrepancies in mixing proportions between two models, the larger are the deviations from the diagonal line. Consequently, this type of graph is a great visual aid in assessing differences between mixing models. The set of four XY graphs plotting the discrepancies in mixing proportions between the reference mixing model (MM3) and another mixing model is referred to below as the *discrepancy portrait*.

Figure 3-10 is the discrepancy portrait of model MM5. The only difference between mixing models MM3 and MM5 is the QBfA end-member. In model MM3, the water acting as the QBfA end-member is sample #143 (AR hydrofacies), while in model MM5 it is sample #291 (JaF hydrofacies). As the discrepancy portrait shows, both models are very similar. TTA and AMW mixing proportions are almost identical, and the only minor differences are restricted to the low end of RCA mixing proportions and to the high end of QBfA mixing proportions. At any rate, these differences are always smaller than 10%. It can be concluded, then, that the change in the QBfA end-member from sample #264 to sample #291 has very few practical implications from a mixing perspective.

However, model MM5 is clearly poorer than model MM3 as the coverage for model MM5 is slightly lower (77.9%) and chloride deviations are the largest among all the mixing models tested (see Table 3-6 above).

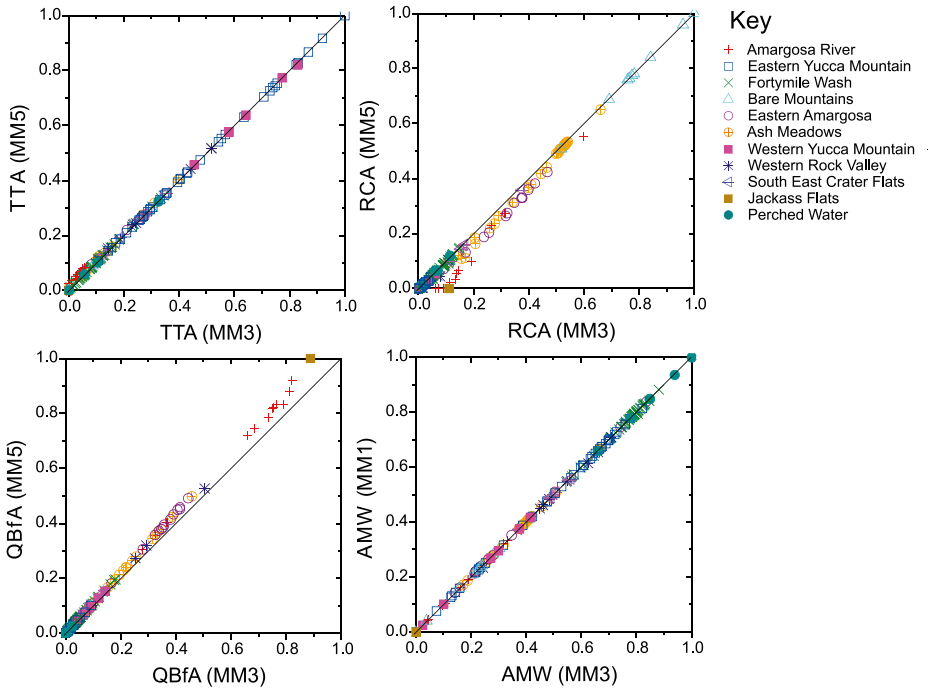

Figure 3-10. *Mixing proportions for mixing model MM5 (TTA=211, RCA=264, QBfA=291, AMW=345) compared to those in the reference mixing model (MM3).*

3.3.3 Mixing models MM1 and MM2

Mixing models MM1 and MM2 are treated together because their discrepancy portraits are very similar, as shown by Figures 3-11 and 3-12. Mixing proportions calculated with MM1 are very similar to those computed with the reference model (MM3). Mixing proportions calculated with MM2 depart somewhat more from the reference model (see QBfA discrepancy plot in both figures), but the overall behaviour is the same.

MM1 differs from the reference model only in the AMW end-member, whereas MM2 differs also in the QBfA end-member (see Table 3-6 above). MM1 has one degree of separation with respect to MM3 and MM2 has two.

Both MM1 and MM2 have precipitation sample #6221 as the AMW end-member (as opposed to perched water sample #345 in MM3). This is the reason why the largest differences in mixing proportions between these models and the reference model affect the AMW component. In both cases, discrepancies of up to 20% can be found in waters where the AMW end-member is dominant (e.g. most of the samples from the FmW hydrofacies). This behaviour is common to all mixing models with precipitation sample #6221 as the AMW end-member. In other words, mixing models with sample #6221 as the AMW end-member underestimate the amount of the AMW component in the mixture by as much as 20% (compared to models with sample #345 as the AMW end-member). The origin of this underestimation was already identified in Section 2.4.1 (Total system exploratory analysis): the compositional gap between the precipitation samples and all the groundwater samples (see, e.g. Figure 2-7). Because this compositional gap does not exist between the perched waters and the groundwaters, when a perched water is used as the AMW end-member, the whole range of mixing proportions from 0 to 100% AMW is obtained, whereas this range is limited to 0–80% when a precipitation sample is used as the AMW end-member.

Apart from this major difference, minor variations (< 10%) are also seen in the low end of the TTA component, and even smaller ones (< 5%) in the low end of the RCA component in both mixing models (in model MM2, samples from the AR hydrofacies can have RCA mixing proportions up to 10% lower than in the reference model).

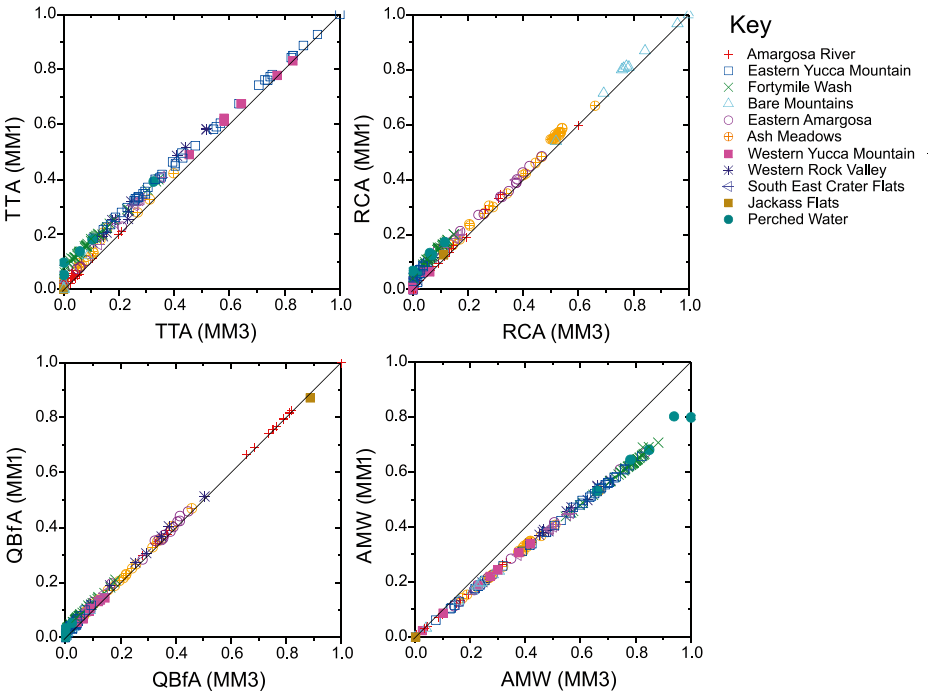

Figure 3-11. *Mixing proportions for mixing model MM1 (TTA=211, RCA=264, QBfA=143, AMW=6221) compared to those in the reference mixing model (MM3).*

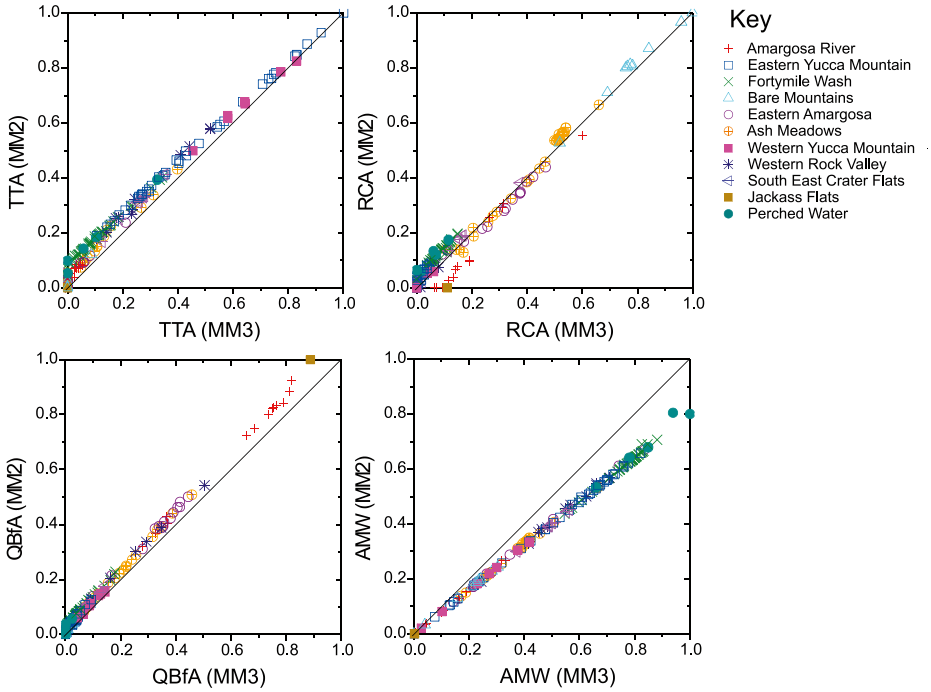

Figure 3-12. *Mixing proportions for mixing model MM2 (TTA=211, RCA=264, QBfA=291, AMW=6221) compared to those in the reference mixing model (MM3).*

3.3.4 Mixing models MM4 and MM6

Mixing models MM4 and MM6 are also treated together because their discrepancy portraits are similar. These two models differ from the reference model more than any previous one. This is clearly seen in Figures 3-13 and 3-14 mainly in the RCA and AMW graphs. MM6 has only the TTA end-member in common with the reference model, whereas MM4 also has the QBfA end-member in common with the reference model. In other words, MM4 has two degrees of separation with respect to the reference model and MM6 has three.

The largest discrepancies affect the RCA component, where the differences in mixing proportions may be as much as 50%. This is the case, for example, for the representative samples of the AM hydrofacies. In the reference model this cluster of samples has a 50% contribution from the RCA end-member (the other 50% comes from the AMW end-member), while this contribution is almost 100% in mixing models MM4 and MM6 (both mixing models have sample #40, one of the representative samples of the AM hydrofacies, as the RCA end-member). The RCA graph in both figures clearly shows that models MM4 and MM6 highly overestimate the contribution of the RCA end-member to the chemistry of most waters in the final dataset (except for a few AR samples in mixing model MM6).

As with the AMW component (both MM4 and MM6 have precipitation sample #6221 as the AMW end-member), the discrepancies with the reference model are also important, not only for large AMW mixing proportions. At the high end, the differences can reach 25% and at the low end as much as 45%. The largest discrepancies are found, in both mixing models, in samples from the Ash Meadows, Eastern Amargosa and South East Crater Flat hydrofacies (those samples with the highest contribution of the RCA end-member).

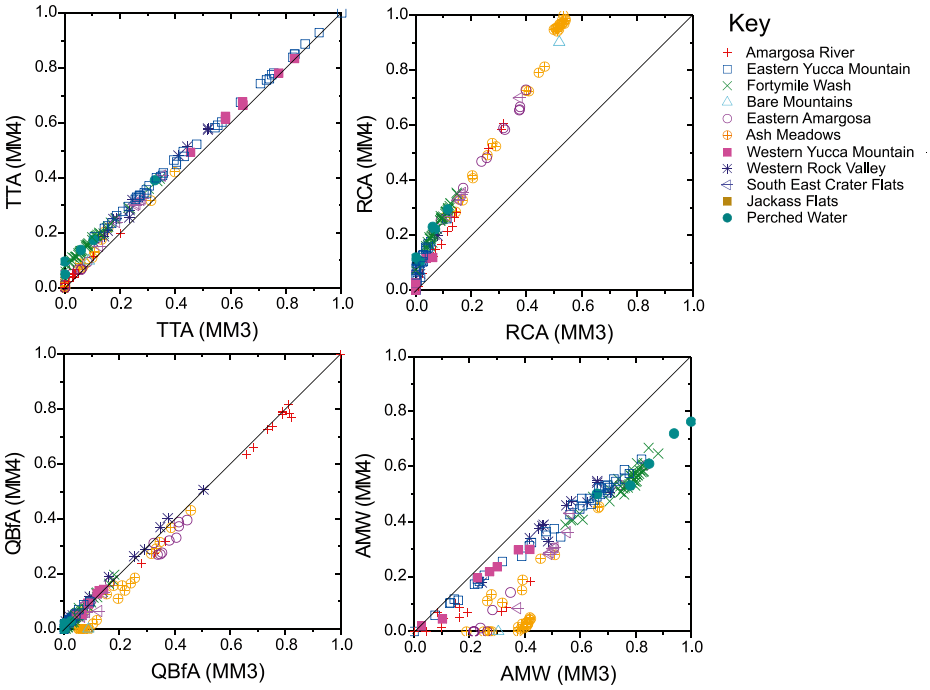

Figure 3-13. *Mixing proportions for mixing model MM4 (TTA=211, RCA=40, QBfA=143, AMW=6221) compared to those in the reference mixing model (MM3).*

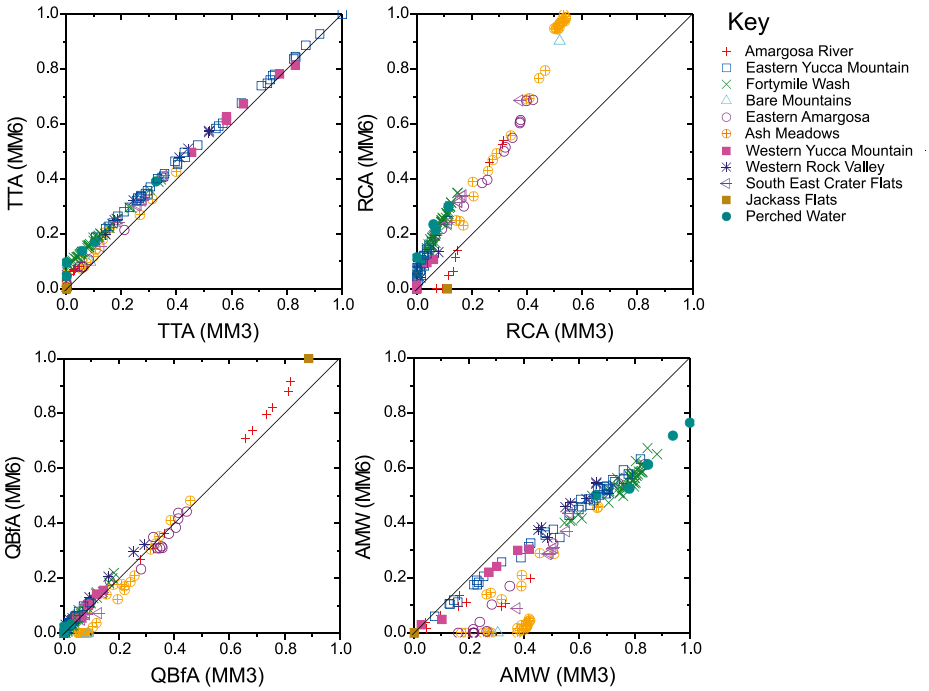

Figure 3-14. *Mixing proportions for mixing model MM6 (TTA=211, RCA=40, QBfA=291, AMW=6221) compared to those in the reference mixing model (MM3).*

3.3.5 Comparison of mixing proportions: a final assessment

The previous sections have shown how mixing proportions differ between mixing models, using mixing model MM3 as a reference. The differences, visually exposed by discrepancy portraits, range from negligible (MM5), to moderate (MM1 and MM2) to fairly large (MM4 and MM6). More quantitatively, taking mixing model MM3 as a reference, the deviation ε of mixing proportions for sample *i* in mixing model *M* can be calculated as:

$$\varepsilon_i^M = \sqrt{\sum_{k=1}^{4} (X_{ik} - X_{ik}^M)^2} \ ,$$

where X_{ij} is the mixing fraction of end-member *k* in sample *i* for the reference model and X_{ik}^M the corresponding mixing fraction for model *M*. The average deviation for mixing model *M*, $\overline{\varepsilon}^M$, is obtained summarising the n_M samples inside the mixing polyhedron of each mixing model:

$$\overline{\varepsilon}^M = \frac{1}{n_M} \sum_{i=1}^{n_M} \varepsilon_i^M \ .$$

Figure 3-15 plots these deviations, by means of box and whiskers diagrams, for mixing models MM1, MM2, MM4, MM5 and MM6, always remembering that these deviations are taken with respect to mixing model MM3 serving as the reference model. The box is delimited by the 25th and 75th percentiles, while the whiskers mark the maximum and minimum values. The square near the centre of the box is the mean value. Values have been converted from mixing fractions, as returned by the equations above, to mixing percentages for plotting purposes.

These quantitative results are in complete agreement with the qualitative visual appreciation made in previous sections with the discrepancy portraits. Mixing model MM5 is the closest to the reference model, with a mean deviation of only 2.1%. Next come models MM1 (11.0%) and MM2 (12.2%), and finally models MM6 (25.6%) and MM4 (25.8%). As for the *maximum* deviations (i.e. the samples with the maximum difference in mixing proportions compared to the reference model), these range from 17% for MM5, 25% for MM1 and MM2, and 60% for MM4 and MM6.

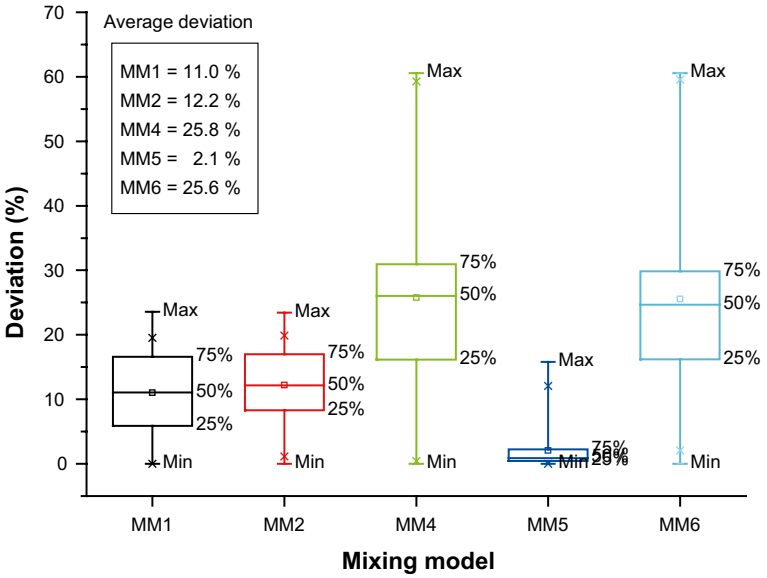

Figure 3-15. *Box and whiskers plot for mixing proportion deviations. Deviations are measured with mixing model MM3 as a reference. The average deviation for each mixing model is given numerically and ranges from 2.1% for MM5 to 25.8% for MM4.*

Figure 3-16 classifies the models according to: (i) the number of end-members different to those in the reference model (what has been called the degree of separation), (ii) the model ranking, taking into account coverage and compositional deviations for chloride (see Table 3-6 above) and (iii) the average deviation of mixing proportions as computed by the equations above (and graphically shown in Figure 3-15). In Figure 3-16 symbols refer to the hydrofacies to which the end-member belongs, while the relative position of the symbol in the row refers to the type of end-member, so that the first symbol refers to the TTA end-member, the second to the RCA end-member, the third to the QBfA end-member and the last to the AMW end-member. Finally, the colour of the box gives an idea of how different the mixing proportions are compared to the reference model (in a qualitative scale from negligible, to small, to large).

A first analysis of Figure 3-16 shows surprisingly that model MM5, the worst *in terms of ranking* (i.e. low coverage and large chloride deviations), is the model that is most similar to the reference model *in terms of mixing proportions* (negligible differences in mixing proportions compared to the reference model MM3: green outline). The only difference between models MM3 and MM5 is the QBfA end-member; in the reference model this end-member is defined by sample #143+ and in model MM5 by sample #291■. Clearly, the impact of swapping the QBfA end-member is almost irrelevant in terms of mixing proportions, but significant in terms of how well the actual chemistry of a sample is reconstructed by means of these mixing proportions. It can be interesting to recall here how the chemistry of a sample is reconstructed. Two things are needed: the mixing proportions and the composition of the end-members. For example, the reconstructed chloride content of a sample is computed as follows:

$$Cl_{Sample} = \frac{Cl_{TTA} \cdot TTA\% + Cl_{RCA} \cdot RCA\% + Cl_{QBfA} \cdot QBfA\% + Cl_{AMW} \cdot AMW\%}{100},$$

where Cl_{TTA} is the chloride content of the sample acting as the TTA end-member (i.e. sample #211 in all mixing models, whose Cl content is 5.50 mg/L), and TTA% is the mixing proportion (%) of the TTA end-member in the sample. The definition of the other terms in the equation follows from this one. So, if the mixing proportions are very similar (for a particular sample) in two mixing models (i.e. TTA%, RCA%, etc are similar), but the composition of the end-member is quite different in the two mixing models (i.e. Cl_{TTA}, Cl_{RCA}, etc are different), the reconstructed chemistry of the sample can greatly differ from the actual chemistry in one mixing model but not in the other. Obviously, one mixing model would be better than the other (the one with the reconstructed chemistry closer to the actual one). In this sense, mixing model MM5 is a less proper mixing model because the reconstructed chemistry (for a conservative element like chloride) differs greatly from the actual chemistry *for many samples in the final dataset*. In summary, to assess the suitability of a mixing model, all the relevant aspects must be taken into account, and mixing proportions is only one of them.

From a practical point of view, if mixing proportions is the most important "relevant aspect" of a mixing model, then little distinguishes model MM3 from MM5. On the other hand, differences are large when the reconstructed chemistry is relevant. Since in this context *both* aspects are highly relevant, it can be concluded that model MM3 is "better" than model MM5. And because the only difference between both mixing models is the QBfA end-member, it can also be concluded that sample #143+ is a better QBfA end-member than sample #291■.

Looking again at Figure 3-16 it can be seen that model MM5 is the only one that does not follow the trend of "the higher the degree of separation, the lower the ranking" in the models (blue arrow). This is the one trend that can be expected if the end-member waters in model MM3 are more appropriate than the rival end-members, so that the more end-members are changed, the more the quality of the resulting mixing model is degraded. The models following this trend, i.e. MM3-MM1-MM4-MM2-MM6, also roughly follow "the mixing proportions trend" in the sense that a model further away from the reference model also has larger discrepancies in mixing proportions. As a result of the good correlation between the two relevant aspects of a mixing model (accuracy in the reconstruction of the chemistry and similarity between mixing proportions) for the models following the trend marked with a blue arrow in Figure 3-16 it can be said that the end-members in model MM3 are more suitable at explaining the Yucca Mountain hydrogeological system than the rival ones in the other mixing-models, and that the differences in mixing proportions are merely a reflection of the inability of the rival end-members to accurately model the chemistry of the samples.

From this point of view, sample #40⊕ is evidently not a good RCA end-member for the Yucca Mountain hydro-system because the mixing models that use it as the RCA end-member have, at the same time, large differences in the computed mixing proportions (compared to the reference model) *and* larger deviations in the reconstructed chemistry (compared to the actual chemistry of the samples). The impact of changing the AMW end-member (from sample #345● to sample #6221▽) or the QBfA end-member (from sample #143+ to sample #291■) is much smaller, which means that these rival end-members are not as different as sample pair #40⊕/#264△ is.

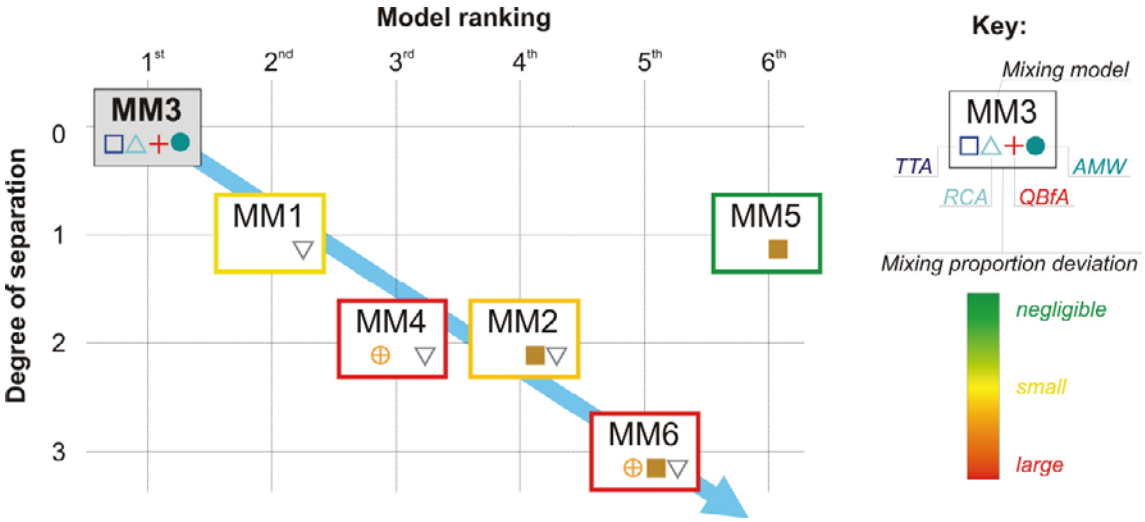

Figure 3-16. *Classification of mixing models in terms of ranking, degree of separation from reference model MM3 and deviation of mixing proportions with respect to MM3. Only the end-members that differ from those in the reference model are shown (▽: Precipitation; ●: perched water; △: Bare Mountain; ⊕: Ash Meadows; □: Eastern Yucca Mountain; +: Amargosa River; ■: Jackass Flat).*

4 Conclusions

The following conclusions are drawn from the study:

- The Yucca Mountain hydro-system is composed of a complex mixture of several water types (groundwaters, pore waters, perched waters, surface waters and precipitation) that interact through the surface, the unsaturated zone and several aquifer systems (the Palaeozoic Carbonate Aquifer, the Tertiary Tuffs Aquifer and the Quaternary Basin-fill Aquifer).
- The raw dataset consists of 397 water samples, of which 254 are groundwater samples, 6 are perched water samples, 81 are pore water samples, 17 are surface water samples and 39 are precipitation samples. The groundwater samples were grouped into 10 hydrofacies according to general chemistry and geographical location.
- The general chemistry of all these waters is rather dilute, dominating the low-TDS waters of the sodium bicarbonate type, although obvious trends towards calcium-magnesium bicarbonate-sulphate type and calcium-magnesium sulphate (-chloride) type of higher TDS exist.
- The median chloride concentration of the samples in the raw dataset is 11.4 mgL^{-1} and the median TDS is 368.0 mgL^{-1}, clearly demonstrating the dilute character of the waters in the Yucca Mountain area. Bicarbonate is the most important anion, with a median concentration of 162 mgL^{-1}, followed by sulphate, with a median concentration of 28.8 mgL^{-1}. Among the cations, sodium is principal, with a median content of 67.3 mgL^{-1}, followed by Ca (19 mgL^{-1}), potassium (6.1 mgL^{-1}) and finally magnesium (2.1 mgL^{-1}).
- Several trends, threshold values, limiting values and outliers have been discovered in the exploratory analysis. Together, these regularities point to the existence of common processes that shape the chemistry of the Yucca Mountain waters.
- The hydrofacies exploratory analysis has permitted the identification of several samples in which evaporation, ion exchange, dissolution and/or precipitation of mineral phases have drastically changed their chemistry. These samples have been excluded from the final dataset, as the main objective of the report is to assess the *general* constraints on the mixing of waters in the Yucca Mountain system. A total of 240 samples (out of the initial 397) have been used in the final dataset.
- The hydrofacies exploratory analysis has also permitted the identification of several samples that can act as potential end-member waters during mixing. The chemistry of all these samples has been compiled in several tables.
- The analysis performed with the M3 code has two parts. In the first part, 13 potential end-member waters have been used to compute the coverage of each combination of end-member waters. The coverage is the percentage of waters in the final dataset that can be explained by pure mixing of the chosen end-members. This analysis has shown that the Yucca Mountain waters are best explained by the mixture of four end-member waters: (1) a carbonate water representative of the Palaeozoic Carbonate Aquifer (sample #264 from the Bare Mountains hydrofacies), (2) a water representative of the Tertiary Tuffs Aquifer (sample #211 from the Eastern Yucca Mountain hydrofacies), (3) a water representative of the Quaternary Basin-fill Aquifer (either samples #143 from the Amargosa River hydrofacies, or samples #291 from the Jackass Flat hydrofacies) and (4) a “meteoric” water that could be a precipitation sample (#6221), a surface water sample (#275) or a perched water sample (#345).

- Six mixing models have been finally selected and tested (MM1 to MM6). A ranking procedure based on coverage and accuracy in the reconstruction of the chemistry of the samples from the computed mixing proportions has allowed the identification of the "best" mixing model, MM3, which has been taken as the reference model. All the other mixing models have been benchmarked against it. The picture that has emerged from this mixing model is the following:

  1. The reference mixing model has sample #211 as the TTA end-member, sample #264 as the RCA end-member, sample #143 as the QBfA end-member and sample #345 as the AMW end-member. The coverage is 81.4%, i.e. 195 samples out of 240 fall within the mixing polyhedron. Overall, the highest contribution to the chemistry of the samples in the final dataset comes from the AMW (49%), followed by the TTA (19%), the RCA (17%) and the QBfA (15%). Also, the AMW contribution is the most evenly spread among the samples.
  2. The Eastern and Western Yucca Mountain hydrofacies samples are almost a binary mixture of the TTA and AMW end-members. The presence of an AMW component in these waters is rather surprising and points to the comparatively widespread presence of an "old" meteoric water in many shallow sections of the local aquifers around Yucca Mountain.
  3. Most Ash Meadows samples are almost a binary mixture of the RCA and AMW end-members (with a small contribution, ~8%, of the QBfA end-member). This correlates with a discharge of the regional Palaeozoic Carbonate Aquifer along the Gravity Fault, followed by a mixture of the carbonate waters with (old) meteoric waters during ascent.
  4. The samples from the Central Amargosa Valley (Amargosa River, Eastern Amargosa, Fortymile Wash and Western Rock Valley hydrofacies) are particularly interesting because they occupy the area down-gradient of Yucca Mountain. From the point of view of mixing, these waters are dominated by the QBfA and AMW end-members, although they always have contributions from at least one other end-member water. By hydrofacies, Amargosa River samples have the highest contribution of the QBfA end-member (between 75% and 100%), followed by the Eastern Amargosa samples (around 40%) and the Fortymile Wash samples (less than 20%). The Western Rock Valley samples have a varied contribution of the QBfA, between 0 and 50%. The "extra" contribution could be the TTA (as in one subset of the Western Rock Valley samples), the RCA (as in the Eastern Amargosa samples), or both (as in the Fortymile Wash samples). The high contribution of the RCA end-member in most samples of the Eastern Amargosa hydrofacies is compatible with their position intersecting the Gravity Fault.

- In summary, the ternary mixing that characterises most samples in the Central Amargosa Valley is a clear indication that the aquifers in the area are not completely sealed. On the contrary, it seems that mixing between chemically contrasting waters is widespread down-gradient of Yucca Mountain. This can negatively impact the Regional Carbonate Aquifer in the case of a containment failure in the repository as there appears to be a connection between the upper aquifers (Tertiary Tuffs and Quaternary Basin-fill Aquifers) and the lower carbonate aquifer.
- As a final point, it is important to note that M3 has been successfully applied to a complex system where mixing is not the only process that has modelled the chemistry of the groundwaters. The methodological procedure followed in this report can be extended to other sedimentary environments.

5 References

SKB's (Svensk Kärnbränslehantering AB) publications can be found at www.skb.se/publications.

Beatley J C, 1976. Vascular plants of the Nevada Test Site and central-southern Nevada: ecologic and geographic distributions. Oak Ridge, TN: Technical Information Center, Office of Technical Information, U.S. Energy Research and Development Administration.

Bedinger M S, Langer W H, Reed J E, 1989. Ground-water hydrology. In: Bedinger M S, Sargent K A, Langer W H (eds). Studies of geology and hydrology in the Basin and Range Province, southwestern United States, for isolation of high-level radioactive waste. Professional Paper 1370–F, U.S. Geological Survey, Denver, Colorado, pp 28–35.

Belcher W R, Faunt C C, D'Agnese F A, 2002. Three-dimensional hydrogeologic framework model for use with a steady-state numerical ground-water flow model of the Death Valley regional flow system, Nevada and California. Water-Resources Investigations Report 01-4254, U.S. Geological Survey, Denver, Colorado.

Claassen H C, 1985. Sources and mechanisms of recharge for ground water in the west-central Amargosa desert, Nevada: a geochemical interpretation. Professional Paper 712-F, U.S. Geological Survey, Denver, Colorado.

Craig H, 1961. Isotopic variations in meteoric waters. Science, 133, pp 1702–1703.

CRWMS M&O, 2007. Saturated zone site-scale flow model. MDL-NBS-HS-000011 REV 03, Appendix A, Sandia National Laboratories, Las Vegas, USA.

D'Agnese F A, Faunt C C, Turner A K, Hill M C, 1997. Hydrogeologic evaluation and numerical simulation of the Death Valley regional ground-water flow system, Nevada and California. Water-Resources Investigations Report 96–4300, U.S. Geological Survey, Denver, Colorado.

Dilles J H, Gans P B, 1995. The chronology of Cenozoic volcanism and deformation in the Yerington area, western Basin and Range and Walker Lane. Geological Society of America Bulletin, 107, pp 474–486.

Eddebbarh A A, Zyvoloski G A, Robinson B A, Kwicklis E M, Reimus P W, Arnold B W, Corbet T, Kuzio S P, Faunt C, 2003. The saturated zone at Yucca Mountain: an overview of the characterization and assessment of the saturated zone as a barrier to potential radionuclide migration. Journal of Contaminant Hydrology, 62-63, pp 477– 493.

Gershenfeld N, 1999. The nature of mathematical modeling. Cambridge: Cambridge University Press.

Gómez J B, Laaksoharju M, Skårman E, Gurban I, 2006. M3 version 3.0: Concepts, methods, and mathematical formulation. SKB TR-06-27, Svensk Kärnbränslehantering AB.

Gómez J B, Laaksoharju M, Skårman E, Gurban I, 2009. M3 version 3.0: Verification and validation. SKB TR-09-05, Svensk Kärnbränslehantering AB.

Grose T L, Smith G I, 1989. Geology. In: Bedinger M S, Sargent K A, Langer W H (eds). Studies of geology and hydrology in the Basin and Range Province, southwestern United States, for isolation of high-level radioactive waste. Professional Paper 1370–F, U.S. Geological Survey, Denver, Colorado, pp 5–19.

Hales J E, 1972. Surges of maritime tropical air north-ward over the Gulf of California: Monthly Weather Review, 100, pp 298–306.

Hales J E, 1974. Southwestern United States summer monsoon source – Gulf of Mexico or Pacific Ocean? Journal of Applied Meteorology, 13, pp 331–342.

Hardyman R F, Oldow J S, 1991. Tertiary tectonic framework and Cenozoic history of the central Walker Lane, Nevada. In: Raines G L , Lisle R E, Schafer R W, Wilkinson W H (eds). Geology and ore deposits of the Great Basin: proceedings of the Great basin Symposium, Reno/Sparks, Nevada, 1–5 april 1990. Reno: Geological Society of Nevada, Vol. 1, pp 279–301.

Laaksoharju M, Skårman C, Skårman E, 1999. Multivariate mixing and mass balance (M3) calculations, a new tool for decoding hydrogeochemical information. Applied Geochemistry, 14, pp 861–871.

Laaksoharju M, Skårman E, Gómez J B, Gurban I, 2009. M3 user's manual. Version 3.0. SKB TR-09-09, Svensk Kärnbränslehantering AB.

Luckey R R, Tucci P, Faunt C C, Ervin E M, Steinkampf W C, D'Agnese F A, Patterson G L, 1996. Status of understanding of the saturated-zone ground-water flow system at Yucca Mountain, Nevada, as of 1995. Water-Resources Investigations Report 96-4077, U.S. Geological Survey, Denver, Colorado.

Meijer A, 2002. Conceptual model of the controls on natural water chemistry at Yucca Mountain, Nevada. Applied Geochemistry, 17, pp 793–805.

Oliver T A, Patterson G L, 2002. Hydrochemical facies in ground water near Yucca Mountain, Nevada. Geological Society of America Abstracts with Programs, 34, p 396.

Parkhurst D L, Appelo C A J, 1999. User's guide to PHREEQC (version 2): a computer program for speciation, batch-reaction, one-dimensional transport, and inverse geochemical calculations. Water-Resources Investigations Report 99-4259, U.S. Geological Survey, Denver, Colorado.

Peterson F F, 1981. Landforms of the Basin & Range province defined for soil survey: Nevada Agricultural Experiment Station, Max C. Fleischmann College of Agriculture, University of Nevada, Reno. (Technical Bulletin 28.)

Plummer L N, Busby J F, Lee R W, Hanshaw B B, 1990. Geochemical modeling of the Madison aquifer in parts of Montana, Wyoming and South Dakota. Water Resources Research, 26, pp 1981–2014.

Rogers A M, Harmsen S C, Meremonte M E, 1987. Evaluation of the seismicity of southern Great Basin and its relationship to the tectonic framework of the region. Open-File Report 87-408, U.S. Geological Survey, Denver, Colorado.

Sawyer D A, Fleck R J, Lanphere M A, Warren R G, Broxton D E, Hudson M R, 1994. Episodic caldera volcanism in the Miocene southwestern Nevada volcanic field: revised stratigraphic framework, $^{40}Ar/^{39}Ar$ geochronology, and implications for magmatism and extension. Geological Society of America Bulletin, 106, pp 1304–1318.

Snow J K, Wernicke B P, 1989. Uniqueness of geological correlations: an example from the Death Valley extended terrain. Geological Society of America Bulletin, 101, pp 1351–1362.

Sonnenthal E L, Bodvarsson G S, 1999. Constraints on the hydrology of the unsaturated zone at Yucca Mountain, NV from three-dimensional models of chloride and strontium geochemistry. Journal of Contaminant Hydrology, 38, pp 107–156.

Stewart J H, 1988. Tectonics of the Walker Lane belt, western Great Basin Mesozoic and Cenozoic deformation in a zone of shear. In: Ernst W G (ed). Metamorphism and crustal evolution of the western United States. Englewood Cliffs, NJ: Prentice-Hall, pp 683–713.

Stewart J H, Crowell J C, 1992. Strike-slip tectonics in the Cordillera region, western United States. In: Burchfiel B C, Lipman P W, Zoback M L (eds). The Cordilleran orogen: conterminous U.S. Boulder, CO: Geological Society of America, pp 609–628.

Stuckless J S, Dudley W W, 2002. The geohydrologic setting of Yucca Mountain, Nevada. Applied Geochemistry, 17, pp 659–682.

Sweetkind D S, Belcher W R, Faunt C C, Potter C J, 2004. Geology and hydrogeology. In: Belcher W R (ed). Death Valley regional ground-water flow system, Nevada and California – hydrogeologic framework and transient ground-water flow model. Scientific Investigation Report 2004-5205, U.S. Geological Survey, Denver, Colorado, Chapter B.

Thomas J M, Welch A H, Dettinger M D, 1996. Geochemistry and isotope hydrology of representative aquifers in the Great Basin Region of Nevada, Utah, and adjacent areas. Professional Paper 1409-C, U.S. Geological Survey, Denver, Colorado.

Vaniman D T, Chipera S J, Bish D L, Carey J W, Levy S S, 2001. Quantification of unsaturated-zone alteration and cation exchange in zeolitized tuffs at Yucca Mountain, Nevada, USA. Geochimica et Cosmochimica Acta, 65, pp 3409– 3433.

von Seggern D H, Brune J N, 2000. Seismicity in the southern Great Basin, 1868–1992. In: Whitney J W, Keefer W R (eds). Geologic and geophysical characterization studies of Yucca Mountain, Nevada. Denver, CO: U.S. Geological Survey. (Digital Data Series 58), Chapter J.

White A F, Chuma N J, 1987. Carbon and isotopic mass balance models of Oasis Valley – Fortymile Canyon Groundwater Basin, southern Nevada. Water Resources Research, 23, pp 571–582.

Wright L A, Greene R C, Cemen I, Johnson F C, Prave A R, 1999. Tectonostratigraphic development of the Miocene-Pliocene Furnace Creek Basin and related features, Death Valley region. In: Wright L A, Troxel B W (eds). Cenozoic basins of the Death Valley region. Boulder, CO: Geological Society of America. (Special Paper 333), pp 87–114.